THE UNIVERSITY OF MANITOBA

INDIVIDUAL AND INTERACTIVE INFLUENCE OF TEMPERATURE, STRESS, PHYSICAL AGING AND MOISTURE ON CREEP, CREEP RUPTURE AND FRACTURE OF EPOXY MATRIX AND ITS COMPOSITE

By

CHANDRA VISWANATHAN

A thesis
Submitted to the Faculty of Graduate Studies
in partial fulfillment of the
requirements for the degree of
Master of Science

DEPARTMENT OF MECHANICAL AND INDUSTRIAL ENGINEERING
WINNIPEG, MANITOBA
FEBRUARY 2001

THE UNIVERSITY OF MANITOBA

FACULTY OF GRADUATE STUDIES

*****

COPYRIGHT PERMISSION PAGE

INDIVIDUAL AND INTERACTIVE INFLUENCE OF TEMPERATURE, STRESS, PHYSICAL AGING AND MOISTURE ON CREEP, CREEP RUPTURE AND FRACTURE OF EPOXY MATRIX AND ITS COMPOSITE

BY

CHANDRA VISWANATHAN

A Thesis/Practicum submitted to the Faculty of Graduate Studies of The University of Manitoba in partial fulfillment of the requirements of the degree

of

MASTER OF SCIENCE

ACKNOWLEDGEMENTS

I take this oppurnity to thank ***Dr. R. Jayaraman*** for his guidance and encouragement throughout this course of this work.

I would like to thank ***Beoing Canada Technology Ltd., Winnipeg Division*** for allowing us to manufacture the composite panels using its facility. I would also like to acknowledge the technical assistance of ***Mr. Don Mardis, Mr. John Van Drop and Mr. Mike Boskwick*** for their technical assistance.

My special thanks to my friends, ***Uttara and Chithra*** for their help and support during last three years. Last but not the least, I would like to thank all my family members, especially ***my parents*** for their constant support and encouragement.

ABSTRACT

Two major concerns in using polymer composites for load bearing structural applications are time dependent degradation in modulus and strength, measured by creep and creep rupture tests. Previous studies on creep of polymer composites focused on the individual and interactive effect of one or more of factors such as Stress-Temperature, Stress-Temperature-Physical Aging and Stress-Temperature-Moisture. While the effect of stress, temperature, and moisture on creep rupture is well documented, limited studies have focussed on the effect physical aging on creep rupture of polymer composites. No effort has so far been made to study the combined effect of the above factors on creep and creep rupture of polymer composites. Hence, the present investigation was undertaken to experimentally study the individual and interactive effect of temperature, stress, physical aging, and moisture on creep (linear and non-linear region), creep rupture and fracture of a thermoset epoxy resin (F263) and its composite (Hexcel Corporation's F263 epoxy resin reinforced with T 300 carbon fibers). Transverse creep compliance (S_{22}) and creep rupture time for unidirectional composite were measured and compared with that of the resin to delineate the effect of fibers on the time dependent behavior of the resin. Both composite and resin exhibited linear creep upto a stress level of 7 MPa. Moisture (M) accelerated creep through plasticization (reduction in the Glass transition temperature (T_g)) of matrix resin of the composite and this creep acceleration was found to be equal to creep acceleration by a temperature increase equivalent to decrease in T_g. Physical aging (PA) retarded creep. The interactive effect of aging and moisture reduced the magnitude of matrix plasticization as compared to non-aged samples containing the

same amount of moisture. The interactive influence of all the other factors on the influence of temperature on creep was not observed. However, interactive influence of physical aging and moisture on the effect of stress on creep was observed, when moisture and physical were considered together. For a given temperature and stress level, the creep rupture time of composite was found to be less than that of resin. While moisture accelerated creep-rupture for both the resin and the composite, physical aging accelerated the creep rupture for composite and retarded that of the resin. Similar to creep, the interactive influence of aging and moisture caused a reduction in the magnitude of creep rupture acceleration when compared to the non-aged material at the same moisture level.

TABLE OF CONTENTS

LIST OF FIGURES

LIST OF TABLES

CHAPTER 1

INTRODUCTION

A composite is a mixture of a reinforcement material (such as fiber) and a matrix (polymer or resin) / binder material. Composite materials are classified into three broad categories depending on type, geometry, and orientation of the reinforcement phase: (1) Particulate, (2) Discontinuous fibers or whisker, and (3) Continuous fibers. Particulate composites consist of particles of aspect ratios $\left(\frac{L}{d}\right)$ 1 to 20 randomly dispersed within the matrix. Discontinuous fiber composites contain short fibers or whiskers as reinforcing phase with aspect ratios 20 to 100. These short fibers can be either all oriented along one direction or randomly oriented. Continuous fiber composites (used in this thesis) have an aspect ratio greater than 100 and are reinforced by continuous fibers and lead to high reinforcing efficiency. Continuous fiber composites, made up of several prepreg layers (a prepreg is a single layer of continuous fiber in a matrix) are divided into three types:

(1) Unidirectional composite – fibers are parallel to each other

(2) Multidirectional composite – fiber orientation vary from layer to layer

(3) Textile composite – fibers are woven like textile cloth

Composite materials influence the daily lives of most people in industrialized societies. Of particular interest are the carbon-reinforced composites which have good combinations of stiffness, strength and fatigue resistance. Their major usage is in the aerospace industry, where their performance characteristics are essential to a wide variety of demanding applications such as the wing to fuselage fairing in commercial aircraft, spacecraft, missiles etc. Many commercial airliners fly with parts of primary structure

and much of the interior furnishings and trim, made from composites. Many types of sporting and leisure goods, such as boats, gliders, sailboards, skis and racquets, use composite materials extensively in their construction.

Polymer composites are viscoelastic in nature (i.e. their behavior is a combination of viscous and elastic behavior). While being used for load bearing structural applications, polymer composites exhibit time dependent degradation in modulus and strength, as a consequence of viscoelasticity of the polymer matrix. The time dependent modulus and strength of composite materials are measured by creep and creep rupture tests, respectively. Since characterizing the time dependent modulus and strength for the entire service life is impossible, accelerated testing and extrapolation procedures are used to extrapolate creep data obtained over a short time to a time frame beyond the experimental time window.

Composites used in aerospace industries are either multidirectional or textile composite. Since fiber orientation in a multidirectional composite varies from layer to layer, characterizing each composite laminate lay-up sequence for time dependent strength and modulus is costly and time consuming. The preferred route by many researchers is to measure creep and creep rupture data for unidirectional composites and use them with a suitable model (such as lamination theory), to predict creep and creep rupture data of multidirectional and textile composites. The ongoing research at the University of Manitoba has chosen this path and this thesis is focused on developing creep and creep rupture data for unidirectional composites required for such modeling. In the past, a majority of creep studies focussed on the influence of stress and temperature on creep and creep rupture. However, limited studies were carried out on the individual

influence of moisture and physical aging. No effort has so far been made to study the combined effect of temperature, stress, physical aging, moisture and fiber volume fraction on creep and creep rupture of polymer composites and a knowledge of this is necessary in modeling and predicting the creep and creep rupture.

Unidirectional composites are orthotropic; i.e. materials having at least three mutually perpendicular planes of symmetry. Thus, to completely characterize the stress or strain of a unidirectional composite under in-plane loading, we need four compliance constants: S_{11}, S_{12}, S_{22}, and S_{66}. The Hooke's law is written as:

$$\begin{bmatrix} \varepsilon_1 \\ \varepsilon_2 \\ \gamma_6 \end{bmatrix} = \begin{bmatrix} S_{11} & S_{12} & 0 \\ S_{12} & S_{22} & 0 \\ 0 & 0 & S_{66} \end{bmatrix} \begin{bmatrix} \sigma_1 \\ \sigma_2 \\ \tau_6 \end{bmatrix}$$

σ_1, ε_1 = Longitudinal stress and strain [Along the fiber direction (0°)]
(Fiber dominated property)

σ_2, ε_2 = Transverse stress and strain [Direction perpendicular to fibers (90°)]
(Matrix dominated property)

τ_6, γ_6 = Shear stress and strain measured using a unidirectional specimen with fibers oriented at an angle (10°) to the loading axis

$S_{11}, S_{22}, S_{66}, S_{12}$ = Longitudinal, Transverse, Shear and In-plane transverse compliance respectively

Experimentally, S_{11} and S_{22} are obtained from uniaxial tests (tension tests) on specimens cut parallel and perpendicular to the fiber direction of a unidirectional composite, respectively. S_{11} and S_{22} are determined using strains from axially mounted strain gages. S_{12} can be determined from transversely mounted strain gage on either specimen. S_{66} is

determined from the difference between measured strains using two strain gages mounted at $\pm 45°$ to the fiber axis.

The present research was undertaken to investigate experimentally the individual and interactive effect of temperature, stress, physical aging, moisture, and fiber volume fraction on creep (linear and non-linear region), fracture and creep rupture of a thermoset epoxy polymer matrix (Hexcel corporation's F263) reinforced with unidirectional carbon fibers (T300). The present study is limited to measuring transverse creep compliance (S_{22}) to determine the influence of carbon fibers on the matrix. Modeling and prediction of long term creep and creep rupture properties was beyond the scope of the present work. However, the main aim of the present work was to generate experimental creep, fracture and creep rupture data, which would be used in future modeling and prediction of long-term creep and creep rupture properties.

ORGANIZATION OF THESIS

In Chapter 2, a brief review of research done to date on individual and interactive effect of one or more factors such as stress, temperature, physical aging, moisture and fiber volume fraction on creep, creep rupture and fracture of polymer composites is discussed. The experimental work and material used are described in Chapter 3. Results and Discussion of this experimental work are presented in Chapter 4. Finally, a conclusion of this research is summarized in Chapter 5.

CHAPTER 2

LITERATURE REVIEW

2.0 INTRODUCTION

Two major concerns in using polymer composites for load bearing structural applications are time dependent degradation in modulus (creep) and strength (creep rupture), as a consequence of viscoelasticity of matrix (resin). Factors that affect creep and creep rupture of polymer composites are (1) Temperature, (2) Stress, (3) Physical aging, and (4) Moisture. In addition, if the effect of fiber volume fraction on creep and creep rupture on polymer matrix is known, then creep and creep rupture of polymer composite of any volume fraction may be determined using the matrix and fiber volume fraction properties, thus eliminating testing procedure for every volume fraction of fibers. Hence volume fraction of fibers is also included as a factor in this study. In order, to predict long term creep compliance and strength of any polymeric composite structure, it is necessary to understand the individual and interactive effect of the above variables on creep and creep rupture of polymer composites. In addition to creep and creep rupture, it is important to understand the influence of above variables on fracture behavior of polymer composites. The fracture energy data obtained from fracture tests will be useful in creep rupture modeling. Definition of creep and creep rupture is discussed in section 2.1. Brief reviews of the previous research performed in these areas are discussed in sections 2.2 to 2.6.

2.1 DEFINITION

2.1.1CREEP

Creep is defined as the time dependent deformation of a material under constant load or stress. Creep in polymers, unlike metals is viscoelastic i.e. exhibit time dependent elastic strain that can be recovered over a period of time after removal of load.

To determine creep compliance of a material, a constant load is applied to a tensile specimen maintained at constant temperature and the resulting strain is measured as a function of time. This time dependent strain is used to determine creep compliance. Creep behavior is divided into two regions: Linear creep and non-linear creep. In linear creep, creep compliance is independent of stress. In non-linear creep, creep compliance is dependent on stress.

2.1.2CREEP RUPTURE

Creep rupture is defined as time dependent degradation of strength of a material under constant stress. It is performed by applying constant load or stress to a specimen until it fractures completely. The time at which the fracture occurs is termed as creep rupture time.

In addition to stress and temperature, the other factors that influence creep, creep rupture and fracture behavior of polymers composites are the physical aging and moisture. The effect of stress, temperature, physical aging and moisture on creep, creep rupture and fracture are reviewed in the following sections.

2.2 EFFECT OF TEMPRATURE/STRESS

2.2.1 ON CREEP

Temperature accelerates creep resulting in increase of creep compliance with increase in temperature. This behavior has been well documented in the temperature range of RT-200°C for epoxy resin and carbon/epoxy composites by Yeow et al. [1], Dillard et al. [2], Brinson et al. [3] and Raghavan and Meshii [4]. In the linear creep region, it has been observed that compliance remains same at different stress levels for a given temperature. Since it is not possible to conduct creep experiments for the entire service life, much effort has been extended in the pursuit of accelerated procedures for creep characterization of composite systems and using models to extrapolate these results to obtain the creep compliance at service conditions beyond the experimental time window. One such extrapolation technique, which has gained wide spread acceptance for a material that exhibited linear creep and that has been used in this thesis, is the Time Temperature Superposition Principle (TTSP). A brief review of TTSP is given below.

Time Temperature Superposition Principle (TTSP):

TTSP states that time and temperature are equivalent to the extent that the data at one temperature can be superimposed on to the data at the other temperature by shifting the creep curve along time axis [2]. In other words, creep compliance curves at different temperatures are of same shape but only shifted in time. TTSP implies that creep compliance at time 't' at a temperature 'T' is equivalent to creep compliance at temperature 'T_o' at a reduced time 'ξ'. This can be mathematically expressed as,

$$E(T,t)=E(T_o,\xi) \qquad \text{---------- (2.1)}$$

where $\xi = \frac{t}{a_T(T)}$ ---------- (2.2)

T_o - reference temperature , t -real time, T - Temperature, ξ - reduced time,

a_T - Temperature shift factor

The creep compliance curves at 5 MPa for resin in the temperature range of 60-230°C is shown in Figure 2.1. The compliance curves at temperature greater than 60°C are then shifted horizontally (in log time) to longer times (i.e. to the right) such that they superimpose on to the curve at reference temperature of 60°C. The resulting master curve at a reference temperature of 60°C is shown in Figure 2.2. Using short-term compliance data at several temperatures and then shifting the curves horizontally, one can obtain a smooth master curve (shown in Figure 2.2) valid over many decades of time at an arbitrary reference temperature using TTSP. The amount of shift required is known as temperature shift factor (a_T). A linear plot of shift factor versus inverse temperature shown in Figure 2.3 can be modeled by Arrhenius theory to yield activation energy for creep process. This can be used to predict shift factor at any temperature. TTSP has been successfully used by several researchers [1, 3, and 6] in linear creep region to predict creep compliance of epoxy resin and carbon/epoxy composites with different fiber orientations (10°, 90°). The shift factors obtained using TTSP were found to be independent of fiber orientation with respect to load direction.

At a given temperature and time it can be observed that the compliance values at two stresses is not the same shown in Figure 2.4, i.e. the material is non-linear in behavior (i.e. an increase in stress is accompanied by a disproportionate increase in the

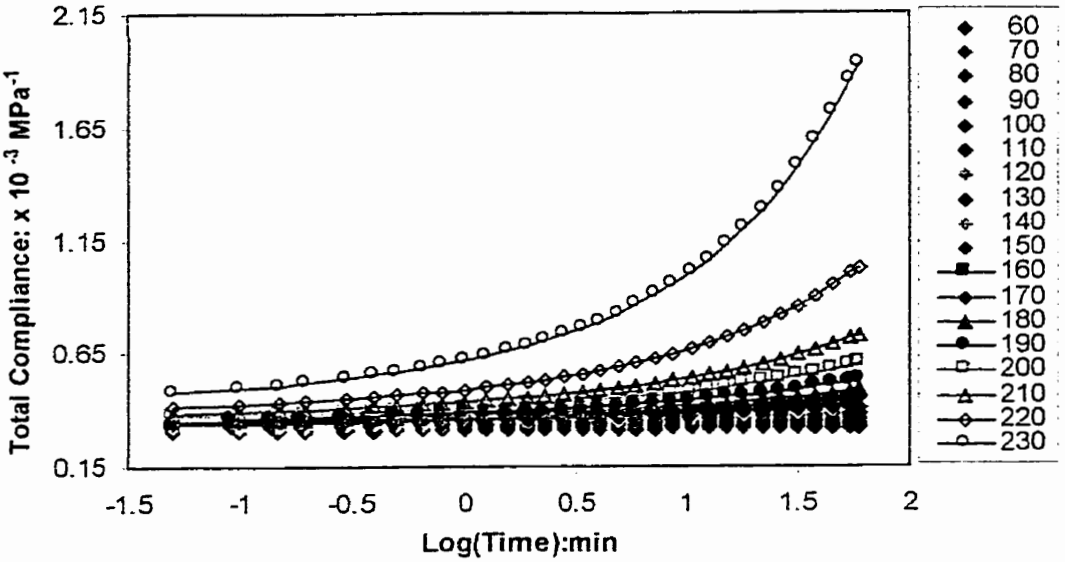

Figure 2.1: Compliance curves at 5 MPa for resin at various temperatures

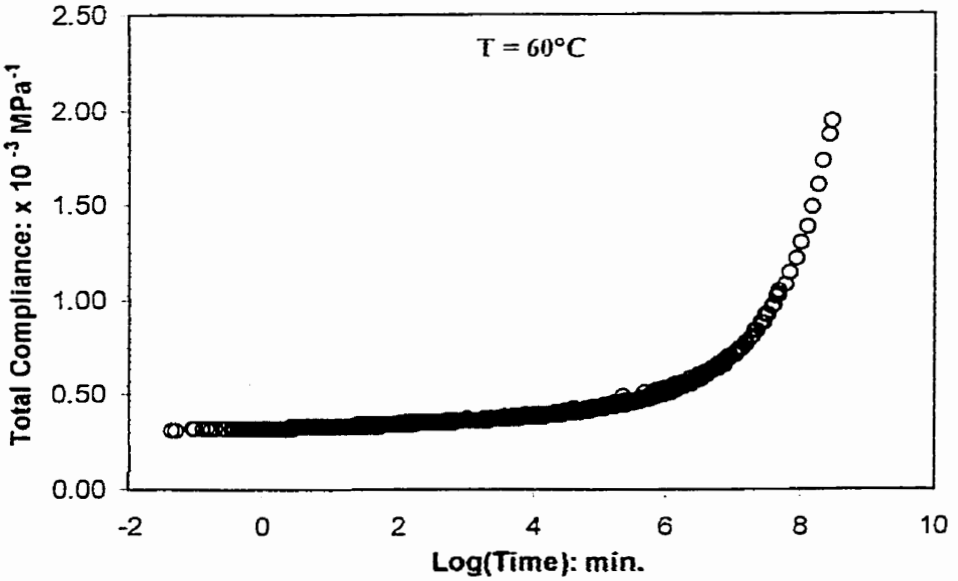

Figure 2.2: Master creep at 5 MPa curve for resin

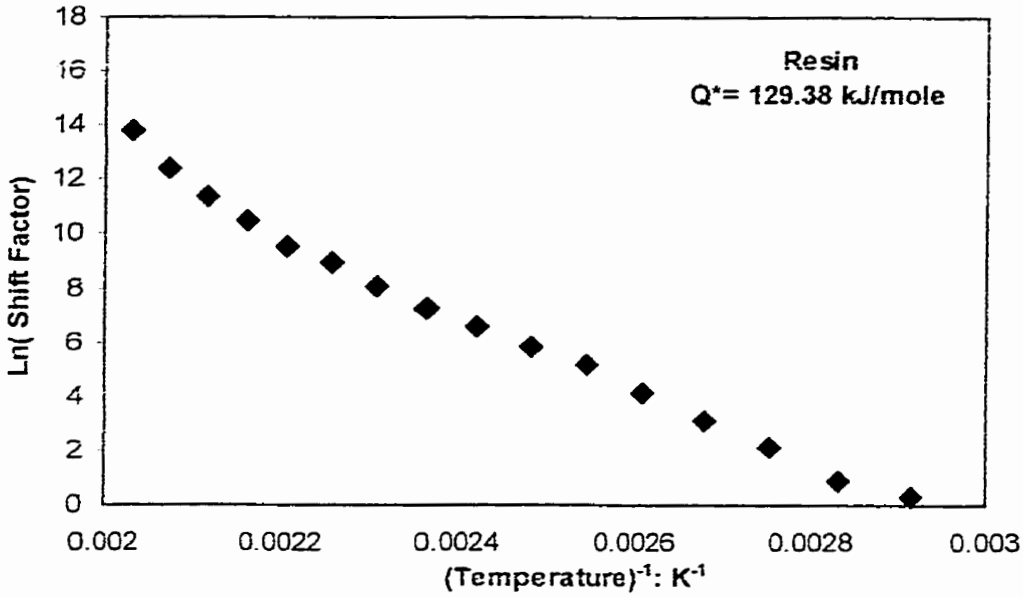

Figure 2.3: Plot of shift factor versus inverse temperature

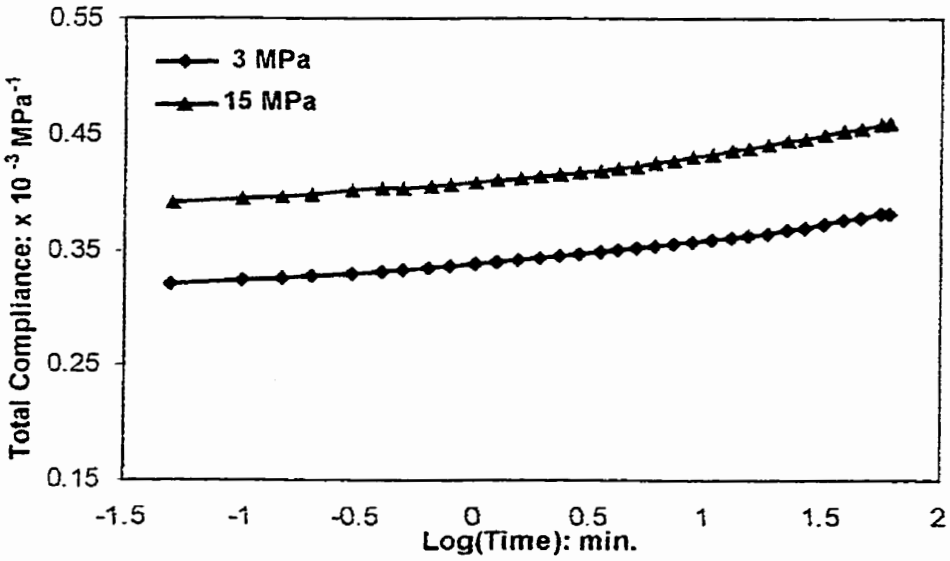

Figure 2.4: Compliance curves at two different stress levels

time dependent strain). TTSP is no longer valid for non-linear creep region. To determine the creep compliance beyond the experimental time window, another extrapolation technique namely, Time Temperature Stress Superposition principle (TTSSP) was used in non-linear creep region.

2.2.2 ON CREEP RUPTURE

In addition to creep, creep rupture [2-5,10,11] of polymers and polymer composites have received considerable attention over the years. Experimental studies pursued to date have shown rupture time to decrease with increase in temperature at a given stress. Rupture time also decreases with increase in stress at a given temperature. Dillard et al. [2] have shown the rupture time of multidirectional graphite /epoxy to vary between 10 to 10^4 min. in the temperature range of 143-193°C and Raghavan and Meshii [10-11] have shown the rupture time of 90° carbon/epoxy to vary between 10^1 to 10^5 min. at stress levels 30-45 MPa in the temperature range of 23-160°C.

2.2.3 ON FRACTURE

The influence of temperature on fracture behavior of polymer composites has been well documented [8-12]. The fracture strength and fracture energy of epoxy resin [9, 10] and 90° carbon epoxy composites [9, 11] has been shown to decrease with increase in temperature. Decrease in fracture energy with temperature has been correlated with fracture surface by few researchers [9, 13]. Cantell and Moloney [13] correlated the

decrease in fracture energy with fracture surface of unfilled and filled particulate epoxy resin in the temperature range of RT to 105°C. They observed the fracture surface at room temperature to be dominated by coarse river like structure. With increase in the temperature the coarse structure gradually disappeared and fracture surface became smoother. Similar trend in fracture behavior of epoxy resin and correlation of this with fracture energy in the temperature range of RT- 279°C was reported by Raghavan and Meshii [9].

2.3 EFFECT OF PHYSICAL AGING

When an amorphous polymer is cooled rapidly to a temperature below its glass transition temperature (Tg), its specific volume is initially in a non-equilibrium state and slowly approaches equilibrium value with time as shown Figure 2.5. This process of slow evolution towards an equilibrium state is known as ***Physical Aging*** [14].

Physical aging affects the mechanical properties of the polymer, often resulting in a material that is stiffer in response and more brittle, so that the compliance is decreased (or modulus is increased).

2.3.1 ON CREEP

Physical aging has been found to decrease creep and stress relaxation rates [14]. Physical aging shifts the creep (compliance) curves to longer times due to reduction in creep rate shown in Figure 2.6. A well-documented technique [14] to quantify the effect of physical aging on creep is through a series of short-term creep tests. A short-term test, also known as momentary test is one in which the test duration is about ($1/10^{th}$) the aging time prior to testing. In these tests, the material is initially quenched from above glass

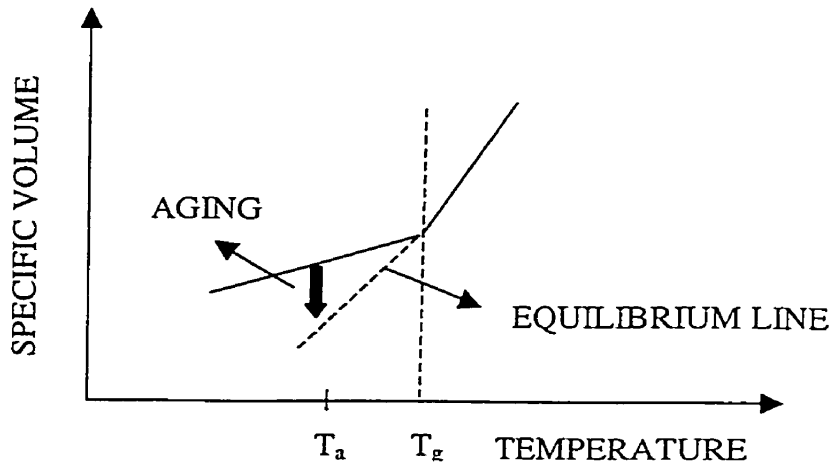

Figure 2.5: Origin of Physical Aging

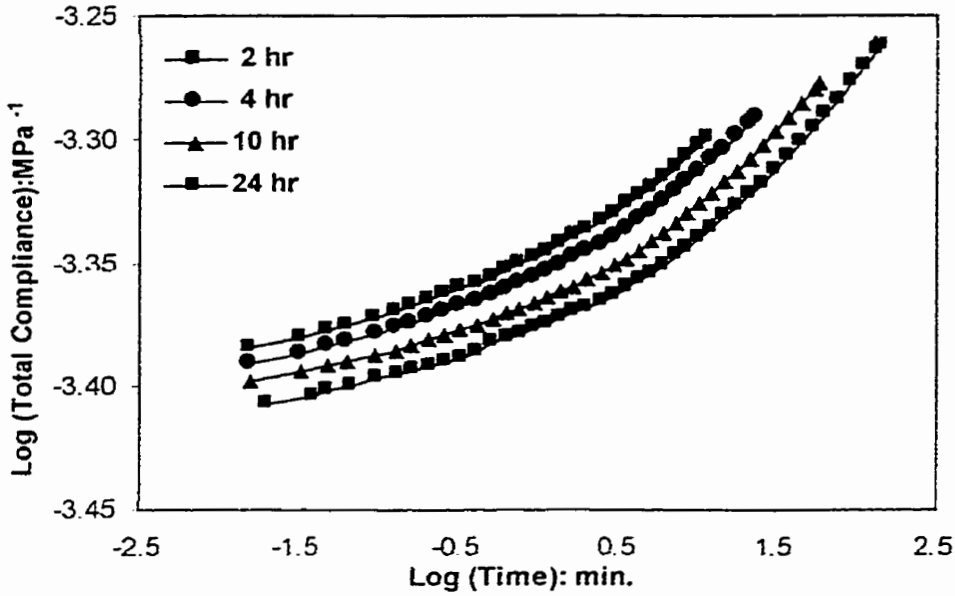

Figure 2.6: Compliance curves at different aging times

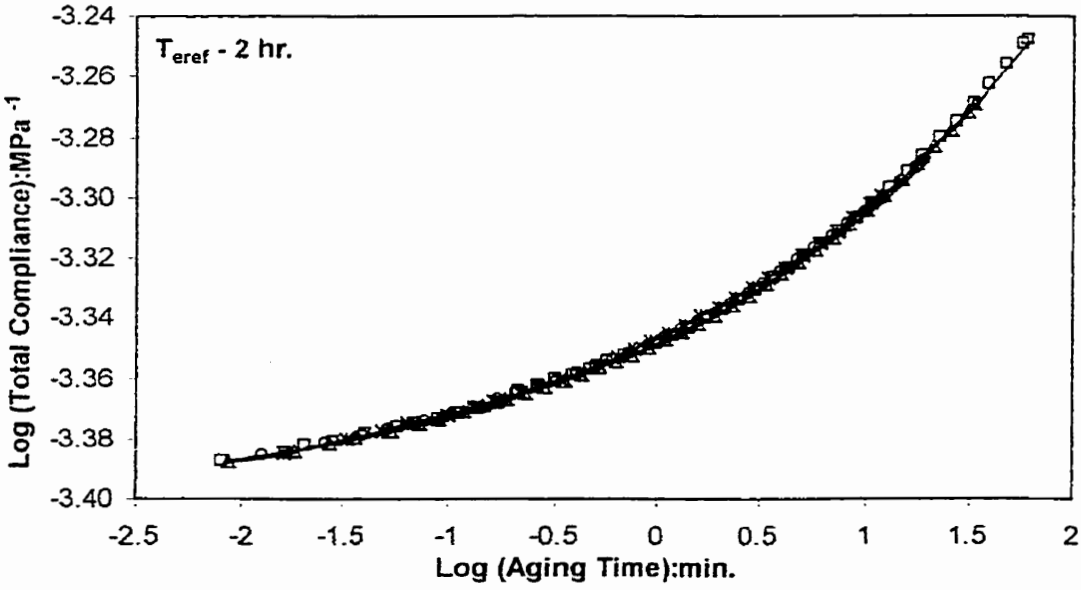

Figure 2.7: Momentary master curve

transition temperature (T_g) to the test temperature below glass transition temperature (T_g). The time that elapses at this temperature after quenching is referred to as aging time (t_e). The material is subjected to a constant stress after a certain aging time (t_e) and the resulting creep strain is determined as a function of time. Creep period is 1/10 of the aging time to avoid simultaneous aging of the material during creep testing. Physical aging reduces the creep rate and shifts the creep curve with aging time as shown in Figure 2.6. The individual compliance curves can be superimposed into a single momentary master curve (MMC) by shifting the curves horizontally (in log time) at any aging time. For e.g. individual compliance curves at different aging times 2, 4, 10 and 24 hours as shown in Figure 2.6 are shifted horizontally along time axis to obtain a master curve at a reference aging time of 2 hr. as shown in Figure 2.7.

The amounts of shift required are called shift factors or aging shift factors. The aging shift factor a_{t_e} changes with aging time as shown in Figure 2.8 and can be mathematically written as

$$a_{t_e} = \left(\frac{t_{eref}}{t_e} \right)^{\mu} \qquad \text{-------- (2.3)}$$

(where)
$$\mu = -\frac{\partial \log a_{t_e}}{\partial \log t_e} = \text{Shift rate} \qquad \text{-------- (2.4)}$$

t_e is the aging time and t_{eref} is the reference aging time

Shift rate (μ) is given by the slope of log shift factor (a_{t_e}) versus log aging time (t_e) as shown in Figure 2.8. Aging shift rate is the most critical parameter in determining

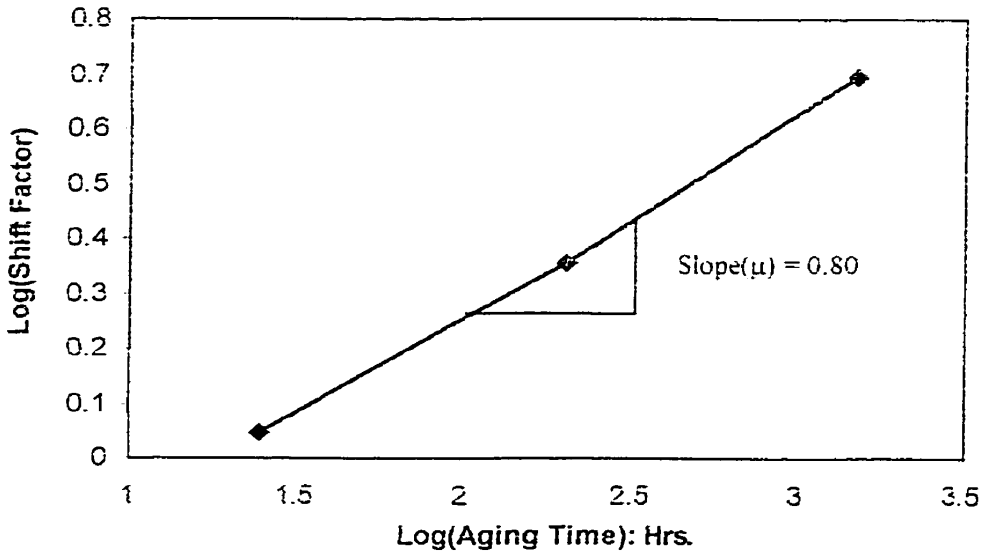

Figure 2.8 A plot of shift factor versus aging time

the effect of physical aging on creep. The shift rate together with the master compliance curve at a reference aging time allow prediction of creep compliance for any aging condition. If the creep time is not short in comparison to the previous aging time then aging occurs during testing which has to be accounted. This led to the development of effective time theory (ETT) proposed by Struik [14] to account for simultaneous aging during creep testing. Details about ETT can be found else where [14, 15-19].

Aging is a characteristic of glassy state and is found in all polymer glasses (i.e. amorphous polymer below T_g), as thoroughly documented by Struik [14]. He developed experimental techniques to isolate physical aging process in polymers from other behaviors by performing short-term creep test as described earlier. Several researchers such as Brinson and Gates [15], Bradshaw and Brinson [16-17], Sullivan [18], Gates[19], Gates and Feldman [20], Veazie and Gates [21], and Wang et al. [22] later adopted Struik's work to study the effect of physical aging on creep of resin and 90°composites. Several experimental studies [14-22] have illustrated that the matrix dominated composite properties of continuous fiber reinforced PMC's, namely transverse response, is affected by physical aging in a similar manner to the pure polymers. They have observed creep compliance to decrease with increase in aging time at a given temperature and stress. Thus, aging shift factor was found to increase with increase in aging time. It has been demonstrated that shift rates found from MMC's showed temperature dependency. In particular near the T_g of a material the shift rate decreased. At T_g, the polymer is in equilibrium and theoretically a shift rate of zero would indicate a

material exhibiting no aging behavior. However, significant scatter in shift rates of epoxy resin and 90° composites have been reported in literature. Struik [14] has also shown that aging decreases with stress, hence the shift rate decreases with increase in stress.

It has also been shown [14, 15, 18-20] that long-term creep curve deviates from momentary behavior after a short time and proceeds at a much slower rate. For materials undergoing physical aging during testing, long term creep prediction using TTSP gave over prediction, since it did not take into account the decrease in creep rate by simultaneous physical aging. Effective time theory (ETT) as proposed by Struik [14] was used by several researchers to predict long-term creep compliance in linear creep region with varying degree of success [14-18]. On the whole, researchers [15, 18-20] could predict with some accuracy creep compliance upto 3 years by using ETT.

2.3.2 ON CREEP RUPTURE

Similar to creep, aging also affects creep rupture. This behavior was observed by Crissman and Mckenna [23] for PMMA. They observed rupture time of PMMA to increase with aging time. Despite the abundance of published creep data, very little effort [23] has so far been made to study the effect of physical aging on creep rupture of polymer composites.

2.3.3 ON FRACTURE

Very limited work has been done to date to study the effect of aging on fracture behavior. One work found is that of Kong [24]. Kong [24] investigated the aging phenomenon on fracture properties of epoxy resin and epoxy resin reinforced with carbon

fibers. He reported that for an aging time of 10^5 min, fracture stress, strain and toughness reduced to about 38.5%, 73.6% and 87.7% from the original stress, strain and toughness of the as received material.

2.4 EFFECT OF MOISTURE

Water accelerates the time dependent response of polymers and polymeric composites in a manner that is analogous to the influence of temperature [25].

2.4.1 MOISTURE ABSORPTION KINETICS

The purpose of this section is to provide information on moisture absorption kinetics, since it is related to conditioning the sample to required moisture content at any temperature.

The simplest model for diffusion of solvent into a solid is given by the linear Fick's law (1855). The rate at which water diffuses into polymer matrix is modeled according to Fick's second law,

$$\frac{\partial c}{\partial t} = D\frac{\partial^2 c}{\partial z^2} \qquad \text{--------- (2.5)}$$

c - moisture concentration within sample

t -time

z - the coordinate coinciding with the thickness direction

D – Diffusion coefficient (temperature dependent)

According to this, the rate of liquid diffusion into the polymer is proportional to the concentration gradient parallel to the diffusion direction. For one dimensional steady state diffusion in the thickness direction, Boundary Conditions:

$$c(z,0) = 0, \quad 0<z<h \qquad h - \text{thickness of laminate}$$

$$c(0,t) = c(h,t) = c_o$$

c_o = maximum moisture concentration and is related to the humidity of the laminate's environment

Equation 2.5 can be solved to yield,

$$\frac{M_t}{M_o} = \frac{4}{h}\left(\frac{Dt}{\pi}\right)^{\frac{1}{2}} \qquad \text{-------- (2.6)}$$

M_t – Moisture content in the laminate at a time t

M_o – Initial moisture content in the laminate

Equation 2.6 can be conveniently rearranged to compute the composite diffusion coefficient as

$$D = \pi\left(\frac{h}{4M_o}\right)^2\left(\frac{M_2 - M_1}{\sqrt{t_2} - \sqrt{t_1}}\right)^2 \qquad \text{--------- (2.7)}$$

M_2 and M_1 are the moisture contents at times t_1 and t_2.

$\frac{M_2 - M_1}{\sqrt{t_2} - \sqrt{t_1}}$ is the linear slope of the plot of weight change versus square root of time.

The above equation was used in calculating diffuison coefficients in this study. The dependence of diffusion coefficient on temperature was modeled using Arrhenius relations,

$$D = D_o \, exp\left(-\frac{E}{RT}\right) \qquad \text{--------- (2.8)}$$

D – Diffusion coefficient at temperature T , E – Activation energy, R - Gas constant.

A linear plot of logarithm of diffusion coefficient versus inverse temperature will yield the activation energy for diffusion, which will be useful in determining D at any temperature which in turn can be used to calculate conditioning time.

The kinetics of water absorption in polymers has been studied for about one and a half centuries beginning with Fick (1855). Increase in moisture content and diffusion coefficient with temperature were observed by several researchers for epoxy resin [26-33] and carbon/epoxy [34-40] composites. Much work has been done in prediction of moisture content in a composite [25-40]. Theoretical models based on one dimensional fickian diffusion were developed by many investigators [25-26, 30-31, 28-29, 40]. Deviations from linear fickian diffusion have been found to occur at elevated temperatures due to a number of causes such as hydrolysis of polymer, moisture diffusing along the fiber matrix interface, voids [27, 41-42]. The effect of fiber type on the diffusion characteristics of a composite was studied by Rao et al. [28, 29, 43], and Rao and Shylaja [39]. Moisture kinetics depends on the material system and within the same material system it varies with exposure conditions. Moisture absorption by composite materials has been found to be function of applied stress. Fahmy and Hurt [44], Neuman and Gad marom [45-46], Janas et al. [47], and Lagrange et al. [48] have shown that applying external tensile stresses increased the diffusion rate and the moisture content at saturation.

However, very limited work has been done to study the effect of physical aging on moisture. Kong [24] investigated the effect of aging on moisture kinetics of epoxy

resin and found that aging reduced the moisture kinetics and moisture content at saturation due to lower free volume. No other work is available on the effect of physical aging on moisture absorption kinetics of resin and composite.

2.4.2 EFFECT OF MOISTURE ON GLASS TRANSITION TEMPERATURE (T_g)

The presence of water within a polymer tends to plasticize the material thereby lowering the glass transition temperature (T_g) of the polymer, reducing the modulus, and accelerating creep process. This phenomenon of plasticization is related to increased molecular mobility of the polymer in the presence of water molecules. It was hypothesized [32] that the moisture increased the free volume, leading to increased molecular mobility. It has been shown by many investigators [32, 33, 35] that T_g lowered by an average of 20°C for each 1 % increase (by volume) of moisture absorption. This lowering of Tg has been used in explaining the effect of moisture on creep in this study.

2.4.3 ON CREEP

Presence of moisture in polymer accelerates the creep process through plasticization. Many researchers have intensively studied the effects of moisture on creep response of epoxy resin [25, 32, 49-50] and carbon/epoxy composites. The effect of moisture was modeled by moisture superposition method [25, 51-55], similar to well known TTSP used to model effect of temperature. Accordingly, the effect of moisture was quantified by means of a moisture dependent shift factor $a_H(m)$, which was coupled with the temperature dependent shift factor $a_T(T)$. Though, in principle, the combined effects of moisture and temperature requires a shift factor function of the form a_{TH} (T, m),

in many circumstances it was possible to coalesce creep data [25] into a master curve by a more convenient product form a_{TH} (T, m) = a_T(T).a_H(m). However, the viscoelastic models developed so far have found to be restricted to linear viscoelastic response and to a limited range of stresses, temperature and moisture content.

2.4.4 ON FRACTURE

The effect of moisture on fracture properties of polymer composites has been investigated by many researchers [25, 32, 34-35, 55-64] on wide range of fiber and matrix material, orientation and moisture levels. Experimental studies have shown that moisture absorption decreases the fracture strength, stiffness and fracture energy of composites in tension, compression, bending or shear to a considerable degree due to plasticization, matrix cracking, fiber-matrix debonding and matrix swelling. Typically, one observes a reduction of 25-80% in the strength of epoxies and 50-80% in the transverse strength of unidirectional reinforced fibrous composites attributable to the effects of water.

2.4.5 ON CREEP RUPTURE

Though a lot of work has been done to date on creep and fracture, limited work has been done to study the effect of moisture on creep rupture. Experimental studies [32, 65-67] completed to date have shown that the moisture-conditioned specimen ruptures faster than unconditioned specimens. However, the combined effect of aging and moisture on creep, creep rupture and fracture data of polymer composites is lacking in literature.

2.5 EFFECT OF FIBER VOLUME FRACTION

2.5.1 ON MOISTURE ABSORPTION KINETICS

Increase in fiber volume has been shown to decrease the moisture content, diffusion coefficient and rate of moisture absorption. This behavior has been observed by Rao et al. [29], Woo and Piggot [31] and Browning [32] for epoxy resin and carbon/epoxy composites. Reduction in moisture content and diffusion coefficient was attributed to decrease in resin in composite.

2.5.2 ON CREEP

Fiber volume fraction also affects the creep response of polymer composites. It has reported that creep of resin is retarded by fiber reinforcement i.e. creep compliance decreases with inclusion of fibers. Such a behavior has been observed on epoxy resin and carbon/epoxy composites by few researchers [4].

2.6 COMBINED EFFECT OF ONE OR MORE PARAMETERS

2.6.1 ON CREEP

The combined effect of two or more of the above variables, such as Stress-Temperature, Stress-Temperature-Fiber volume fraction, Stress-Temperature-Physical Aging-Fiber volume fraction, Stress-Temperature-Moisture has been investigated on creep of resin and composites.

2.6.1.1 STRESS-TEMPERATURE-FIBER VOLUME FRACTION

Though the effect of stress and temperature on creep of epoxy resin and 90° carbon/epoxy composites is well documented [1-7], one researcher [4] has talked about the effect of fiber volume fraction on creep. While creep compliance increases with stress and temperature, it has been found to decrease with fiber volume fraction.

2.6.1.2 STRESS-TEMPERATURE-PHYISCAL AGING-FIBER VOLUME FRACTION

Physical aging retards creep. The effect of stress-temperature-physical aging on polymers and polymer composites has been well documented in the literature [14-22]. However, the effect of stress-temperature-physical aging-fiber volume fraction on creep of polymers and polymer composites is limited [14, 18]. The shift rates for resin and composites varied from one researcher to another. Since stress decreases aging, shift rates also decreased with increase in stress. Shift rates were found to be independent of fiber volume fraction.

2.6.1.2 STRESS-TEMPERATURE-MOISTURE

In contrast to physical aging, moisture accelerates creep through plasticization. The effect of stress-temperature-moisture on epoxy and carbon/epoxy composites in linear and non -linear creep region is limited [25, 49-53].

2.6.1.3 COMBINED EFFECT OF TEMPERATURE, STRESS, PHYSICAL AGING, MOISTURE AND FIBER VOLUME FRACTION

No effort has so far been made to study the combined effect of temperature, stress, physical aging, moisture and fiber volume fracture on creep of polymer composites.

2.6.2 ON CREEP RUPTURE

Although a lot of work has been done to date to study the effect of stress and temperature [8-12] on creep rupture, limited work has been done to date to study the individual effect of physical aging [23] and moisture [32, 65-67] on creep rupture of polymer composites. Creep rupture data on the combined effect of these parameters is lacking in literature.

2.6.3 ON FRACTURE

Considerable work has been done to date to study the individual effect of temperature and moisture on fracture strength, strain and energy of epoxy and carbon/epoxy composites. However, limited work [24] has been done to date to study the effect of physical aging on fracture strength, strain and energy of polymer composites. Fracture data on the interactive effect of temperature, physical aging, moisture and fiber volume fraction on epoxy and its composites is lacking in literature.

2.7 SCOPE OF THE PRESENT INVESTIGATION:

The following can be inferred from the literature review presented in the previous section:

- Influence of stress and temperature on creep (in linear and non-linear viscoelastic region), creep rupture and fracture data is well documented.
- Despite the abundance published creep data in linear creep region, limited work has been done to study the effect of physical aging on non-linear creep region. While published data on the effect of aging on fracture is limited, information regarding the effect of aging on creep rupture data is lacking in literature.
- The influence of moisture on creep (in non-linear creep region) and creep rupture is limited.
- While effect of fiber volume fraction on moisture absorption kinetics is well documented in literature, effect of fiber volume fraction on creep is limited and effect of fiber volume fraction on fracture and creep rupture is lacking in literature.
- No effort has so far been made to study the combined effect of temperature, stress, physical aging and moisture on creep (in linear and non linear viscoelastic region), creep rupture and fracture data

Keeping this background in view, the present investigation was under taken to experimentally study the individual and interactive influence of stress, temperature, physical aging, and moisture on creep (in linear and non-linear creep region), creep rupture and fracture behavior of F263 epoxy resin reinforced with T300 carbon fibers. The pure resin and composite are studied to delineate the effect of fibers on creep and creep rupture.

CHAPTER 3

EXPERIMENTAL PROCEDURE

To obtain the objectives discussed in the chapter 2, four major tests were performed on epoxy resin and its composite,

1. Moisture Absorption Test
2. Tensile test
3. Creep test
4. Creep rupture test

The material studied in this work and the curing procedure used for the material of current study is discussed in sections 3.1 and 3.2. Determination of fiber volume fraction is discussed in section 3.3. Section 3.4 describes the techniques used for sample preparation. The four tests mentioned above are discussed in detail in sections 3.5 to 3.9.

3.1 MATERIAL

The material used in the current study was Hexcel Corporation's F263 epoxy resin and F263 epoxy resin reinforced with T-300 unidirectional carbon fiber. The uncured resin and the composite prepreg were purchased and processed at University of Manitoba to make test specimens.

3.2 CURING PROCESS

Dog-bone shaped specimens of epoxy resin were prepared by casting them using an aluminum mold. Aluminum mold shown in Figure 3.1 was designed as per ASTM D647-88a and specimen dimensions were chosen as per ASTM D638-91. The cure cycle

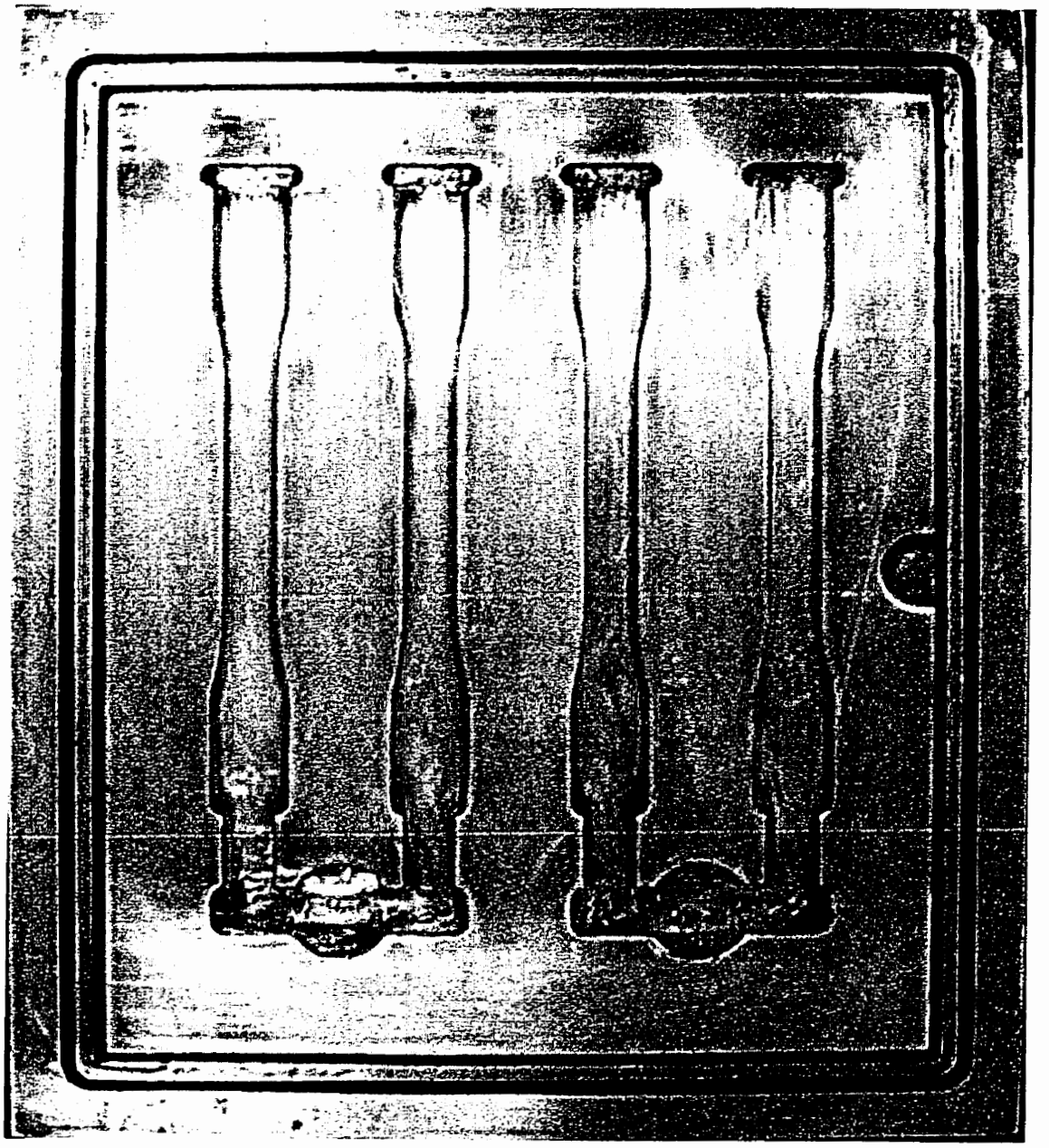

Figure 3.1: Aluminum Mold

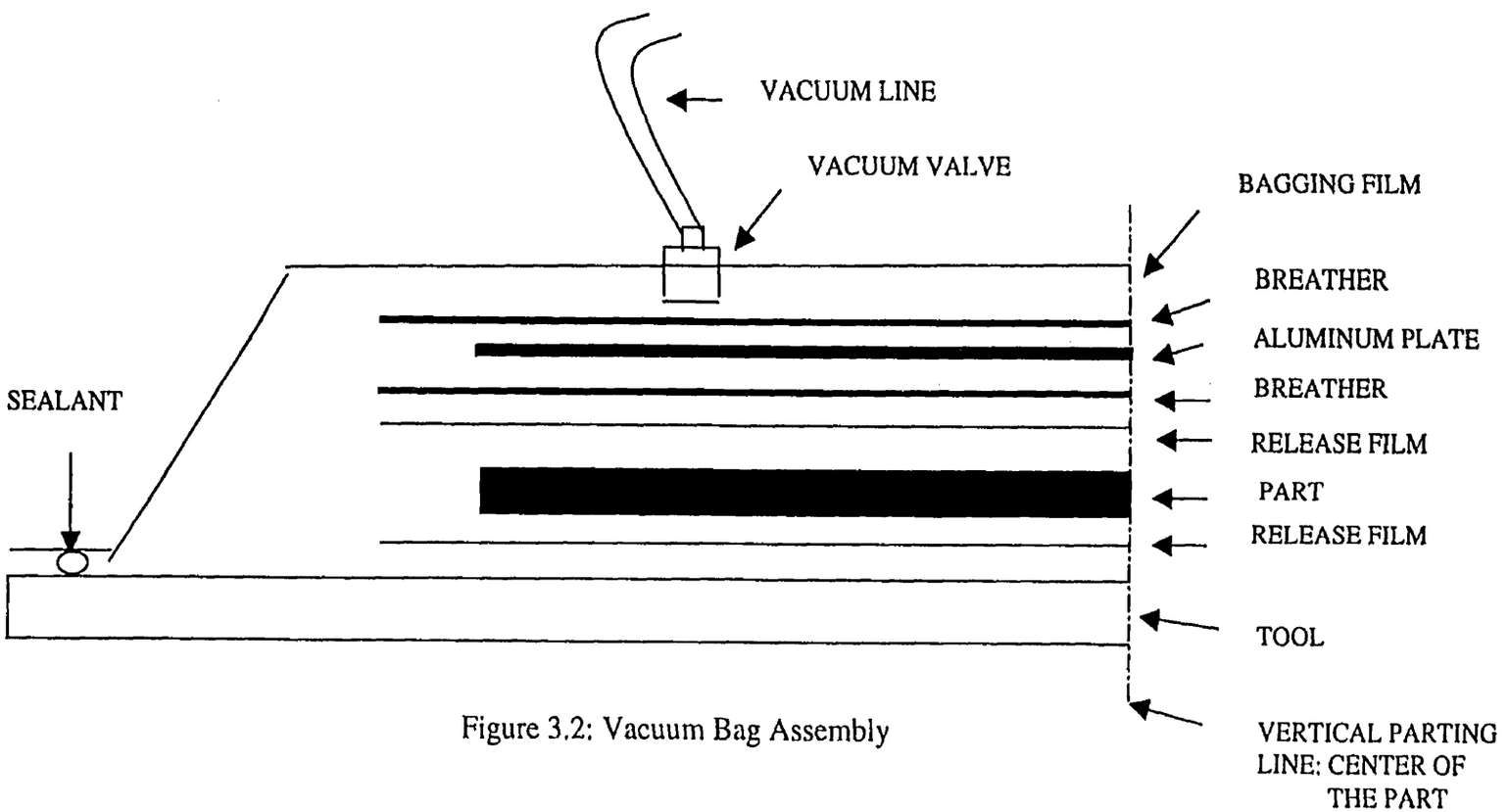

Figure 3.2: Vacuum Bag Assembly

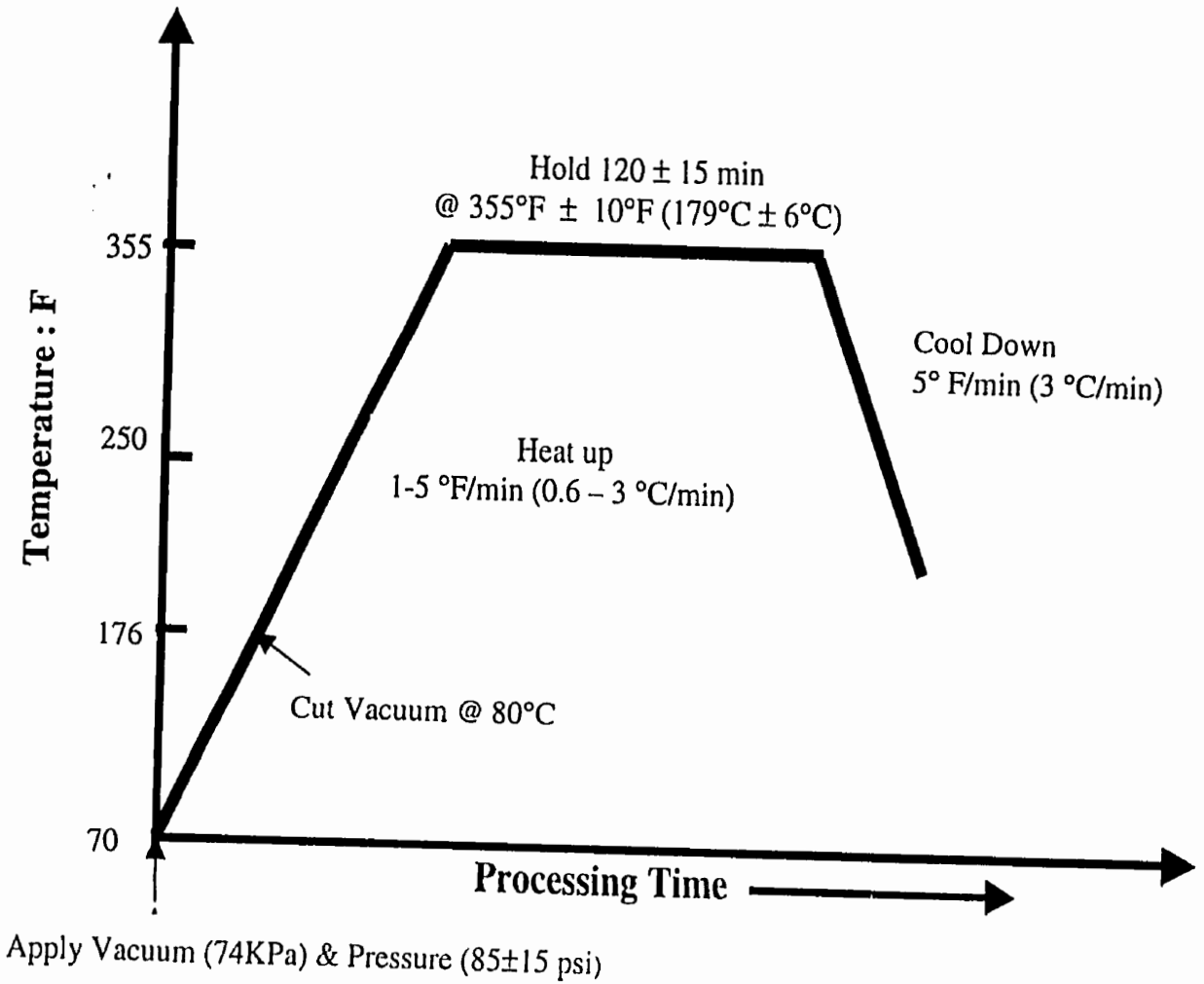

Figure 3.3: Schematic diagram of cure cycle of composite

for the resin involved degassing at 45°C for 10 minutes followed by holding at 90°C for 1 hour and then finally curing at 177°C for 2 hours in nitrogen atmosphere at a pressure of 100 psi. The F263/T300 prepreg supplied by Hexcel Corporation was cut to 12" x 12" sheet, stacked one above the other such that fibers in all layers were parallel to each other and then cured in an autoclave at *Boeing Canada Technology Inc.* Vacuum-bagged lay-up as shown in Figure 3.2 was placed in the autoclave and a vacuum of 22inHg(74 kPa) was applied. The schematic diagram of cure cycle of composite is shown in Figure 3.3. The temperature was raised at the rate of 3°C/min (5°F/min) up to 179°C (355°F) under a autoclave pressure of 85±15 psi and was held for 120 minutes. The vacuum bag was released to atmospheric pressure at 80°C. The entire assembly was cooled at the rate of 3°C/min and then debagged. As received prepreg when cured, resulted in a volume fraction of 54%. In order to study the effect of fiber volume fraction on resin, composite with 71 % fiber volume fraction was manufactured by bleeding the resin using a bleeder. $[0]_8$ and $[0]_{12}$ composite panels were made and the subscripts in $[0]_8$ and $[0]_{12}$, refer to the number of plies.

Thermal analysis by differential scanning calorimetry on epoxy resin indicated that the resin was not fully cured (shown in Figure 3.4). Hence, a postcuring of resin and composite at 230°C for 4 hours was necessary to complete the cross linking reaction.

3.3 DETERMINATION OF VOLUME FRACTION

The volume fraction of the cured composite panels was measured by acid-digestion method, as per ASTM D3171-76 (Re-approved 1990).

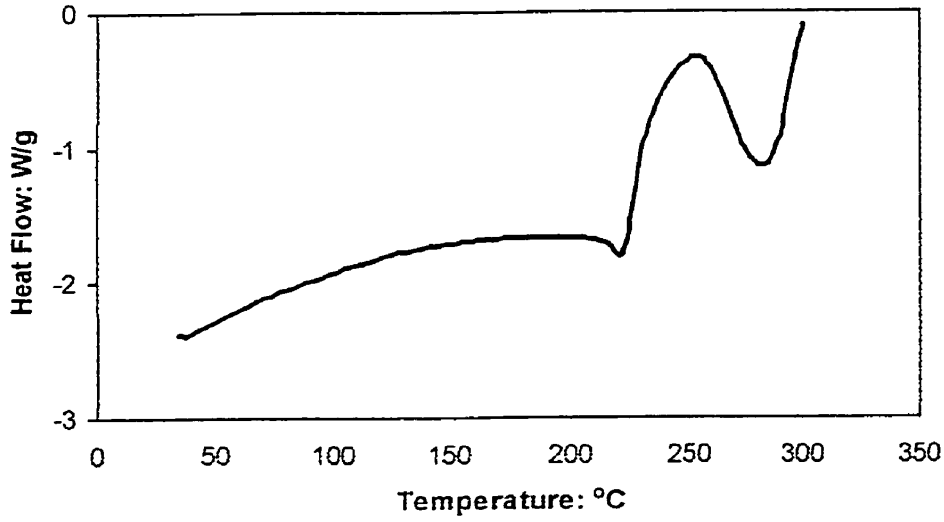

Figure 3.4: Heat Flow versus temperature plot (DSC)

3.3.1 TEST PROCEDURE

To start with, the density of each composite specimen was determined by liquid displacement technique as per ASTM D792. Then, composite specimen of known weight was placed in a flask containing 70% nitric acid (HNO_3). The flask was connected to reflux condensers and heated to 75±1°C to digest the resin matrix. The digestion was carried out for 5 hours until the resin dissolved completely in nitric acid. Undissolved fibers were filtered onto a tarred sintered glass filter crucible under a vacuum of 16.9 Pa(127 torr). The fiber was washed with water and acetone. The crucible with the washed fiber was dried in oven at 100°C for 1 hour. The crucible was then removed from the oven and cooled to room temperature in a desiccator and weighed using an analytical balance to the nearest of 0.0001 g. Fiber volume % was calculated according to following equation:

Fiber, volume % = $[(W/\rho_f) / (w/\rho_c)] \times 100$

where W = weight of fiber in composite [measured after digestion]

w = weight of composite specimen [measured before digestion]

ρ_f = fiber density = 1.76 g/cm^3

ρ_c = composite density

3.4 SPECIMEN PREPARATION

3.4.1 MOISTURE ABSORPTION TEST

Specimens were cut from resin coupons and $[0]_8$ composite panels with 54% and 71% fiber volume fraction with the help of diamond saw at a low speed to avoid heating of specimens. No coolant was used during cutting. The cut edges were made

smooth by polishing with 240 SiC grit paper. Specimen dimensions are given in Table 3.1.

3.4.2 TENSILE TEST

As mentioned earlier (section 3.2), dog bone shaped resin specimens were prepared in an aluminum mold. $[90]_{12}$ composite specimens (54% and 71%) were obtained, by cutting the specimens with their length perpendicular to the fiber direction in the cured composite panels. Resin and Composite specimens were prepared as per ASTM D647-88a and ASTM D3039/D3039M-93. Woven carbon fiber /epoxy composite tabs with 7° bevel angle at the end were bonded to $[90]_{12}$ composite panel with 54% and 71% volume fraction using AF- 191 epoxy adhesive supplied by 3 M company. The adhesive was cured at 177°C for 2 hours in a hot press under a pressure of 45 psi. Strain gages of type WK *(WK-15-125BT-350)* were bonded in the gage area of resin and composite specimens using M bond 610 adhesive which was cured at 177°C for 1.5 hours under a pressure of spring clamp as per recommendations of strain gage manufacturer. A typical tensile test specimen of composite is shown in Figure 3.5. All the specimens were stored in a desiccator prior to testing. The reader is referred to Table 3.1 for specimen dimensions.

3.4.3 CREEP TEST

Creep tests were done on resin and $[90]_8$ composite specimens using two instruments:

(1) Dynamic Mechanical Analyzer (DMA)

Test		Length (mm)	Width (mm)	Thickness (mm)
Moisture Absorption Kinetics & DMA [Effect of moisture on Glass transition temperature (T_g)]	Resin	50.00 ±5.00	5.00±1.00	2.50±0.20
	54 %	50.00 ±5.00	5.00±1.00	1.60±0.20
	71%	50.00 ±5.00	5.00±1.00	1.50±0.20
Tensile	Resin	150.40 ±1.00	12.62±0.20	2.50±0.20
	54 %	127.00 ±1.00	20.32±1.00	2.30±0.20
	71 %	127.00 ±1.00	20.32±1.00	2.20±0.20
	Tab	37.00 ±1.00	20.32±1.00	1.90±0.20
Creep - DMA	Resin	50.00 ±1.00	1.60±0.20	0.42±0.02
	54%	50.00 ±1.00	1.60±0.20	0.42±0.02
	71%	50.00 ±1.00	1.50±0.20	0.42±0.02
Creep - Instron	Resin	150.40 ±1.00	12.62±0.20	2.50±0.20
	54 %	127.00 ±1.00	20.32±1.00	2.50±0.20
	Tab	37.00 ±1.00	20.32±1.00	1.90±0.20
Creep Rupture	Resin	150.40 ±1.00	12.62±0.20	2.50±0.20
	54 %	127.00 ±1.00	19.02±1.00	2.30±0.20
	Tab	37.00 ±1.00	19.32±1.00	1.90±0.20

Table 3.1: Specimen Dimension

Figure 3.5: Tensile test specimen of composite

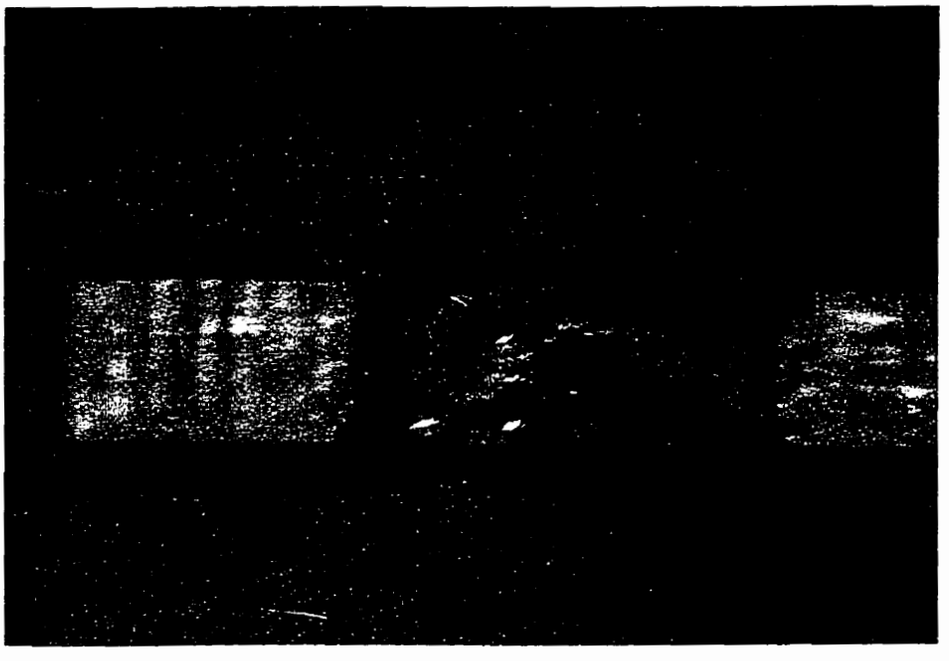

Figure 3.6: Test specimen of composite for creep test (moisture)

(2) Servo-Electric *Instron Model 8562* with a load capacity of ±100kN and equipped with an environmental chamber supplied by *Associated Environmental Systems.*

Dynamic Mechanical Analyzer (DMA): Resin and $[90]_8$ composite specimens with 54% and 71% fiber volume fraction were prepared as discussed in section 3.4.1 and 3.4.2.

Instron: Preparation of resin and $[90]_{12}$ composite specimens with 54% fiber volume fraction were as described in section 3.4.2. In order to prevent the moisture attack, strain gaged (WK-125BT-350) sections of specimens were coated with AE 15 adhesive and RTV silicone rubber supplied by Micromeasurements Group (Figure 3.6). The AE 15 adhesive and silicone rubber were cured at 100°C for 1.5 hours as per manufacturer's recommendation.

3.4.4 CREEP RUPTURE TEST

Resin and $[90]_{12}$ composite with 54 % fiber volume fraction specimens were prepared as discussed in section 3.4.2. Strain gages were not bonded to the specimens.

3.5 MOISTURE ABSORPTION TEST

Moisture absorption tests were carried out to determine moisture absorption kinetics that could be used to determine the conditioning time required to obtain a certain amount of moisture content. Two types of moisture absorption tests, (1) Water Immersion test and (2) Relative Humidity test, were performed on resin, and $[0]_8$ composite with 54% and 71% volume fractions. For water immersion test, the specimens were tested as

per ASTM D5229/D5229M-92 and for relative humidity test, the specimens were tested as per ASTM E104 and DIN 50 008.

For both water immersion and humidity tests, the specimens were first dried in oven at 80°C for 48 hours, cooled in a desiccator and immediately weighed.

3.5.1 WATER IMMERSION TEST

Weighed specimens were then immersed in distilled water bath maintained at 23°, 50°, 60°, 80°C. Five specimens were immersed at each temperature. Specimens were removed from water bath at 24 hours interval, dried clean of water, visually inspected for any discoloration, cracking, and weighed. After weighing the test specimens were returned to the water bath. The test continued until the specimens reached a constant weight.

3.5.2 RELATIVE HUMIDITY TEST

Relative humidity tests were performed at room temperature, 60°C and 80°C at three different humidity levels viz.35%, 50% and 75%. Five specimens were used at each humidity level. Tests at 60°C and 80°C were performed using an environmental chamber manufactured by Associated Environmental Systems. For room temperature tests, the desired humidity was obtained in a glass jar using sulfuric acid solution as per ASTM E104 and DIN 50 008. Weighed specimens were kept in the environmental chamber and inside the glass jar to study the effect of relative humidity on moisture absorption kinetics at 80°C, 60°C and room temperature, respectively. Specimens were removed from humidity chamber and glass jar at 24 hours interval, weighed and visually inspected for any discoloration. After weighing the specimens were kept in the humidity chamber and

glass jar. The test continued until the specimens reached a constant weight. The data were modeled using Fick's law to obtain moisture kinetic parameters and saturation moisture content.

3.5.3 EFFECT OF PHYSICAL AGING ON MOISTURE

To determine the effect of physical aging on moisture, test specimens were soaked at 270°C (T_g) for 15 minutes to erase any previous aging, cooled to room temperature and aged at 80°C for 100 hours (4.16 days), 200 hours (8.33 days), 300 hours (12.5 days), and 400 hours (16.6 days) in an oven. The aged specimens were then immersed in distilled water at 80°C until saturation. The weight was periodically measured as per section 3.5.1and this data was modeled to obtain moisture kinetics and saturation moisture content data.

3.5.4 MEASUREMENT OF GLASS TRANSITION TEMPERATURE (T_g)

Glass transition temperature of resin and composite with 54 % and 71 % fiber volume fraction was measured using *TA Instruments 2980 Dynamic Mechanical Analyzer (DMA)*. DMA tests in dual cantilever mode were performed on test specimens conditioned to different degrees of moisture content to obtain glass transition temperature as a function of moisture content. The variation of T_g as a function of moisture content were used to understand the effect of moisture on creep process. Figure 3.7 shows a plot of Temperature versus Tan delta obtained from DMA. T_g was chosen to be the temperature corresponding to the peak value of tan delta.

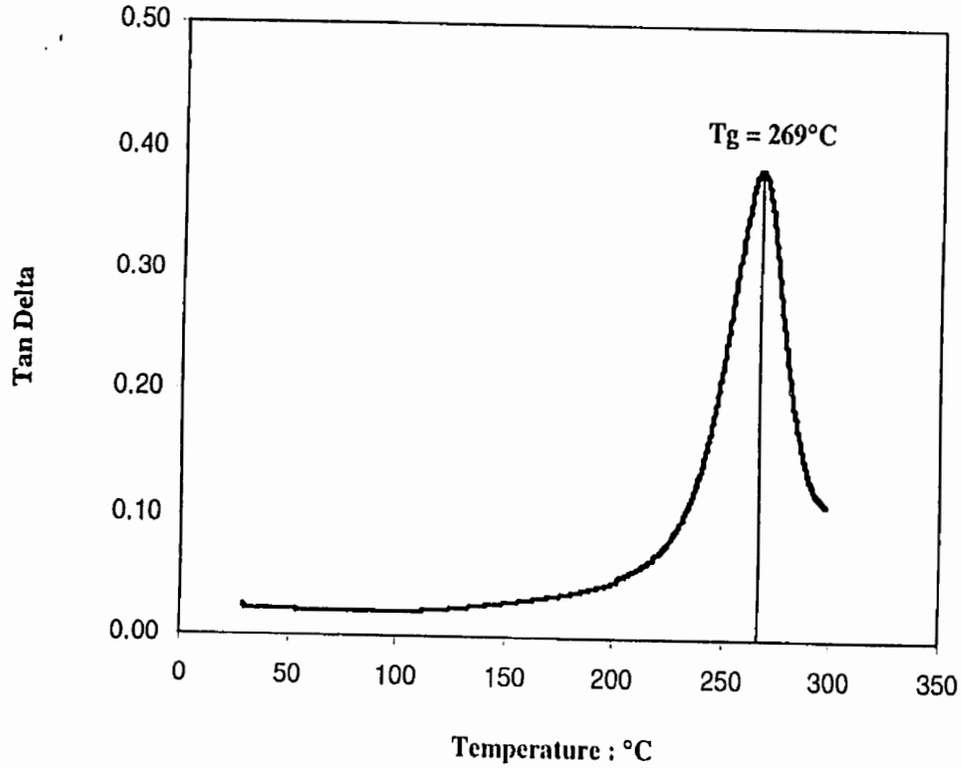

Figure 3.7: A plot of Temperature versus Tan delta (DMA plot)

3.6 TENSILE TEST

Tensile tests were performed to determine the effect of temperature, physical aging, moisture and combined effect of aging and moisture on total fracture energy. These data were required for future creep rupture modeling.

3.6.1 TEST PROCEDURE

The tensile tests were performed on a servo-electric *Instron Model 8562* with a load capacity of ±100kN and equipped with an environmental chamber supplied by *Associated Environmental Systems*. The strain rate used was 10^{-4} s^{-1}. Three specimens were tested at each temperature (shown in Table 3.2). Strain gages of type WK (*WK-15-125BT-350*) manufactured by *Micro Measurements Group* were used to measure strain at different temperatures. The load and strain data were acquired using data acquisition system (*PCI-6032E* data acquisition card and Strain gage conditioner *SCXI-1121*) from National Instruments. Tensile tests were performed on resin and $[90]_{12}$ composite specimens with 54 % volume fraction in the following conditions : Post-cured (PC), physically aged (PA), moisture conditioned (M), aged and moisture conditioned (PA+M) as shown in Table 3.2. For $[90]_{12}$ composite with 71% fiber volume fraction, tensile tests were performed only on postcured specimens.

3.7 CREEP TEST

Constant load creep tests were performed to determine the effect of temperature, stress, physical aging and moisture on creep of resin and $[90]_8$ or $[90]_{12}$ composite with 54% and 71% fiber volume fraction.

Test Condition	Aging Temp./ Immersion Temp.(°C)	Aging Time (Days)	Moisture Content (% Mm)		Test Temperature (°C)						
					RT	80	100	150	180	200	240
Post-cured	–	–	–		✓	✓	✓	✓	✓	✓	✓
Physical Aging	80	1	–		–	✓	–	–	–	–	–
		7									
		16.6									
	150	1	–		–	–	–	✓	–	–	–
		7									
		16.6									
	180	1	–		–	–	–	–	✓	–	–
		7									
		16.6									
	240	1	–		–	–	–	–	–	–	✓
		7									
		16.6									
Moisture	80	–	Resin	54%							
			2.00	2.00	✓	✓	–	✓	✓	–	–
			5.27	3.50	✓	✓	–	✓	✓	–	–
Physical Aging + Moisture	80/80	7	2.00	2.00	–	✓	–	–	–	–	–
		16.6	4.40	2.90		✓					
	150/80	7	2.00	2.00	–	–	–	✓	–	–	–
		16.6	4.40	2.90				✓			
	180/80	7	2.00	2.00	–	–	–	–	✓	–	–
		16.6	4.40	2.90					✓		

Table 3.2: Tensile Testing Scheme

Creep tests were performed on resin and $[90]_8$ or $[90]_{12}$ composite specimens with 54 % volume fraction in the following conditions: Post-cured, physically aged, moisture conditioned, aged and moisture conditioned as shown in Table 3.3.

3.7.1 ON POSTCURED

For post cured specimens, creep tests in the linear region (3,5,7 MPa) and non-linear region (15 MPa) were done using the *DMA*. The specimens were tested in tensile mode. Creep tests in the non-linear region, at stress level greater than 15 MPa were done using *Instron Model 8562* with a load capacity of ±100kN. Creep tests were also performed on $[90]_8$ composite specimens with 71% volume fraction in linear region (3, 5, 7, MPa) and in the non linear region (15 MPa) using *DMA*.

3.7.2 ON PHYSICALLY AGED

To determine the effect of physical aging, short-term creep tests in linear (5,7 MPa) and non-linear region (15 MPa) were done using the *DMA*. The specimens were tested in tensile mode. In non-linear region (for stress level greater than 15 MPa), creep tests were performed on *Instron Model 8562* with a load capacity of ±100kN. Prior to testing all specimens were heated to 270°C for 15 min. to erase any previous aging and cooled to room temperature. The duration of each creep test was $1/10^{th}$ the duration of aging time to prevent further aging of specimens during creep test. The aging times selected for creep segment was 2, 4, 10 and 24 hours and their creep time were 12 min., 24 min., 60 min., and 144 min. respectively.

Test Condition	Aging / Immersion Temp. (°C)	Aging Time (Days)	Moisture Content (% M_m)		Stress (MPa)		Test Temp. (°C)	Creep/Recovery Time (Hrs.)
					Linear	Non-Linear (MPa, % of UTS)		
Postcured (Temperature/ Stress)	-	-	-		3, 5, 7	15, 70%, 85%	60-240	1/0.50: Linear 8-24: Non Linear
Physical Aging	40-240	2,4,10,24	-		5, 7	15, 70%, 85%	40-240	C.T=1/10th A.T.
Moisture	80	-	Resin	54%	5,7	70%, 85%	40-80	1/1: Linear 24/48 : Non-Linear
			2.00	2.00				
			3.00	3.00				
			5.27	3.50				
Combined Effect of Aging and Moisture	80/80	16.6	4.40	2.90	5,7	70%, 85%	40-80	1/1 : Linear 24/48: Non-Linear

Table 3.3: Creep Test Scheme

3.7.3 ON MOISTURE CONDITIONED

Creep tests were performed on moisture conditioned specimens in the Linear and non-linear region using *Instron* equipped with an environmental chamber.

3.7.4 ON PHYSICALLY AGED AND MOISTURE CONDITIONED

To determine the combined effect of aging and moisture, creep tests were performed in linear and non-linear region using *Instron* equipped with an environmental chamber.

3.7.5 COMPARISON OF CREEP DATA

The creep data obtained from DMA and Instron were compared due to following reasons: (a) The strain in DMA samples is obtained using the displacement whereas strain is obtained from strain gage in Instron, (b) DMA samples were very small when compared to Instron samples and there was a possibility that volume fraction in the samples might be different from Instron samples due to specimen preparation, and (c) DMA tests were carried out on dry specimens and moisture conditioned specimens were tested using Instron. Creep tests on dry resin and $[90]_{12}$ composite specimen with 54 % volume fraction using Instron were done at 5 MPa in the temperature range of 60°C – 120°C to ensure that the creep data obtained using DMA is comparable to that obtained using Instron shown in Figures 3.8-3.9. It was observed that creep data obtained from DMA superimpose with that of Instron.

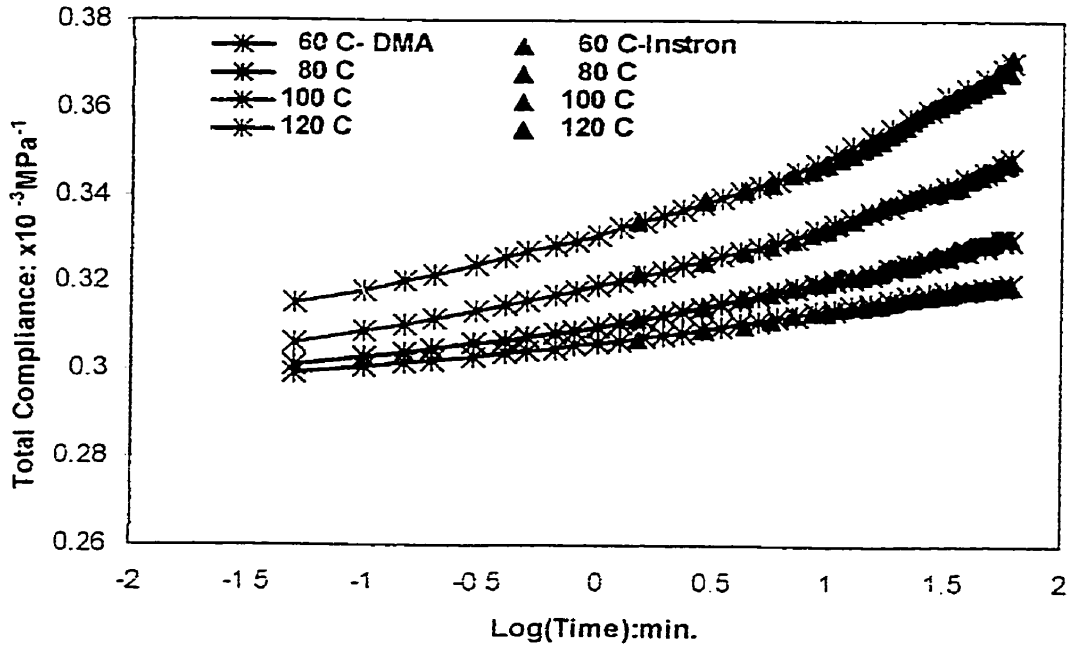

Figure 3.8:Creep data of resin at 5 MPa

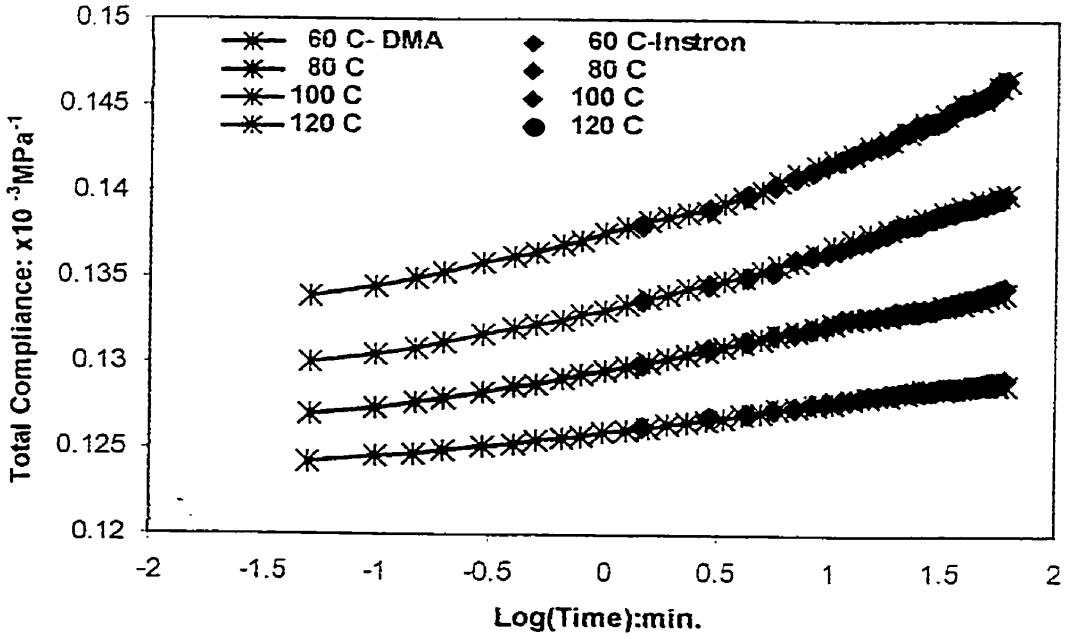

Figure 3.9: Creep data of 54 % V_f at 5 MPa

3.8 CREEP RUPTURE TEST

Creep rupture tests were done to determine the time to fracture at a constant stress.

3.8.1 TEST PROCEDURE

Creep rupture tests on dry samples were carried out in a constant stress machine supplied by *Avery Denison Ltd.* The time to fracture was recorded by built-in timer that automatically shut itself off when test specimens fractured. Specimens were tested at stresses in the range of 30-95% of the ultimate tensile strength. The temperature of the test specimens was monitored with a thermocouple placed near the gage length of the test specimen. The moisture-conditioned specimens were tested in *Instron.*

Creep rupture tests were performed on resin and $[90]_{12}$ composite specimens with 54% fiber volume fraction in the following conditions: Postcured, physically aged, moisture conditioned, aged and moisture conditioned as shown in Table 3.4.

Test Condition	Aging / Immersion Temp. (°C)	Aging Time (Days)	Moisture Content (% M_m)		UTS (%)	Test Temperature (°C)
Postcured (Temperature/ Stress)	-	-	-		40-95	80-240
Physical Aging	80,180,240	16.6	-		70-95	80-240
Moisture	80	XX	Resin 5.27	54% 3.50	70-95	80
Aging + Moisture	80/80	16.6	4.40	2.90	70-95	80

Table 3.4: Creep Rupture testing scheme

CHAPTER 4

RESULTS AND DISCUSSION

The results obtained from experiments elaborated in Chapter 3, are presented and discussed in this chapter. The results of moisture absorption test are presented first. The individual and interactive effect of each parameter such as temperature, stress, moisture, physical aging and fiber volume fraction on creep of both resin and composite are presented and discussed separately in section 4.2 . Section 4.3 discusses the effect of above factors on tensile properties of both materials. Finally, the individual and interactive effect of the above factors on creep rupture of resin and composite are presented and discussed in section 4.4

4.1 MOISTURE ABSORPTION KINETICS

4.1.1 RESIN

4.1.1.1 EFFECT OF TEMPERATURE

Figure 4.1 shows the experimental curves for weight gain during immersion in distilled water at 23°C, 50°C, 60°C and 80°C for resin. The weight gain (or alternatively referred to as "moisture content" in this thesis) increased linearly with $\sqrt{t}$ (immersion time) and reached a plateau value corresponding to the moisture saturation. This behavior is typical of a material that exhibits a fickian behavior in moisture absorption. The increase in temperature increased the rate of moisture absorption as well as the saturation moisture content. Diffusion coefficient 'D' calculated using the slope of curves in Figure 4.1 and the equation given in appendix A for all temperatures is plotted in Figure 4.2. Increase in "D" with temperature is the reason for increase in rate of absorption with

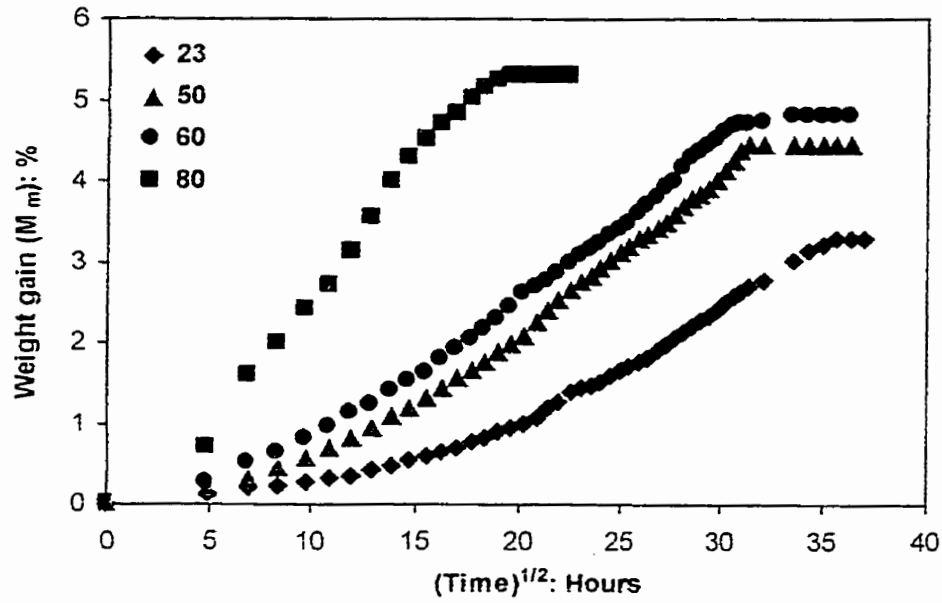

Figure 4.1: Moisture content as function of time for resin immersed in distilled water at various temperatures

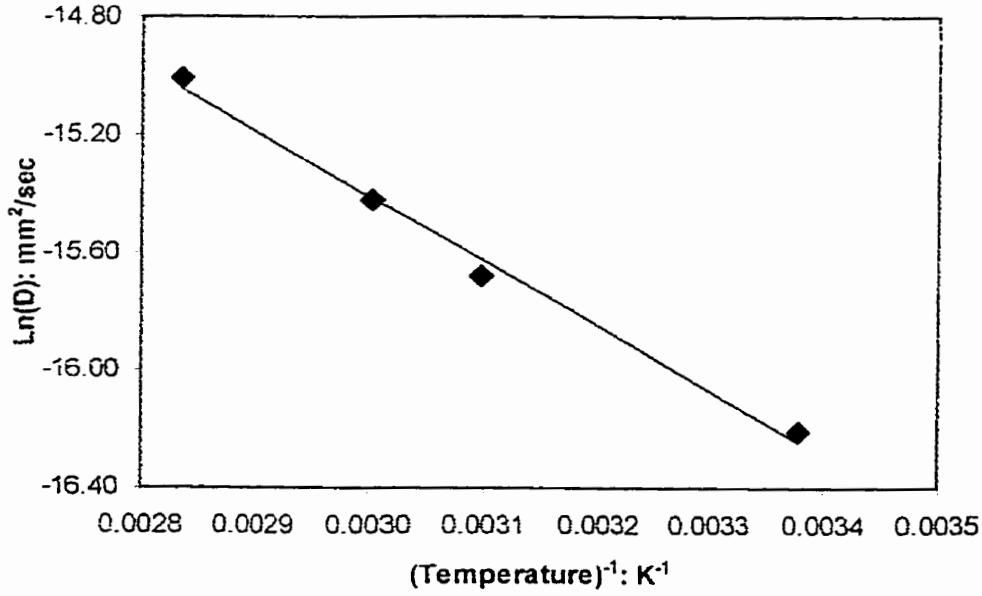

Figure 4.2: Diffusion coefficient for resin as a function of temperature

Temp. (° C)	M_{sat} (%)			Diffusion coefficient(D) (x 10^{-8}) mm^2/sec			Activation energy kJ/mole			Pre-exponential Factor (mm^2/sec)		
	Resin	V_f:54%	V_f:71%	Resin	V_f:54%	V_f:71%	Resin	V_f:54%	V_f:71%	Resin	V_f:54%	V_f:71%
23	3.29	1.80	1.69	9.12	8.52	5.16						
50	4.43	1.95	1.84	15.47	12.92	7.92	18.23	13.63	10.66	8.83	12.18	12.19
60	4.66	2.23	1.98	20.00	14.28	8.10						
80	5.27	3.50	2.50	30.30	16.20	9.53						

Table 4.1: Moisture absorption kinetic parameters for resin and composite immersed in water

temperature. The data in Figure 4.2 was modeled using Arrhenius equation to yield activation energy of 18.23 kJ/mole. Increase in saturation moisture content and diffusion coefficient with temperature was observed by several researchers for epoxy resin [26-33] and is consistent with present results. The magnitude of diffusion coefficient noticed in the present study is consistent with other published literature [26-30, 32, 33]. The diffusion coefficient values for epoxy resin reported in literature varied 0.83 x 10^{-7} to 1.8 x 10^{-7} mm^2/sec^{-1} in the temperature range of 23°C to 70°C. The saturation moisture content (weight gain) and diffusion coefficients at different temperatures, as well as the activation energy and pre-exponential factor values for resin are tabulated in Table 4.1.

4.1.1.2 EFFECT OF PHYSICAL AGING

Figure 4.3 shows the experimental curves for weight gain, during immersion in distilled water at 80°C, for resin samples aged to different times. The curves indicate that the moisture absorption in epoxy follows fickian behavior even in physically aged condition. Moreover, saturation moisture content decreased and the time to reach saturation level increased with increase in aging time. The saturated moisture content was found to decrease by 16.5% after aging for 400 hours (16.6 days) from that of non-aged sample. This is expected since physical aging leads to lower free volume within polymer, thereby decreasing the rate of moisture absorption, diffusion coefficient and saturated moisture content. Similar trend (i.e. decrease in moisture content with increase in aging time) was noticed by Kong [24] for epoxy resin. Kong [24] observed a 20% decrease in

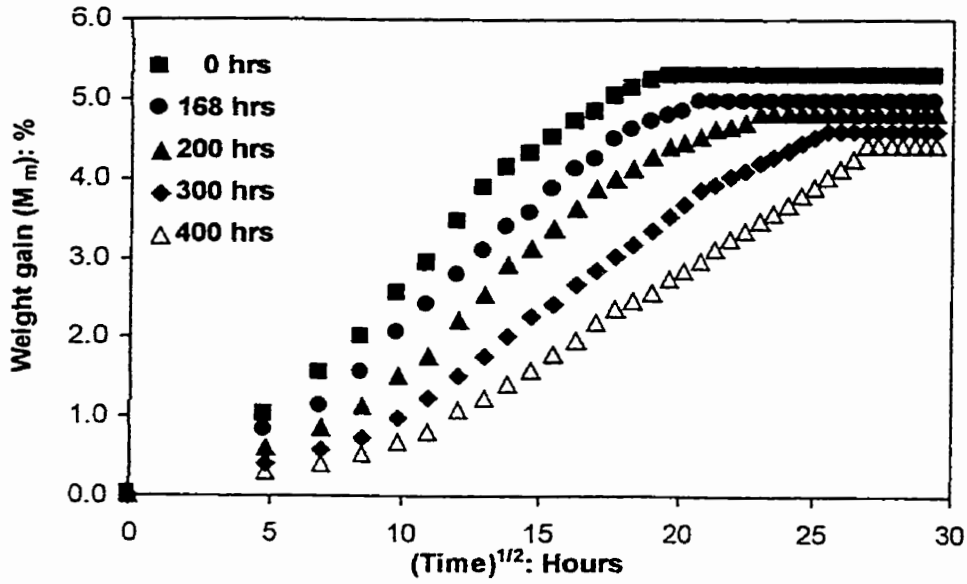

Figure 4.3: Moisture content as function of time for resin immersed in distilled water at 80°C at different aging times

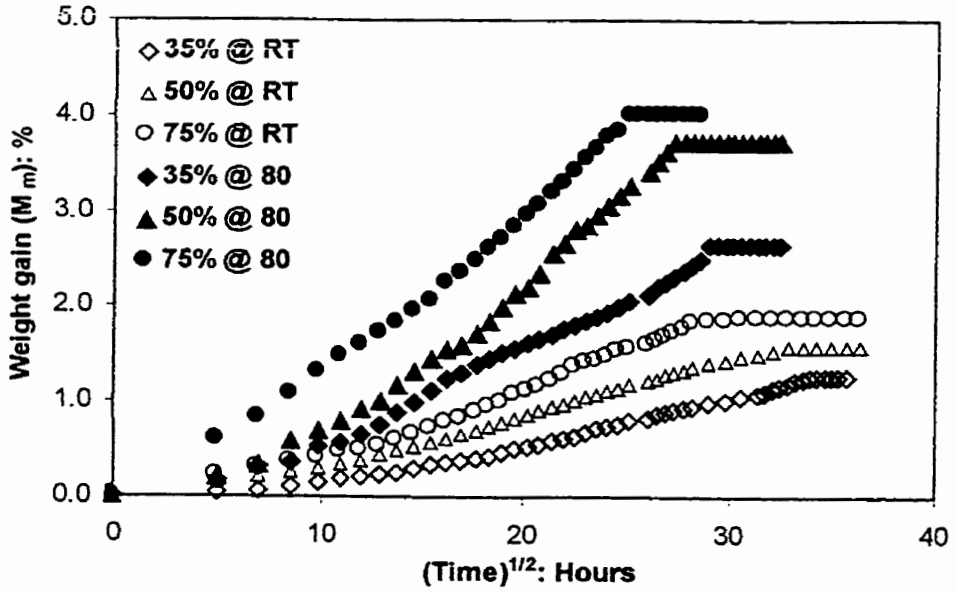

Figure 4.4: Moisture content as a function of time for resin at various temperature and humidity levels

Aging Time (Hours)	M_{sat} (%)		Diffusion coefficient(D) (x 10^{-8}) mm^2/sec	
	Resin	V_f : 54 %	Resin	V_f : 54 %
0	5.27	3.50	30.30	16.20
100	4.95	3.44	25.25	15.90
200	4.89	3.20	24.10	14.20
300	4.60	3.09	23.20	14.00
400	4.40	2.90	20.01	13.40

Table 4.2: Effect of physical aging on moisture absorption kinetic parameters for resin and composite (V_f:54%) at 80°C

moisture content after aging for 166 hours when compared to non-aged samples. The saturation moisture content and diffusion coefficients at different aging times are tabulated in Table 4.2.

4.1.1.3 EFFECT OF RELATVE HUMIDITY

Figure 4.4 shows the experimental curves for weight gain, at different temperatures (23°C and 80°C) and humidity levels (35%, 50% and 75%) for resin. The weight gain increased linearly with $\sqrt{t}$ and reached a plateau value corresponding to the moisture saturation. This behavior is typical of a material that exhibits a fickian behaviour in moisture absorption. Similar to water immersion tests, the increase in temperature and humidity increased the rate of moisture absorption as well as the saturation moisture content. Diffusion coefficient 'D' calculated using the slope of curves in Figure 4.4 and the equation given in Appendix A for all temperatures is plotted in Figure 4.5. Increase in "D" with temperature and humidity is the reason for increase in rate of absorption with temperature and humidity. Such an increase in D with humidity for epoxy resin has been observed by many investigators [26, 29-31, 34]. The magnitude of diffusion coefficient values reported in literature is consistent with present results [26, 29-31, 34]. The plot in Figure 4.5 was modeled using Arrhenius equation to yield activation energy of 5.19 (35%), 5.31 (50%) and 9.15 (75%) kJ/mole. In addition to saturation moisture content and diffusion coefficient, activation energy also increased with humidity and reached a maximum at 100% humidity. Increase in activation energy with humidity observed in the present study, is in contrast to that observed by Woo and Piggot [36]. They found activation energy to be independent of relative humidity. The

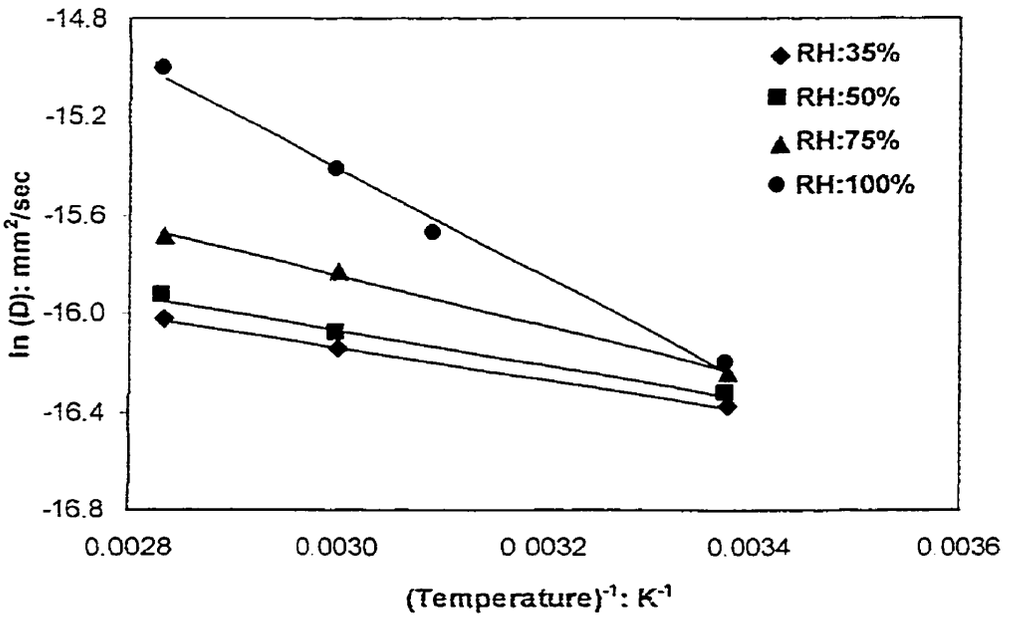

Figure 4.5: Diffusion coefficient for resin as a function of temperature at different humidity levels

Temp. (°C)	RH (%)	M_{sat} (%)		Diffusion coefficient(D) (x 10^{-8} mm^2/sec)		Activation energy (kJ/mole)		Pre-exponential Factor(mm^2/sec)	
		Resin	V_f : 54 %	Resin	V_f : 54 %	Resin	V_f : 54 %	Resin	V_f : 54 %
23	35	1.25	0.78	7.60	7.30	5.19	1.93	14.26	15.64
	50	1.56	0.92	8.10	7.40	5.31	3.83	14.16	14.75
	75	1.85	1.05	8.80	7.80	8.55	4.12	12.76	14.70
	100	3.29	1.80	9.12	8.50	18.23	13.63	8.83	12.18
60	35	2.15	1.15	9.70	8.00				
	50	2.56	1.50	10.30	8.80				
	75	3.34	1.56	13.40	9.50				
	100	4.66	2.23	20.00	14.28				
80	35	2.62	1.59	11.00	8.30				
	50	3.71	1.63	12.00	9.80				
	75	4.00	1.83	15.40	10.30				
	100	5.27	3.50	30.30	16.20				

Table 4.3: Moisture absorption kinetic parameters for resin and composite (V_f : 54%) at various humidity levels

saturation moisture content and diffusion coefficients at different temperatures, as well as activation energy and pre-exponential factor values for resin are tabulated in Table 4.3.

4.1.2 COMPOSITE WITH 54% FIBER VOLUME FRACTION

4.1.2.1 EFFECT OF TEMPERATURE

Figure 4.6 shows the experimental curves for weight gain during i mmersion in distilled water at 23°C, 50°C, 60°C and 80°C for composite with 54% fiber volume fraction. The weight gain increased linearly with $\sqrt{t}$ and reached a plateau value corresponding to the moisture saturation. Similar to epoxy matrix, the increase in temperature increased the rate of moisture absorption as well as the saturation moisture content. Composite with 54% fiber volume fraction absorbed 33.5% less moisture than the resin due to lesser amount of resin in the composite. Diffusion coefficient 'D' calculated using the slope of curves in Figure 4.6 and the equation given in appendix A for all temperatures is plotted in Figure 4.7. Increase in "D" with temperature is the reason for increase in rate of absorption with temperature. Such an increase in moisture content and 'D' were also observed by other investigators [31, 38, 39]. The 'D' values for carbon/epoxy composite reported in literature varies between $0.82 \times 10^{-7} - 2.8 \times 10^{-7}$ mm^2/sec and is consistent with the present data. The plot in Figure 4.7 was modeled using Arrhenius equation to yield activation energy of 13.63 kJ/mole. The saturation moisture content and diffusion coefficients at various temperatures, as well as activation energy and pre-exponential factor values for composite with 54% fiber volume fraction are tabulated in Table 4.1.

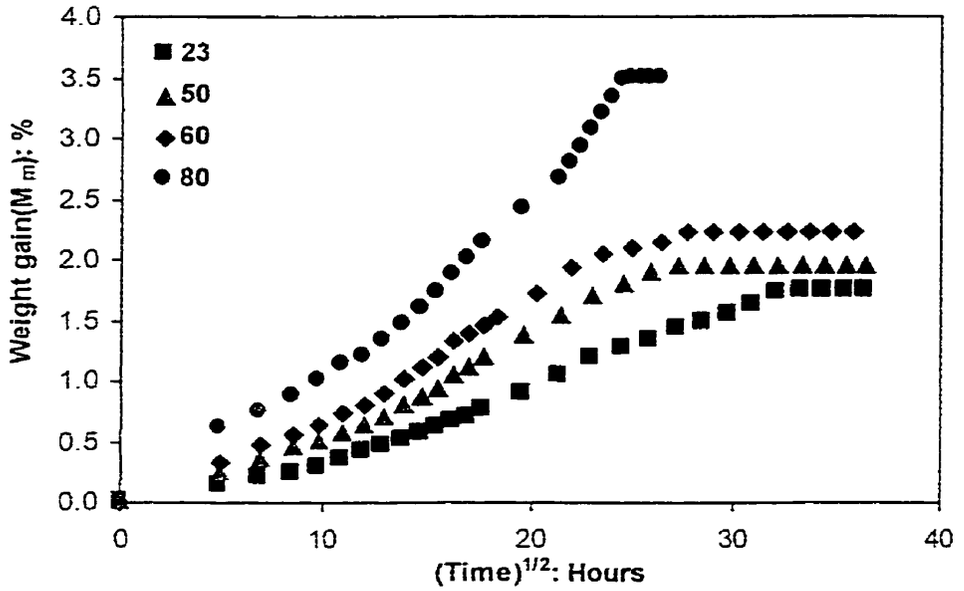

Figure 4.6: Moisture content as function of time for composite (V_f : 54%) immersed in distilled water at various temperatures

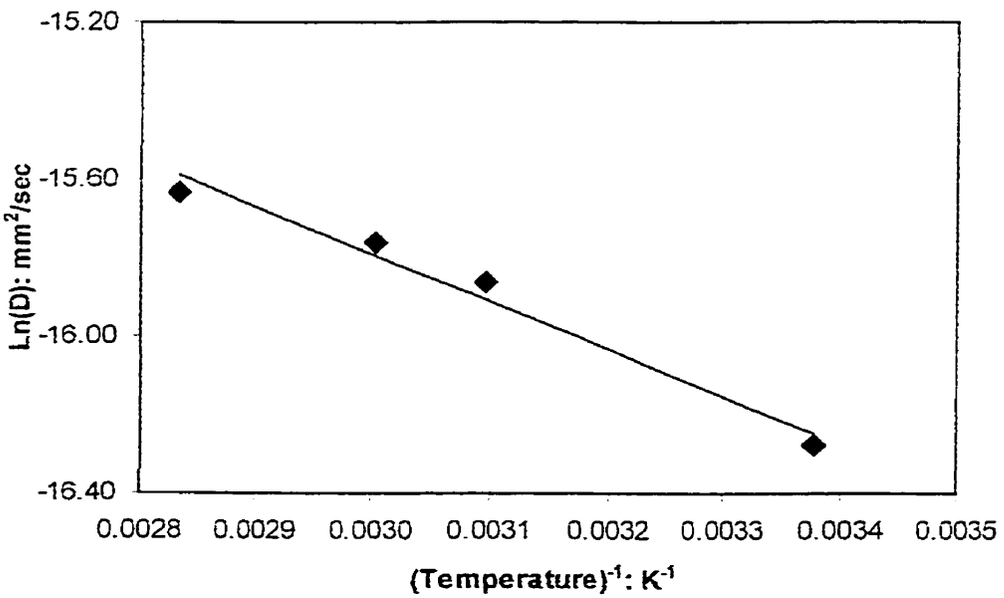

Figure 4.7: Diffusion coefficient for composite (V_f :54%) as a function of temperature

4.1.2.2 EFFECT OF PHYSICAL AGING

Figure 4.8 shows the experimental curves for weight gain during immersion in distilled water at 80°C for composite with 54% fiber volume fraction samples aged to different times. The curves indicate that the moisture absorption in composite follows fickian behavior even in physically aged condition. Moreover, saturation moisture content decreased and the time to reach saturation level increased with increase in aging time. The saturated moisture content was found to decrease by 14.2% after aging for 400 hours when compared to non-aged sample. This is expected since physical aging leads to lower free volume within the polymer, thereby decreasing the rate of moisture absorption, diffusion coefficient and saturated moisture content. The % decrease in moisture content with increasing aging time for composite with 54% fiber volume fraction with increasing aging time was found to be less than that for resin due to lesser amount of resin in composite. The saturation moisture content and diffusion coefficients at different aging times are tabulated in Table 4.2.

Figure 4.9 shows experimental curves for weight gain during immersion in distilled water at various temperatures for composite with 54% V_f aged to 100 hrs. The experimental curves for weight gain during immersion in distilled water at various temperatures for composite aged to 200 hrs is shown is Appendix A. Similar to unaged samples, the weight gain increased linearly with $\sqrt{t}$ and reached a plateau value corresponding to the moisture saturation. The saturation moisture content increased with increase in temperature. Diffuison coefficient 'D' calculated using the slope of curves in Figure 4.9 is plotted in Figure 4.10 for 100 and 200 hours. Increase in "D" with temperature is the reason for increase in rate of absorption with temperature. However it

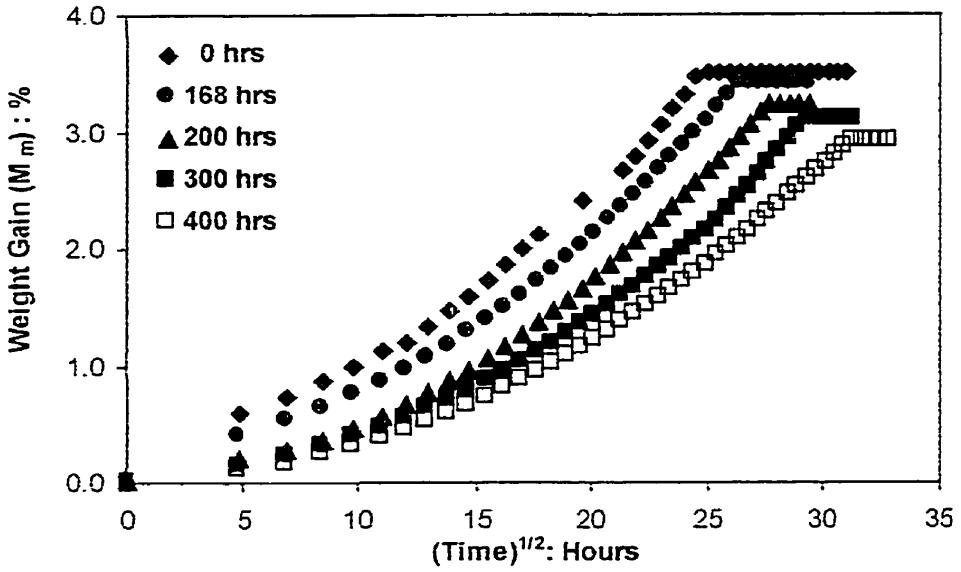

Figure 4.8: Moisture content as function of time for composite (V_f :54%) immersed in distilled water at 80°C at various aging times

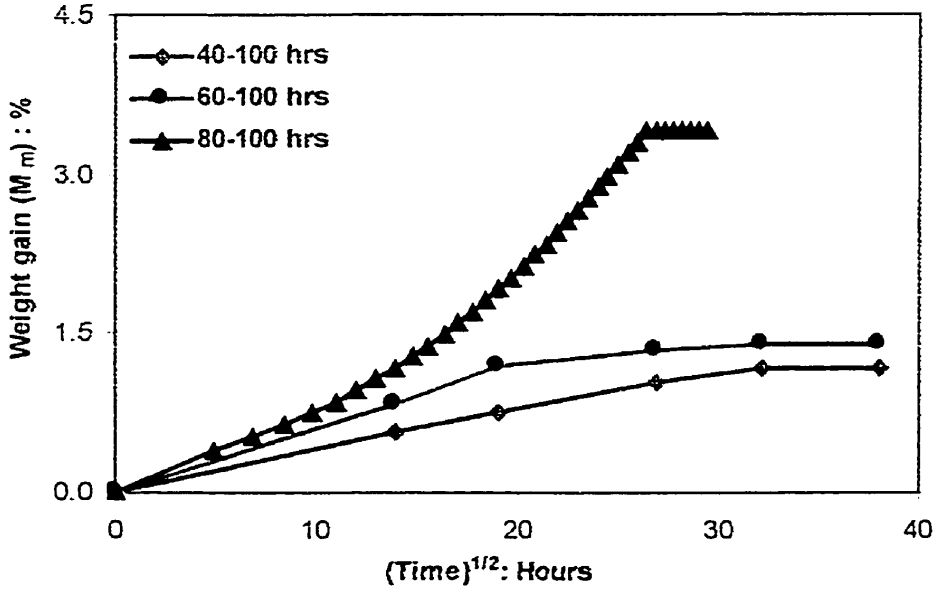

Figure 4.9: Moisture content as function of time for aged composite (V_f :54%) immersed in distilled water at various temperatures

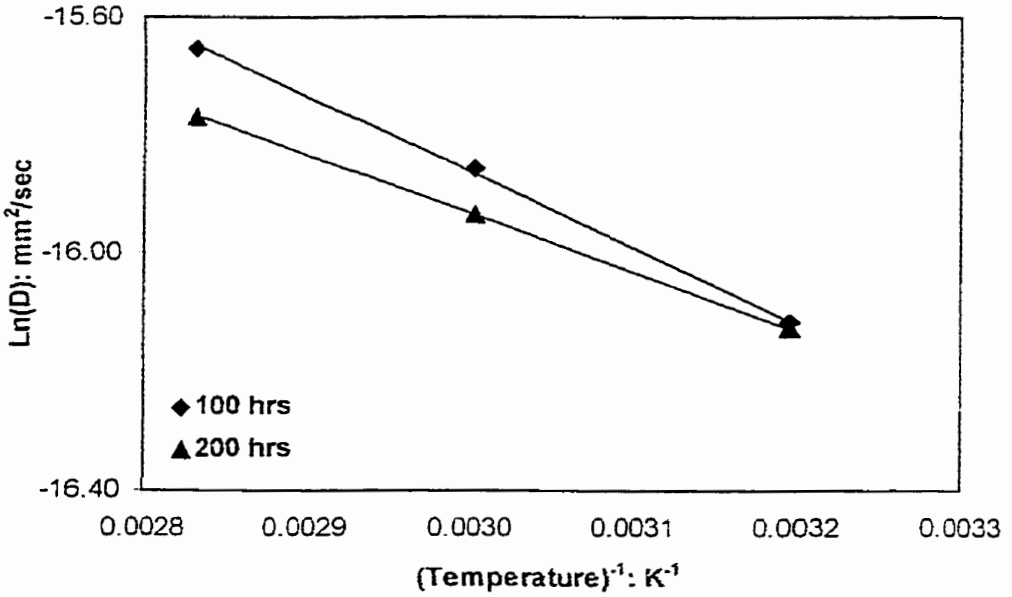

Figure 4.10: Diffusion coefficient for aged composite (V_f :54%) as a function of temperature

Temp. (° C)	M_{sat} (%)			Diffusion coefficient(D) (x 10^{-8}) mm^2/sec			Activation energy kJ/mole			Pre-exponential Factor (mm^2/sec)		
	0 hrs	100 hrs	200 hrs	0 hrs	100 hrs	200 hrs	0 hrs	100 hrs	200 hrs	0 hrs	100 hrs	200 hrs
40	1.95	1.17	1.08	12.20	10.00	9.90						
60	2.23	1.39	1.26	14.28	13.00	12.00	13.63	9.52	8.28	12.18	12.41	12.94
80	3.50	3.40	3.20	16.20	15.90	14.20						

Table 4.4: Moisture absorption kinetic parameters for composite (V_f : 54%) at various aging times

was observed that saturation moisture content and diffusion coefficient as well as activation energy decreased with increase in aging time. The saturation moisture content and diffusion coefficient as well as activation energy and pre-exponential factor values for composite with 54% fiber volume fraction are tabulated in Table 4.4. Though the effect of aging on moisture kinetics of epoxy resin has been investigated by Kong [24] for epoxy resin, no effort has so far been made to study the effect of aging on moisture kinetics of carbon/epoxy composite. Results of this study are the first data on the effect of physical aging on moisture absorption kinetics of composites.

4.1.2.3. EFFECT OF RELATIVE HUMIDITY

Figure 4.11 shows the experimental curves for weight gain for composite with 54% fiber volume fraction at different temperatures (23°C and 80°C) and humidity levels (35%, 50% and 75%). The weight gain increased linearly with $\sqrt{t}$ and reached a plateau value corresponding to the moisture saturation similar to water immersion tests. The saturation moisture content increased with increase in temperature and humidity. The increase in temperature increased the rate of moisture absorption as well as the saturation moisture content. Diffusion coefficient 'D' calculated using the slope of curves in Figure 4.11 and the equation given in appendix A for all temperatures is plotted in Figure 4.12. Increase in "D" with temperature is the reason for increase in rate of absorption with temperature. The data in Figure 4.12 was modeled using Arrhenius equation to yield activation energy of 1.93 (35%), 3.83 (50%), and 4.12 (75%) kJ/mole. The increase in moisture content and D with humidity has been observed by other researchers [26, 29-31, 34, 38] for carbon/epoxy composites in the published literature. However, Woo and

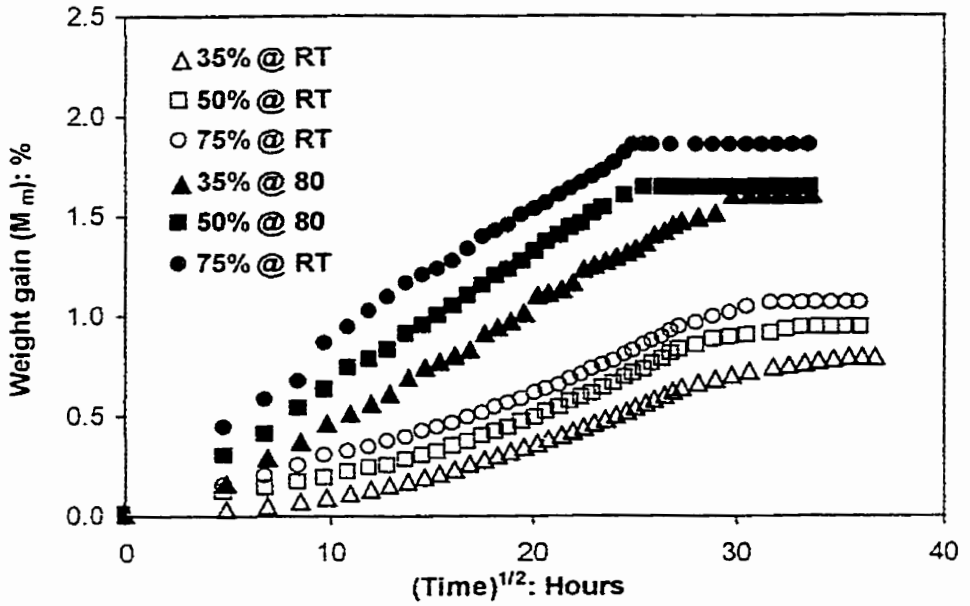

Figure 4.11: Moisture content as function of time for composite (V_f :54%) at various temperature and humidity levels

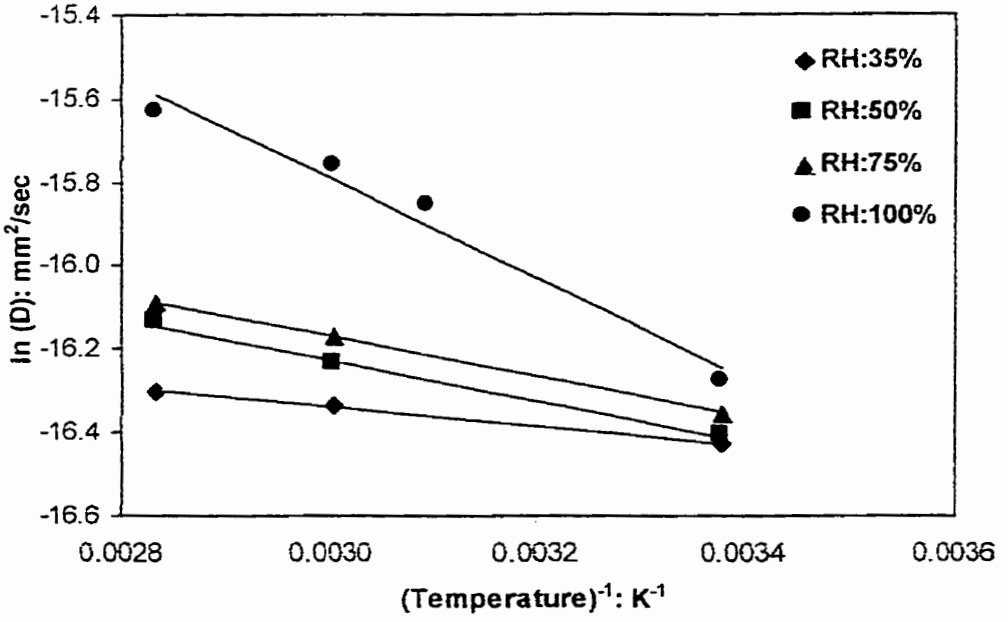

Figure 4.12: Diffusion coefficient for composite (V_f :54%) as a function of temperature at various humidity levels

Piggot [36] have observed activation energy to be independent of humidity. The saturation moisture content and diffusion coefficients at different temperature, as well as activation energy and pre-exponential factor values for composite with 54% fiber volume fraction are tabulated in Table 4.3.

4.1.3 COMPOSITE WITH 71% FIBER VOLUME FRACTION

4.1.3.1 EFFECT OF TEMPERATURE

Figure 4.13 shows the experimental curves for weight gain during immersion in distilled water at 23°C, 50°C, 60°C and 80°C for composite with 71% fiber volume fraction. The weight gain increased linearly with $\sqrt{t}$ and reached a plateau value corresponding to the moisture saturation. Similar to composite with 54% fiber volume fraction, the increase in temperature increased the rate of moisture absorption as well as the saturation moisture content. Composite with 71% fiber volume fraction absorbed 28.5% less moisture than composite with 54% fiber volume fraction due to lesser amount of resin in the composite. Diffusion coefficient 'D' calculated using the slope of curves in Figure 4.13 and the equation given in appendix A for all temperatures is plotted in Figure 4.14. Increase in "D" with temperature is the reason for increase in rate of absorption with temperature. The data in Figure 4.14 was modeled using Arrhenius equation to yield activation energy of 10.66 kJ/mole. The increase in moisture content with temperature can be attributed to volume expansion with temperature. The saturation moisture content and diffusion coefficients at different temperatures as well as activation energy and pre-

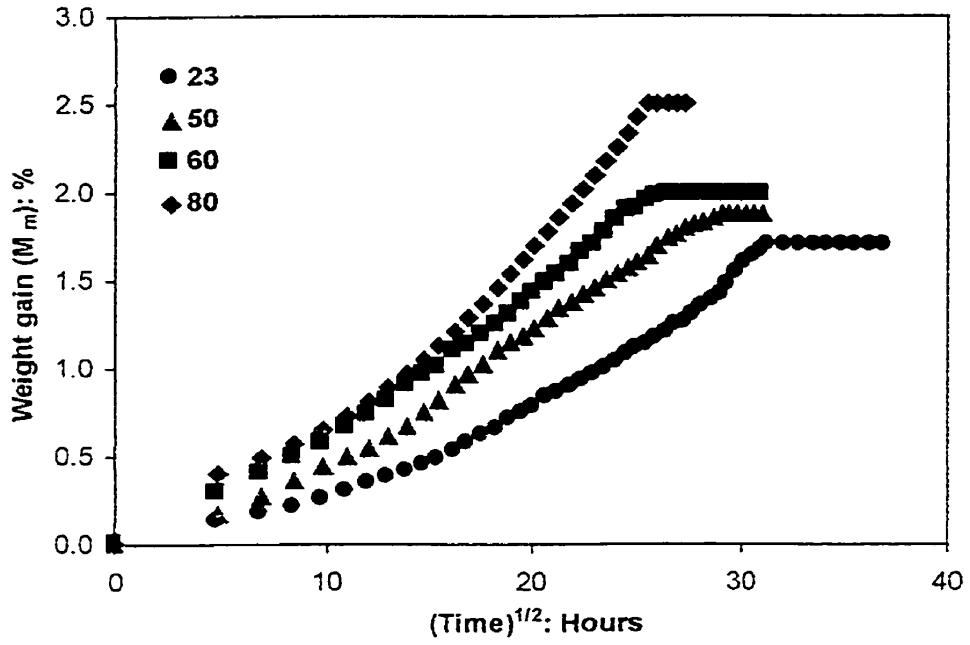

Figure 4.13: Moisture content as function of time for composite (V_f :71%) immersed in distilled water at various temperatures

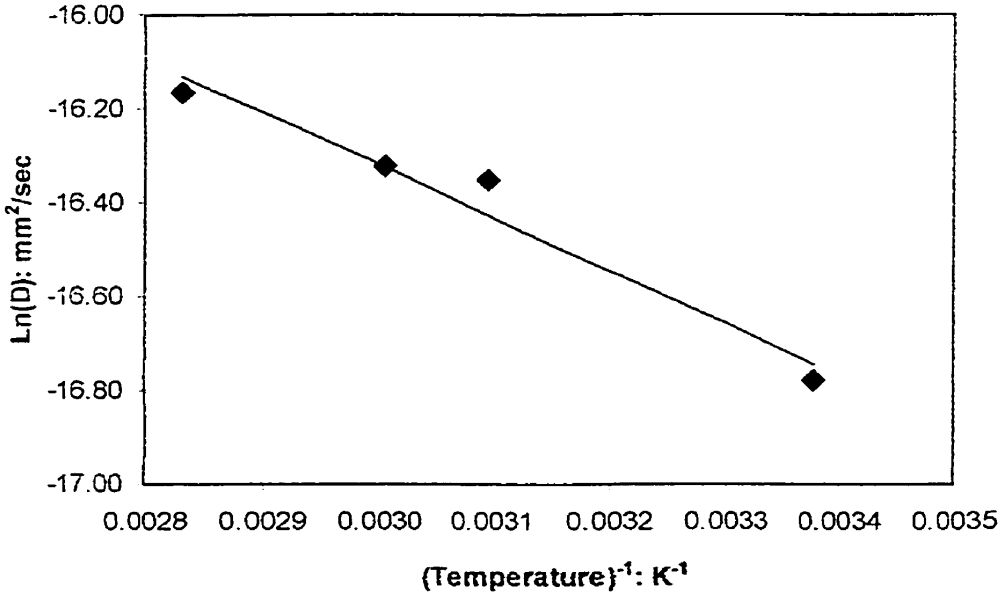

Figure 4.14: Diffusion coefficient for composite (V_f :71%) as a function of temperature

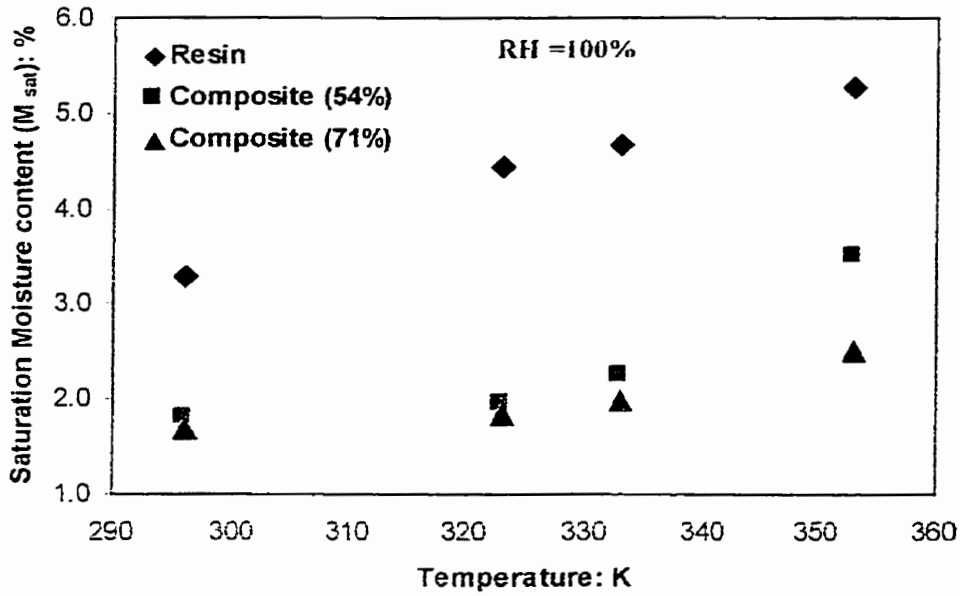

Figure 4.15: Saturation moisture content as a function of temperature for different volume fractions

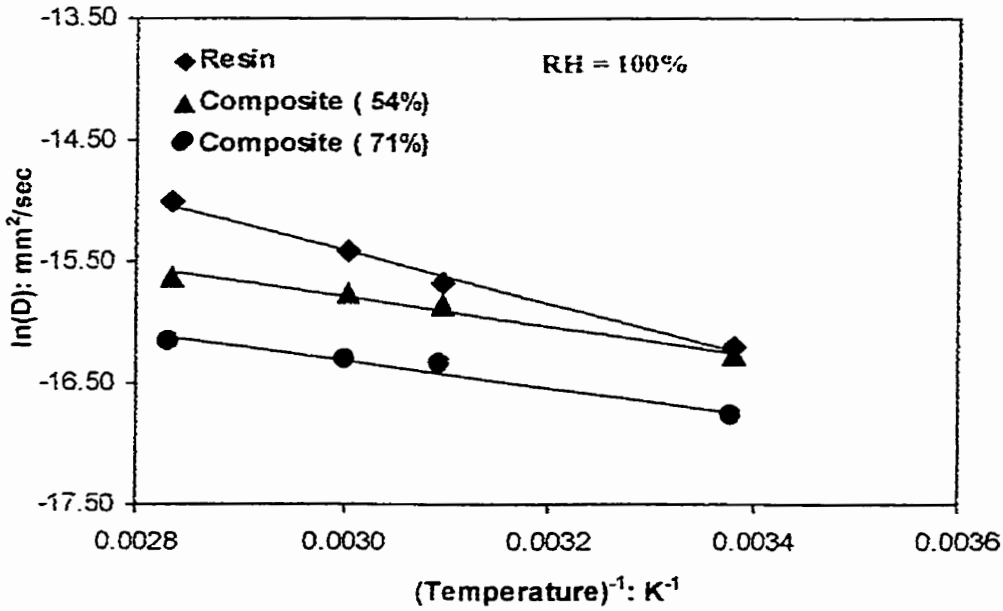

Figure 4.16: Diffusion coefficient as a function of temperature for different volume fractions

exponential factor for composite with 71% fiber volume fraction are tabulated in Table 4.1.

4.1.4 SUMMARY AND EFFECT OF FIBER VOLUME FRACTION ON MOISTURE KINETICS

A plot of saturated moisture content as a function of temperature at 100% relative humidity for resin and composite with 54% and 71% fiber volume fraction is shown in Figure 4.15. As shown in the figure, at a given temperature saturation moisture content decreases with increase in fiber volume fraction. The decrease in moisture content with increase in fiber volume fraction could be due to less amount of resin in composite. Similar to saturation moisture content, Diffusion coefficient 'D' also decreased with increase in fiber volume fraction at a given temperature shown in Figure 4.16 at 100% relative humidity. Similar trend (i.e. decrease in saturation moisture content and diffusion coefficient with increase in fiber volume fraction) was observed at other humidity levels. Such a trend has been observed by other researchers [29, 31, 35] for epoxy resin and carbon/epoxy composites. In addition to saturation moisture content and diffusion coefficient, activation energy also decreased with increase in fiber volume fraction.

4.2 CREEP

4.2.1 EFFECT OF TEMPERATURE/STRESS

4.2.1.1 RESIN

Figure 4.17 shows the experimental total compliance data at 5 MPa for resin in the temperature range of 60°C-230°C. As expected, the creep compliance increases with the increase in temperature and time. TTSP (Time Temperature Superposition Principle)

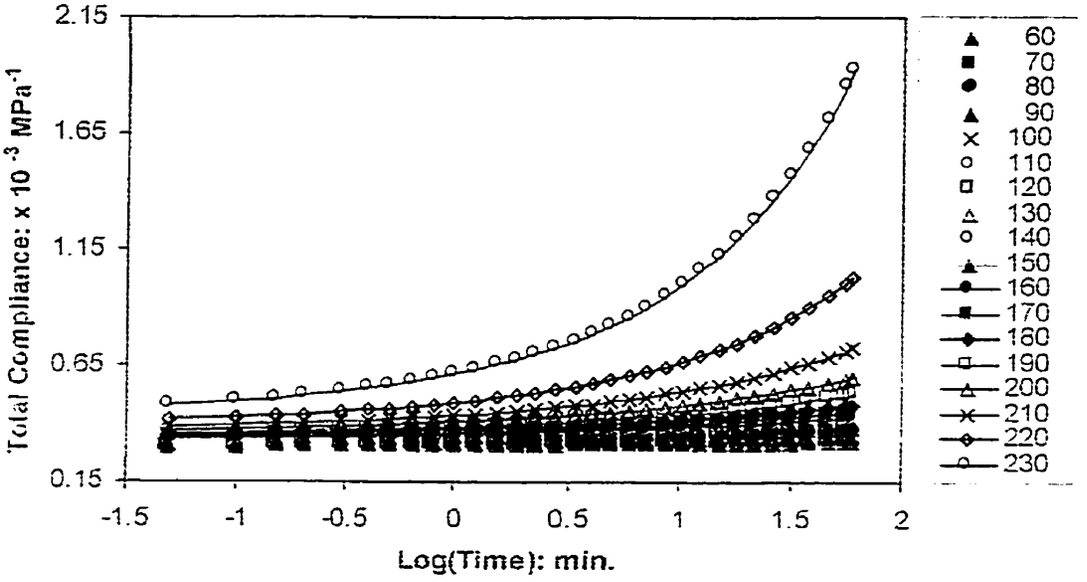

Figure 4.17: Compliance data at 5 MPa for resin

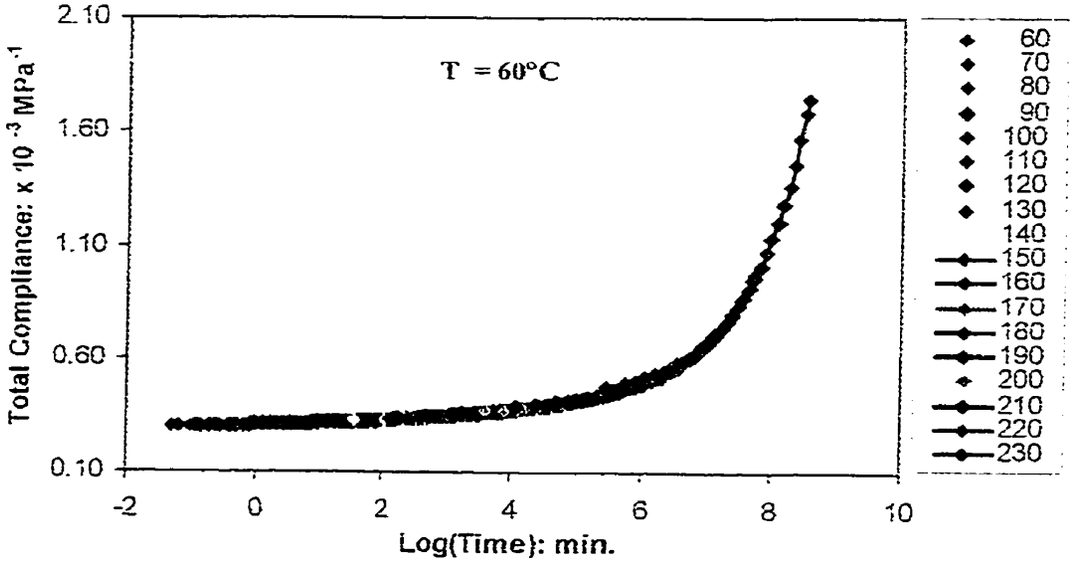

Figure 4.18: Master creep curve at 5 MPa for resin

was used to shift and superimpose the compliance curves at different temperatures to a reference temperature of 60°C. An excellent superposition was obtained indicating that creep at this stress level was well within the linear region. The superimposed creep curve, also known as "Master Creep Curve" for the resin at 5 MPa is shown in Figure 4.18. Since the instantaneous compliance increases with increase in temperature, vertical shifting was used to account for this change before horizontal shifting. Vertical shift factor was obtained from the slope of temperature versus elastic modulus plot obtained using DMA at a frequency of 10Ø Hz shown in Figure 4.19. The relation between instantaneous compliance and temperature for resin is given as $S_o = A + B*T$ (where A is the constant, B is the slope obtained from DMA plot, T is the temperature, S_o is the compliance). This equation was used to calculate the vertical shift between two creep curves at two temperatures (T_1 and T_{ref}) and subtract from (or add to) the creep curve at T_1 to shift it towards that at T_{ref}. The slope and constant values for resin are tabulated in Table 4.5. The experimental creep data at 3,7 and 15 MPa and master curves at 3, 7 MPa is shown Appendix B. Master creep curves at 3, 5, 7 MPa superimpose as shown in figure 4.20 indicating that creep is in the linear region at these stress levels. However, creep curve at 7 MPa deviates from the creep curves at 3 and 5 MPa for time greater than 10^7 minutes. This suggests that creep becomes non-linear beyond 10^7 minutes. It was observed that at a given temperature, increase in stress also accelerates creep process. As shown in Figure 4.21, increase in stress (beyond 7 MPa) increases the creep compliance. Also, creep curves at 15 MPa, 70% and 85% of ultimate tensile strength (UTS) doesn't superimpose at all (shown in figure 4.19 for a temperature of 60°C), suggesting that creep is non-linear at 15 MPa, 70% and 85% of UTS. This suggests that creep becomes non-

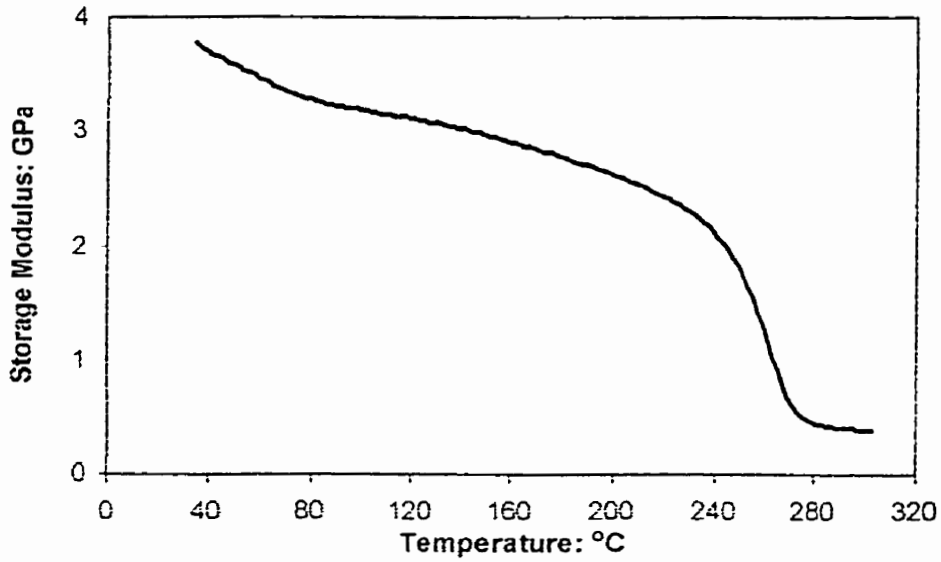

Figure 4.19: Storage modulus versus temperature plot for resin

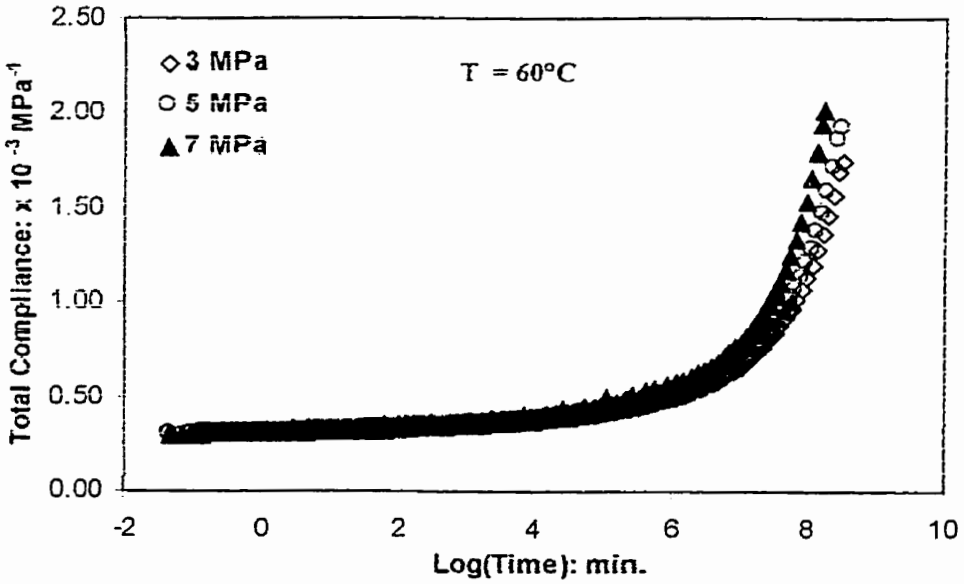

Figure 4.20: Master creep curves at 3, 5, and 7 MPa for resin

Fiber Volume Fraction (%)	Slope(B) ($\times 10^{-7}$) $MPa^{-1}.K^{-1}$	Constant (A) ($\times 10^{-5}$) MPa^{-1}
0 % (Resin)	5.75	9.87
54%	1.57	6.68
71%	1.00	6.70

Table 4.5: Equation parameters for Postcured Specimens

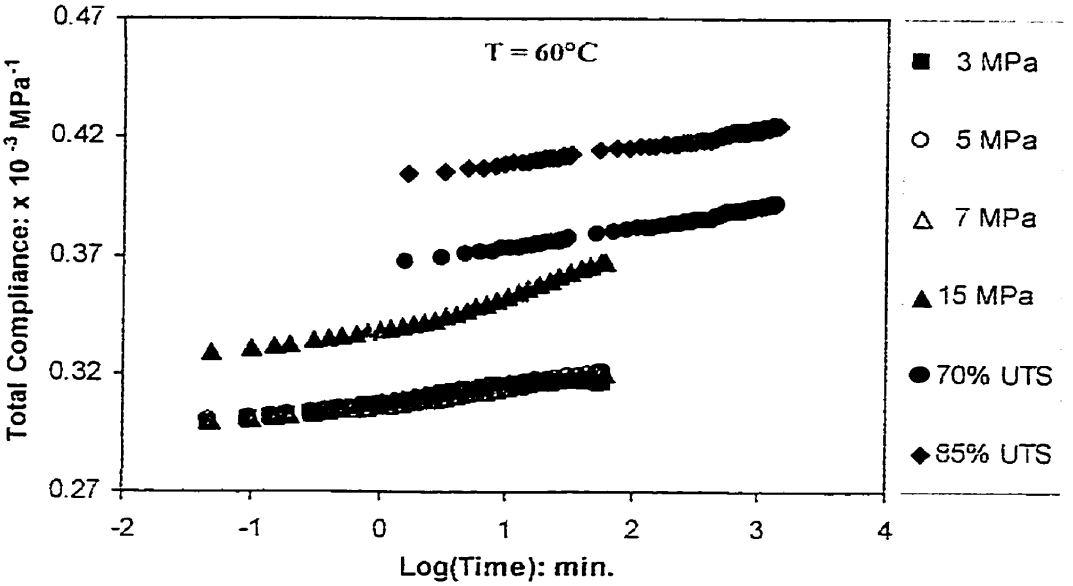

Figure 4.21: Compliance data for resin at 60°C at various stress levels

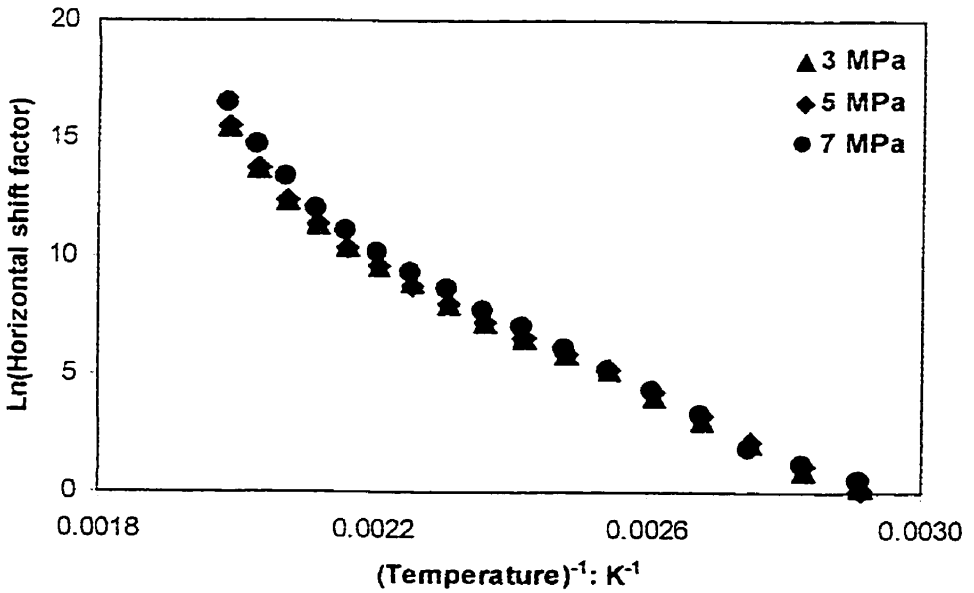

Figure 4.22: Shift factor as a function of inverse temperature at 3, 5, and 7 MPa for resin

Stress (MPa)	Activation Energy (kJ/mole)			Pre-exponential factor		
	Resin	**V_f : 54%**	**V_f : 71%**	**Resin**	**V_f : 54%**	**V_f : 71%**
3	125	193	227	43.90	67.77	77.87
5	126	201	228	45.90	69.52	77.61
7	135	203	227	46.78	69.46	77.53
Ave.	**128**	**199**	**228**	--	--	--

Table 4.6: Activation energy and Pre-exponential factor values of resin, composite with 54% and 71% V_f

linear creep occurs at a stress level above 7 MPa and the time for such transition decreases with increasing stress.

A plot of horizontal shift factor versus inverse temperature of resin at 3, 5 and 7 MPa shown in figure 4.22 is non-linear. Figure 4.22 indicates that shift factors for 3 and 5 MPa superimposes well. Shift factor at 7 MPa superimposes with shift factor at 3 and 5 MPa till 180°C and then deviates beyond 180°C. Assuming that the temperature effect on creep can be modeled using an arrehenius relations, the activation energies were calculated from slopes of horizontal shift factor versus inverse temperature plot (limited to straight line portion) shown in Figure 4.22. The activation energy and pre-exponential factor values for 3,5 and 7 MPa are tabulated in Table 4.6.

4.2.1.2 COMPOSITE WITH 54% FIBER VOLUME FRACTION

Figure 4.23 shows the experimental total compliance data at 5 MPa for $[90]_8$ composite with 54% fiber volume fraction in the temperature range of 60°C-230°C. As expected, the creep compliance increases with the increase in temperature and time. Similar to the resin, TTSP was used to shift and superimpose the compliance curves at different temperatures to a reference temperature of 60°C. An excellent superposition was obtained indicating that creep at this stress level was well within the linear region. The master creep curve for $[90]_8$ composite with 54% fiber volume fraction at 5 MPa is shown in Figure 4.24. Since the instantaneous compliance increases with increase in

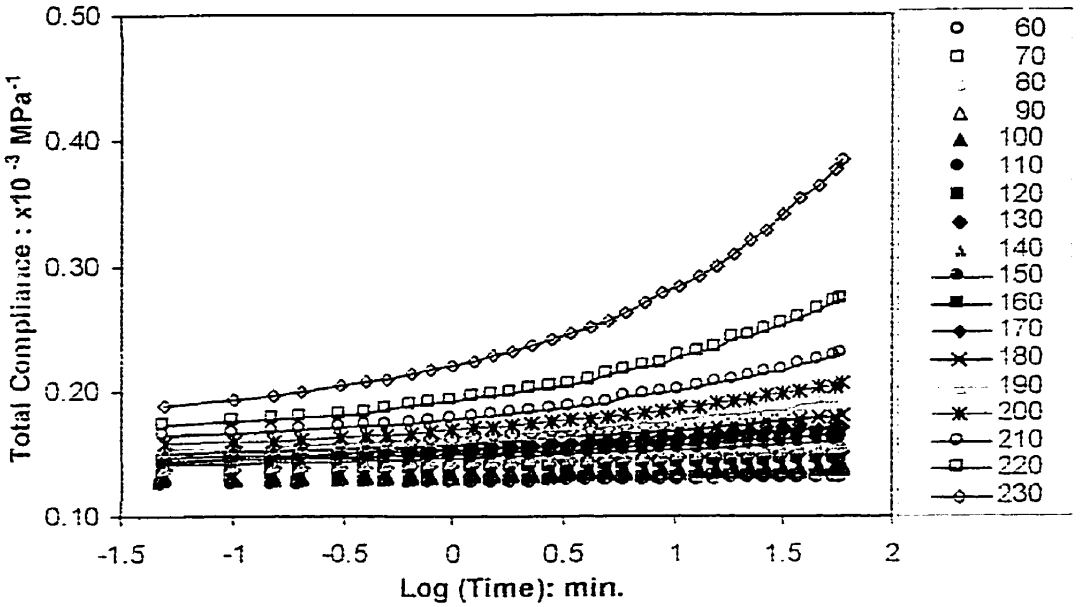

Figure 4.23: Compliance data at 5 MPa for $[90]_8$ composite (V_f :54%)

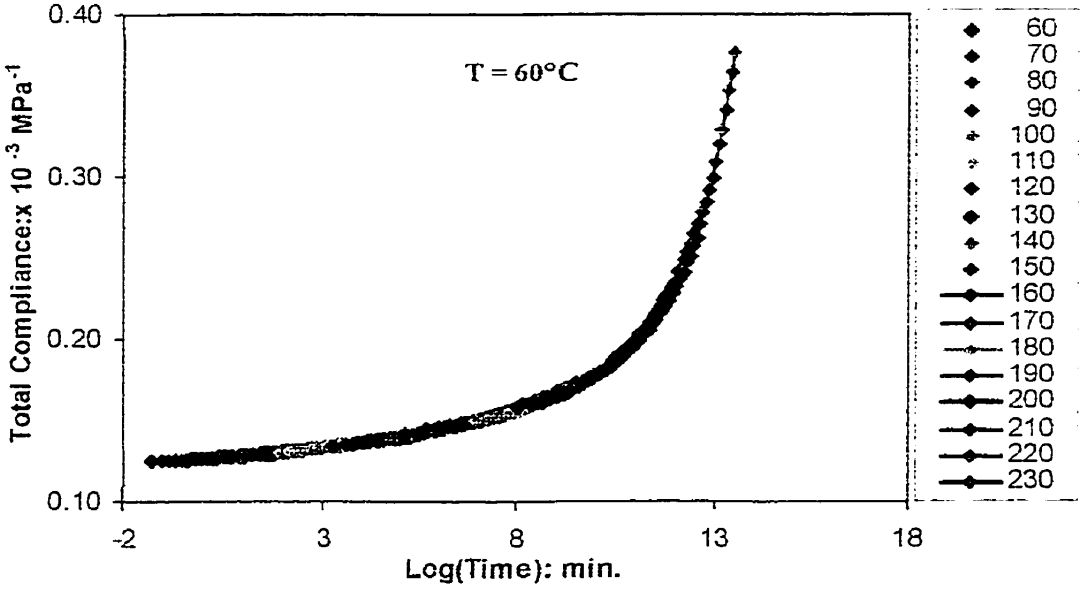

Figure 4.24: Master creep curve at 5 MPa for $[90]_8$ composite (V_f :54%)

temperature, vertical shifting was used to account for this change before horizontal shifting. Similar to resin, vertical shift factor was obtained from the slope of temperature versus elastic modulus plot obtained using DMA at a frequency of 10 Hz. The equation and procedure used to vertically shift a creep curve at a temperature (T_1) to the creep curve at reference temperature (T_{ref}) was same as discussed in section 4.2.1.1. The slope and constant values for $[90]_8$ composite with 54% fiber volume fraction are tabulated in Table 4.5. The experimental creep data at 3,7 and 15 MPa and master curves at 3 and 7 MPa are shown Appendix B. Master creep curves at 3, 5, 7 MPa superimpose as shown in Figure 4.25 indicating that creep is in the linear region at these stress levels. However, creep curve at 7 MPa deviates from the creep curves at 3 and 5 MPa for time greater than 10^7 minutes. This suggests that creep becomes non-linear beyond 10^7 minutes. Also, creep curves at 15 MPa, 70% and 85% of ultimate tensile strength (UTS) doesn't superimpose at all (shown in Figure 4.26 for a temperature of 60°C), suggesting creep to be in non-linear region at 15 MPa, 70% and 85% of UTS. This suggests that transition from linear to non-linear creep occurs at some stress level above 7 MPa and the time for such transition decreases with increasing stress.

A plot of horizontal shift factor versus inverse temperature of $[90]_8$ composite with 54% fiber volume fraction at 3, 5 and 7 MPa shown in figure 4.27 is non-linear. Figure 4.27 indicates that shift factor at 3 and 5 MPa well. Horizontal shift factor at 7 MPa superimposes with shift factor at 3 and 5 MPa till 180°C and then deviates beyond 180°C. Assuming that the temperature effect on creep can be modeled using an arrehenius relations, activation energies were calculated from slopes of horizontal shift

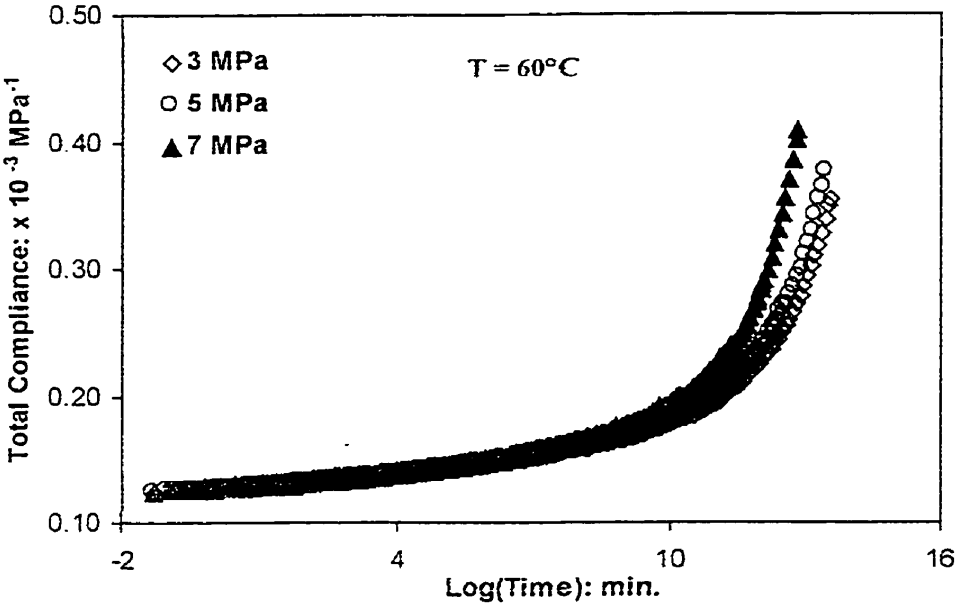

Figure 4.25: Master creep curves at 3, 5, and 7 MPa for $[90]_8$ composite (V_f :54%)

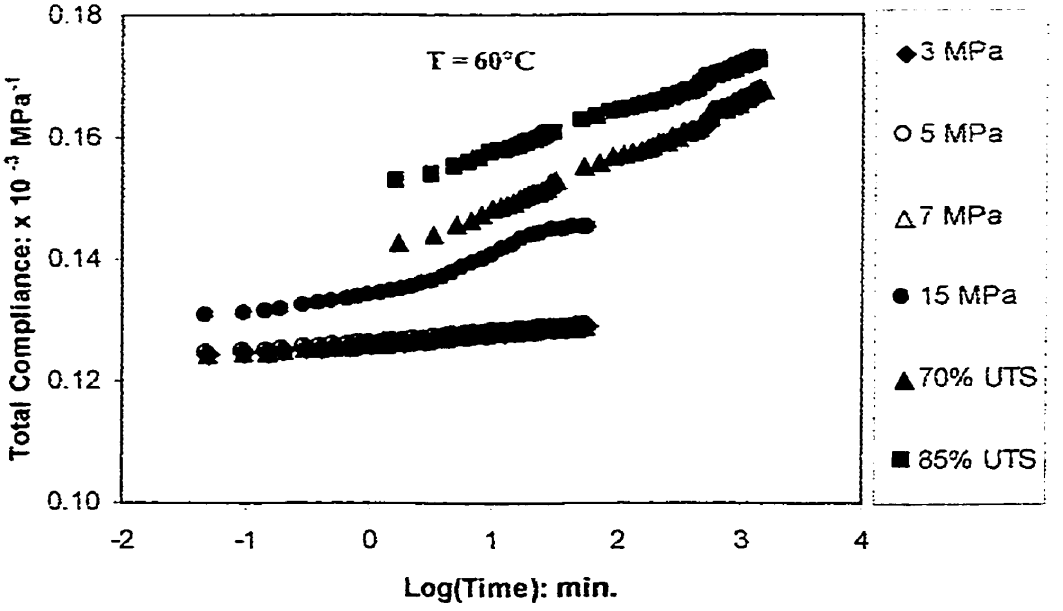

Figure 4.26: Compliance data for $[90]_8$ composite (V_f :54%) at various stress levels

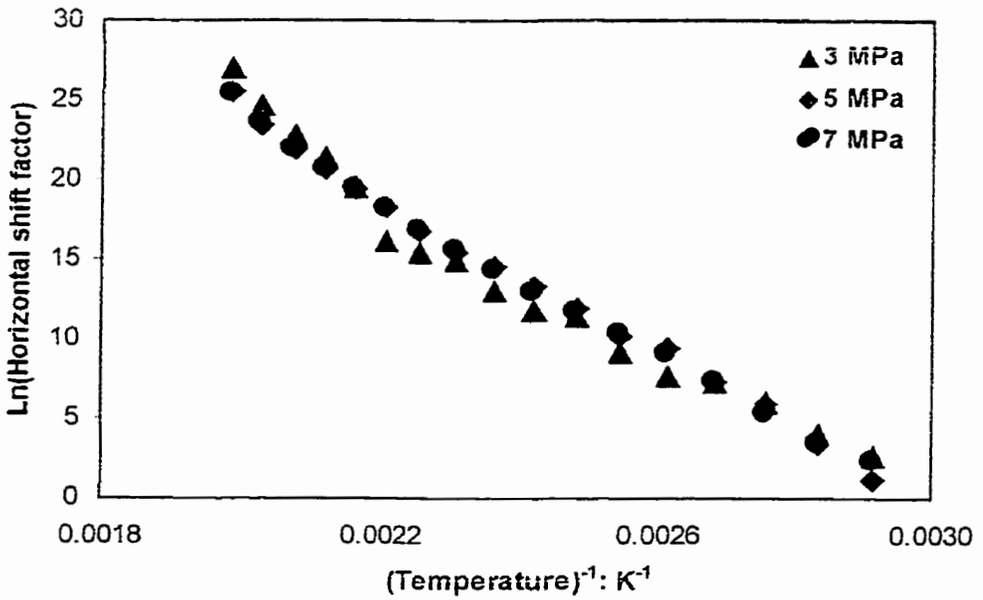

Figure 4.27: Shift factor as a function of inverse temperature at 3, 5, and 7 MPa for $[90]_8$ composite (V_f :54%)

factor versus inverse temperature plot shown in Figure 4.27. The activation energy and pre-exponential factor values for 3, 5 and 7 MPa are tabulated in Table 4.6.

4.2.1.3 COMPOSITE WITH 71% FIBER VOLUME FRACTION

Figure 4.28 shows the experimental total compliance data at 5 MPa for $[90]_8$ composite with 71% fiber volume fraction in the temperature range of 60°C-230°C. As expected, the creep compliance increases with the increase in temperature and time. Similar to 54% composite, TTSP was used to shift and superimpose the compliance curves at different temperatures to a reference temperature of 70°C. An excellent superposition was obtained indicating that creep at this stress level was well within the linear region. The master creep curve for $[90]_8$ composite with 54% fiber volume fraction at 5 MPa is shown in Figure 4.29. Since the instantaneous compliance increased with increase in temperature, vertical shifting was used to account for this change before horizontal shifting. Vertical factor was obtained from the slope of temperature versus elastic modulus plot obtained using DMA at a frequency of 10 Hz. The equation used for vertical shifting was similar to as discussed in section 4.2.1.1. The slope and constant values for $[90]_8$ composite with 71% fiber volume fraction are tabulated in Table 4.5. The experimental creep data at 3,7 and 15 MPa and master curves at 3, 7 MPa is shown Appendix B. Master creep curves at 3 and 5 MPa superimpose as shown in Figure 4.30 indicates that creep is in the linear region at 3 and 5 MPa. However, creep curve at 7 MPa doesn't superimpose with creep curves at 3 and 5 MPa suggesting that creep becomes non-linear beyond 5 MPa. This suggests that transition from linear to non-linear creep occurs at some stress level above 5 MPa.

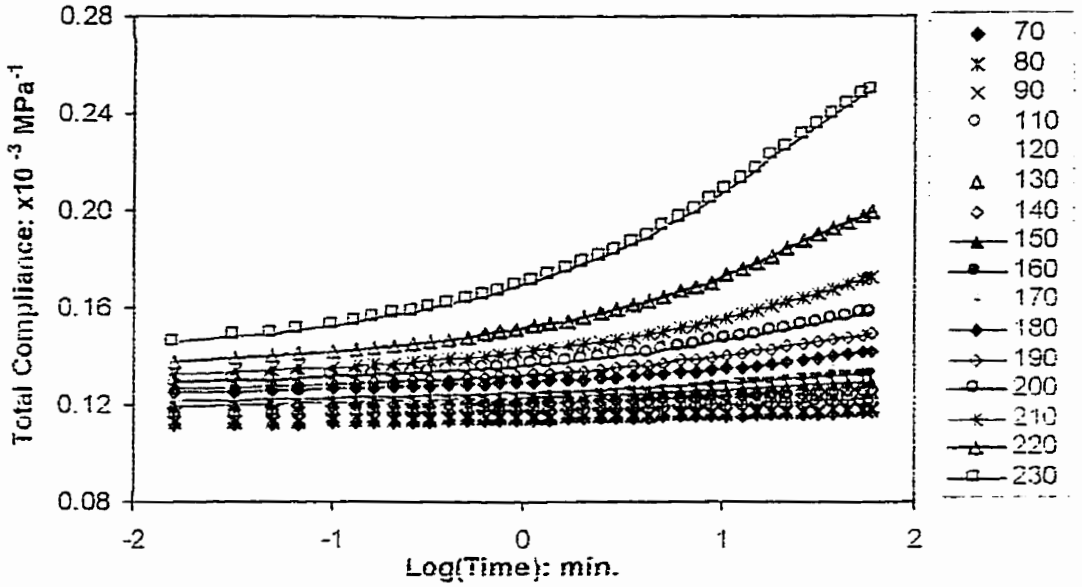

Figure 4.28: Compliance data at 5 MPa for $[90]_8$ composite (V_f:71%)

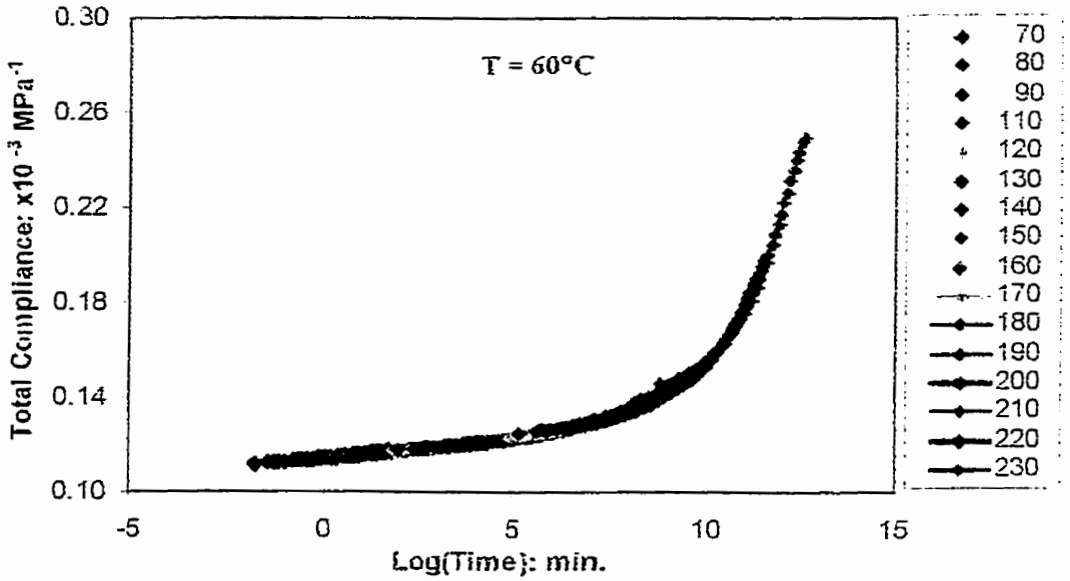

Figure 4.29: Master creep curve at 5 MPa for $[90]_8$ composite (V_f:71%)

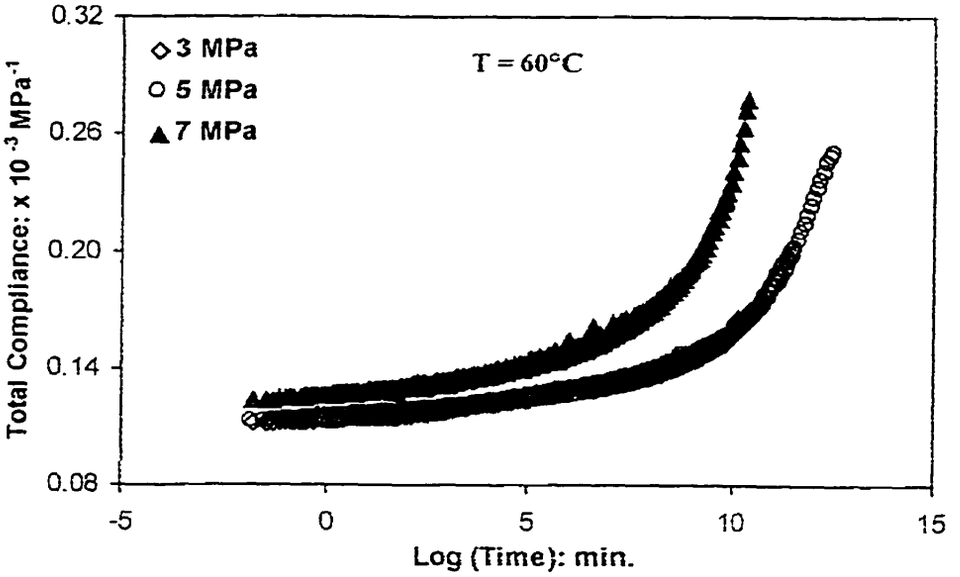

Figure 4.30: Master creep curves at 3, 5, and 7 MPa for $[90]_8$ composite (V_f:71%)

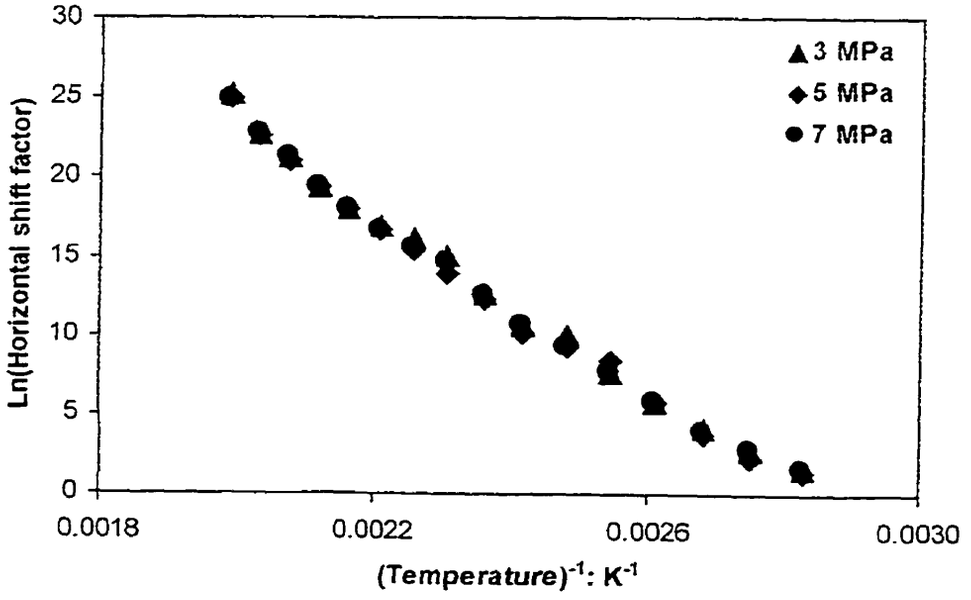

Figure 4.31: Shift factor as a function of inverse temperature at 3, 5, and 7 MPa for $[90]_8$ composite (V_f:71%)

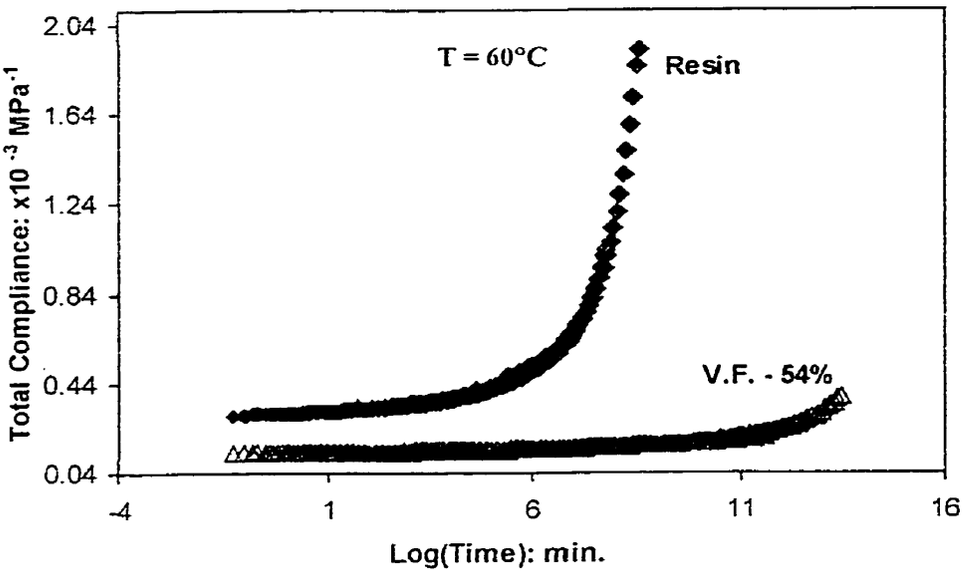

Figure 4.32: Master creep curve at 5 MPa for resin and $[90]_8$ composite (V_f :54%)

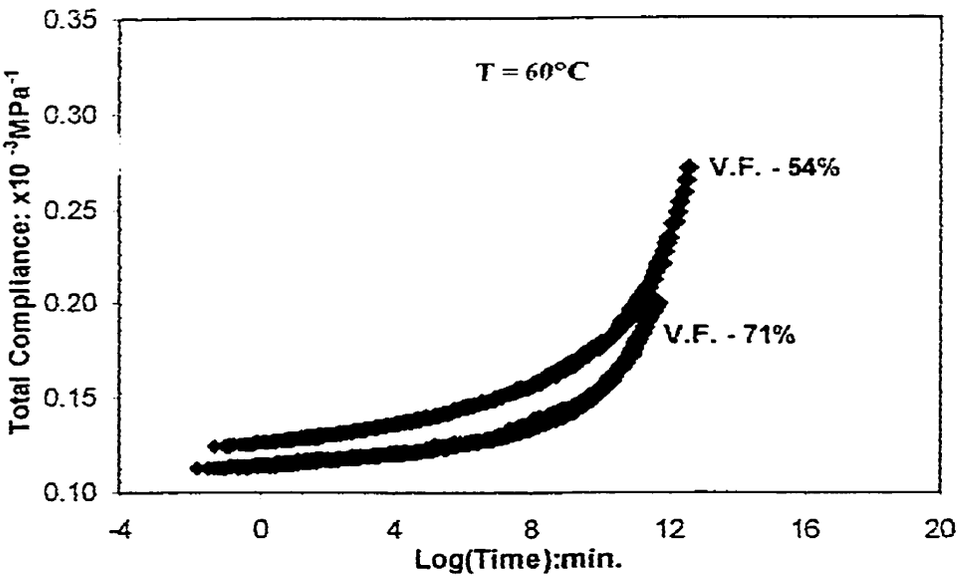

Figure 4.33: Master creep curve at 5 MPa for $[90]_8$ composite with 54% V_f and 71% V_f

A plot of horizontal shift factor versus inverse temperature of $[90]_8$ composite with 71% fiber volume fraction at 3, 5 and 7 MPa shown in Figure 4.31 is non-linear. Figure 4.31 indicates that shift factor at 3 and 5 MPa well. Horizontal shift factor at 7 MPa superimposes with shift factor at 3 and 5 MPa till 150°C and then deviates beyond 150°C. Assuming that the temperature effect on creep can be modeled using an arrhenius relations, activation energies were calculated from slopes of horizontal shift factor versus inverse temperature plot shown in figure 4.31. The activation energy and pre-exponential constant values for 3, 5 and 7 MPa are tabulated in Table 4.6.

4.2.1.4 SUMMARY AND EFFECT OF FIBER VOLUME FRACTION ON CREEP

A comparison of master curves at 5 MPa for resin and 54% composite and for 54% and 71% composite as shown in Figures 4.32-4.33 indicate that creep of resin is retarded by fiber reinforcement (creep compliance decreases with inclusion of fibers). The limit of linear creep region for resin and 54% composite was found to be 7 MPa. However, for 71% composite, the limit of linear creep region was found to be about 5 MPa. Though the limit of linear creep region remained the same for both the resin and the 54% composite, it changed for 71% composite. An increase in fiber volume fraction decreased the creep compliance reducing the creep rate and increased the activation energy (tabulated in Table 4.6).

4.2.2 EFFECT OF PHYSICAL AGING

4.2.2.1 RESIN

Figure 4.34 shows the creep curves for resin that was physically aged for various times at 80°C. As shown in the figure, creep compliance at a given creep time decreased with increase in the aging time, modulus increased. This indicates that creep is retarded by physical aging. The short-term creep curves (momentary) at different aging times were horizontally shifted and superimposed to a reference aging time of 2 hours using TTSP. The master curve of resin at 80°C is shown in Figure 4.35. Despite horizontal shifting, some amount of vertical shifting was needed to account for change in instantaneous compliance with aging time. This vertical shifting was determined from the relation between instantaneous compliance with aging time at various temperatures. This relation was determined using DMA and is given in Table 4.7. The individual master curves for resin at 5 MPa, 7 MPa, 15 MPa, 70% and 85% UTS in the temperature range of 40°C-240°C are shown in Appendix C. A double log plot of horizontal shift factor versus aging time is shown in Figures 4.36-4.38 in the temperature range of 40°C-240°C at 5, 7 and 15 MPa. It is observed that the shift factor increases with increase in aging time at various temperatures. In addition, the aging temperature also affects the rate of physical aging and this is characterized by aging shift rate (μ), which is the slope of the plot in Figures 4.36-4.38. A plot of shift rate as a function of temperature at different stress levels is shown in Figure 4.39. The shift rate slightly increased with temperature and then remained constant except at 200°C, where it peaked. However, the sudden increase in shift rate at 200°C is not fully understood and is thought to be due to process induced residual stresses. Further experimentation is required to understand and

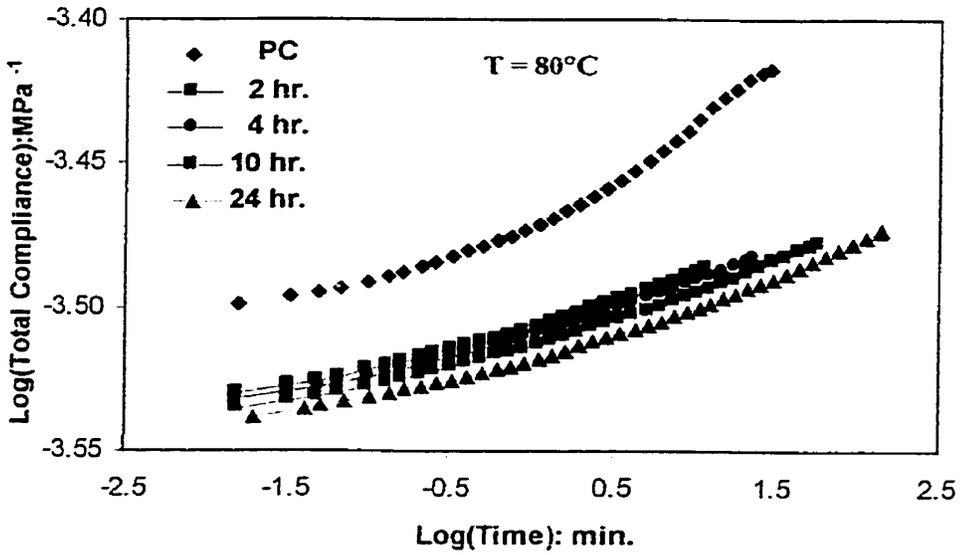

Figure 4.34: Compliance data at 5 MPa for resin at 80°C at various physical aging times

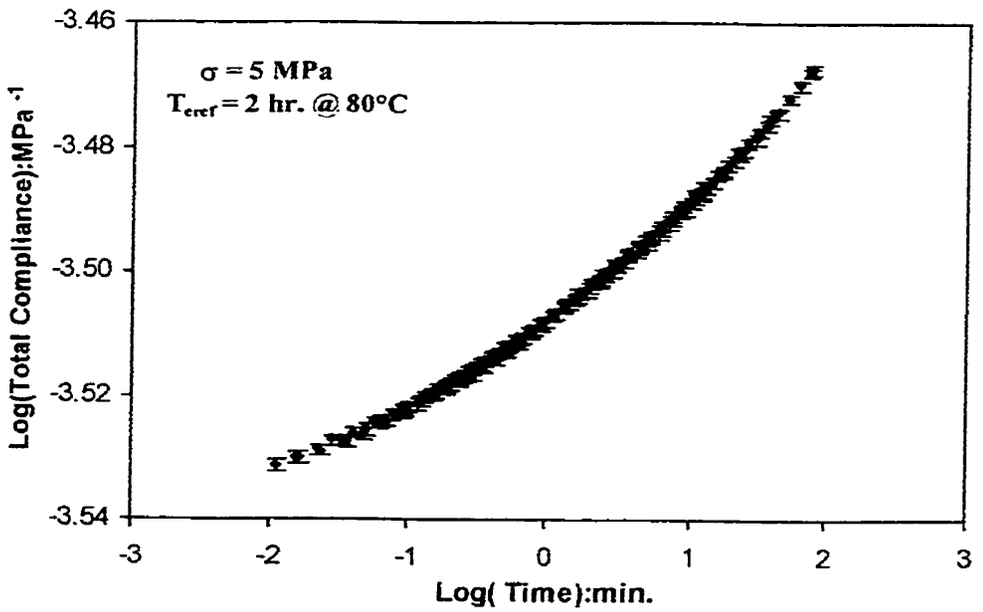

Figure 4.35: Momentary master curve at 5 MPa for resin at 80°C

Temperature (°C)	Slope(B) $MPa^{-1}.Hr^{-1}$		Constant (A) (x 10^{-4}) MPa^{-1}	
	Resin	V_f - 54%	Resin	V_f - 54%
40	1.89×10^{-9}	7.14×10^{-8}	1.11	2.57
60	1.48×10^{-8}	7.43×10^{-8}	1.12	2.64
80	5.28×10^{-8}	1.50×10^{-7}	1.14	2.68
110	-	1.07×10^{-7}	-	1.17
150	-	9.49×10^{-8}	-	1.21
180	1.80×10^{-7}	6.23×10^{-7}	1.38	3.71
200	1.49×10^{-7}	9.06×10^{-7}	1.68	4.26
210	3.40×10^{-7}	3.72×10^{-6}	1.68	4.72
240	3.93×10^{-7}	3.19×10^{-6}	2.13	6.67

Table 4.7: Vertical shift factor for physically aged specimens

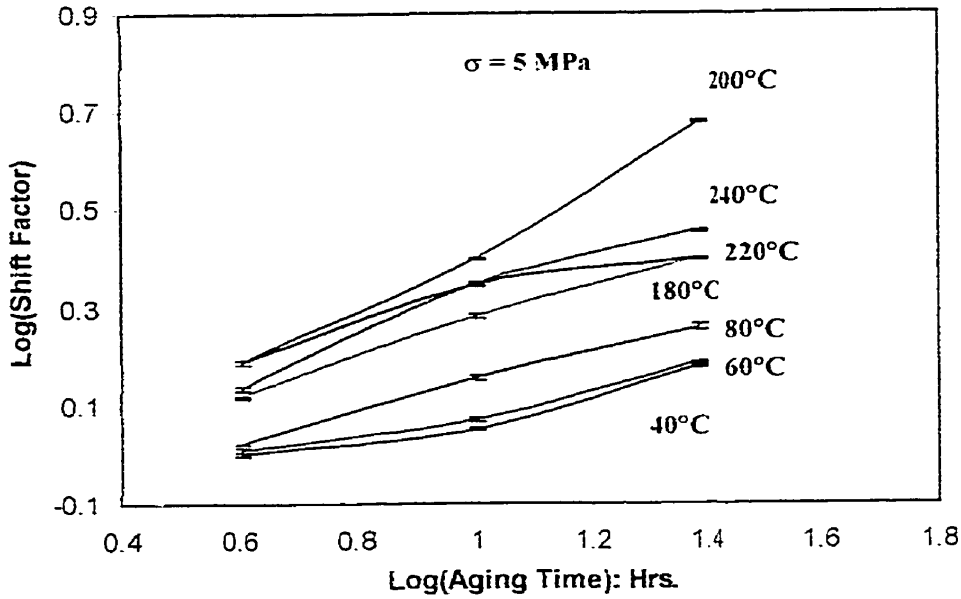

Figure 4.36: Aging shift factor for resin as a function of aging time at 5 MPa

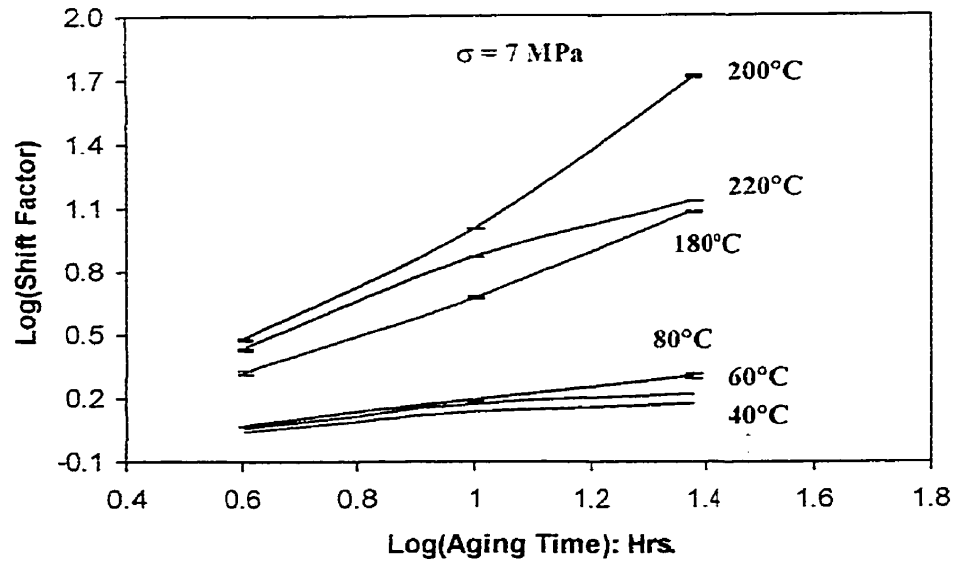

Figure 4.37: Aging shift factor for resin as a function of aging time at 7 MPa

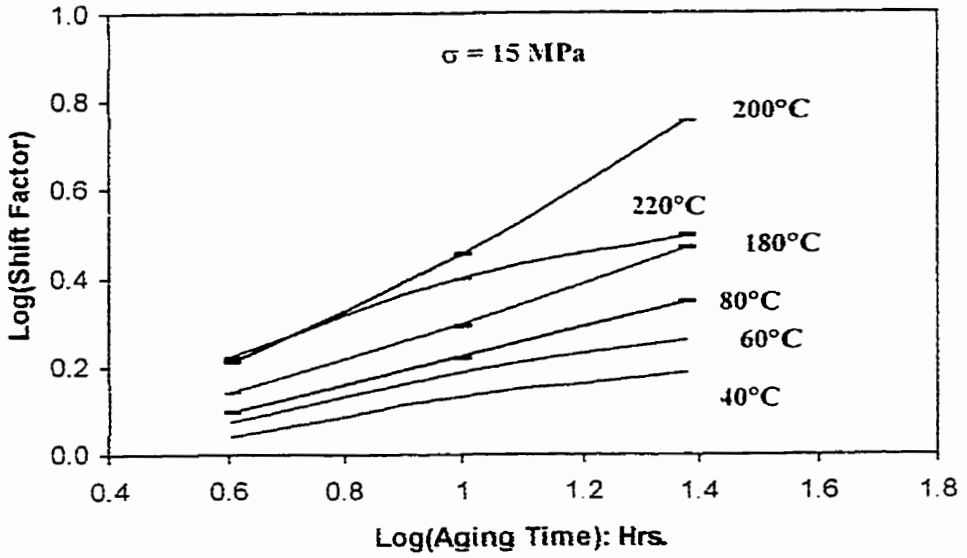

Figure 4.38: Aging shift factor for resin as function of aging time at 15 MPa

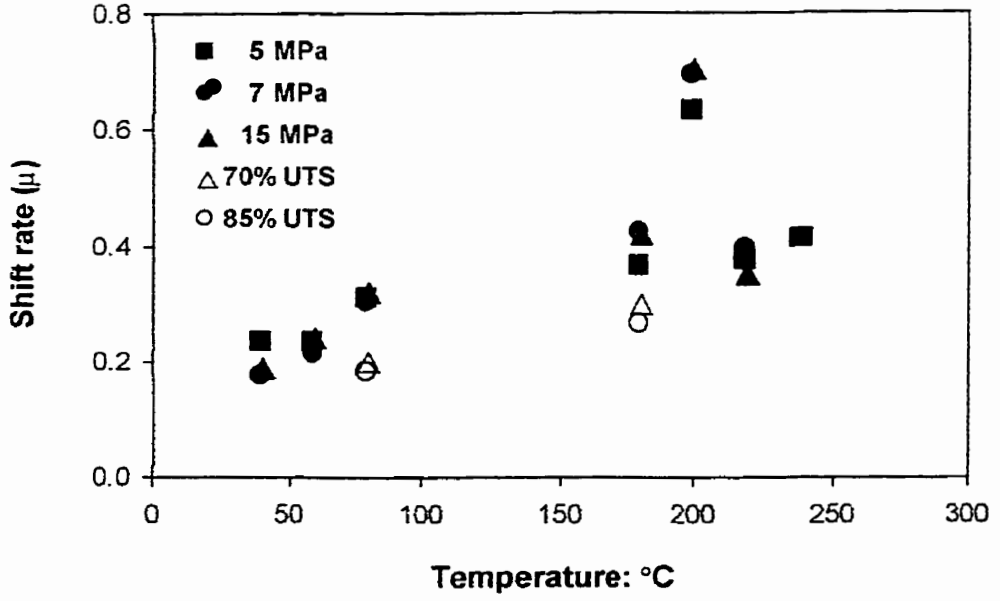

Figure 4.39: Shift rate for resin as a function of temperature at various stress levels

characterize this behavior. The shift rate of resin varied between 0.3 to 0.7. Wang et al. [22] also observed shift rates between 0.3-0.8 for Fiberite 954-2 resin in the temperature range of 140-200°C, which is consistent with the present results. Though the shift rate values reported in literature [14-22] varies from one researcher to another, the magnitude and temperature dependence of shift rates observed in this study is consistent with the other published literature [14-22].

The shift rate remained constant at 5, 7 and 15 MPa for any given temperature. However, beyond 15 MPa (i.e at 70% and 85% UTS), the shift rate decreased at a given temperature. Similar effect of stress on shift rate was noticed by Struik [14]. He has explained this behavior to be due to partial erasing of aging by applied stress. The shift rate will be a useful parameter in determining aging shift rate which are required, in modeling of creep.

4.2.2.2 COMPOSITE WITH 54% FIBER VOLUME FRACTION

Figure 4.40 shows the compliance data at 5 MPa for $[90]_8$ composite with 54% volume fraction that was physically aged for various times at 80°C. As shown in the Figure 4.40, at a given creep time decreased with increase in the aging time, modulus increased. This indicates that physical aging retards creep. Similar to resin, the short-term creep curves (momentary) at different aging times were horizontally shifted and superimposed to a reference aging time of 2 hours using TTSP. The master curve of $[90]_8$ composite with 54% volume fraction at 80°C is shown in Figure 4.41. Despite horizontal shifting, some amount of vertical shifting was needed to compensate for the increase in instantaneous compliance with aging time. Vertical shift factors at different temperatures

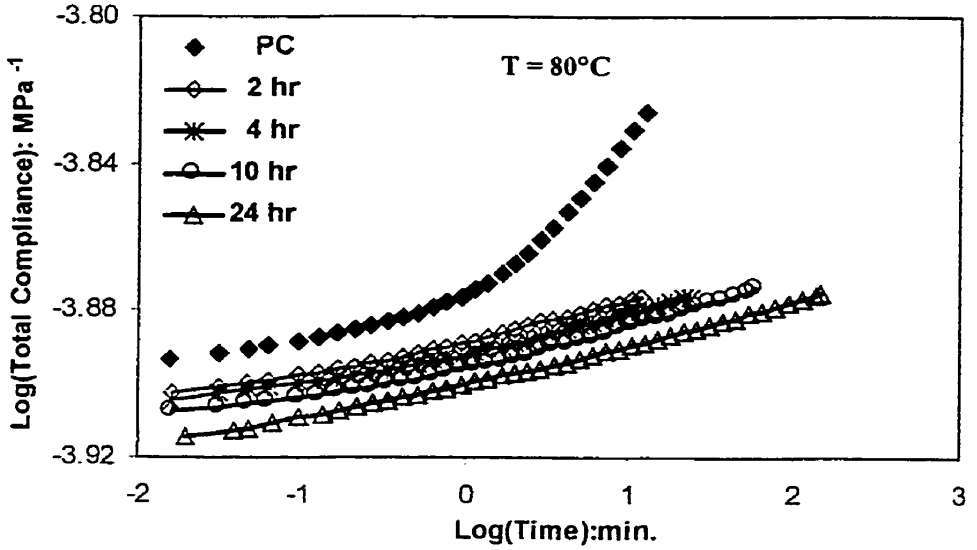

Figure 4.40: Compliance data at 5 MPa for $[90]_8$ composite (V_f :54%) at 80°C at various physical aging times

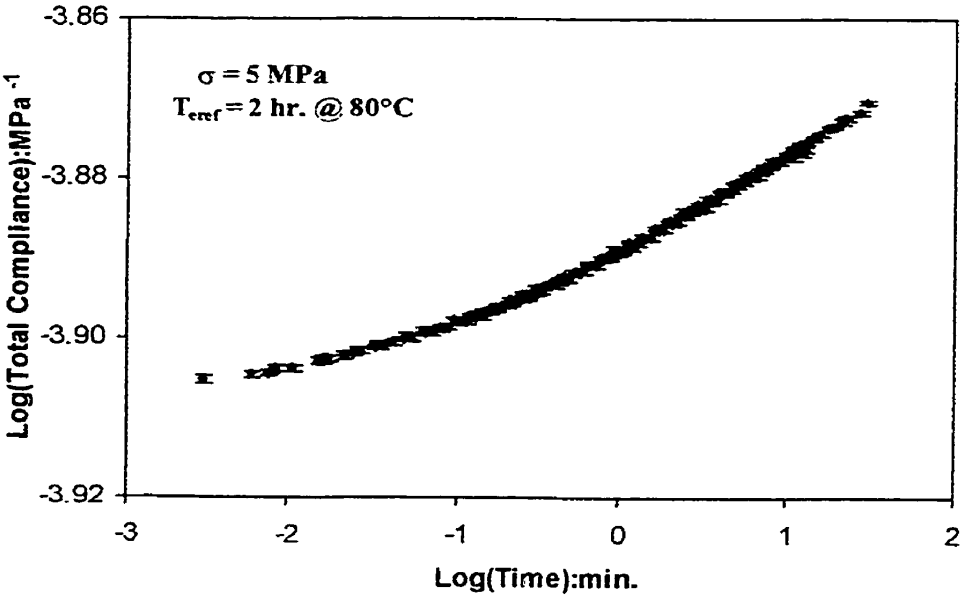

Figure 4.41: Momentary master curve at 5 MPa for $[90]_8$ composite (V_f :54%) at 80°C

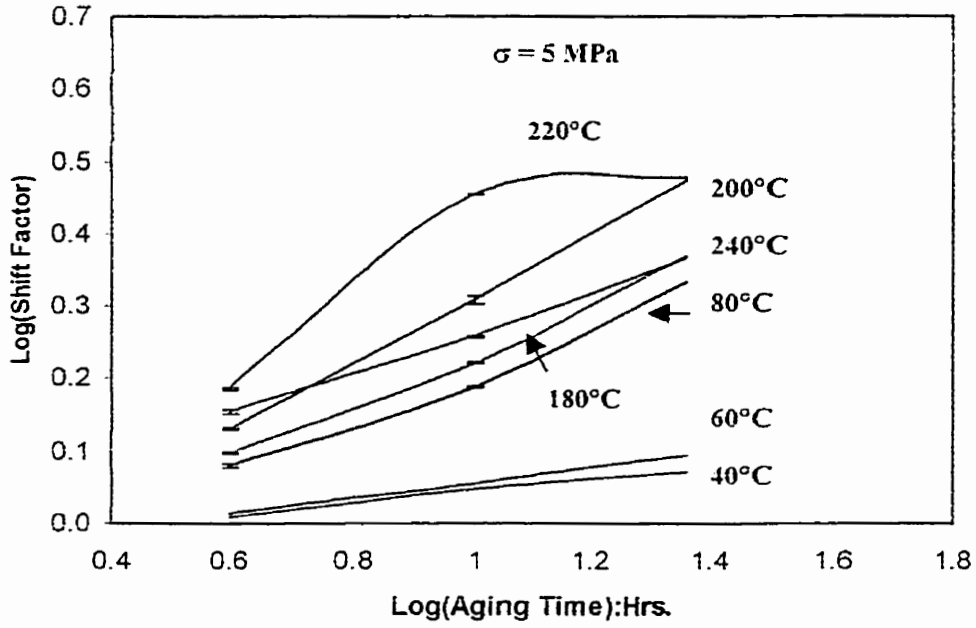

Figure 4.42: Aging shift factor for composite (V_f :54%) as a function of aging time at 5 MPa

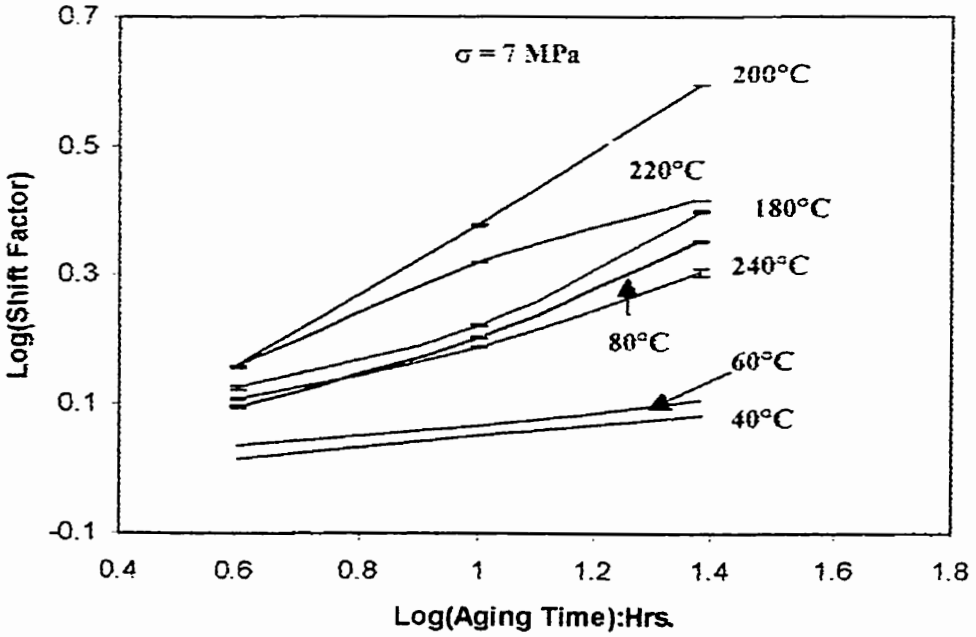

Figure 4.43: Aging shift factor for composite (V_f :54%) as a function of aging time at 7 MPa

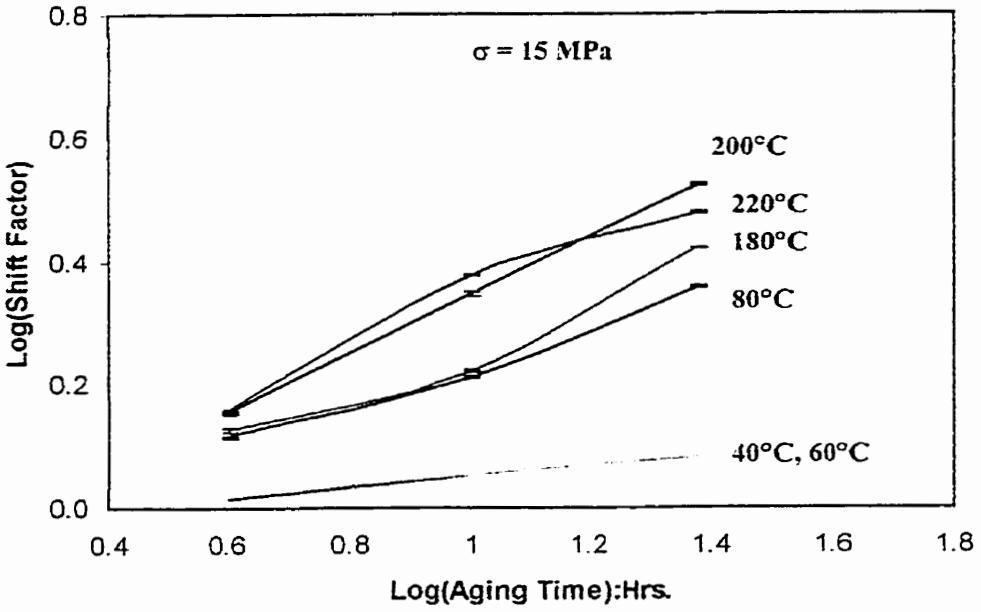

Figure 4.44: Aging shift factor for composite (V_f :54%) as a function for aging time at 15 MPa

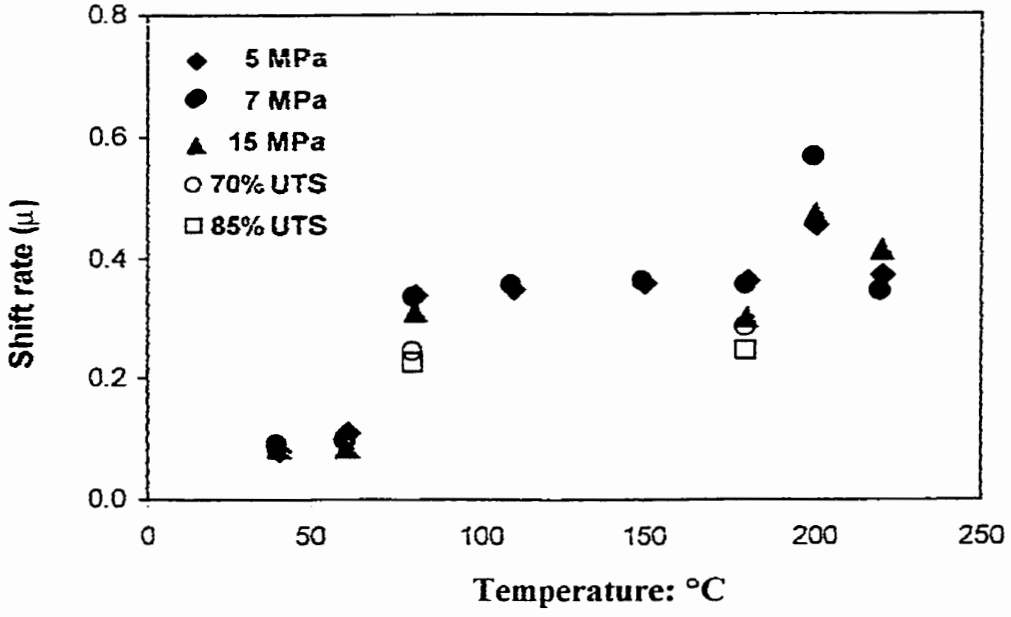

Figure 4.45: Shift rate for composite (V_f :54%) as a function of temperature at various stress levels

for are tabulated in Table 4.7. The individual master curves of $[90]_8$ composite with 54% volume fraction at 5 MPa, 7 MPa, 15 MPa, 70% and 85% of UTS in the temperature range of 40°C-240°C are given in Appendix C. It was observed that horizontal shift factor increased with increase in aging time at different temperatures. In addition, the aging temperature also affects the rate of physical aging and this is characterized by aging shift rate (μ), which is the slope of the plot in Figures 4.42-4.44. A plot of shift rate as a function of temperature at different stress levels is shown in Figure 4.45. Similar to resin, the shift rate of 54% composite slightly increased with temperature and then remained constant except at 200°C, where it peaked. Such a sudden increase in shift rate was also noticed by Gates and Feldman [20] at around 210-215°C for IM7/K3B (carbon/polyimide composite). However, the sudden increase in shift rate at 200°C is not fully understood and is thought to be due to process induced residual stresses. Further experimentation is required to understand and characterize this behavior. The shift rate of 54% composite varied between 0.3 to 0.55. Wang et al. [22] also observed between 0.3-0.8 for 954-2 composite in the temperature range of 140-200°C, which is consistent with the present results. Similar to the resin, the magnitude and temperature dependence of shift rates observed in this study for 54% composite is consistent with the other published literature [14-22].

The shift rate remained constant at 5, 7 and 15 MPa for any given temperature. However, beyond 15 MPa (i.e. at 70% and 85% UTS), the shift rate decreased at a given temperature. Similar influence of stress on shift rate was noticed by Struik [14]. He has explained this behavior to be due to partial erasing of aging by applied stress. The shift

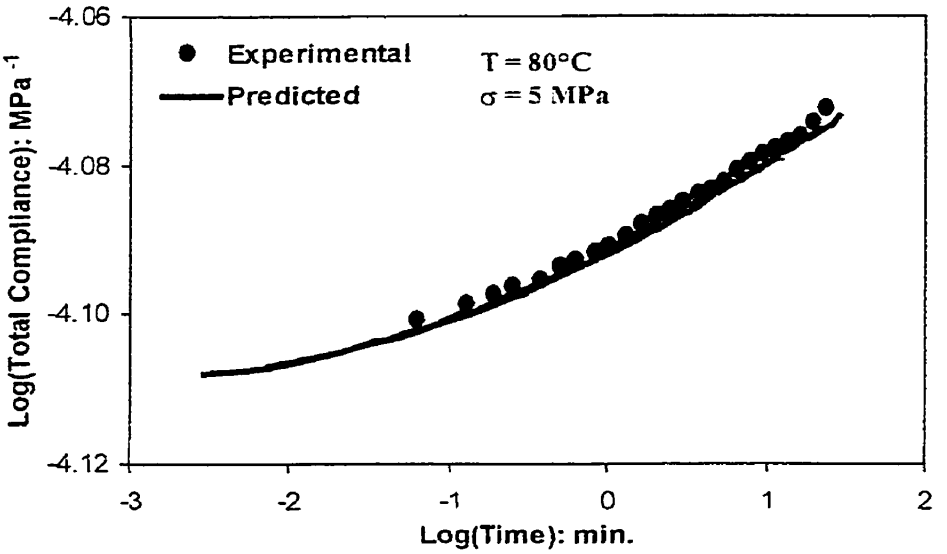

Figure 4.46: Experimental and Predicted compliance data at 5 MPa for composite (V_f :54%) at 80°C

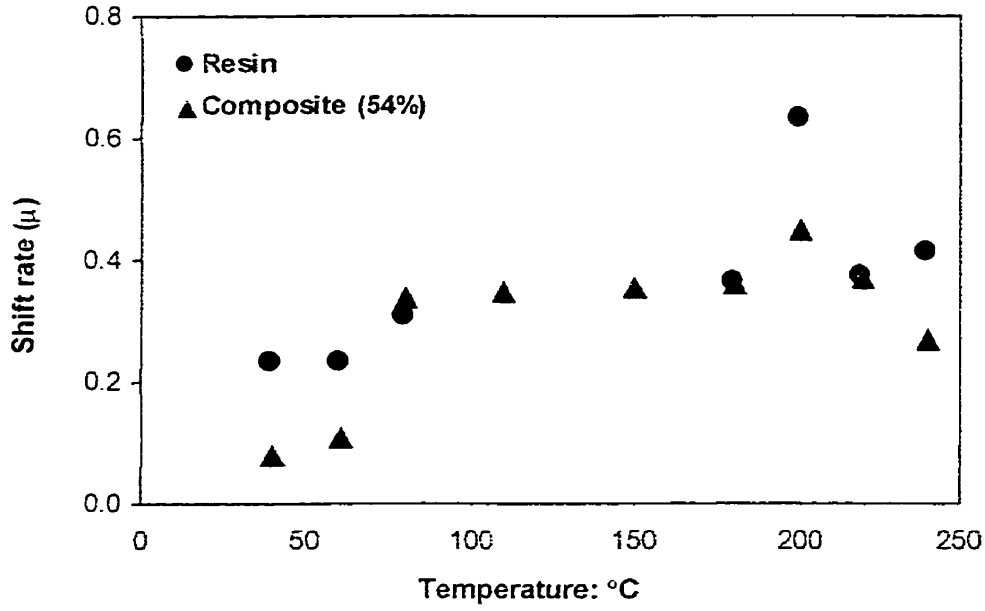

Figure 4.47: Shift rate as a function of temperature for resin and composite (V_f: 54%) at 80°C at 5 MPa

rate will be a useful parameter in determining aging shift rate which are required, in modeling of creep.

To validate the shifting procedure, total compliance data was predicted for an aging time of 1500 hours at 80°C and compared with experimental compliance data aged for 1500 hours at 80°C. The log(horizontal shift factor) versus log(aging time) plot at 80°C for composite was extrapolated to obtain shift factor for an aging time of 1500 hours. The master curve for a reference aging time of 2 hours, shown in Figure 4.41 was shifted using the extrapolated shift factor to obtain creep curve for composite for an aging time of 1500 hours. Figure 4.46 shows the superposition of predicted and experimental compliance data at 80°C. Excellent correlation is observed and this validates the shifting procedure and shift factors obtained in the study.

4.2.2.3 SUMMARY AND EFFECT OF FIBER VOLUME FRACTION ON PHYSICAL AGING

Figure 4.47 shows a plot of shift rate as a function of temperature for resin and 54% composite at 5 MPa. The magnitude of shift rates was found to be same for resin and 54% composite. This is expected since the property of $[90]_8$ composite is dominated by matrix properties. Shift rates were found to be independent of fiber volume fraction except at 200°C. Similar trend in shift rates with fiber volume fraction was noticed by Struik [14], Sullivan [18], and Wang et al. [22].

4.2.3 EFFECT OF MOISTURE

4.2.3.1 RESIN

Figure 4.48 shows experimental total compliance data at 5 MPa for dry (0%) and moisture conditioned (5.27%) at various temperatures. It can be inferred from the Figure 4.48 that the magnitude and the rate of creep increases with increase in moisture content at a given temperature. Similar trend has been reported in literature [25, 49, 50, 54] and has been explained in terms of plasticization of matrix by the absorbed moisture. Rate of creep in a polymer is determined by the mobility of polymer chains. Since the mobility of polymer chains decreases drastically with decrease in temperature below T_g, creep rate of a polymer at a temperature T_1 is determined by how far below the temperature T_1 is from T_g. Since the introduction of moisture in a polymer decreases T_g as shown in Figure 4.49, the mobility of a polymer with moisture will be more than a dry polymer at T_{test} below T_g. This is because $(T_g^{wet} - T_{test,\,1}^{wet})$ which influences molecular mobility for a wet sample will be more than $(T_g^{dry} - T_{test,\,2}^{dry})$ for a dry sample. If the above explanation is valid, then temperature T_{test} for dry and wet sample can be varied such that $(T_g^{wet} - T_{test,\,1}^{wet}) = (T_g^{dry} - T_{test,\,2}^{dry})$. Hence the creep of dry sample tested at a temperature $T_{test,\,2}$ will be equal to that of a wet sample at $T_{test,\,1}^{wet}$ i.e. $[T_{test,\,2}^{dry} = [(T_g^{dry} - T_g^{wet}) + T_{test,\,1}^{wet}]]$ (Please note that $T_{test}^{dry} > T_{test}^{wet}$). A plot of moisture content as a function of glass transition temperature (T_g) is shown in Figure 4.49. As shown in Figure 4.49, T_g of resin decreases from 270°C (0% moisture content) to 179°C (5.27% moisture content) i.e. a total decrease of 91°C. Thus, the total compliance of 5.27% moisture conditioned sample at 80°C was found to be same as that of dry sample at 170°C, shown in Figure 4.50. Similarly, the total compliance of 5.27% moisture conditioned samples at 40°C and 60°C

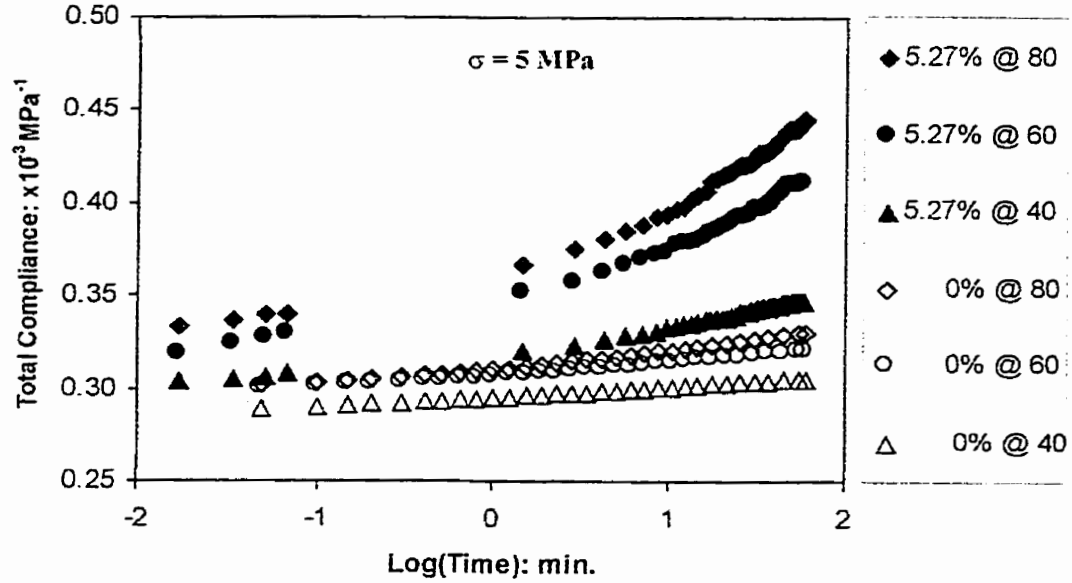

Figure 4.48: Compliance data at 5 MPa for dry and moisture conditioned resin at various temperatures

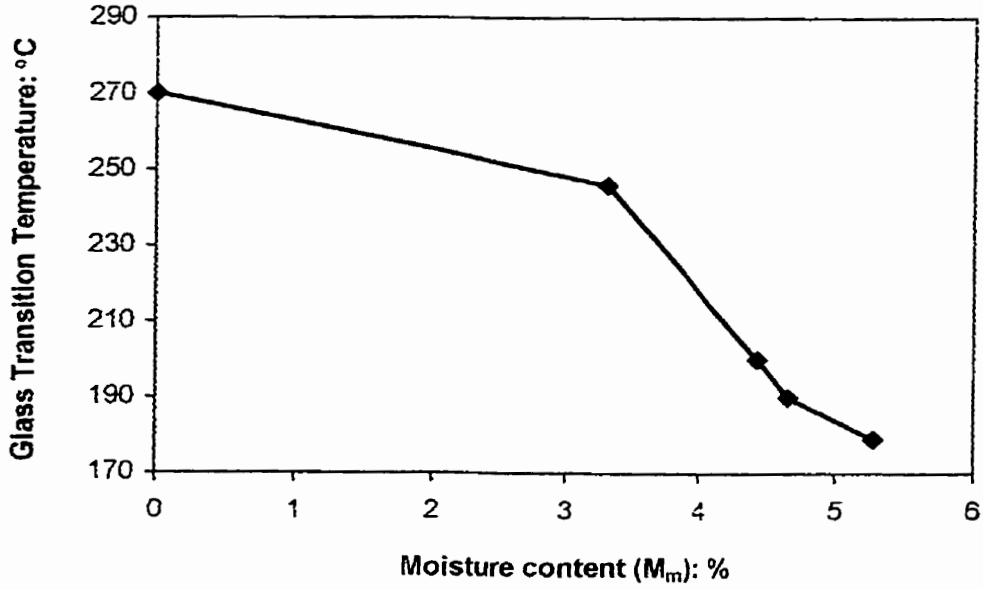

Figure 4.49: Glass transition temperature of resin as a function of moisture content

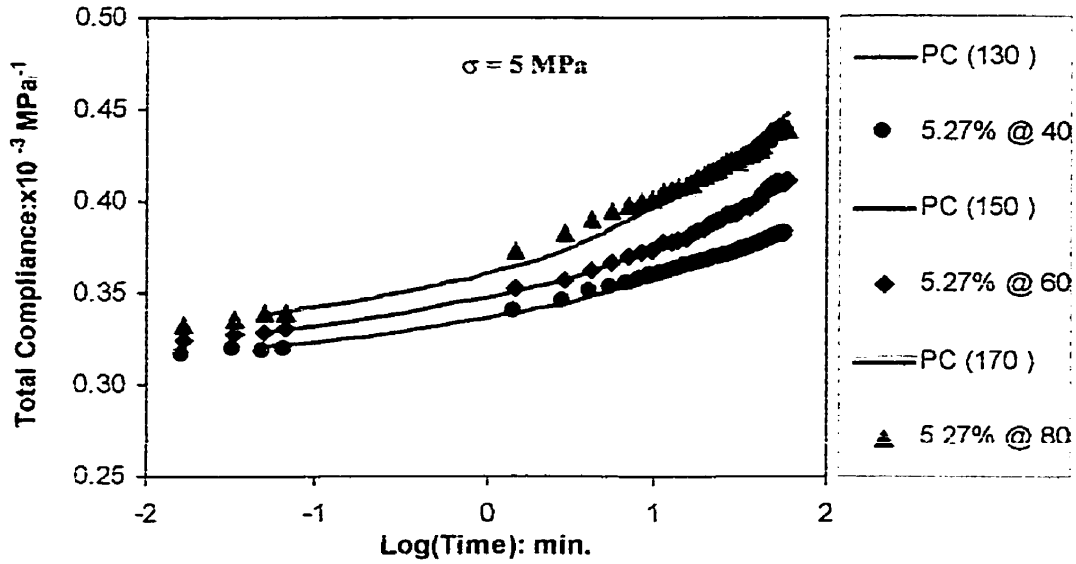

Figure 4.50: Validation of mechanism of creep acceleration by moisture for resin at 5 MPa

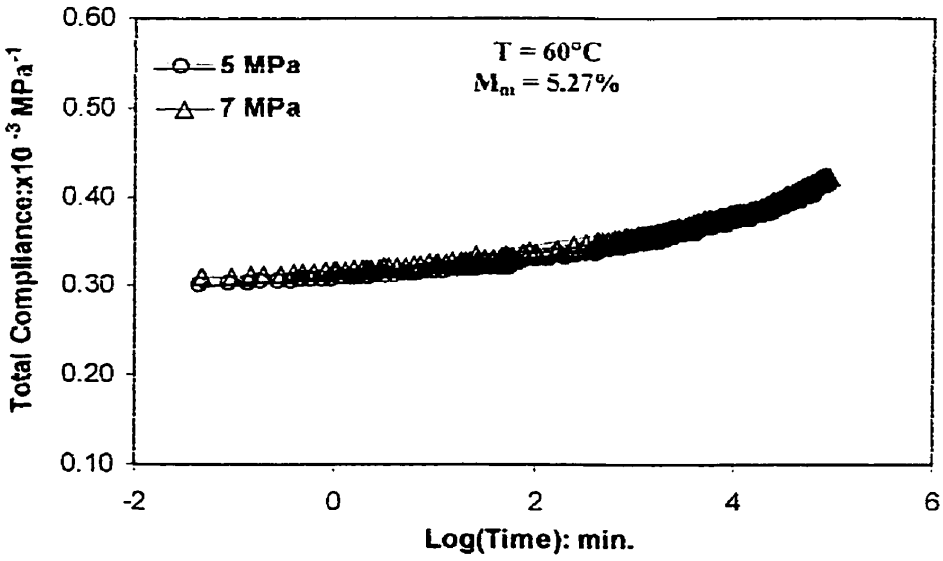

Figure 4.51: Master creep curve at 5 and 7 MPa for moisture conditioned resin

Fiber Volume Fraction (%)	Slope(B) (x 10^{-7}) $MPa^{-1}.K^{-1}$			Constant (A) (x 10^{-5}) MPa^{-1}		
	2%	3%	5.27%/3.50%	2%	3%	5.27%/3.50%
0 (Resin)	5.72	5.73	5.74	9.51	9.25	9.15
54	1.52	1.53	1.55	6.66	6.70	6.70

Table 4.8: Equation parameters for moisture conditioned specimens

was found to be same as that of dry sample at 130°C and 150°C respectively. Similar trend was observed for resin at 7 MPa shown in Appendix D. The experimental compliance data for 2% and 3% moisture conditioned resin at 5 MPa, 7 MPa, 70%UTS and 85% UTS at various temperatures is shown in Appendix D.

The compliance curves for moisture content, at different temperatures were shifted and superimposed to a reference temperature of 60°C using TTSP. Horizontal and vertical shifting were used to obtain a smooth master curve. Vertical shift factor was obtained from the slope of temperature versus modulus plot. The modulus values were obtained from the slope of stress-strain plot for given moisture content at different temperatures. The equation and vertical shifting procedure was similar to as discussed in section 4.2.1.1. The slope and constant values for various moisture contents are tabulated in Table 4.8. Figure 4.51 shows the master creep curve of moisture conditioned (5.27%) resin at 5 and 7 MPa at 60°C. It was observed that creep curve at 5 MPa superimposes with creep curve at 7 MPa, suggesting creep to be in the linear region at these stress levels. This suggests that moisture does not influence the linear-nonlinear creep transition in resin. Master creep curves for 2 % and 3% moisture conditioned resin at 5 and 7 MPa are shown in Appendix D. However, creep curves at 70% and 85% UTS (shown in Appendix D) didn't superimpose suggesting creep to be in non-linear region beyond 7 MPa, similar to dry resin.

Figure 4.52 shows a plot of horizontal shift factor as a function of temperature for 5.27% moisture conditioned resin at 5 and 7 MPa. The superposition of shift factors at 5 and 7 MPa indicates creep to be in the linear region at these stress levels. The plot of shift factor of resin as a function of temperature for 2 % and 3% moisture contents is

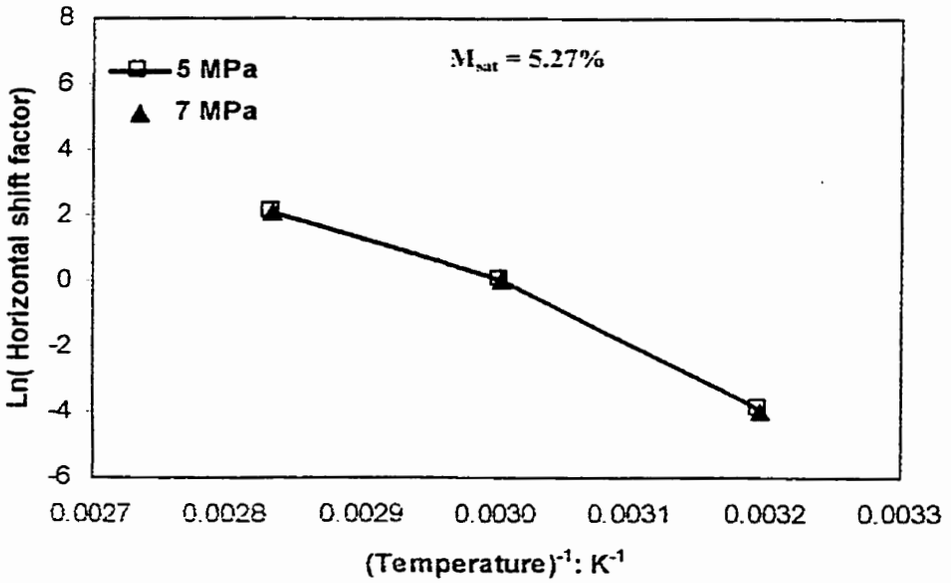

Figure 4.52: Shift factor for moisture conditioned resin as a function of temperature at 5 and 7 MPa

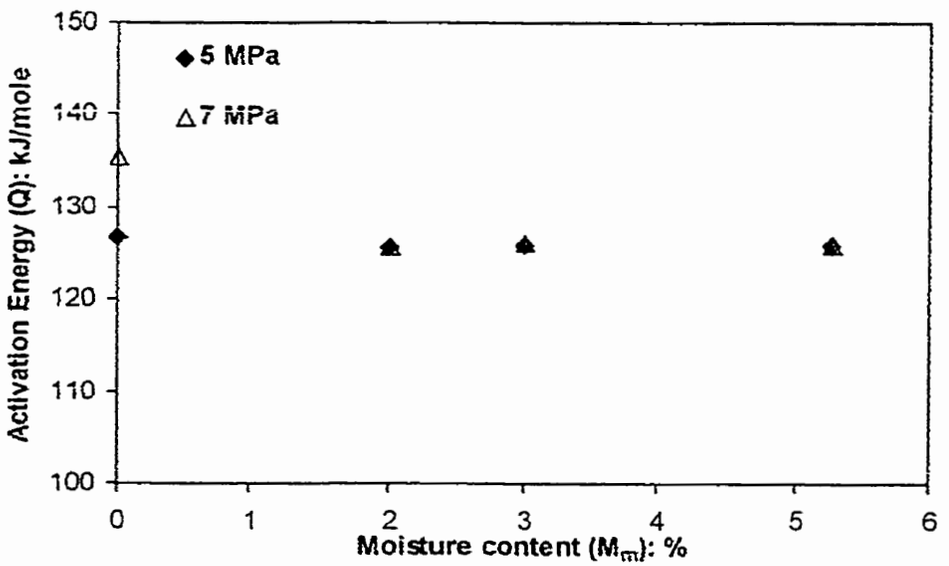

Figure 4.53: Activation energy of resin as function of moisture content at 5 and 7 MPa

Stress (MPa)	Activation Energy (kJ/mole)						Pre-exponential factor					
	Resin			V_f : 54%			Resin			V_f : 54%		
	2%	3%	5.27%	2%	3%	3.50%	2%	3%	5.27%	2%	3%	3.50%
5	124	125	125	197	198	199	55.1	51.8	49.4	69.4	66.4	62.9
7	125	126	127	198	199	200	55.1	51.8	49.5	69.5	66.5	63.0

Table 4.9: Activation energy and Pre-exponential factor values for moisture conditioned resin and composite (V_f : 54%) at various stress levels

shown in Appendix D. Activation energy was determined from the slope of the plot shown in Figure 4.52. The activation energies of dry (0%) and moisture conditioned (2, 3, & 5.27%) resin were found to be nearly same shown in Figure 4.53, indicating that creep acceleration was due to plasticization. The activation energy and pre-exponential factor values for resin at different moisture contents are tabulated in Table 4.9. During modeling on creep the effect of moisture is accounted for through this pre-exponential factor.

4.4.3.2 COMPOSITE WITH 54% FIBER VOLUME FRACTION

Figure 4.54 shows experimental total compliance data at 5 MPa for dry (0%) and moisture conditioned (5.27%) $[90]_{12}$ composite with 54% volume fraction at different temperatures. Similar to resin, it can be inferred from the Figure 4.54 that the magnitude and the rate of creep increases with increase in moisture content at a given temperature Moisture accelerates creep process through plasticization (reduction in T_g) of matrix (resin) as discussed in section 4.2.3.1. A plot of moisture content as a function of glass transition temperature (T_g) is shown in Figure 4.55. As shown in Figure 4.55, T_g of 54% composite decreases from 270°C (0% moisture content) to 221°C (3.50% moisture content) i.e. a total decrease of 49°C. Thus, the total compliance of 3.50% moisture conditioned sample at 80°C was found to be same as that of dry sample at 130°C, shown in Figure 4.56. Similarly, the total compliance of 3.50% moisture conditioned samples at 40°C and 60°C was found to be same as that of dry sample at 90°C and 110°C respectively. Similar trend was observed for composite at 7 MPa shown in Appendix D. The experimental compliance data for 2% and 3% moisture conditioned composite at 5 MPa, 7 MPa, 70% and 85% UTS at different temperatures is shown in Appendix D.

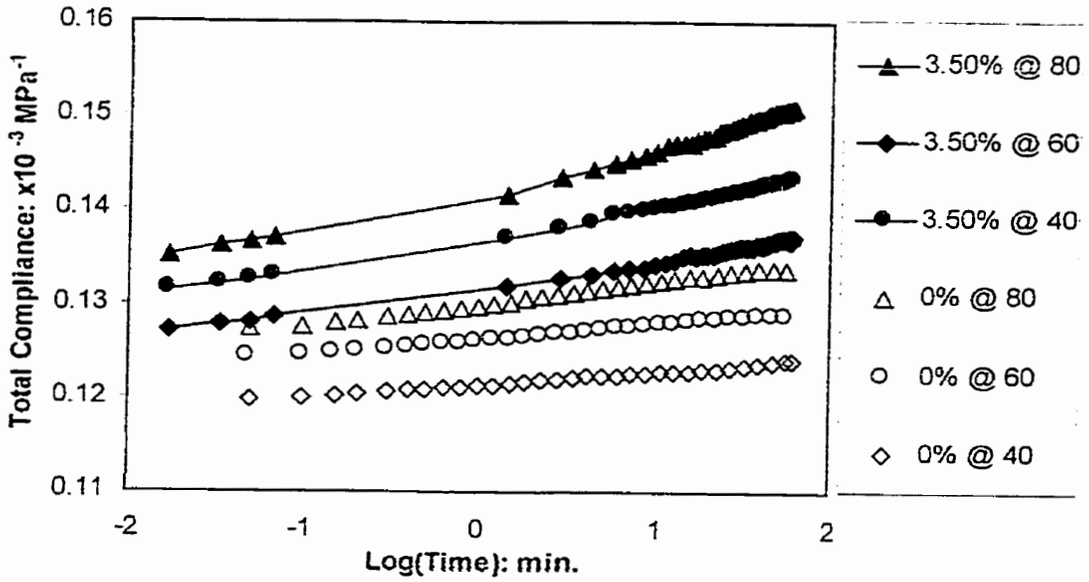

Figure 4.54: Compliance data at 5 MPa for dry and moisture conditioned $[90]_{12}$ composite (V_f : 54%) at various temperatures

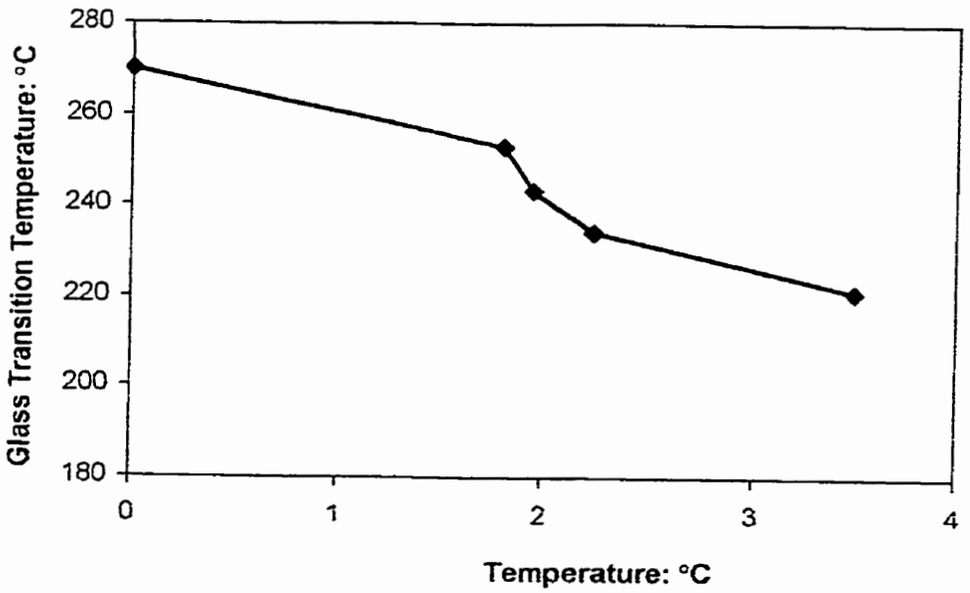

Figure 4.55: Glass transition temperature of $[90]_8$ composite (V_f :54%) as a function of moisture content

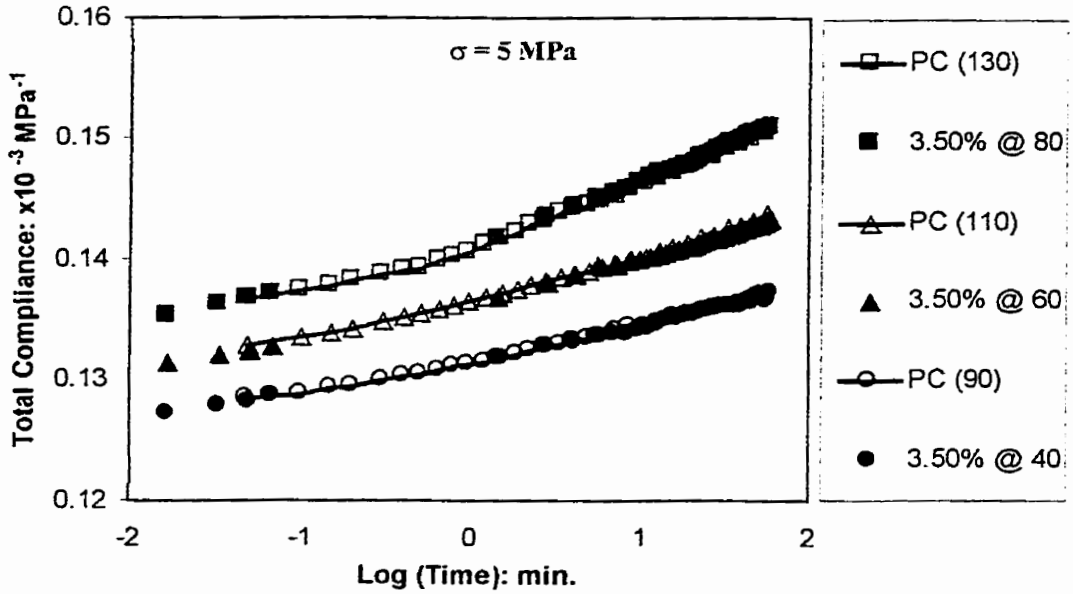

Figure 4.56: Validation of mechanism of creep acceleration by moisture for composite (V_f :54%) at 5 MPa

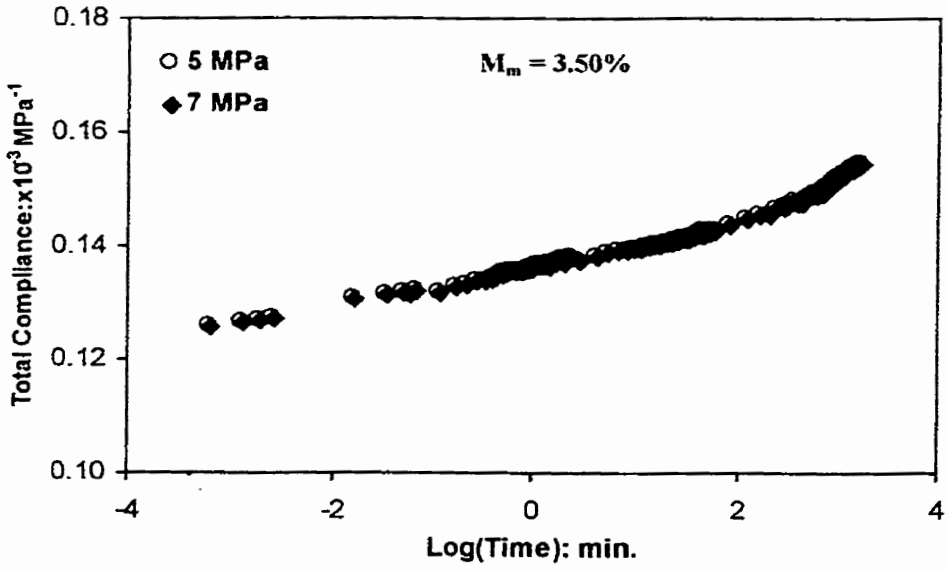

Figure 4.57: Master creep curve at 5 and 7 MPa for moisture conditioned $[90]_{12}$ composite (V_f :54%)

Similar to resin, the compliance curves at different temperatures were shifted and superimposed to a reference temperature of 60°C using TTSP. Horizontal and vertical shifting were used to obtain a smooth master curve. The modulus values were obtained from the slope of stress-strain plot for given moisture content at different temperatures. The equation and vertical shifting procedure was same as discussed in section 4.2.1.1. The slope and constant values for various moisture contents are tabulated in Table 4.8. Figure 4.57 shows the master creep curve of moisture conditioned composite at 5 and 7 MPa at 60°C. Similar to resin, it was observed that creep curve at 5 MPa superimposes with creep curve at 7 MPa, suggesting creep to be in linear region at these stress levels. Similar to resin, moisture does not influence the linear-non linear creep transition. However, creep curves at 70% and 85% UTS didn't superimpose suggesting creep to be in non-linear region beyond 7 MPa.

Figure 4.58 shows a plot of horizontal shift factor as a function of moisture content at 5 and 7 MPa. It was observed that shift factor increased with increase in moisture content. The superposition of shift factors at 5 and 7 MPa indicates creep to be in linear region at these stress levels. The plot of shift factor of composite as a function of temperature at 2 % and 3% moisture contents is shown in Appendix D. Similar to resin, activation energy was determined from the slope of plot shown in Figure 4.58. The activation energies of dry (0%) and moisture conditioned (2, 3, & 3.50%) composite were found to be nearly same shown in Figure 4.59, indicating that creep acceleration was due to plasticization of matrix (resin). The activation energy ands pre-exponential factor values for $[90]_{12}$ composite with 54% volume fraction at different moisture contents mare tabulated in Table 4.9.

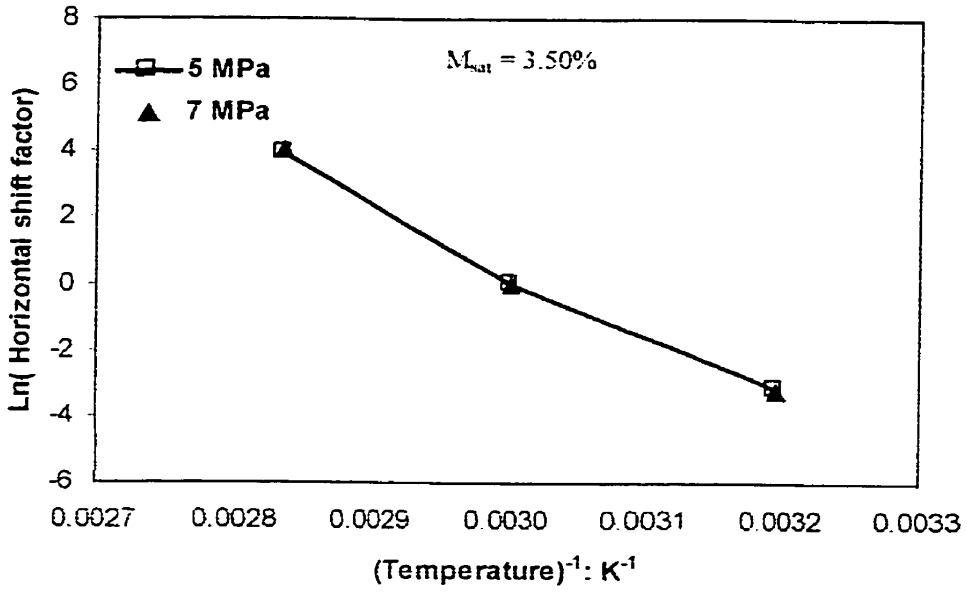

Figure 4.58: Shift factor for moisture conditioned $[90]_{12}$ composite (V_f :54%) as a function of temperature at 5 and 7 MPa

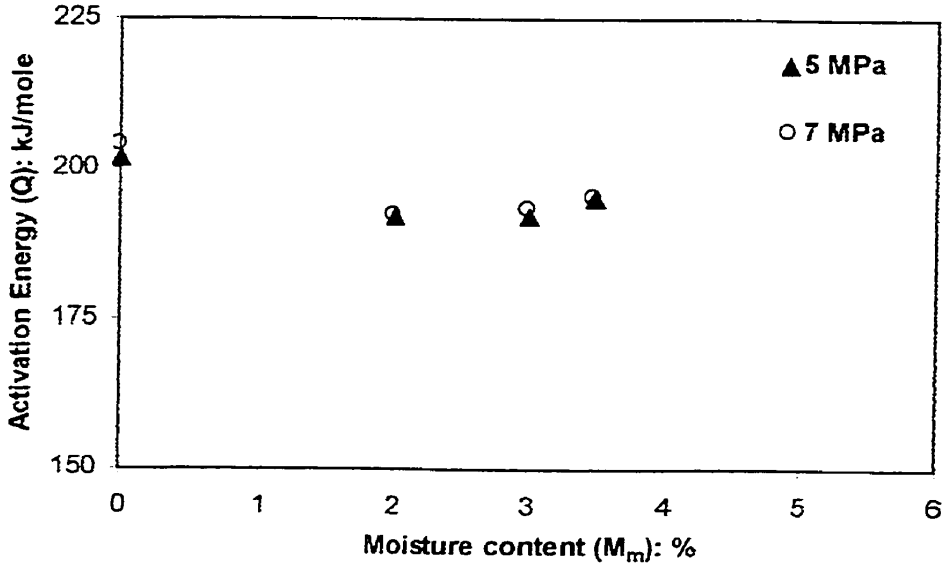

Figure 4.59: Activation energy of $[90]_{12}$ composite (V_f :54%) as a function of moisture content at 5 and 7 MPa

4.2.4 INTERACTIVE EFFECT OF STRESS, TEMPERATURE, MOISTURE, PHYSICAL AGING AND FIBER VOLUME FRACTION

4.2.4.1 RESIN

Figure 4.60 shows experimental total compliance data at 5 MPa for aged and moisture conditioned (16.6 days, 4.40%) resin at various temperatures. The experimental total compliance data at 7 MPa, 70% and 85% UTS is shown in Appendix E. TTSP was used to shift and superimpose the compliance curves to a reference temperature of 60°C. Horizontal and vertical shifting were used to obtain a smooth master curve shown in Figure 4.61 at 5 and 7 MPa. Vertical shift factor was obtained from the slope of temperature versus modulus plot. The modulus values were obtained from the slope of stress-strain plot at different temperatures for aged (16.6 days) resin with 4.40% moisture content. The equation and procedure used to vertically shift a creep curve at a temperature (T_1) to the creep curve at reference temperature (T_{ref}) was same as discussed in section 4.2.1.1. The slope and constant values are tabulated in Table 4.10. It was observed that creep curve at 5 MPa does not superimpose with creep curve at 7 MPa, suggesting creep to be in the non-linear region at above 5 MPa. This suggests that aging and moisture in combination, influences the linear-nonlinear creep transition in resin. A plot of shift factor as a function of temperature is shown in Figure 4.62. Superposition of shift factors at 5 and 7 MPa indicates that creep mechanism is not altered.

In order to understand the interactive effect, the compliance data at 5 MPa for postcured (PC), Aged (PA –16.6 days), Moisture conditioned (M – 5.25%), and Aged-Moisture conditioned (PA+M: 16.6 days + 4.40%) resin at 80°C are plotted together shown in Figure 4.63. As shown in Figure 4.63, aging retards creep and moisture

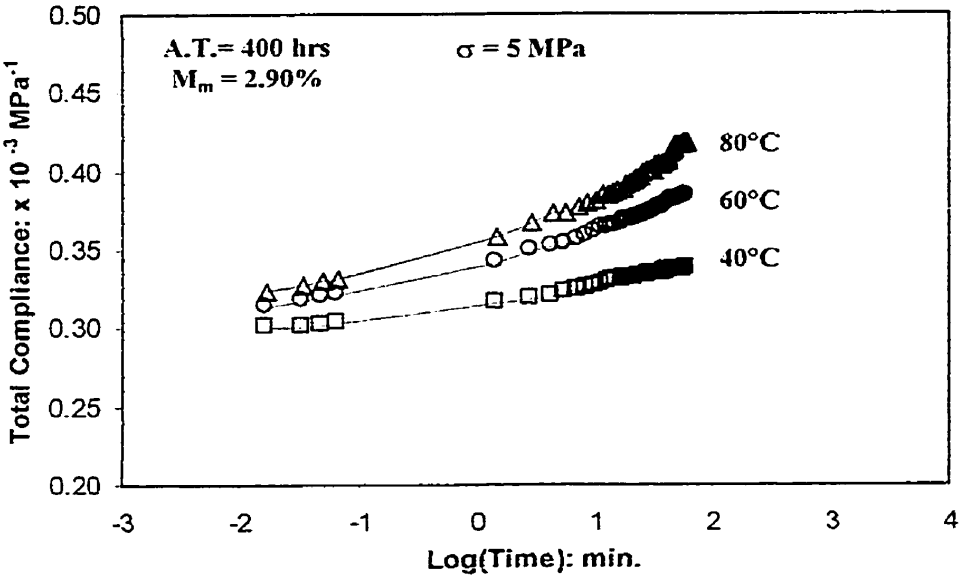

Figure 4.60: Compliance data at 5 MPa for aged-moisture conditioned resin at various temperatures

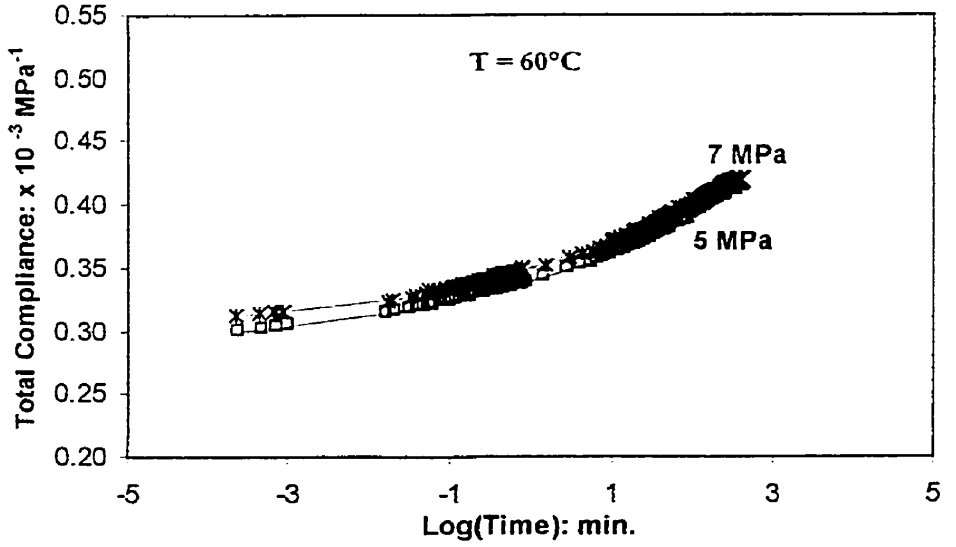

Figure 4.61: Master creep curve at 5 MPa and 7 MPa for aged-moisture conditioned resin

Fiber Volume Fraction (%)	Slope(B) ($\times 10^{-7}$) $MPa^{-1}.K^{-1}$	Constant (A) ($\times 10^{-5}$) MPa^{-1}
0 % (Resin)	5.70	9.30
54%	1.50	6.50

Table 4.10: Equation parameters for Aged – moisture conditioned specimens

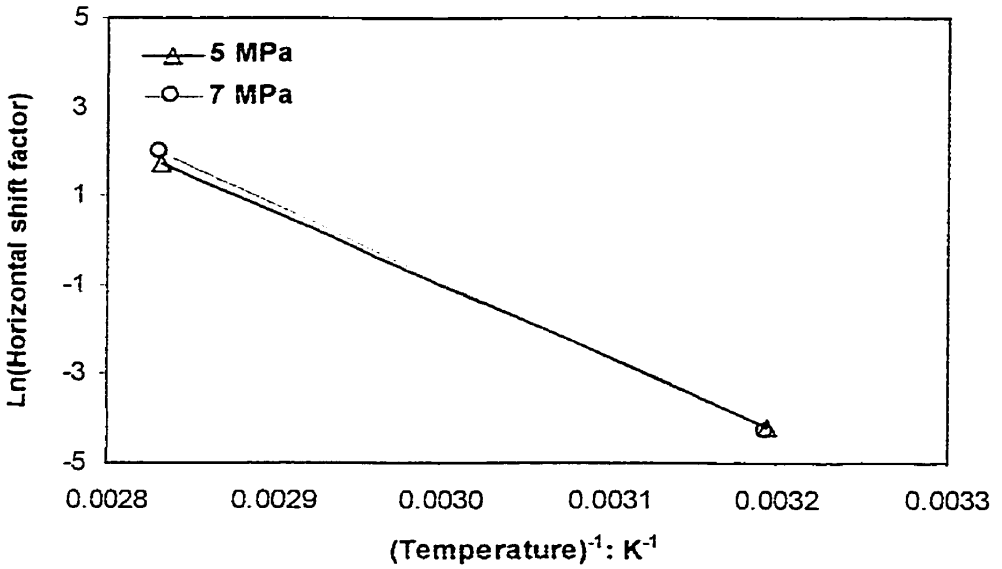

Figure 4.62: Shift factor for aged-moisture conditioned resin as a function of temperature at 5 MPa and 7 MPa

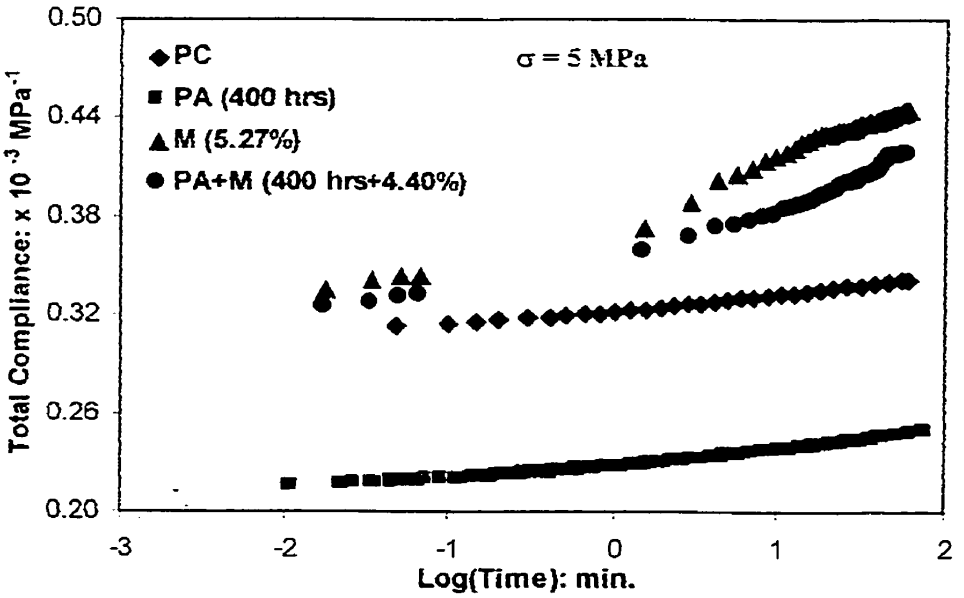

Figure 4.63: Compliance data at 5 MPa for postcured, aged, moisture conditoned and aged-moisture conditioned resin at 80°C

Moisture level (%)		Aging condition (Hrs.)	Tg(°C)		$\Delta T_g = T_g^{dry} - T_g^{wet}$	
Resin	**V_f : 54%**		**Resin**	**V_f : 54%**	**Resin**	**V_f : 54%**
0	0	Unaged	270	270	-	-
5.27	3.50	Unaged	179	221	91	49
4.95	3.44	Unaged	181	222	89	48
		168	183	226	87	44
4.89	3.20	Unaged	182	223	88	47
		200	187	227	83	43
4.60	3.09	Unaged	184	224	86	46
		300	189	230	81	40
4.40	2.90	Unaged	185	225	85	45
		400	190	231	80	39

Table 4.11: Reduction of glass transition temperature at different moisture contents

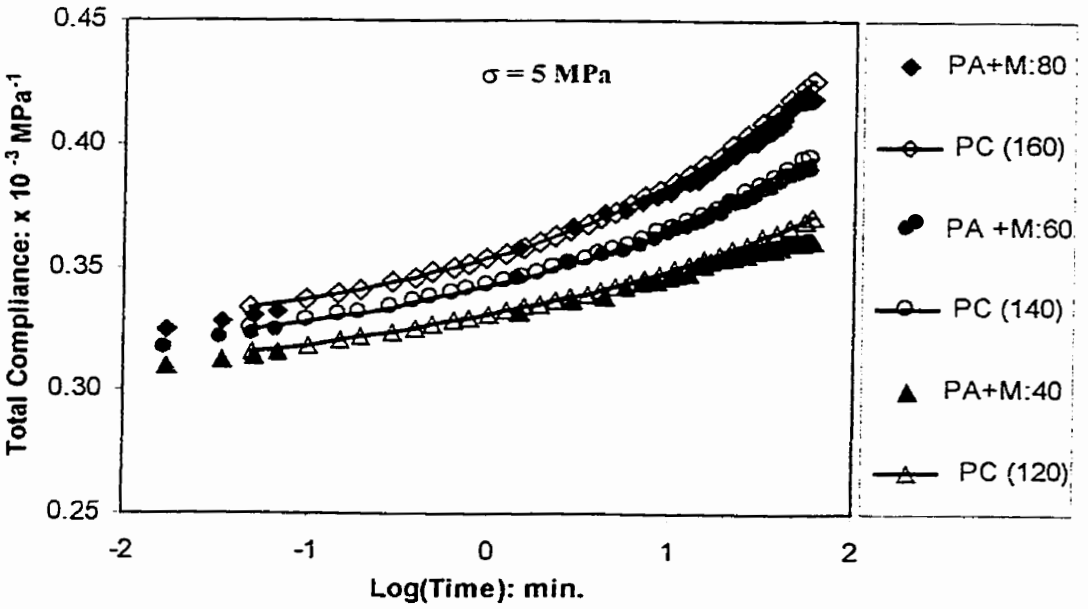

Figure 4.64: Validation of mechanism for interactive influence of aging and moisture for resin at 5 MPa

Stress (MPa)	Activation Energy (kJ/mole)		Pre-exponential factor	
	Resin	V_f : 54%	Resin	V_f : 54%
5	120	190	51.8	63.4
7	122	195	48.7	61.9

Table 4.11: Activation energy and Pre-exponential factor values for aged-moisture conditioned resin and composite (V_f : 54%) at various stress levels

accelerates creep. The creep acceleration for combined effect of aged –moisture conditioned sample at a constant temperature was found to be less than that non-aged moisture conditioned sample. The difference in creep acceleration was found to be due to difference in magnitude of matrix plasticization, between non-aged and aged resin, by absorbed moisture as shown in Table 4.11. A non-aged sample with 4.40% moisture content experienced a reduction in Tg by 85°C, while the aged samples experienced a reduction in T_g by 80°C for the same amount of moisture. The creep of aged resin with 4.4% moisture content at 80°C was found to be same as that of non-aged sample at 160°C shown in Figure 4.64. However, the creep of non-aged sample at 80°C is same as creep of non-aged dry sample with 4.40% moisture content. Similarly, compliance of aged resin with 4.4% moisture content at 40°C and 60°C were found to be same as that of non-aged dry sample at 120°C and 140°C respectively. Similar results were obtained at 7 MPa shown in Appendix E. Thus, it can be concluded that combined effect of aging and moisture decreased the magnitude of plasticization as compared to non-aged samples containing the same amount of moisture for a given temperature and stress level. The activation energy and pre-exponential factor values for resin are tabulated in Table 4.12

4.2.4.2 COMPOSITE WITH 54% FIBER VOLUME FRACTION

Figure 4.65 shows experimental total compliance data at 5 MPa for aged and moisture conditioned (16.6 days, 2.90%) 54% composite at different temperatures. TTSP was used to shift and superimpose the compliance curves to a reference temperature of 60°C. Horizontal and vertical shifting was done to obtain a smooth master curve shown in Figure 4.66 at 5 and 7 MPa. Vertical shift factor was obtained from the slope of

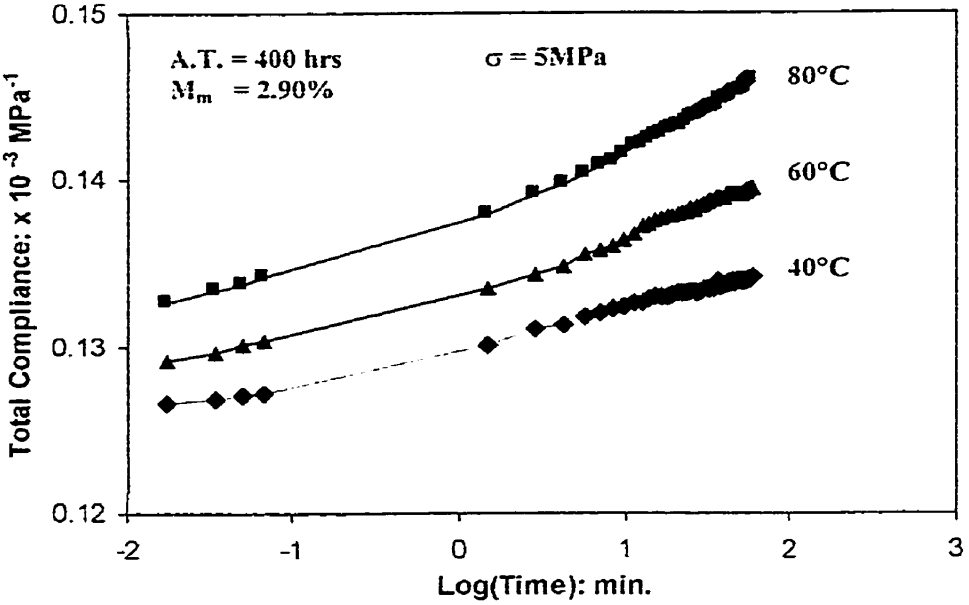

Figure 4.65: Compliance data at 5 MPa for $[90]_{12}$ aged-moisture conditioned composite (V_f:54%) at various temperatures

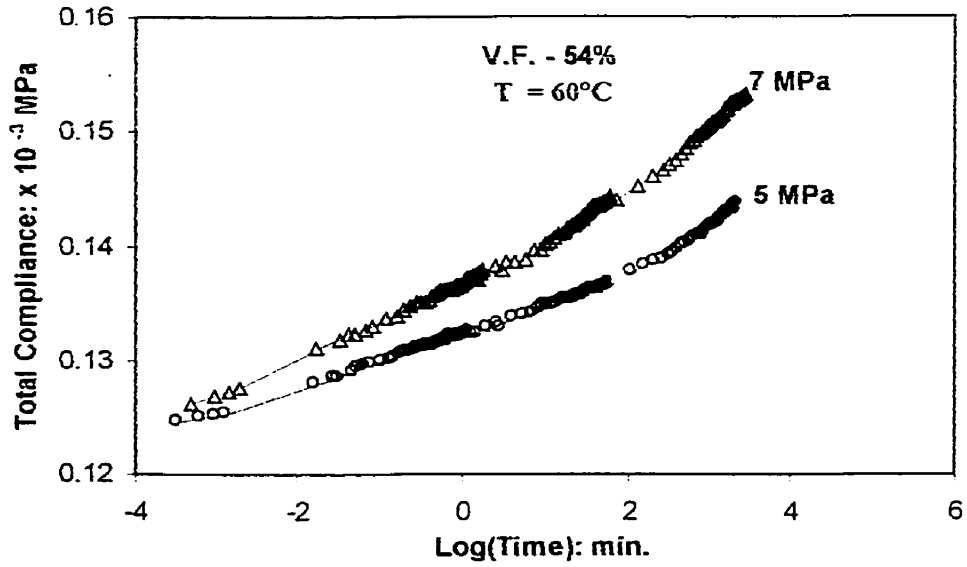

Figure 4.66: Master creep curve at 5 MPa and 7 MPa for $[90]_{12}$ aged-moisture conditioned composite (V_f:54%)

temperature versus modulus plot. The modulus values were obtained from the slope of stress-strain plot at different temperatures for aged (16.6 days) resin with 4.40% moisture content. The equation and vertical shifting procedure was same as discussed in section 4.2.1.1. The slope and constant values are tabulated in Table 4.10. Similar to resin, it was observed that creep curve at 5 MPa does not superimpose with creep curve at 7 MPa, suggesting creep to be in the non-linear region at above 5 MPa. This suggests that aging and moisture in combination, influences the linear-nonlinear creep transition in composite. The effect of stress is very apparent in composite than in resin. A plot of shift factor as a function of temperature shown in Figure 4.67. Similar to resin, shift factors at 5 MPa superimposes with that of 7 MPa .

In order to delineate the interactive effect, compliance data at 5 MPa for Postcured (PC), Aged (PA —16.6 days), Moisture conditioned (M – 3%), and Aged-Moisture conditioned (PA+M= 16.6 days + 2.90%) composite sample at 80°C are plotted together as shown in Figure 4.68. As shown in Figure 4.68, aging retards creep and moisture accelerates creep of matrix. The creep acceleration for combined effect of aged–moisture conditioned composite sample at a constant temperature was found to be less than that non-aged moisture conditioned sample similar to resin. The difference in creep acceleration was found to be due to difference in magnitude of matrix (resin) plasticization, between non-aged and aged resin, by absorbed moisture as shown in Table 4.11. For absorbed moisture content of 3% of non-aged samples experienced a reduction in T_g by 45°C, while the aged samples experienced a reduction in T_g by 39°C for the same moisture content. The creep of aged composite with 2.90% moisture content at

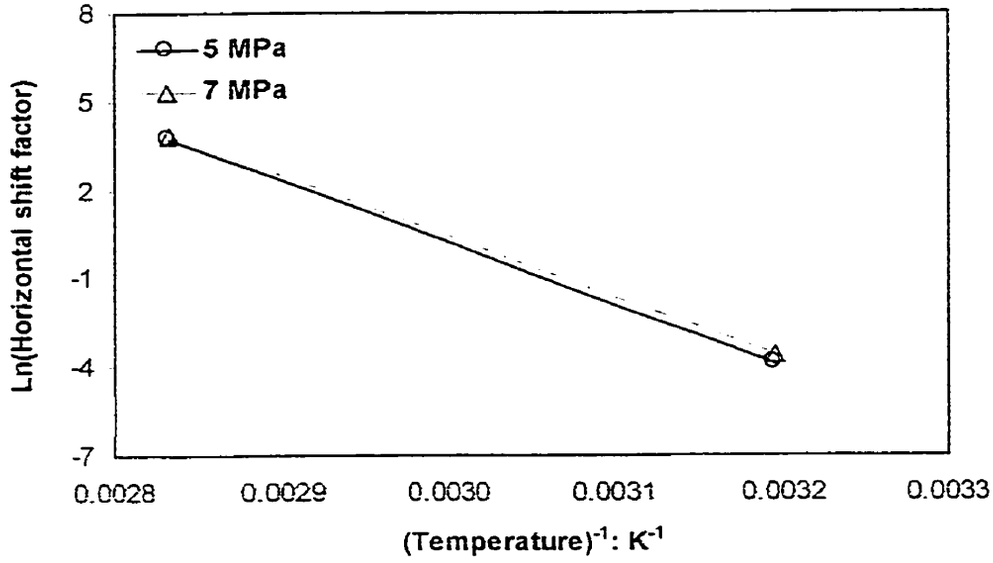

Figure 4.67: Shift factor for $[90]_{12}$ aged-moisture conditioned composite (V_f : 54%) as a function of temperature at 5 MPa and 7 MPa

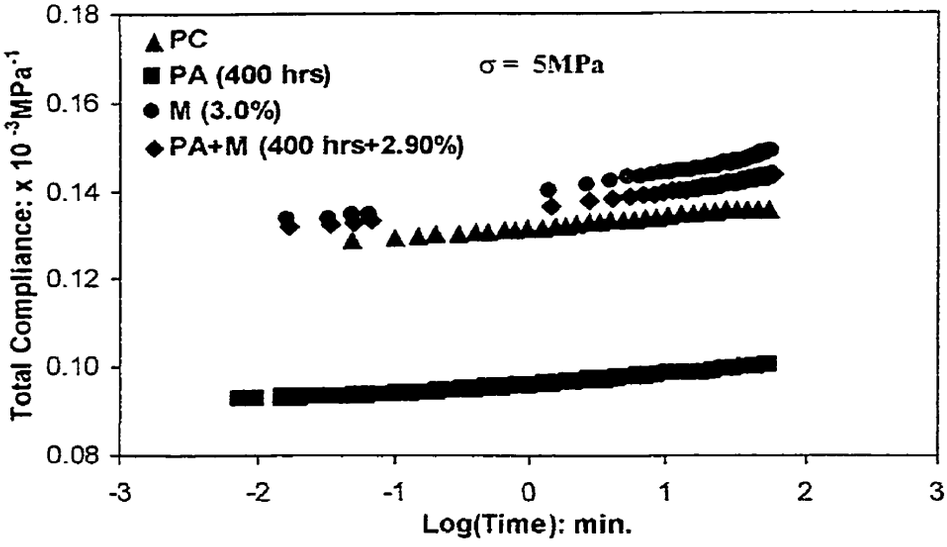

Figure 4.68: Compliance data at 5 MPa for postcured, aged, moisture conditioned and aged-moisture conditioned composite (V_f : 54%) at 80°C

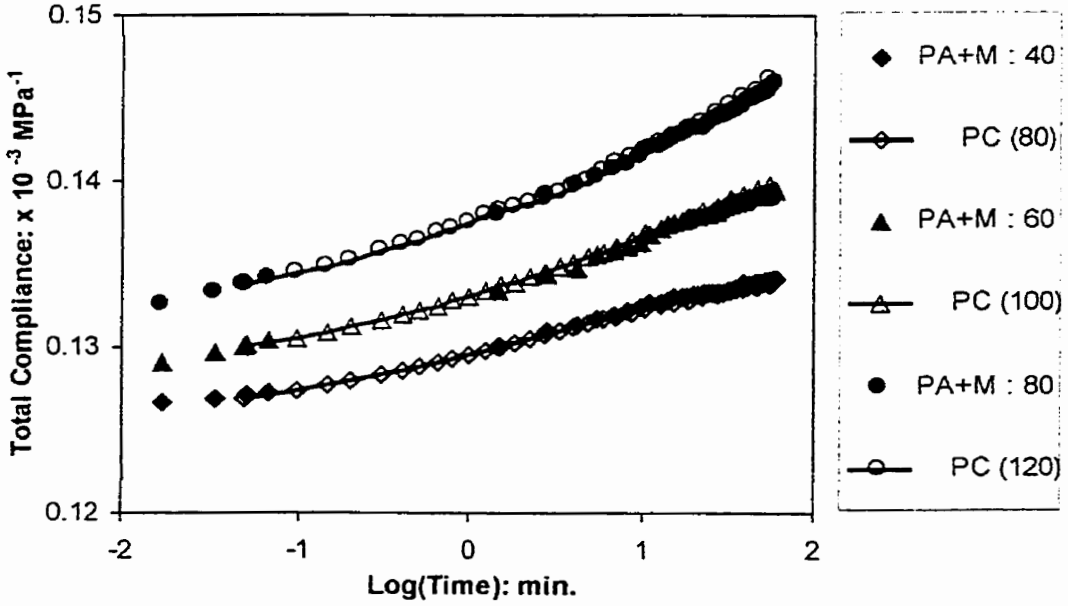

Figure 4.69: Validation of mechanism for interactive influence of aging and moisture for composite (V_f: 54%) at 5 MPa

80°C was found to be same as that of non-aged sample at 120°C shown in Figure 4.69. Similarly, compliance of aged resin with 2.90% moisture content at 40°C and 60°C were found to be same as that of non-aged dry sample at 100°C and 80°C respectively. Similar results were obtained at 7 MPa shown in Appendix E. Combined effect of aging and moisture decreased the magnitude of plasticization of matrix (resin) as compared to non-aged samples containing the same amount of moisture for a temperature and stress level. The activation energy and pre-exponential factor values for composite are tabulated in Table 4.12.

4.3 FRACTURE

The fracture tests were done to determine the individual and interactive effect of temperature, physical aging and moisture on total fracture energy. This fracture energy data will be used for creep rupture modeling ~~by the successor to the author of this thesis~~.

4.3.1 RESIN

4.3.1.1 EFFECT OF TEMPERATURE

Figure 4.70 shows the stress-strain plot of resin in the temperature range of RT-180°C. The strength decreased with increase in temperature and fracture strain increased with increase in temperature. A plot of total fracture energy as a function of temperature is shown in Figure 4.71. Fracture energy is the energy absorbed by a specimen when it fractures and was measured from the area under stress-strain curve at different temperatures. The total fracture energy was found to decrease with increase in temperature. The total fracture energy decreased from 170 kJm^{-3} at room temperature (295 K) to a value of 96 kJm^{-3} at 180°C (453 K).

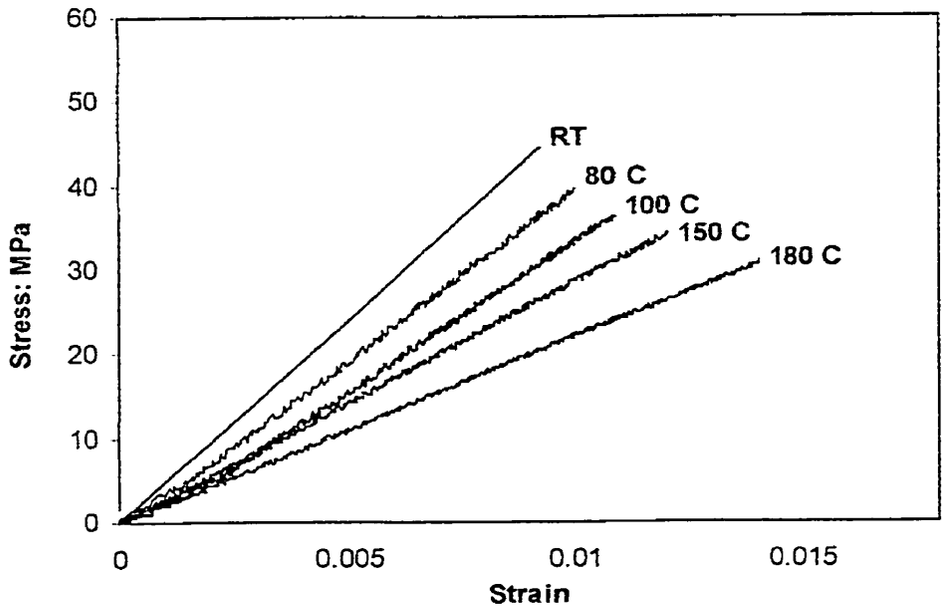

Figure 4.70: Stress-Strain plot of resin at different temperatures

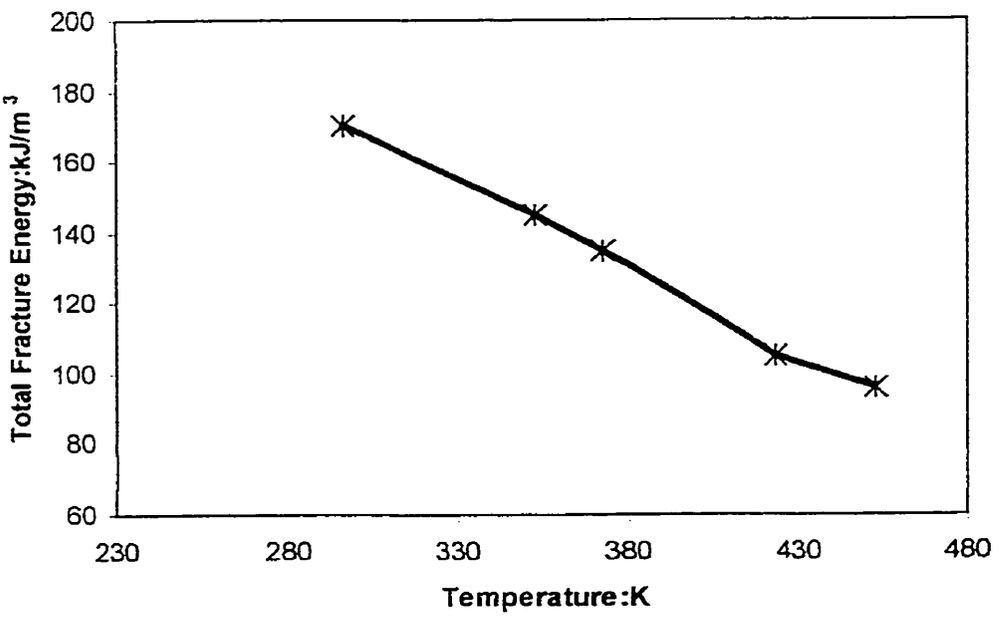

Figure 4.71: Total fracture energy of resin as a function of temperature

4.3.1.2 EFFECT OF AGING

The stress strain plot of resin at different aging times at 80°C is shown in figure 4.72. The stress strain plot of resin at 150°C and 180°C is shown in Appendix E. The fracture stress, strain and fracture energy values at values temperatures are tabulated in Table 4.13. Figure 4.73 shows a plot of total fracture energy as a function of aging time at different temperatures. Total fracture energy of the resin decreased with increase in aging time at all temperatures until about 168 hours(7 days). However, an increase in fracture energy was observed after aging for 168 hours (7 days) at all temperatures and then decreased again. The higher fracture energy for 7 days of aging as compared to 1 day appears to corroborate the explanation based on residual stresses. It is possible that any decrease in energy due to aging is offset by an increase in energy due to reduction in residual stresses. The fracture energy decreased by 73.5 %, 67.5% and 66.6% after aging for 400 hours (16.6 days) at 80°C, 150°C and 180°C from that of non-aged samples. Similar trend was observed by Kong [24] for epoxy resin. The magnitude of % reduction in fracture stress, strain and fracture energy reported by Kong [24] for epoxy resin is consistent with present result. He observed 80%, 46.3% and 41% decrease in fracture energy, fracture stress and strain respectively after aging for 1666 hours at 140°C when compared to non-aged sample.

4.3.1.3 EFFECT OF MOISTURE

A stress strain plot of resin at different moisture contents at 80°C is shown in figure 4.74. Similar results were obtained at 150°C and 180°C, whose plots are shown in

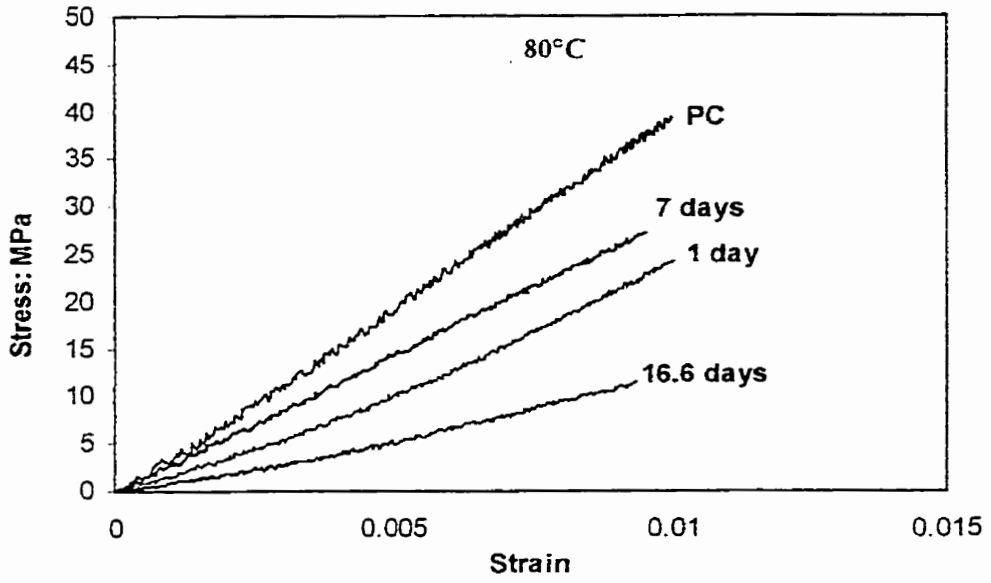

Figure 4.72: Stress-Strain plot of resin at 80°C at various physical aging times

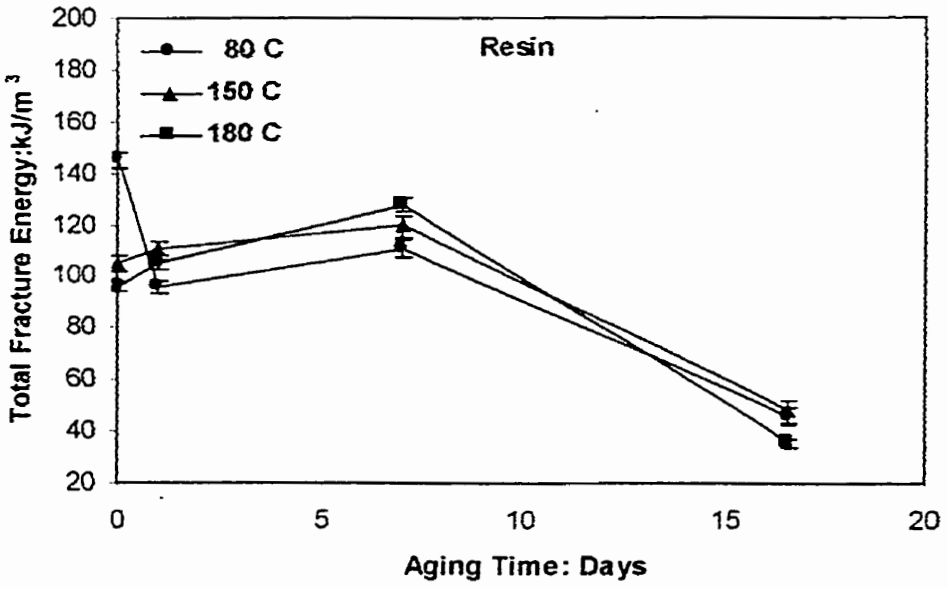

Figure 4.73: Total fracture energy of resin as a function of aging time

	A.T (Days)	80°C	150°C	180°C
Stress (MPa)	0	39.0±0.50	33.0±1.00	30.0±1.00
	1	24.0 ± 1.00	33.2±1.25	33.0±1.00
	7	27.0±1.00	33.1±1.150	33.6±0.70
	16.6	11.0±2.00	9.5±1.50	8.26±0.80
% Reduction in Stress	1	38.4	-	-
	7	30.7	-	-
	16.6	71.7	71.2	72.4
Strain (%)	0	0.89±0.04	1.13±0.04	1.40±0.04
	1	1.02±0.04	1.06 ±0.041	1.09
	7	0.95±0.04	0.93±0.05	1.2±0.02
	16.6	0.92±0.05	0.99±0.05	0.86±0.05
Total Fracture Energy(kJm^{-3})	0	170±1.20	145±1.05	105±1.00
	1	95±2.08	110±3.50	105±2.51
	7	110±3.21	120±1.08	127±2.51
	16.6	45±3.51	47±2.08	35±1.52
% Reduction in Fracture Energy	1	34.4	24.1	-
	7	35.3	17.2	-
	16.6	73.5	67.5	66.6

Table 4.13: Effect of aging on tensile properties of resin

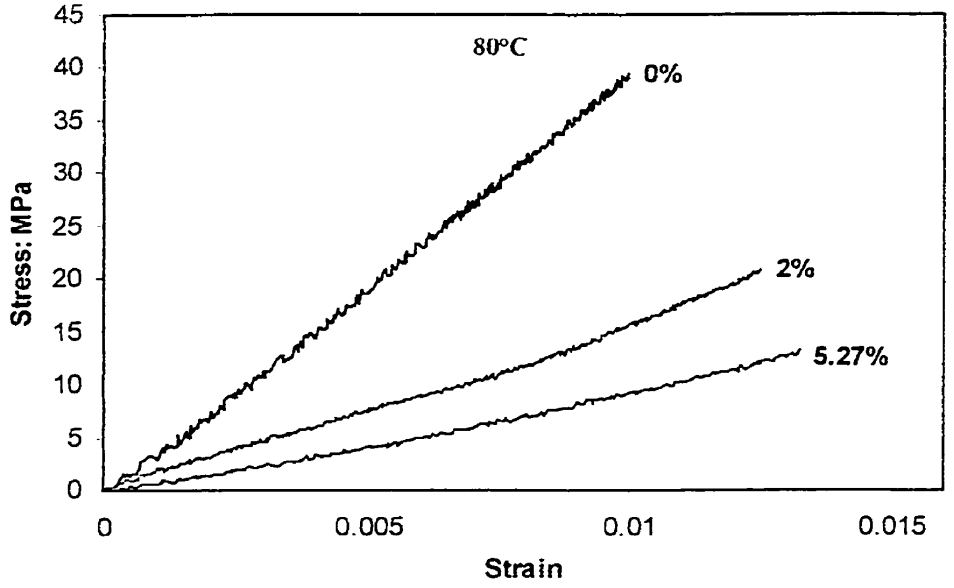

Figure 4.74: Stress-Strain plot of resin at 80°C at different moisture contents

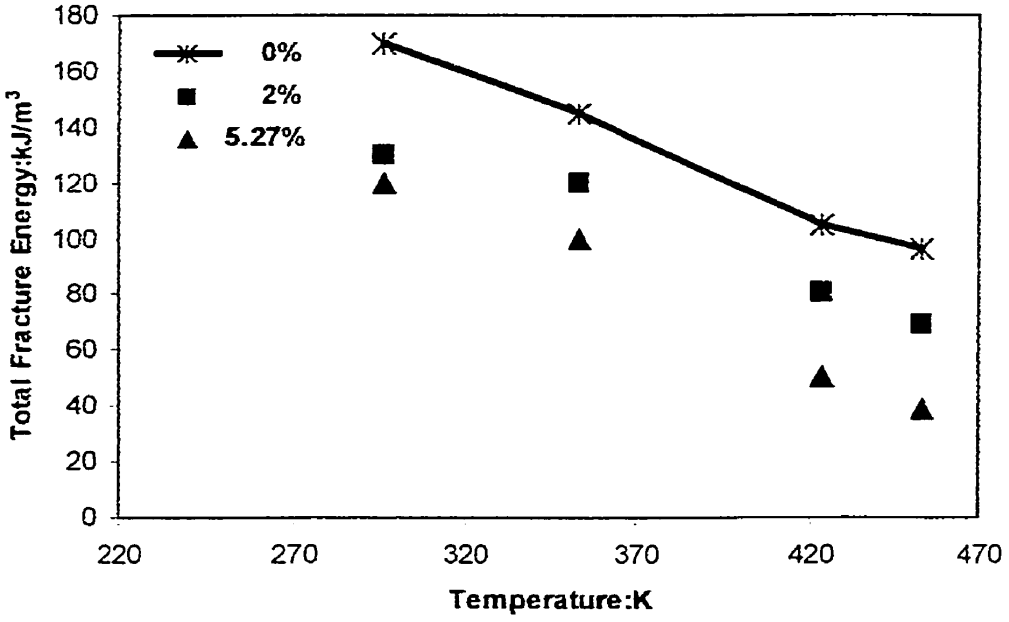

Figure 4.75: Total fracture energy of resin as a function of temperature at various moisture contents

	Mm (%)	80°C	150°C	180°C
Stress (MPa)	0	39±0.5	33±1.0	30±1.0
	2	20 ± 1.7	17±1.25	21±1.32
	5.27	13±0.75	9.8±1.52	7.4±1.6
% reduction in Stress	2	48.4	48.4	30
	5.27	66.6	70.3	75.3
Strain (%)	0	0.89±0.04	1.13±0.04	1.40±0.04
	2	1.25±0.04	0.89 ±0.02	0.89±0.015
	5.27	1.32±0.05	1.50±0.03	1.55±0.02
Total Fracture Energy(kJm^{-3})	0	170±1.20	145±1.05	105±1.0
	2	100±0.88	80±2.08	69±1.0
	5.27	40.0±.03	35±.04	25±.025
% reduction in Fracture Energy	2	41.0	44.8	29.1
	5.27	76.4	75.8	76.2

Table 4.14: Effect of moisture on tensile properties of resin

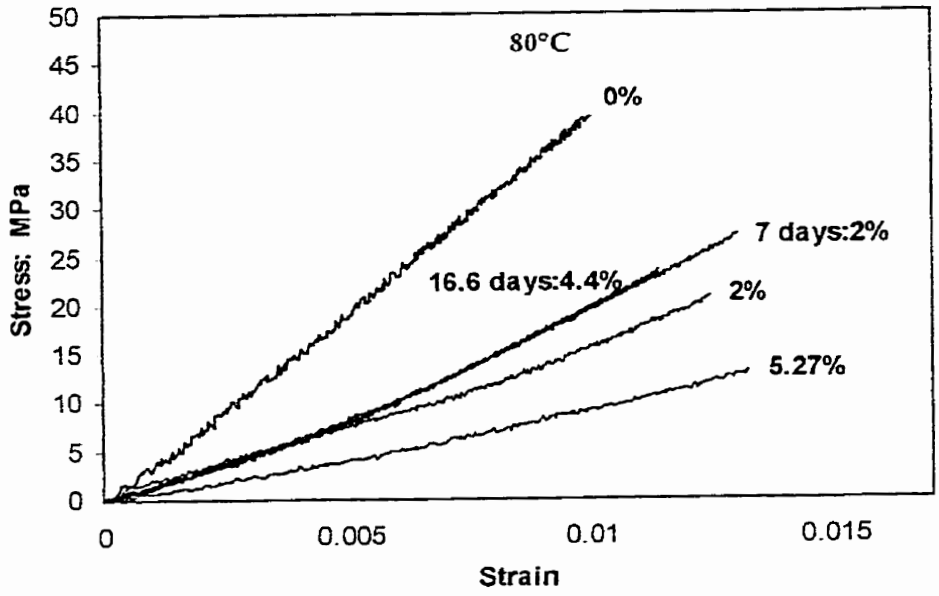

Figure 4.76: Stress-Strain plot of resin at 80°C at various physical aging times and moisture contents

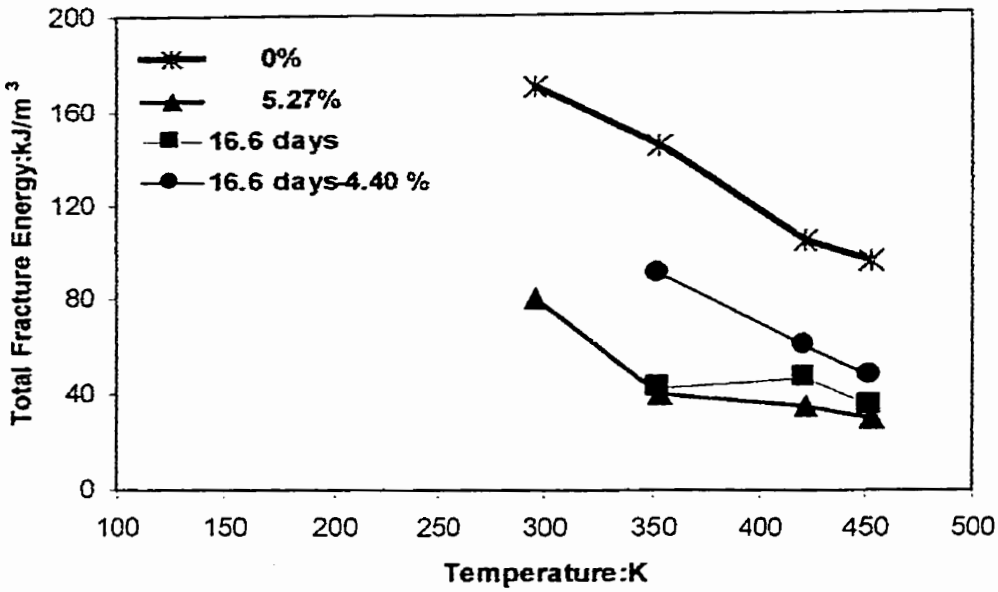

Figure 4.77: Total fracture energy of resin as a function of temperature at various aging times and moisture contents

	Mm (%)	80°C	150°C	180°C
Stress (MPa)	0	39.0±0.50	33.0±1.00	30±1.00
	7/2	27.0 ± 1.70	29.6±1.25	21.2±1.32
	16.6/4.4	23.2±0.75	18.0±1.52	12.0±1.60
% Reduction in Stress	7/2	30.0	10.3	29.3
	16.6/4.4	41.0	45.3	59.7
Strain (%)	0	0.89±0.04	1.13±0.04	1.40±0.04
	7/2	1.30±0.04	1.40 ±0.02	1.43±0.015
	16.6/4.4	1.07±.03	0.95±0.03	0.92±0.03
Total Fracture Energy(kJm^{-3})	0	170±1.20	145±1.05	105±1.0
	7/2	110±0.88	105±2.08	90±1.0
	16.6/4.4	90±1.03	60±1.00	48±1.05
% Reduction in Fracture Energy	7/2	35.4	27.5	14.2
	16.6/4.4	47.0	58.6	54.2

Table 4.15: Combined effect of aging and moisture on tensile properties of resin

Appendix E. The fracture stress, strain and total fracture energy values are tabulated in 4.14. Figure 4.75 shows the effect of moisture content on total fracture energy at different temperatures. At a given temperature, total fracture energy decreases with increase in moisture content.

4.3.1.4 COMBINED EFFECT OF AGING AND MOISTURE

Figure 4.76 shows the stress strain plot of resin at 80°C conditioned to various moisture levels and physical aging times. The fracture stress, strain and fracture energy values are tabulated in Table 4.15. Total Fracture energy as a function of temperature at different moisture contents and aging times is shown in Figure 4.77. While aging and moisture alone decreased fracture energy, combined effect of aging and moisture resulted in fracture energy higher than that of non-aged moisture conditioned specimen for a given moisture content and temperature. The total fracture energy of aged (16.6 days) resin with 4.40% moisture content was found to be higher than that of non-aged moisture conditioned sample at a given temperature.

4.3.2 COMPOSITE WITH 54% FIBER VOLUME FRACTION

4.3.2.1 EFFECT OF TEMPERATURE

Figure 4.78 shows the stress-strain plot of $[90]_{12}$ composite with 54% volume fraction in the temperature range of RT-180°C. Similar to resin, the strength decreases with increase in temperature. Figure 4.79 shows a plot of total fracture energy as a function of temperature. Fracture energy is the energy absorbed when specimen fractures and was measured from the area under stress-strain curve. Similar to resin, the fracture

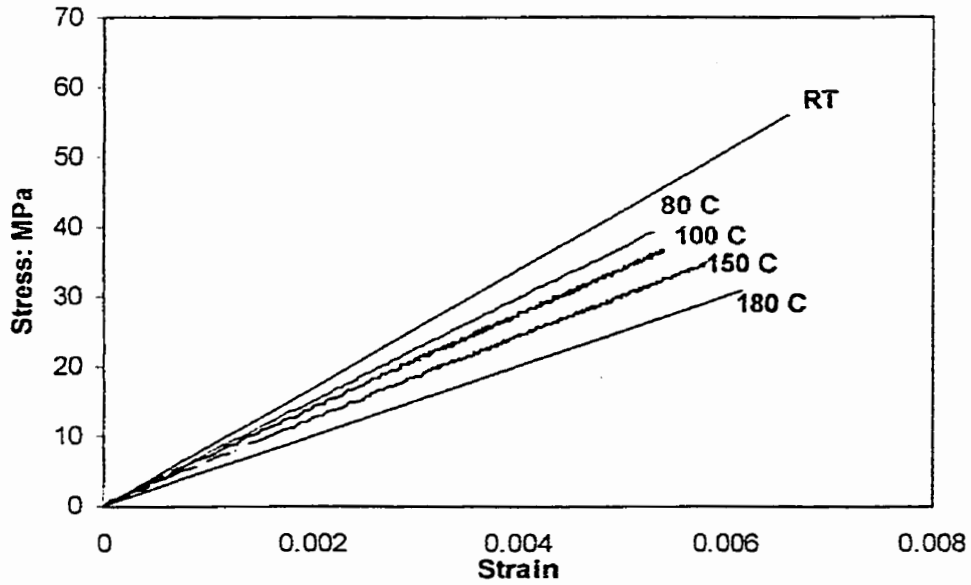

Figure 4.78: Stress-Strain plot of $[90]_{12}$ composite (V_f :54%) at different temperatures

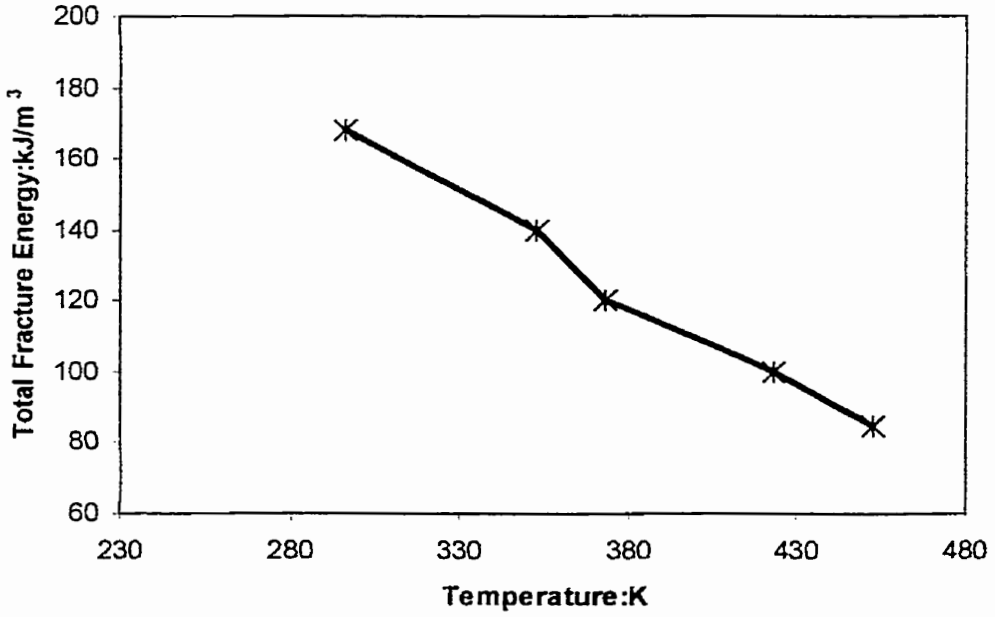

Figure 4.79: Total fracture energy of $[90]_{12}$ composite (V_f :54%) as a function of temperature at different temperatures

energy of composite decreases with increase in temperature. The fracture energy decreased from 168kJm^{-3} at room temperature to 85 kJm^{-3} at 180°C (453 K). Similar decrease in fracture energy with temperature was observed by Raghavan and Meshii [9] and Miyano et al [11] for carbon/epoxy composites and is consistent with the present results.

4.3.2.2 EFFECT OF AGING

The stress strain plot of $[90]_{12}$ composite with 54% volume fraction at different aging times at 80°C is shown in Figure 4.80. The stress strain plot of composite at 150°C and 180°C is shown in Appendix E. The fracture stress, strain and fracture energy values at different temperatures are tabulated in Table 4.16. Figure 4.81 shows a plot of total fracture energy as a function of aging time at different temperatures. Though the total fracture energy decreased with increase in aging time at 80°C, an increase in fracture energy was observed at 150°C and 180°C after aging for 400 hours (16.6 days). The total fracture energy of 400 hours aged composite at 150°C and 180°C was found to be higher than that of non-aged sample. The higher fracture energy at 150°C and 180°C for 16.6 days of aging as compared to 1 and 7 days could be due to relaxation of residual stresses induced during processing. However, fracture energy decreased drastically after aging for 1000 hours (41.6 days) at 180°C. Similar trend was observed by Kong [24] for carbon/epoxy composite. He noticed a decrease of 38.5%, 73.6% and 87.8% in fracture stress, strain and energy after 1666 hours of aging at 140°C from that of non-aged sample.

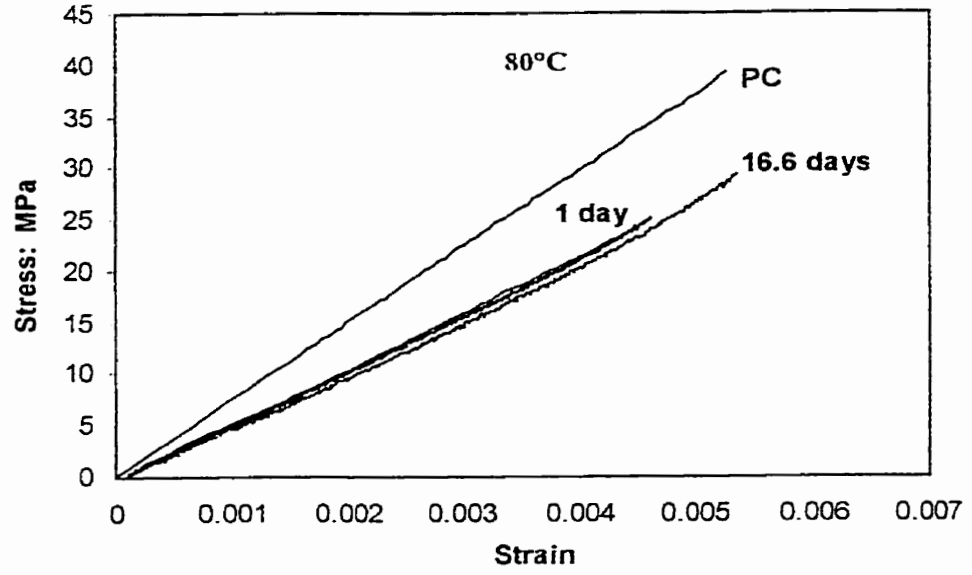

Figure 4.80: Stress-Strain plot for $[90]_{12}$ composite (V_f :54%) at various physical aging times at 80°C

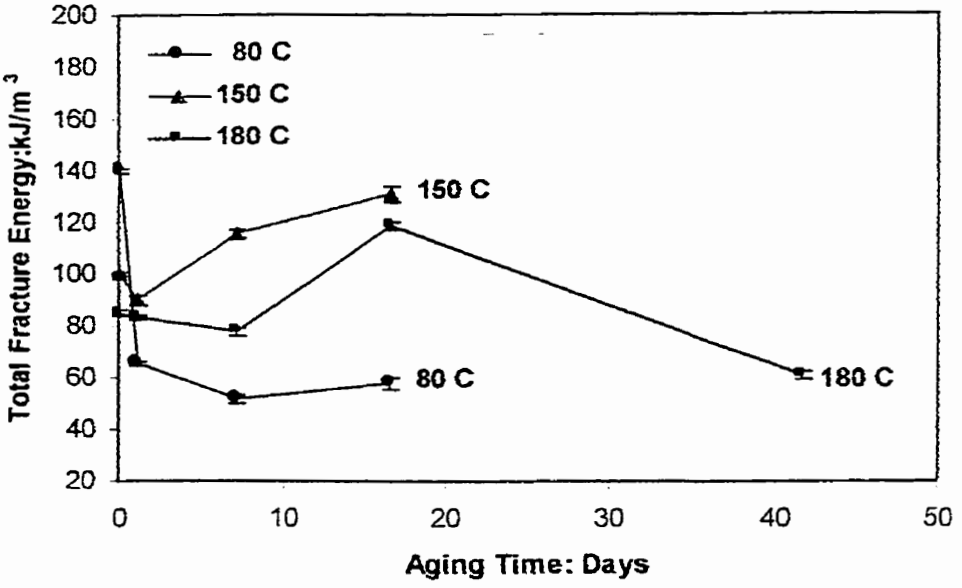

Figure 4.81: Total fracture energy of $[90]_{12}$ composite (V_f :54%) as a function of aging time at various temperatures

	A.T (Days)	80°C	150°C	180°C
Stress (MPa)	0	39.0±0.50	34.0±1.00	30.0±1.0
	1	29.0 ± 1.70	33.2±1.25	31.0±1.32
	7	22.0±0.75	35.0±1.52	32.0±1.60
	16.6	25.5±1.50	38.0±1.00	35.0±1.52
	41.6	-	-	15.0
% reduction in Stress	1	25.6	2.35	-
	7	43.5	-	-
	16.6	34.6	-	-
	41.6	-	-	50
Strain (%)	0	0.52±0.03	0.48±0.03	0.61±0.03
	1	0.54±0.04	0.54 ±0.02	0.51±0.02
	7	0.57±0.04	0.76±0.02	0.54±0.03
	16.6	0.58±0.03	0.92±0.04	0.83±0.04
	41.7	-	-	0.45
Total Fracture Energy(kJm^{-3})	0	140±1.0	100±1.50	85±0.88
	1	65±0.88	90±2.08	83±1.00
	7	51±1.60	115±1.52	77±1.50
	16.6	58±2.29	131±2.08	118±1.50
	41.6	-	-	50
% Reduction in Fracture Energy	1	53.5	10.0	2.35
	7	63.5	-	9.41
	16.6	58.5	-	-
	41.6	-	-	41.70

Table 4.16: Effect of aging on tensile properties of $[90]_{12}$ composite with 54% V_f

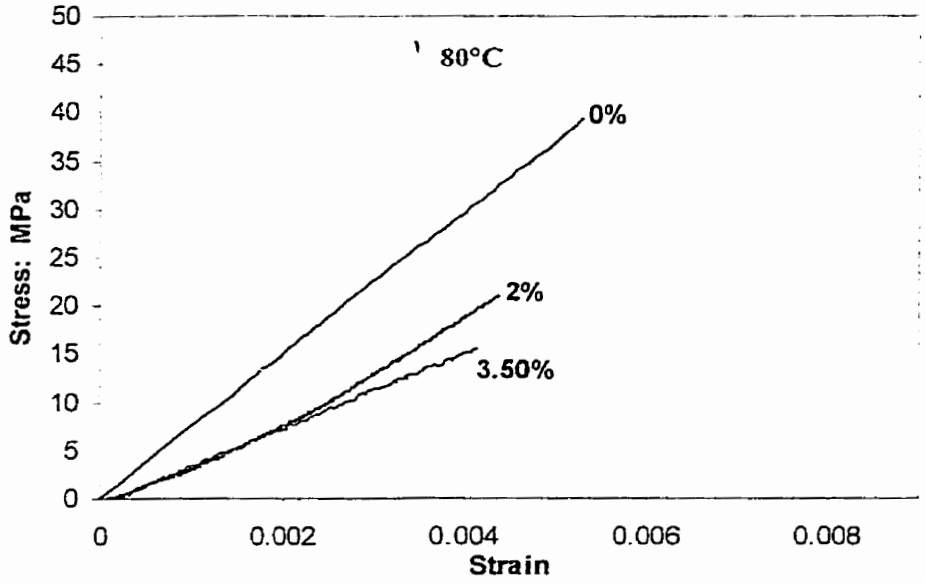

Figure 4.82: Stress-Strain plot of $[90]_{12}$ composite (V_f :54%) at various moisture contents at 80°C

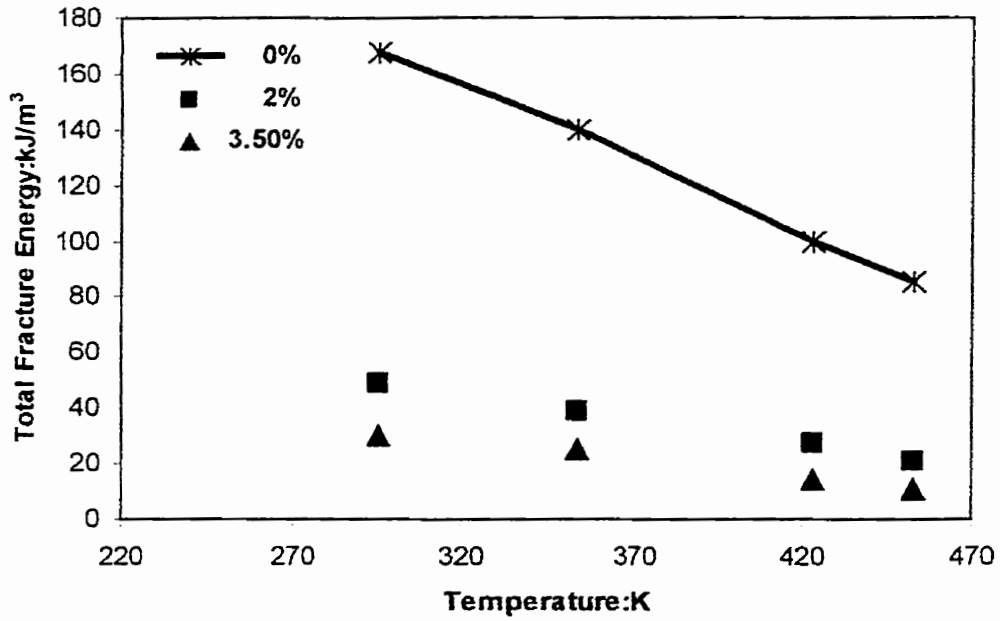

Figure 4.83: Total fracture energy of $[90]_{12}$ composite (V_f :54%) as a function of temperature at various moisture contents

	Mm (%)	80°C	150°C	180°C
Stress (MPa)	0	39.0±0.5	34.0±1.0	30.0±1.0
	2	21.0 ± 1.7	20.0±1.25	16.0±1.32
	3.5	15.5±0.75	11.4±1.52	8.6±1.60
% Reduction in Stress	2	46.1	41.1	46.6
	3.5	60.0	66.4	71.3
Strain (%)	0	0.52±.025	0.48±0.025	0.61±0.03
	2	0.53±0.04	0.50 ±0.02	0.36±0.015
	3.5	0.43±0.02	0.40±0.01	0.42±.03
Total Fracture Energy(kJm^{-3})	0	140±1.00	100±1.50	85±0.88
	2	39±0.88	27±2.08	21±1.00
	3.5	25±1.20	14.6±2.00	10.8±1.50
% Reduction in Fracture Energy	2	72.0	73.0	75.3
	3.5	82.1	85.4	87.3

Table 4.17: Effect of moisture on tensile properties of $[90]_{12}$ composite with 54% V_f

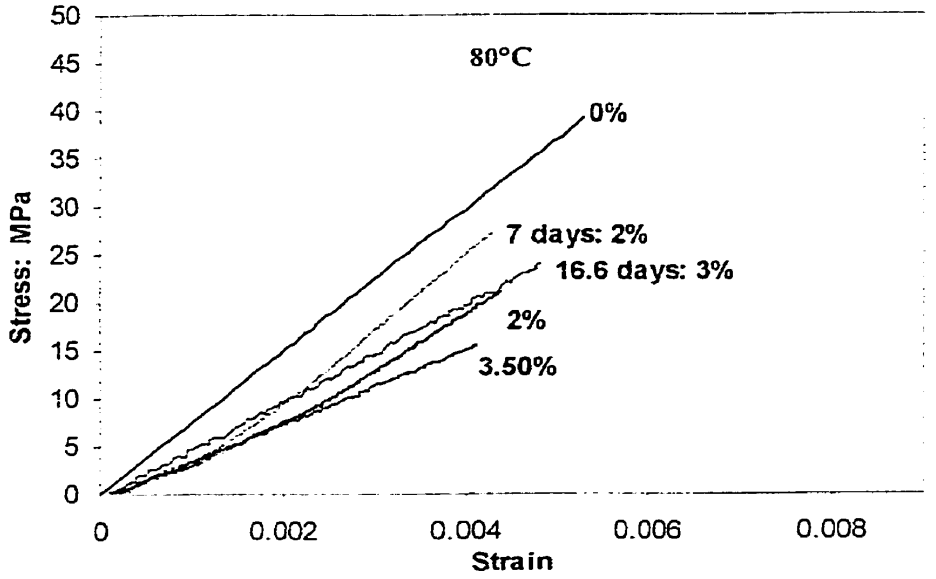

Figure 4.84: Stress-Strain plot of $[90]_{12}$ composite (V_f :54%) at various moisture contents and physical aging times

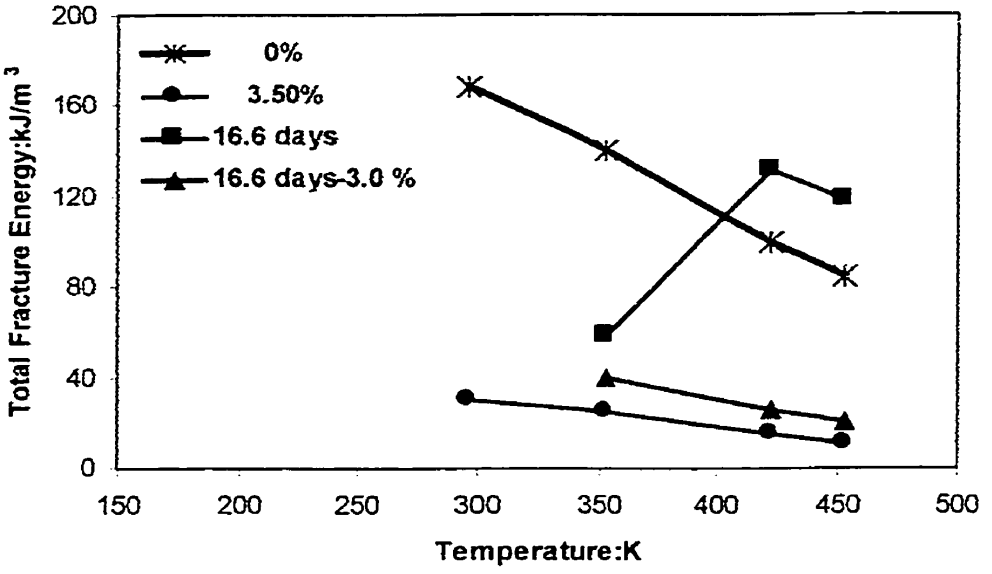

Figure 4.85: Total fracture energy of $[90]_{12}$ composite (V_f :54%) as a function of temperature at various moisture contents and physical aging times

	Mm (%)	80°C	150°C	180°C
Stress (MPa)	0	39.0±0.50	34.0±1.00	30±1.00
	7/2	27.0 ± 1.70	24.0±1.25	31±1.32
	16.6/3	24.0±0.75	19.7±1.52	13.6±1.60
% Reduction in Stress	7/2	30.7	29.4	-
	16.6/3	38.4	42.0	54.6
Strain (%)	0	0.52±.025	0.48±0.025	0.61±0.03
	7/2	0.51±0.04	0.52 ±0.02	0.43±0.015
	16.6/3	0.52±025	0.46±0.015	0.39±0025
Total Fracture Energy(kJm^{-3})	0	140±1.00	100±1.50	85±0.88
	7/2	49±0.88	38±2.08	31±1.00
	16.6/3	40±0.88	25.4±2.08	20.14±1.00
% Reduction in Fracture Energy	7/2	65.0	62.0	63.5
	16.6/3	71.4	75.0	76.3

Table 4.18: Combined effect of aging and moisture on tensile properties of $[90]_{12}$ composite with 54% V_f

4.3.2.3 EFFECT OF MOISTURE

A stress strain plot of $[90]_{12}$ composite with 54% volume fraction at different moisture contents at 80°C is shown in figure 4.82. The stress strain behavior of $[90]_{12}$ composite with 54% volume fraction at 150°C and 180°C is shown in Appendix E. The fracture stress, strain and total fracture energy values are tabulated in Table 4.17. Figure 4.83 shows the effect of moisture content on fracture energy at different temperatures. The fracture energy decreased with increase in moisture content at all temperatures.

4.3.2.4 COMBINED EFFECT OF AGING AND MOISTURE

Figure 4.84 shows the stress strain plot of $[90]_{12}$ composite with 54% volume fraction at 80°C at different moisture contents and physical aging times. The fracture stress, strain and fracture energy values are tabulated in Table 4.18. Total fracture energy as a function of temperature at different moisture contents and aging times is shown in Figure 4.85. The total fracture energy of aged composite with 3% moisture content was found to be higher than non aged moisture conditioned sample (3.5%) at a given temperature.

4.4 CREEP RUPTURE

4.4.1 RESIN

4.4.1.1 EFFECT OF TEMPERATURE/STRESS

Figure 4.86 shows the rupture time of resin as a function of % of ultimate tensile strength at different temperatures. It was observed that rupture time decreases with

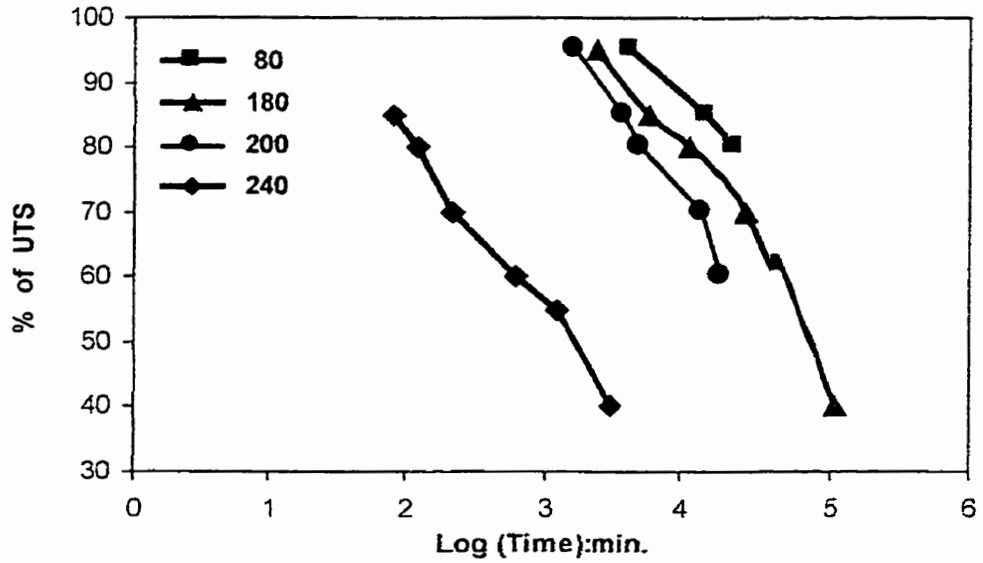

Figure 4.86: Creep rupture time for resin at various temperatures

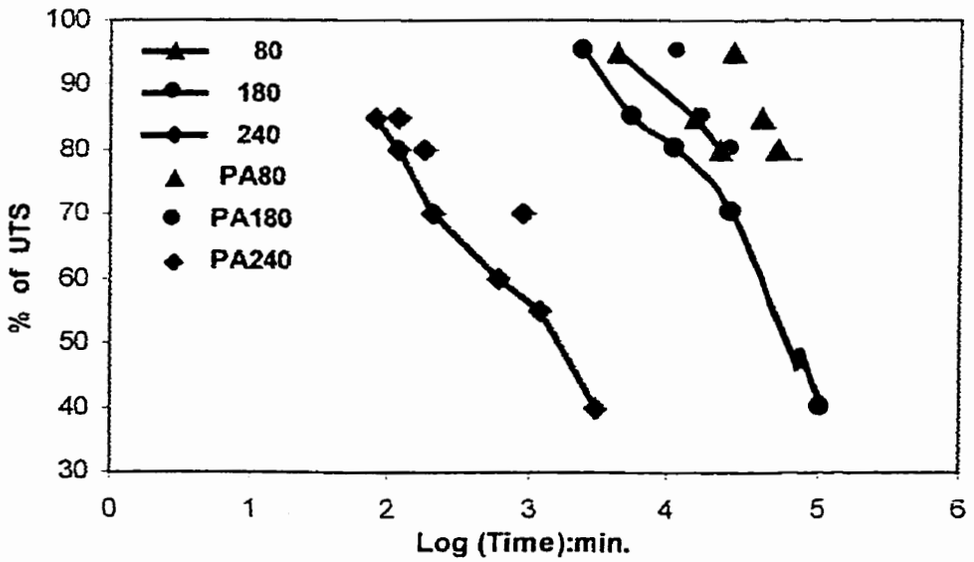

Figure 4.87: Creep rupture time for physically aged (400 hrs) resin at various temperatures

increase in temperature and stress level. Similar trend has been observed by several researchers [1, 3, 8]. The rupture time varied from 80 to 10^5 minutes.

4.4.1.2 EFFECT OF PHYSICAL AGING

Figure 4.87 shows the effect of aging on rupture time. Aging shifts the rupture time to right i.e. takes longer times to rupture when compared to non-aged samples. In other words, physical aging increased the creep rupture time for resin. This could be due to reduction in creep rate as compared to non-aged samples. Similar behavior was observed for PMMA polymer by Crissman and Mckenna [23]. However, they found the creep rupture time to decrease after 11 days of aging for a given stress level.

4.4.1.3 EFFECT OF MOISTURE

Figure 4.88 shows rupture time as a function of % of ultimate tensile strength at 80°C. In contrast to aging, moisture accelerates the creep process, there by shifting the rupture time to left i.e. to shorter times. Moisture accelerated the creep rate and decreased the creep rupture time when compared to non-aged samples. Many researchers have observed such creep rupture acceleration in the past [35, 65-67].

4.4.1.4 COMBINED EFFECT OF AGING AND MOISUTRE

The creep rupture time of aged resin was longer than for non-aged resin for a given moisture content as shown in Figure 4.88 (PC:Postcured, PA:Physically Aged (400

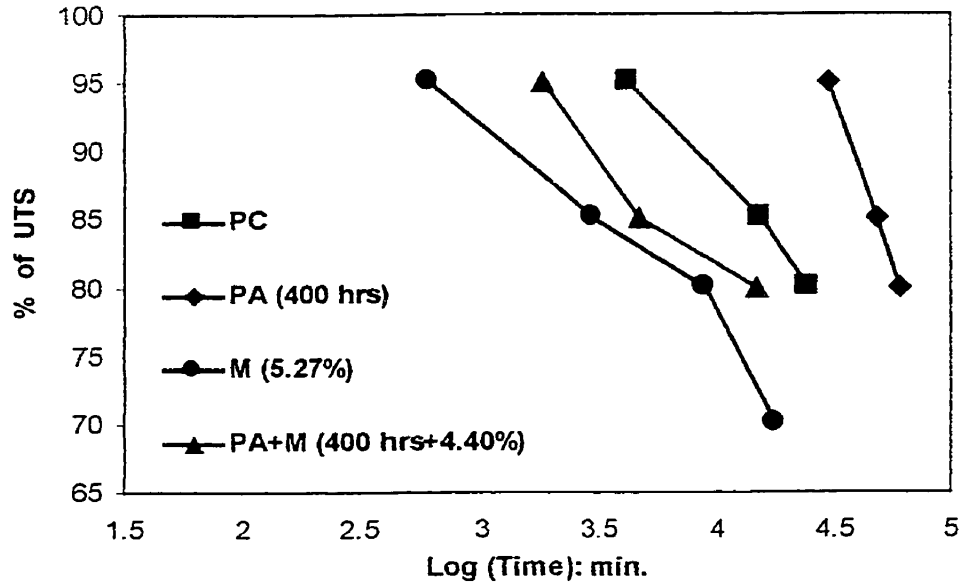

Figure 4.88: Creep rupture time for postcured, physically aged, moisture-conditioned and aged-moisture conditioned resin at 80°C

hours), M: Moisture-conditioned (5.27%), PA+M: Aged & Moisture conditioned (400 hours+4.40%)). It was observed during the discussion on interactive effect of moisture and physical aging on creep that creep rate of PA+M would be slower than that of M sample for a given moisture, temperature and stress level. This was attributed to reduction in the magnitude of plasticization in the aged state. Similar trend was observed in fracture energy i.e. the fracture energy of PA+M were higher than that of M sample for a given moisture and temperature. Hence it is expected that the creep rupture time of PA+M specimens would be longer than that of M specimens for a given, temperature and stress level. Results of this study are the first data on the combined effect of aging and moisture on creep rupture of resin.

4.4.2 COMPOSITE WITH 54% FIBER VOLUME FRACTION

4.4.2.1 EFFECT OF TEMPERATURE / STRESS

Figure 4.89 shows the rupture time of $[90]_{12}$ composite with 54% volume fraction as a function of % of ultimate tensile strength at different temperatures. Similar to resin, rupture time decreased with increase in temperature and stress level. Similar trend was observed by other investigators [1, 3, 8]. Rupture time varied from 45 to 10^4 minutes.

4.4.2.2 EFFECT OF PHYSICAL AGING

Figure 4.90 shows the effect of aging on rupture time. In contrast to resin, aging shifts the rupture time to right i.e. takes shorter time to rupture. In other words, aging decreased the creep rupture time when compared to non-aged samples.

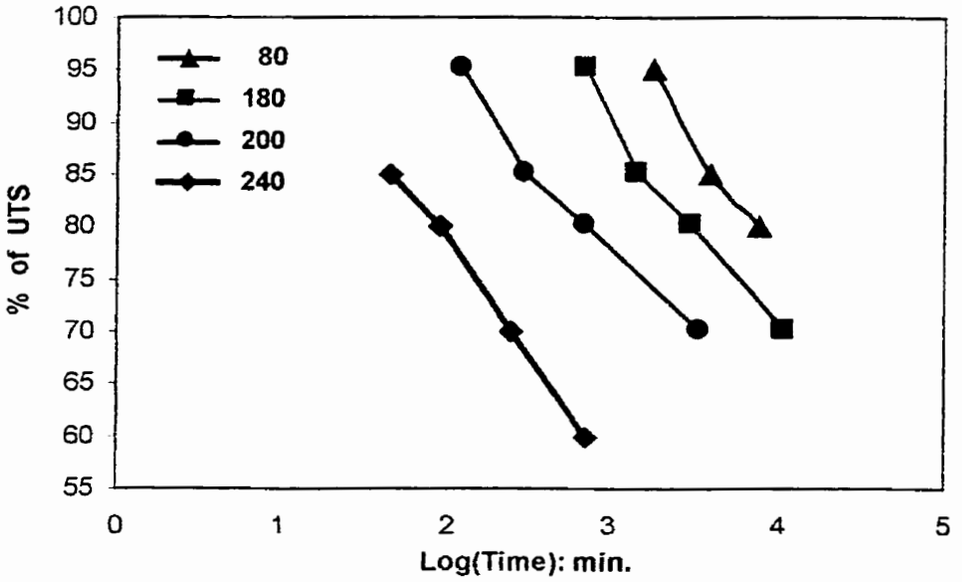

Figure 4.89: Creep rupture time for $[90]_{12}$ composite (V_f: 54%) at various temperatures

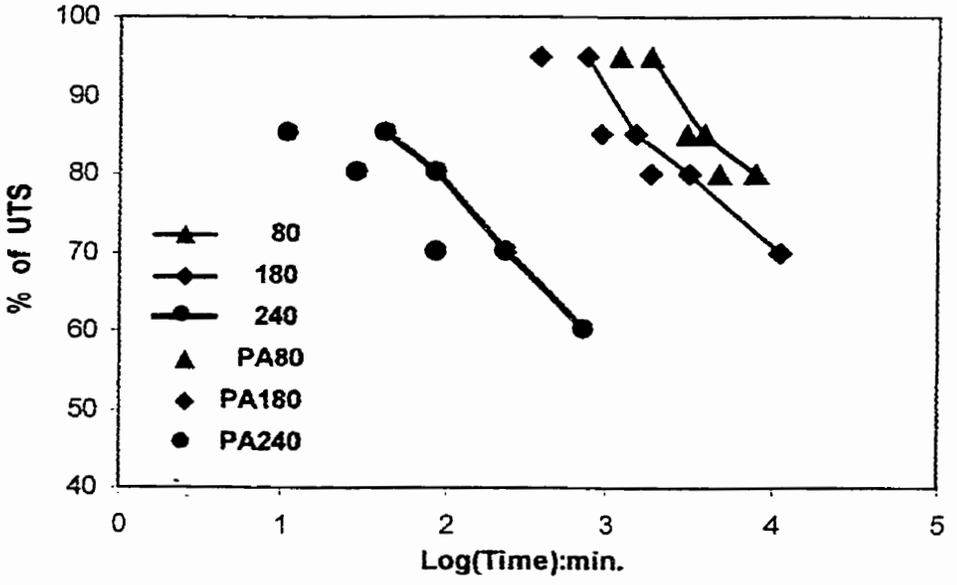

Figure 4.90: Creep rupture time for physically aged (400hrs) $[90]_{12}$ composite (V_f: 54%) at various temperatures

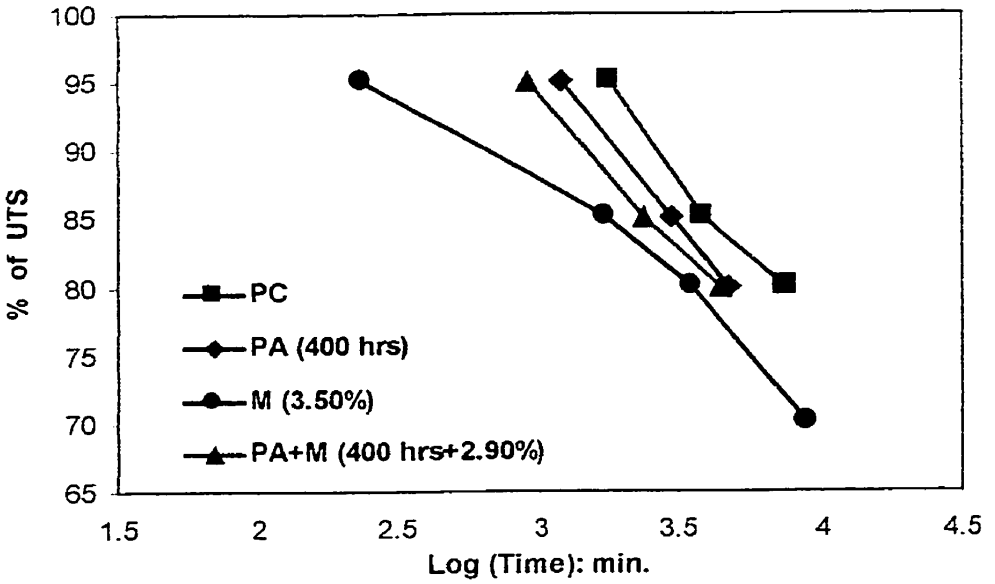

Figure 4.91: Creep rupture time for postcured, physically aged, moisture conditioned, and aged-moisture conditioned composite (V_f: 54%) at 80°C

4.4.2.3 EFFECT OF MOISTURE

Figure 4.91 shows rupture time as a function of % of ultimate tensile strength at 80°C. In contrast to aging, moisture accelerates the creep process, there by shifting the rupture time to ~~right~~ left i.e. to shorter times. Similar to resin, moisture accelerated the creep rate and decreased the creep rupture time for composite when compared to non-aged samples. Many researchers have observed such creep rupture acceleration in the past [46, 64-66].

4.4.2.4 COMBINED EFFECT OF AGING AND MOISUTRE

Similar to resin, the creep rupture time of aged composite was longer than for non-aged composite shown in Figure 4.91 (PC:Postcured, PA: Physically Aged (400 hours), M: Moisture Conditioned (3.50%), PA+M: Aged & Moisture conditioned (400 hours+3.30%)). It was observed during the discussion on interactive effect of moisture and physical aging on creep that creep rate of PA+M would be slower than that of M sample for a given moisture, temperature and stress level. This was attributed to reduction in the magnitude of plasticization in the aged state. Similar trend was observed in fracture energy i.e. the fracture energy of PA+M were higher than that of M sample for a given moisture and temperature. Hence it is expected that the creep rupture time of PA+M specimens would be longer than that of M specimens for a given % UTS, temperature and stress level. Results of this study are the first data on the combined effect of aging and moisture on creep rupture of composite.

CHAPTER 5

CONCLUSION

Experimental study of individual and interactive influence of stress, temperature, physical aging, and moisture on creep, fracture and creep rupture of an epoxy and a composite has been completed. In addition, the interactive influence of aging and moisture on moisture absorption kinetics has also been studied. Results of this study are summarized below.

5.1 MOISTURE ABSORPTION KINETICS

- Saturation moisture content, diffusion coefficient and rate of moisture absorption, for the resin and the composite, increased with increase in temperature and relative humidity.
- Introduction of carbon fibers decreased the saturation moisture content, the diffusion coefficient and the rate of moisture absorption for the resin.
- Activation energy for moisture absorption decreased with increase in fiber volume fraction.
- Physical aging decreased the saturation moisture content, the diffusion coefficient and the rate of moisture absorption for the resin and the composite.

5.2 CREEP

5.2.1 Effect of temperature/stress

- Increase in temperature and stress accelerated creep of resin (i.e. magnitude and rate of creep increased with increase in temperature and stress).

- Introduction of carbon fibers retarded the creep of the resin (i.e. magnitude and creep rate decreased).
- Resin and composite exhibited linear creep until 7 MPa. Above 7 MPa, creep became nonlinear for both the resin and the composite (54%).
- For composite with 71% fiber volume fraction, the stress limit for linear creep was found to be 5 MPa.
- Time for transition from linear to non-linear creep at a constant applied stress decreased with increase in applied stress.

5.2.2 Effect of Physical aging

- Physical aging retarded creep (i.e. shifted the creep curve to longer times).
- Effect of physical aging on creep could be modeled by Time-Aging Time Superposition principle.
- Shift rate increased with aging temperature and decreased with stress.
- Shift rate was found to be independent of fiber volume fraction i.e. effect of physical aging on creep was found to be of same magnitude for both the resin and the composite

5.2.3 Effect of Moisture

- Moisture accelerated the creep of the resin and composite through plasticization of matrix (i.e. reduction in T_g)

- The creep of the moisture conditioned sample at a temperature T_1 was shown to be equivalent to the creep of a dry sample at higher temperature T_2 [$T_2 = T_1 + (T_g^{dry} - T_g^{wet})$].
- Activation energy for creep of moisture conditioned sample was found to be same as that of dry sample for both the resin and the composite.
- Moisture did not alter the stress limit for linear creep for both the resin and the composite.

5.2.4 Combined effect of Temperature, Stress, Physical aging and Moisture

- Combined effect of aging and moisture decreased the magnitude of plasticization of matrix (resin) (i.e. the magnitude of decrease in T_g was lower than that for the moisture conditioned sample)
- Hence, the creep of physically aged-moisture conditioned resin and the composite (PA+M) was less than that of moisture conditioned resin and the composite.
- The activation energy for creep was found to be the same for the resin and composite, for all conditions (such as postcured (PC), physically aged(PA), moisture-conditioned(M), and physically aged and moisture conditioned (PA+M)). Hence, it can be concluded that the effect of temperature on creep is same for all the conditions investigated in this study. However, the pre-exponential factors varied for all the test conditions. The pre-exponential factor for Postcured (PC) > Moisture (M)> Physical aging and moisture (PA+M) > Physical aging (PA).
- While the stress limit for linear to non-linear creep transition was found to be same for postcured (PC), physically aged (PA), and moisture conditioned (M) resin and the

composite, it changed for physically aged and moisture conditioned (PA+M) resin and the composite

5.3 FRACTURE

- Fracture energy for resin and the composite decreased with increase in temperature.
- Individually, physical aging and moisture decreased the fracture energy for the resin and the composite.
- At a given temperature, the fracture energy of physically aged and moisture conditioned (PA+M) resin and the composite was found to be higher than that of moisture conditioned (M) but lower than that of physically aged (PA) resin and the composite.

5.4 CREEP RUPTURE

- With increase in temperature and stress, creep rupture time decreased for the resin and the composite.
- Creep rupture time for physically aged resin was found to be higher than that for non-aged resin (Postcured:PC). Creep rupture time for physically aged composite was found to be less than that for non-aged composite (PC). However, current results are limited to one aging time and further experimentation is required at other aging times to verify the observed effect of physical aging on creep rupture.
- The creep rupture time for the moisture conditioned resin and composite was lower than that for postcured resin and composite, at a given temperature and stress.

- For a given temperature and stress level, the creep rupture time for physically aged and moisture conditioned (PA+M) resin and the composite was found to be higher than that for moisture conditioned (M), but less than that for physically aged (PA) resin and the composite.

Based on these results the following conclusion can be drawn on interactive influence of temperature, stress, physical aging, moisture and fiber volume fraction on creep, fracture and creep rupture of resin and composite

- Interactive influence of the other factors on the influence of temperature on creep was not observed.
- Interactive influence of physical aging and moisture on the effect of stress on creep was observed, when moisture and physical aging were considered together.
- Physical aging and moisture influenced each other on their effect on creep and creep rupture.

REFERENCES

1. Y.T. Yeow, D.H. Morris and H.F. Brinson; Time Temperature behavior of a unidirectional graphite/epoxy composite*; Composite materials, Testing and Design(Fifth conference), ASTM STP 674*, (1979), pp.263-281
2. D. Dillard, D.H. Morris, and H.F Brinson; Creep and creep rupture of laminated graphite/epoxy composites; *A report prepared for National Aeronautics and Space Adminstration , VPI-E-81-3, Materials and Physical Sciences Branch, Ames Research Center,Moffett Field,CA*, (1981)
3. H.F Brinson, D.H. Morris, and D. Dillard; Environmental effects and viscoelastic behavior of laminated graphite/epoxy composites; *Environmental Degradation of Engineering Materials in Aggressive environment, Proceedings of 2nd International Conference on Environmental Degradation of Engg. Materials*, pp. 445-453,(1981)
4. J. Raghavan and M. Meshii; Creep of Polymer Composites, *Composite Science and Technology*, (1997), pp.1-16
5. S.Y. Zhang and X.Y. Xiang; Constitutive of viscoelasticty of PMC with creep damage; *24th International SAMPE Technical Conference*, Vol.24, (1992), pp.319-328
6. David W.Scott, James S. Lai, and Abdul-Hamid Zureick; Creep behavior of FRP; *Journal of Reinforced Plastics and Composites*, Vol.14, (1995), pp.588-617
7. R.N Yancy and Marek-Jerzy Pindera; Micromechanical analysis of the creep response of unidirectional composites; *Journal of Engineering Materials And Technology*, Vol.112, (1990), pp.157-163

8. J. Raghavan and M. Meshii; Creep rupture of polymer composites; *Composite Science and Technology*, Vol.57, (1997), pp.375-388

9. J. Raghavan and M. Meshii; Prediction of Creep rupture of unidirectional carbon fiber reinforced polymer composite, *Materials Science and Engineering A: Structural Materials properties, Microstructure and Processing*, Vol.A197, (1995), pp.237-249

10. S. Yamini and R. J. Young; The mechanical properties of epoxy resins : Part 2, Effect of plastic deformation upon crack propogation; *Journal of Materials Science*, Vol.15, (1980), pp.1823-1831

11. Yasushi Miyano, Manabu Kanemitsu, Takeshi Kunio and Howard A. Kuhn; Role of matrix resin on fracture strength of unidirectional CFRP; *Journal of Composite Materials*, Vol.20, (1986), pp.520-537

12. T.A. Chenock and H.A. Aglan; Fracture behavior of advanced composites at elevated temperatures, *International SAMPE Symposium and Exhibition How Concept becomes Reality 36th International SAMPE Symposium and Exhibition*,Vol.32, (1991), pp.1147-1160

13. W.J. Cantwell and Anne C. Roulin-Moloney; Fractography and Failure Mechanisms of Unfilled and Particulate Filled Epoxy Resins, *Fractography and Failure of Mechanisms of Polymers and Composites by Anne C. Rouling-Moloney*, Elsevier Applied Science, (1989), pp.233-289

14. L.C.E. Struik; Physical Aging in Amorphous polymer and other materials, *Elsevier Scientific Publishing Company*, Amsterdam-Oxford, New York, (1978)

15. L.C. Brinson And T.S.Gates; Effects of Physical Aging on Long-Term Creep of Polymers and Polymer Matrix Composites; *National Technical Memorandum*, (1994), pp.1-15

16. R.D. Bradshaw and L.C. Brinson; Physical Aging in Polymers and Polymer Composites: An analysis and Method for Time-Aging Time Superposition; *Polymer Engineering and Science*, Vol.37, No.1, (1997), pp.31-44

17. R.D. Bradshaw, L.C. Brinson; Recovering Nonisothermal Physical Aging Shift factors Via Continuous Test data:Theory and Experimental Results; *Journal of Engineering Materials and Technology*, Vol. 119, (1997), pp.233-241

18. J.L.Sullivan; Creep and Physical aging of composites; *Composites Science and Technology*,Vol.39, (1990),pp. 207-232

19. Thomas S. Gates; High Temperature Effects on Polymeric Composites; *ASTM STP 1174, American Society for Testing and Materials*; (1993), pp.201-221

20. Thomas S. Gates and Mark Feldman; Effects of Physical Aging at Elevated Temperatures on the Viscoelastic Creep of IM7/K3B; Composite materials: *Testing and Design (Twelfth vol.), ASTM STP 1274, American Society for Testing and Materials*, (August 1996), pp7-36

21. D.R. Veazie and T.S. Gates; Compressive Creep of IM7/K3B Composite and the Effects of Physical Aging on Viscoelastic Behavior; *Experimental Mechanics*, Vol. 37, No.1, (1997), pp.62-68

22. Y.Z.Wang, Parvatareddy, T.Chang, N.Iyengar, D.A.Dillard and K.L.Reifsnider; Physical Aging Behavior of High Performance Composites; *Composites Science and Technology*, Vol.54, (1995), pp.405-415

23. John M. Crissman, Gregory B. Mckenna; Physical and chemical aging in PMMA in creep and creep rupture behavior; *Journal of Polymer Science, Part B, Polymer Physics*,Vol.28, (1990), pp.1463-1473

24. E.S.W. Kong; Physical Aging in Epoxy Matrices and Composites; *Advances in Polymer Science 80, Springer-Verlag Berlin Heidelberg*, (1986)

25. Y. Jack Weitsman; Effects of Fluids on Polymeric Composites-A Review, Report MAES98-5.0-CM, University of Tennessee, Knoxville, TN, (1998)

26. George S. Springer and A.C. Loos; Moisture absorption of Graphite-Epoxy composites immersed in liquids and humid air; *J. Composite materials*, Vol.3, (1979) pp.131-147

27. Dewimille, J. Thoris, R. Mailfert and A.R. Bunsell; Hydrothermal aging of an unidirectional glass fibers epoxy composite during water immersion; ; *Economic Computation and Economic Cybernetics studies and Research Aug.26-29,1980 Paris Fr, Pergamon Press,(Int Ser on the strength and Fracture of Materials and Structures) Oxford, Engl*, Vol.1, pp597-612, (1980)

28. R.M.V.G.K.Rao, Manas Chanda and N. Balasumbrmanian; Factors affecting moisture absorption in polymer composites: Part I Influence of internal factors; *Journal of Reinforced Plastics and Composites*, Vol.3, (1984), pp246-256

29. R.M.V.G.K.Rao, N. Balasumbrmanian and Manas Chanda; Factors affecting moisture absorption in polymer composites: Part II Influence of external factors; *Journal of Reinforced Plastics and Composites*, Vol.3, (1984), pp233-243

30. Monica S.W. Woo and Micheal R. Piggot; Moisture absorption of resin and composites:1 Epoxy homopolymer and copolymer; *American Society for Testing and Materials*, Vol.9, (1987), pp.162-166

31. Monica S.W. Woo and Micheal R. Piggot; Moisture absorption of resin and composites:II. Diffusion in carbon and glass reinforced epoxies; *American Society for Testing and Materials*, Vol.9, (1987), pp.162-166

32. Charles E. Browning; The mechanisms of elevated temperature property losses in high performance structural epoxy resin matrix materials after exposures to high humidity environments; *Polymer Engineering and Science*, Vol.18, No.1, (1978), pp.16-24

33. W.J. Milkos, J.J.C. Seferis, A. Apicella and l. Nicholais; Evaluation of structural changes in epoxy systems by moisture absorption-desorption and dynamic mechanical studies; *Polymer Composites*, Vol.3, No.3, (1982), pp.118-124

34. Chi-Hung Shen and George S. Springer; Moisture absorption and desorptiopn of composite material; *Journal of Composite Materials*, Vol.10, (1975), pp.2-20

35. C.E. Browning, G.E. Husman and J.M. Whitney; Moisture effects in epoxy matrix composites; *Composites Materials: Testing and Design(Fourth Conference), ASTM STP 617, American society For Testing And Materials*, (1977), pp. 481-496

36. Blaga; Water absorption characteristics of graphite composites: Effect of outdoor weathering; *Polymer Composites*, Vol.2, No.1, (1981), pp.13-17

37. J. M. Marshall, G.P. Marshall and R.F. Pinzelli; The diffusion of liquids into resins and composites; *Polymer Composites*, Vol.3, No.3, (1982), pp.131-137

38. Marten Blikstad, Peter O.W. Sjoblom and Thomas R. Johannesson; Long term moisture absorption in graphite/epoxy angle ply laminates; *Journal of Composite Materials*, Vol.18, (1984), pp.32-46

39. Srihari, Shylaja and Rao, R.M.V.G.K.; Hygrothermal characterization and diffusion studies on carbon epoxy composites, *Journal of Reinforced Plastics and Composites*; Vol.18, (1999), pp.921-930,

40. C.E Browning and J.T. Hartness; Effect of moisture on the properties of high performance structural resins and composites; Composites Materials: *Testing and Design(Third Conference), ASTM STP 546, American society For Testing And Materials*, (1974), pp. 284-302

41. J.F. Harper and M. Naeem; The moisture absorption of glass fiber reinforced vinyl ester and polyster composites; *Materials and Design*, Vol.10 No.6, (1989), pp.297-300

42. Ghorbel and D. Valentin; Hygrothermal effects on the physio-chemical properties of pure/glass reinforced polyster and vinyl ester resin; *Composites Polymer Composites*, Vol.14, No.4, (1993), pp.324-334

43. R.M.V.G.K.Rao, N. Balasumbrmanian and Manas Chanda; Hydrothermal effects on chopped fiber/woven fabric reinforced epoxy composites Part A: Moisture absorption characteristics; *Journal of Reinforced Plastics and Composites*, Vol.3, (1991), pp233-243

44. A.A. Fahmy and J.C. Hurt; Stress dependence of water diffuison in epoxy resin; *Polymer Composites*, Vol.1, (1980), pp.77-80

45. Neuman and Gad marom; Stress dependence of the coefficient of moisture diffusion in composite material; *Polymer Composites*; Vol. 6 n1, (1985), pp.9-12

46. Neuman and Gad marom; Prediction of moisture diffusion parameters in composite material under stress; *Journal of Composite Materials*; Vol.21,(1987)

47. V.F. Janas, L.S. Smith and R.L. McCullough; The effects of tension on the absorbance of water into resin and glass filled and crosslinked polyster; *Polymer Composites*, Vol.7, No.6, (1986), pp.455-462

48. R. Lagrange, Ch. Melennec, R. Jacquemet; Influence of stress conditions of the moisture diffusion of composites in distilled water and in natural sea water; *Durability of Polymer based composite systems for structural applications, Elsevier Applied Science*, (1991), pp.385-392

49. M. Marchetti, S.Tizzi and C. Tessi; Creep behavior of graphite-epoxy composites: Temperature and moisture effects; *Advances in fracture research (Fracture 84), Proceedings of the 6th International Conference on fracture*,(1984), pp. 3029-3036

50. Won Hee Han and Gregory B. Mckenna; *Annual Technical conference – ANTEC,Conference Proceedings Materials of the 1997 55th Annual Technical Conference*, Vol. 2, (1997), pp.1539-1545

51. David A. Douglas and Yechiel Weitsman; Stresses due to environmental conditioning of crossply graphite/epoxy laminates; *Economic Computation and Economic Cybernetics studies and Research Aug.26-29,1980 Paris Fr, Pergamon Press,(Int Ser on the strength and Fracture of Materials and Structures) Oxford, Engl*, Vol.1, pp529-542, (1980)

52. D.L. Flaggs and W.F. Crossman; Analysis of viscoelastic response of composite laminates during hyrothermal exposure; *Journal of Composite Materials*, Vol.15,(1980), pp.21-39

53. John Z. Wang, V. Dave, W. Glasser and D.A. Dillard; The effect of moisture sorption on the creep behaviors of fibers; *High Temperature and Environmental Effects on Polymeric Composites, ASTM STP 1174*, (1993), pp. 186-200

54. E.M. Woo; Moisture temperature equivalency in creep analysis of a hetergenous matrix carbon fiber epoxy matrix composite; *Composites*, Vol.25, No.6, (1994), 425-430

55. G.E. Springer; Environmental effects on glass fiber reinforced polyster and vinyl ester composites; *Journal of composite materials*,Vol.14, (1980), pp.213-235

56. R.J. Morgan, J.E. O'Neal, and D.L. Fanter et al;The effect of moisture on the physical and mechanical integrity of epoxies; *Journal of Materials Science*, Vol.15, , (1980), pp.751-764

57. B.L. Lee, R.W. Lewis and R.E. Sacher; Environmental effects on the mechanical properties of glass fiber/epoxy resin composites; *Proceedings of the Annual Meeting and Techincal Conference- Numerical Control Society Proc. Of the Int Conf on Comps Mater*, 2nd, (ICCM2), (1978), pp1560-1580

58. Ronald E. Allred; The effect of temperature and moisture content on flexural response of Kevlar/Epoxy laminates: Part I [0/90] filament orientation; *Journal of Composite Materials*, Vol.15, (1981), pp.117-132

59. K.W. Thomson and L.J. Broutman; The effect of water on the fracture surface energy of fiber reinforced composite material; *Polymer Composites*, Vol.3, No.3, (1982), pp.113-117

60. I.M. Daniel, G. Yaniv and G. Peimanidis; Hygrothermal and strain rate effects on properties of graphite/epoxy composites; *Journal of Engineering Materials and Technology*, Vol.110, (1988), pp.169-173

61. Suong V. Hoa, Sui Lin, And Jirui R. Chen; Effect of moisture content on the mechanical properties of PPs composite material; *Advances in Thermoplastic matrix composite Materials, ASTM STP 1044, American society For Testing And Materials*, (1989), pp. 213-230

62. James P. Lucas and Ben C. Odegard; Moisture effects on Mode I interlaminar fracture toughness of a graphite fiber thermoplastic matrix composites; *Advances in Thermoplastic matrix composite Materials, ASTM STP 1044, American society For Testing And Materials*, (1989), pp. 231-247

63. Selzer, R; Friedrich ,R; Mechanical properties and failure behaviour of carbon fiber-reinforced polymer composites under the influence of moisture; *Composites-Part A: Applied Science and manufacturing*, Vol.28, (1997), pp.595-604

64. Shin E. Eugene, Dunn Calin; Fouch, Eric; Morgan, Roger J; Wilenski, Mark; Drzal, Lawerence T.; Durability and critical fundamental aging mechanisms of high temperature polymer matrix carbon fiber composites: Part II *American Society of Mechanical Engineers, Materials Division (Publication) MD ASME Materials Division Proceedings of 1995 ASME International Mechanical Engineering Congress exposition*, Vol.69-1, (1995), pp.191-200

65. Rotem and S. Elizov; Effect of temperature and marine environment on the rupture strength of fibrous composite materials; *Proceedings of Riso International Symposium on Metallurgy and Materials Science Fatigue and Creep of composite materials, Proceedings of the 3rd Riso International Symposium on Metallurgy and Materials Science*, (1982), pp308- 310

66. M.G. Phillips; Predictions of long term stress rupture life for glass fiber reinforced polyster composites in air and aqueous environments; *Composites*, Vol.14, No.3, (1983), pp.270-275

67. R.C. Wyatt, L.S. Norwood and M.G. Phillips; The stress rupture behavior of graphite laminates; *Composite Structures*, Applied Science Publisher,(1981), pp.79-91

APPENDIX - A

Calculation of Diffusion Coefficient

$$D_x = \left(\frac{h}{4M_m}\right)^2\left(\frac{M_2 - M_1}{\sqrt{t_2} - \sqrt{t_1}}\right)^2\left(1+\frac{h}{L}+\frac{h}{w}\right)^{-2}$$

h = Thickness of the specimen, L = Length of the specimen, w = Width of the specimen

M_m = Maximum moisture content

$\left(\frac{M_2 - M_1}{\sqrt{t_2} - \sqrt{t_1}}\right)$ = m = linear slope of weight change versus square root of time data

Resin

Temperature (T) = RT , m= 0.0882 , w =5 mm, h = 2.33 mm, L = 37.63 mm,

M_m = 3.29 %

$$D_x = \left(\frac{2.33}{4\times3.29}\right)^2(0.0882)^2\left(1+\frac{2.33}{37.63}+\frac{2.33}{5.00}\right)^{-2}\left(\frac{1}{3600}\right)$$

D_x= 9.115 x 10^{-8} mm^2/sec

Composite with 54% fiber volume fraction

Temperature (T) = RT, m= 0.0593, w =5.31 mm, h = 1.62 mm, L = 37.90 mm,

M_m = 1.80%

$$D_x = \left(\frac{1.62}{4\times1.80}\right)^2(0.0593)^2\left(1+\frac{1.62}{37.90}+\frac{1.62}{5.31}\right)^{-2}\left(\frac{1}{3600}\right)$$

D_x= 8.56 x 10^{-8} mm^2/sec

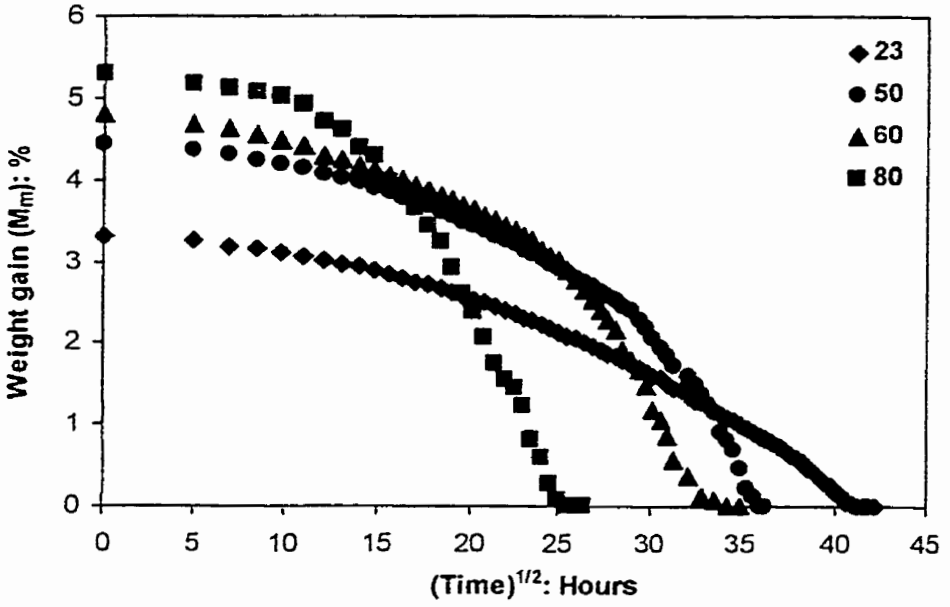

Figure A1: Desorption curves for resin at various temperatures

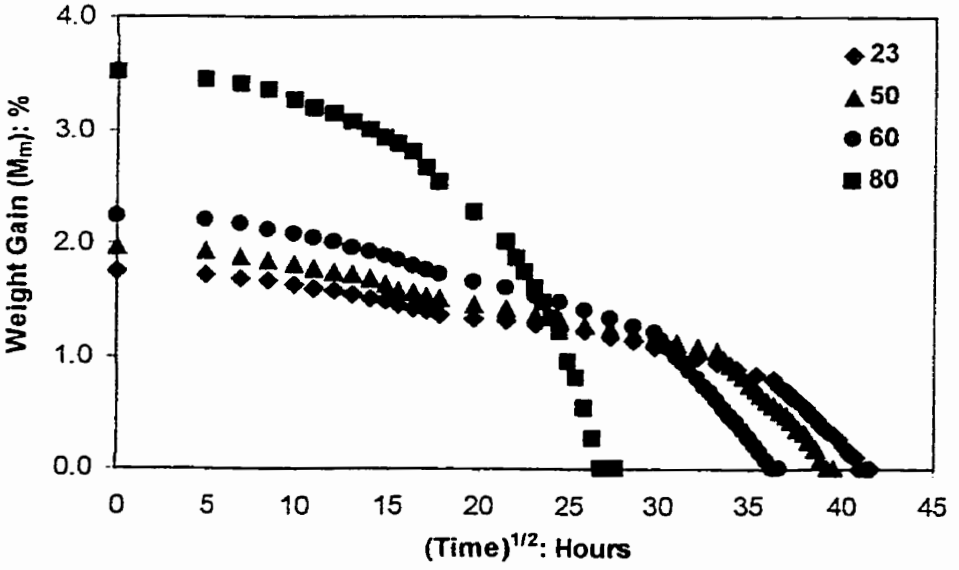

Figure A2: Desorption curves for composite (V_f :54%) at various temperatures

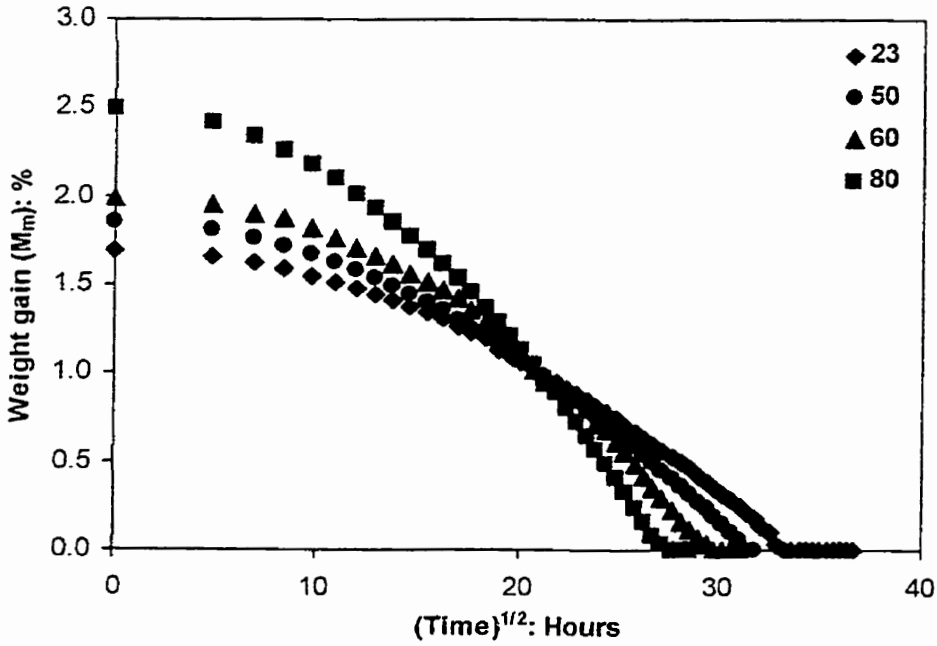

Figure A3: Desorption curves for composite (V_f :71%) at various temperatures

APPENDIX - B

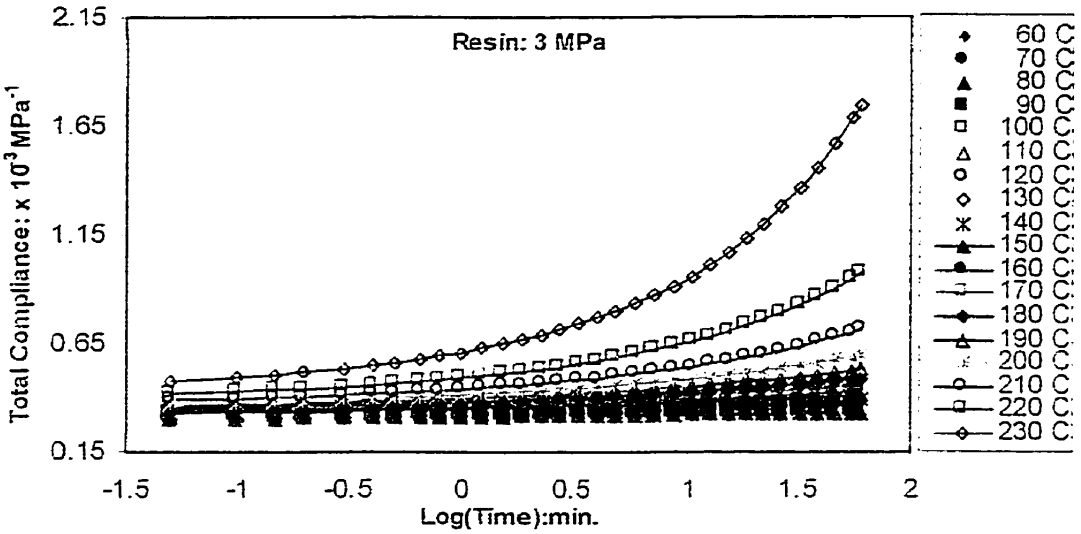

Figure B1: Compliance data at 3 MPa for resin at various temperatures

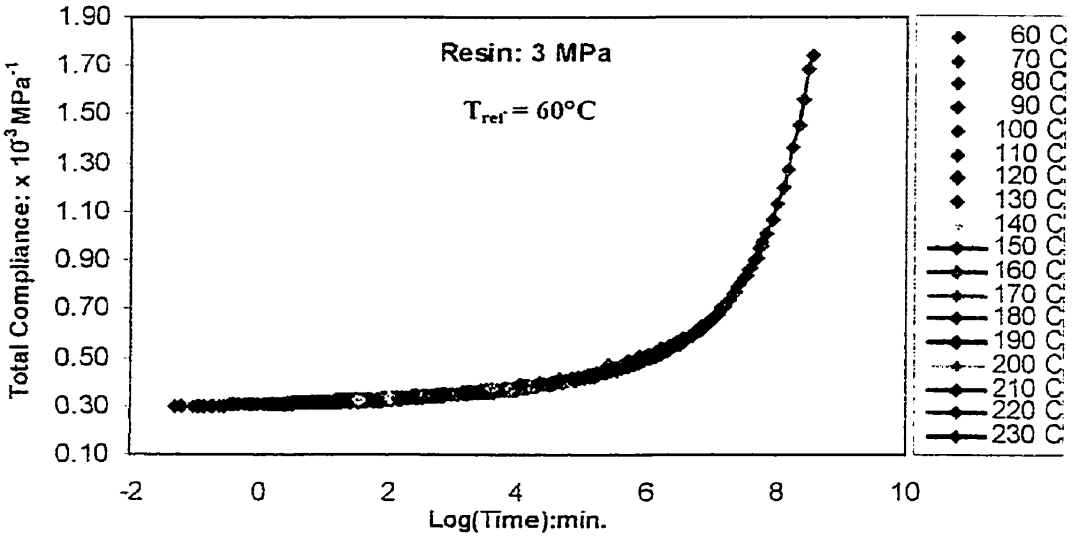

Figure B2: Master creep curve at 3 MPa for resin

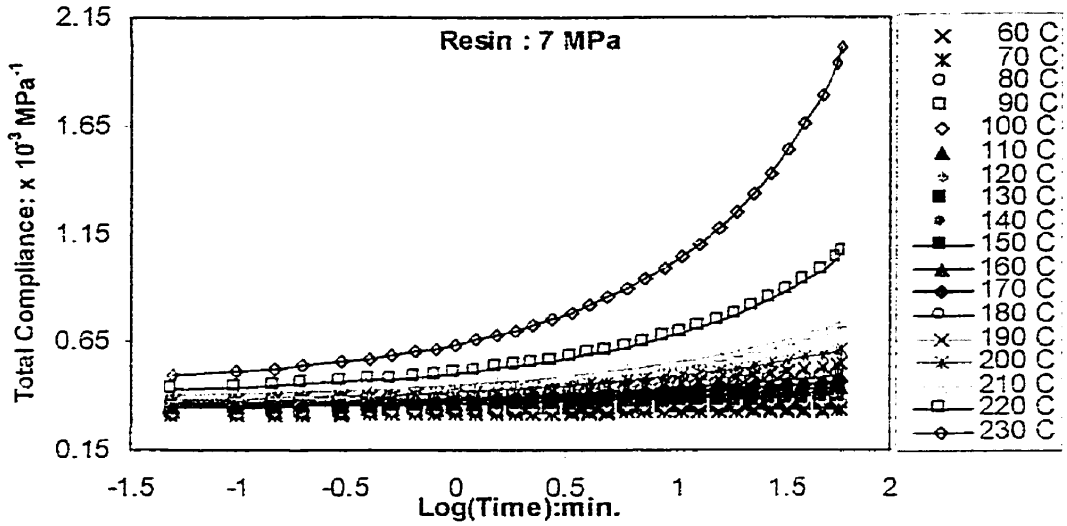

Figure B3: Compliance data at 7 MPa for resin at various temperatures

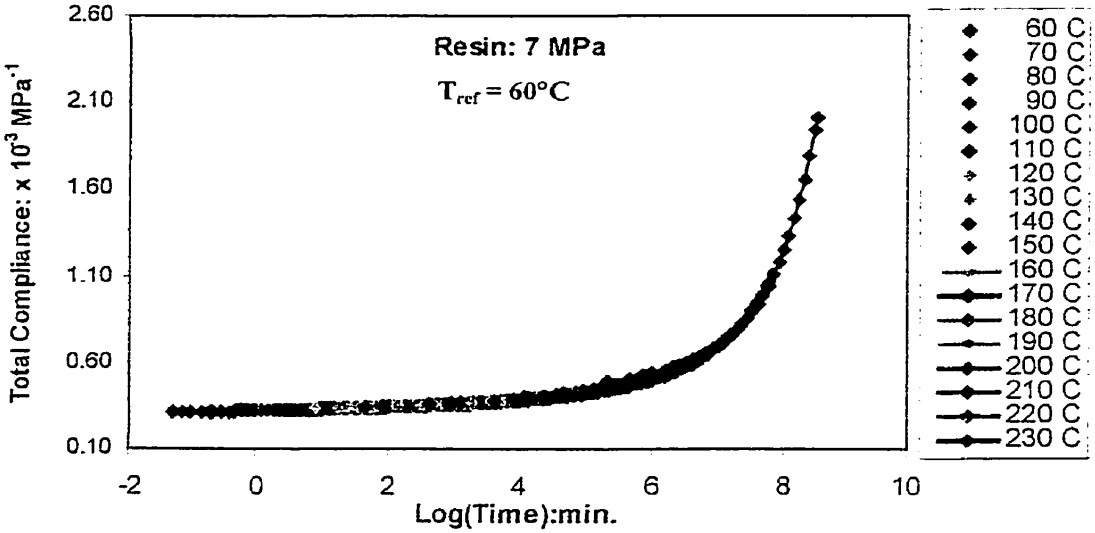

Figure B4: Master creep curve at 7 MPa for resin

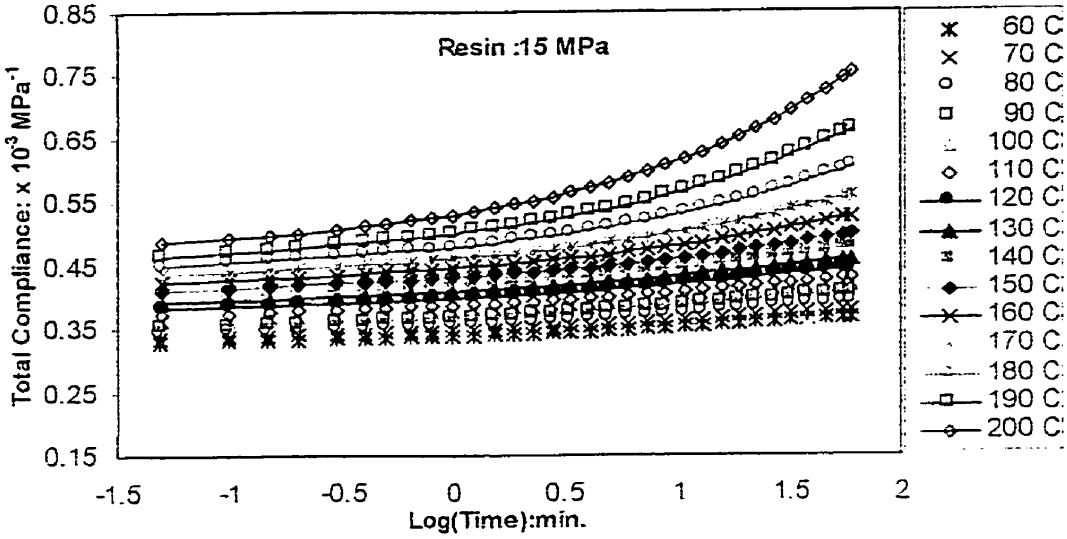

Figure B5: Compliance data at 15 MPa for resin at various temperatures

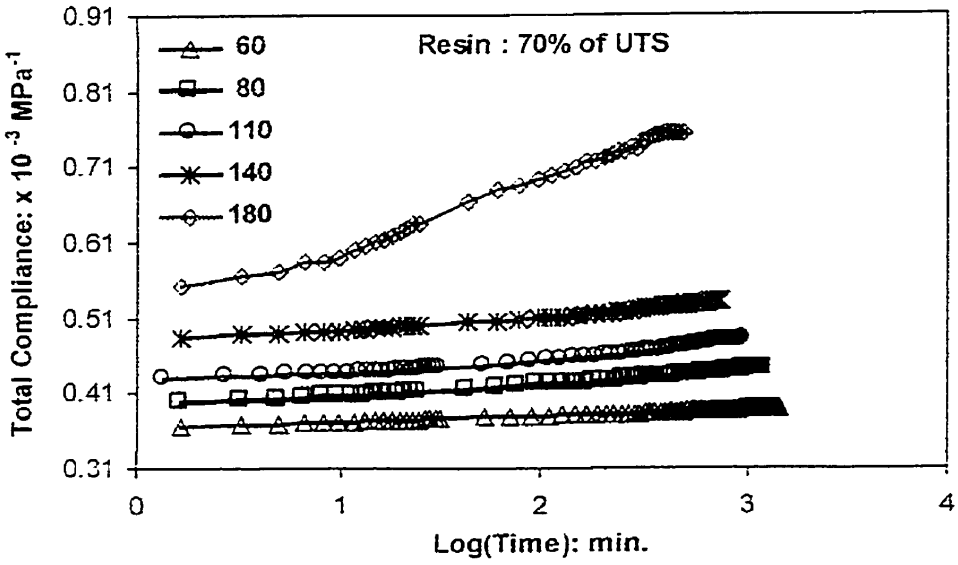

Figure B6: Compliance data at 70% of UTS for resin at various temperatures

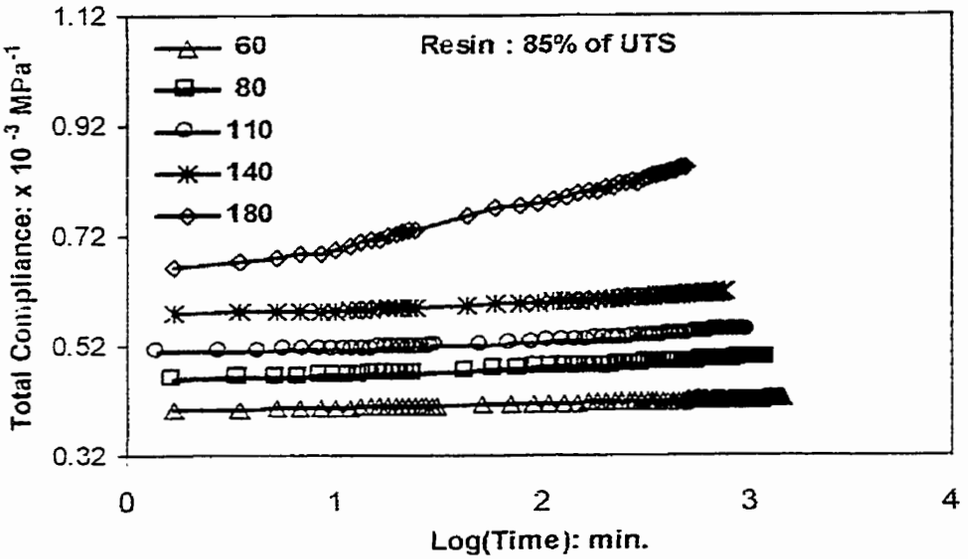

Figure B7: Compliance data at 85% of UTS for resin at various temperatures

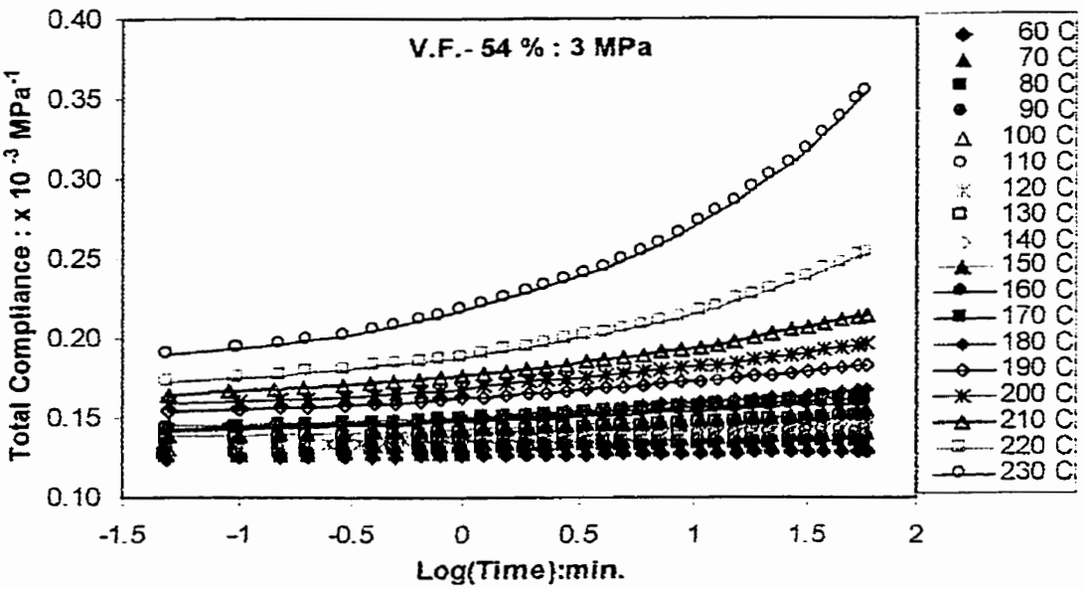

Figure B8: Compliance data at 3 MPa for $[90]_8$ composite (V_f :54%) various temperatures

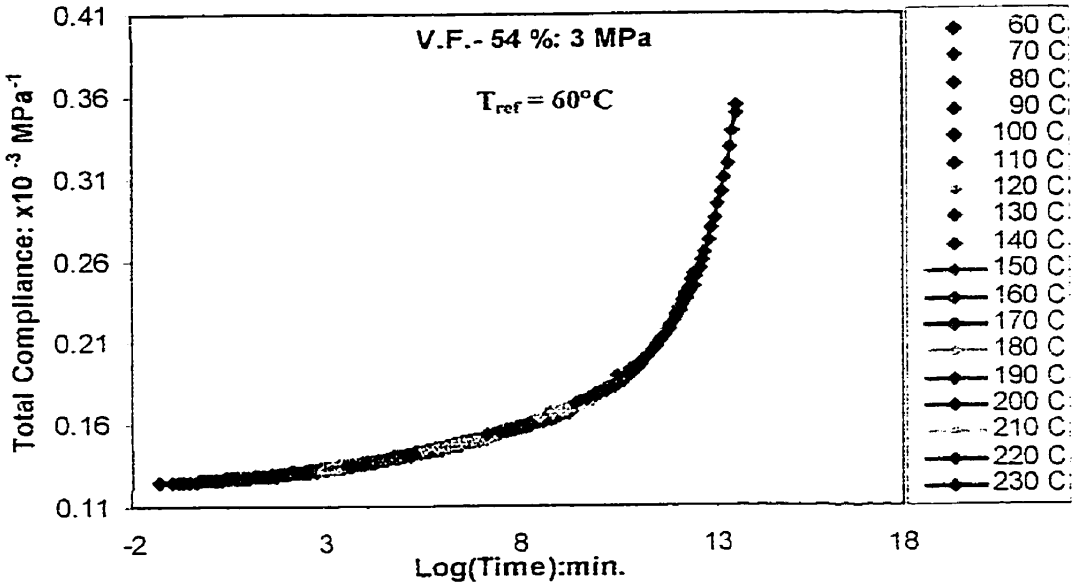

Figure B9: Master creep curve at 3 MPa for $[90]_8$ composite (V_f:54 %)

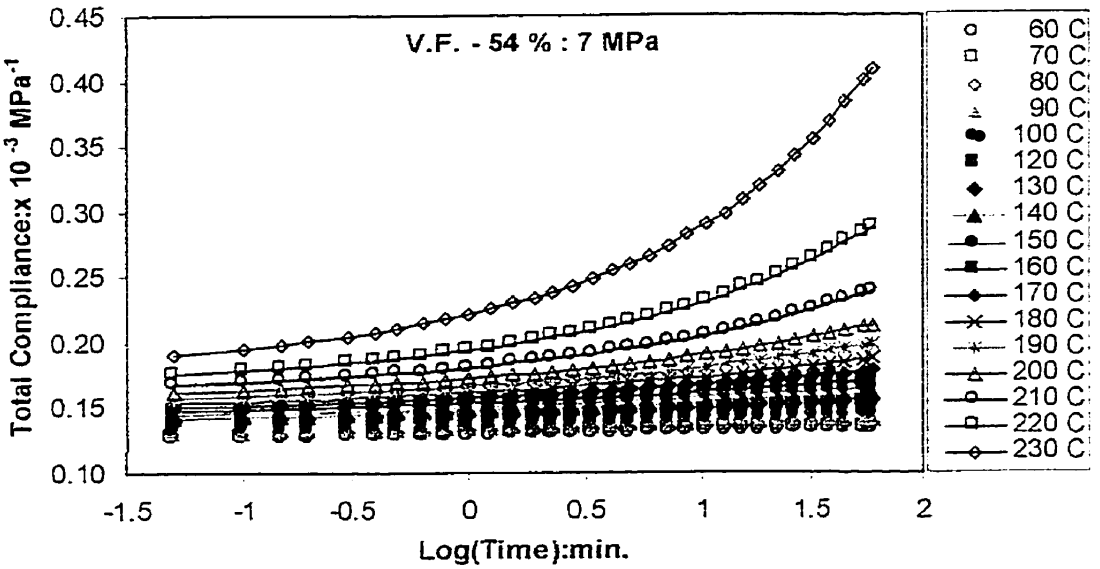

Figure B10: Compliance data at 7 MPa for $[90]_8$ composite (V_f:54%) at various temperatures

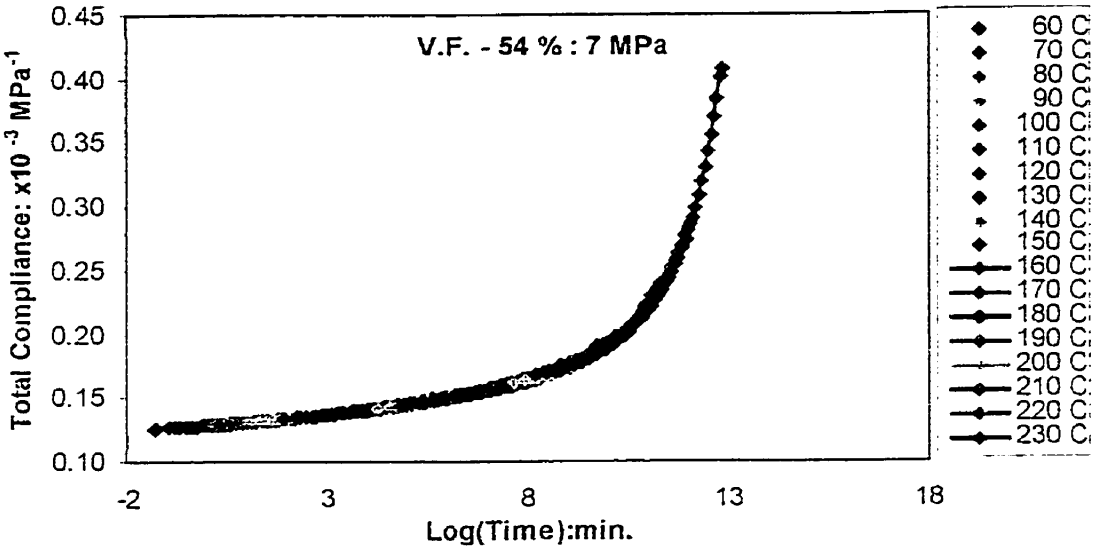

Figure B11: Master creep curve at 7 MPa for $[90]_8$ composite (V_f:54 %)

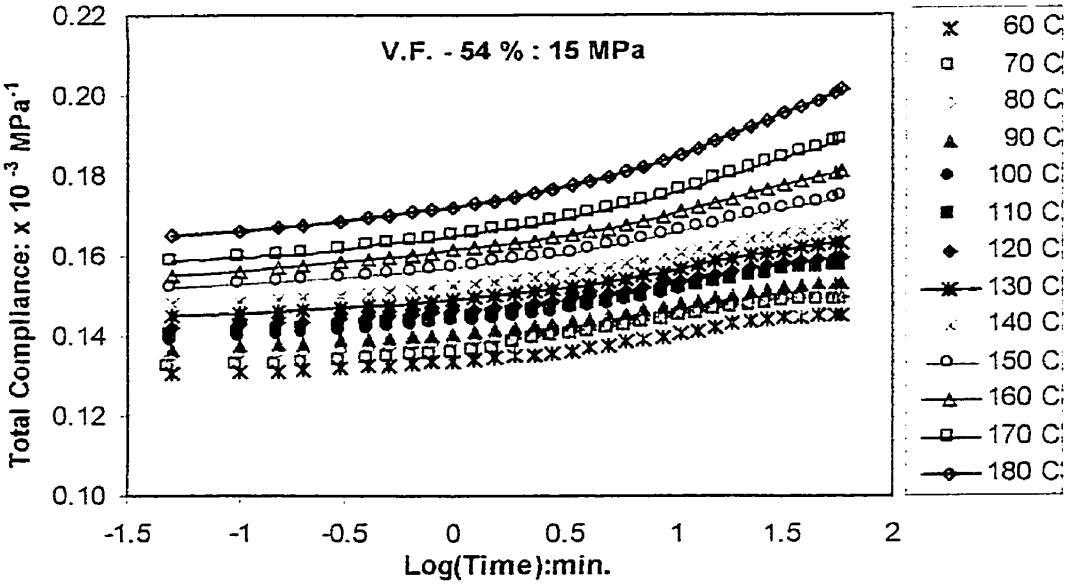

Figure B12: Compliance data at 15 MPa for $[90]_8$ composite (V_f :54%) at various temperatures

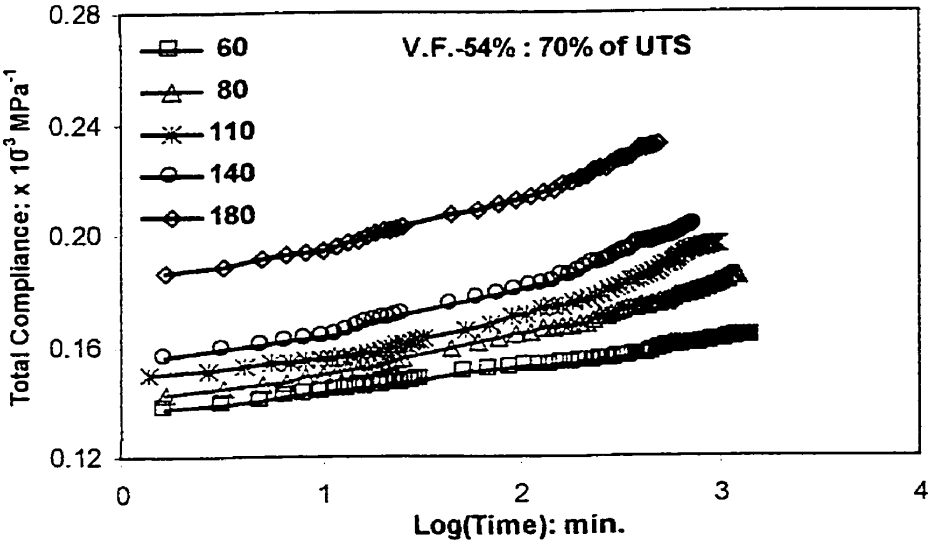

Figure B13: Compliance data at 70% of UTS for $[90]_8$ composite (V_f :54%) at various temperatures

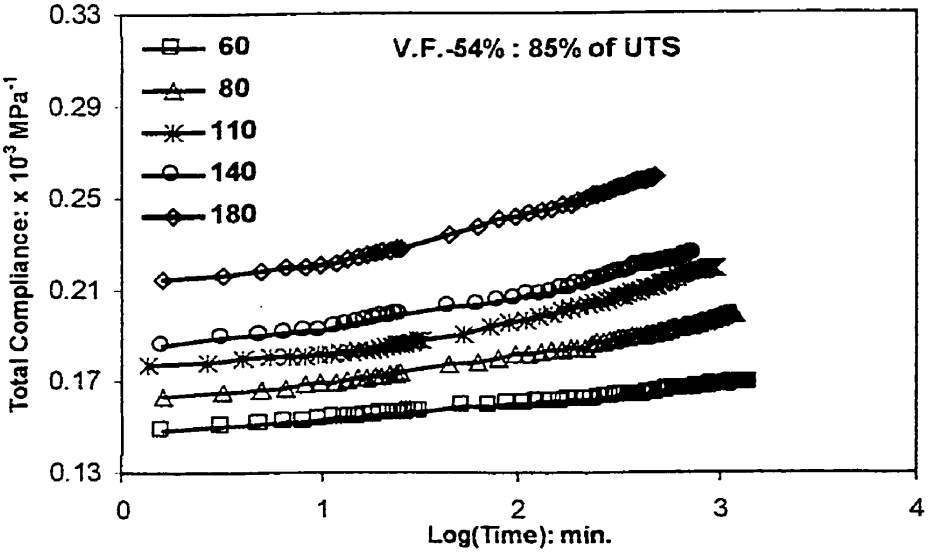

Figure B14: Compliance data at 85% of UTS for $[90]_8$ composite (V_f :54%) at various temperatures

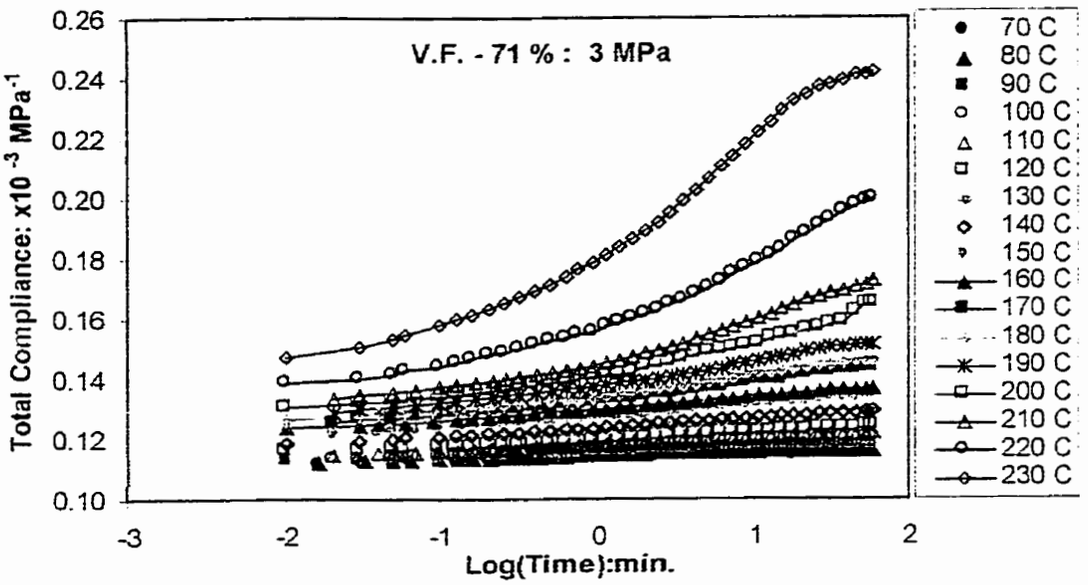

Figure B15: Compliance data at 3 MPa for $[90]_8$ composite (V_f: 71%) at various temperatures

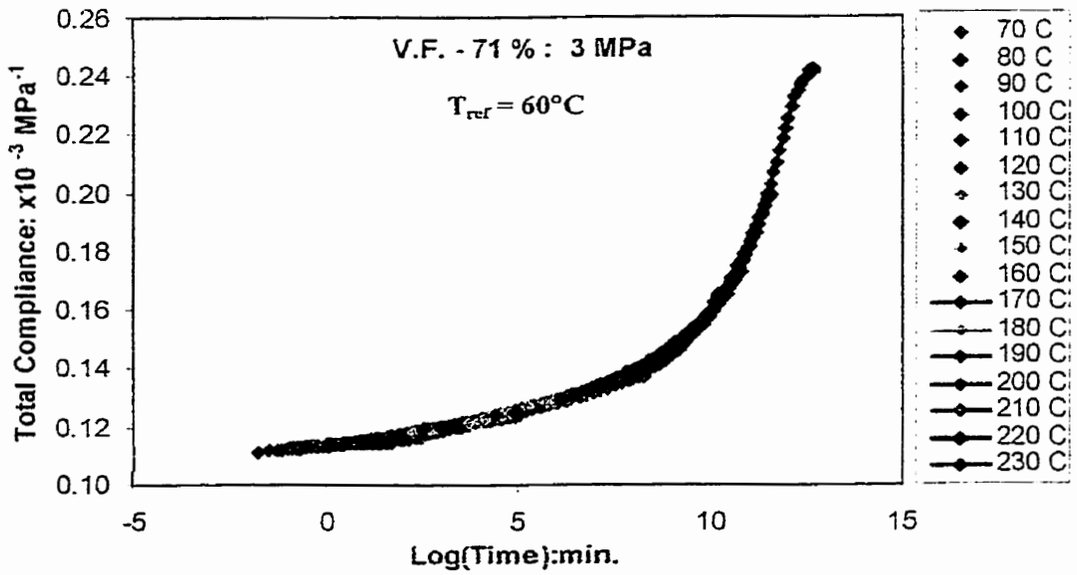

Figure B16: Master creep curve at 3 MPa for $[90]_8$ composite (V_f: 71%)

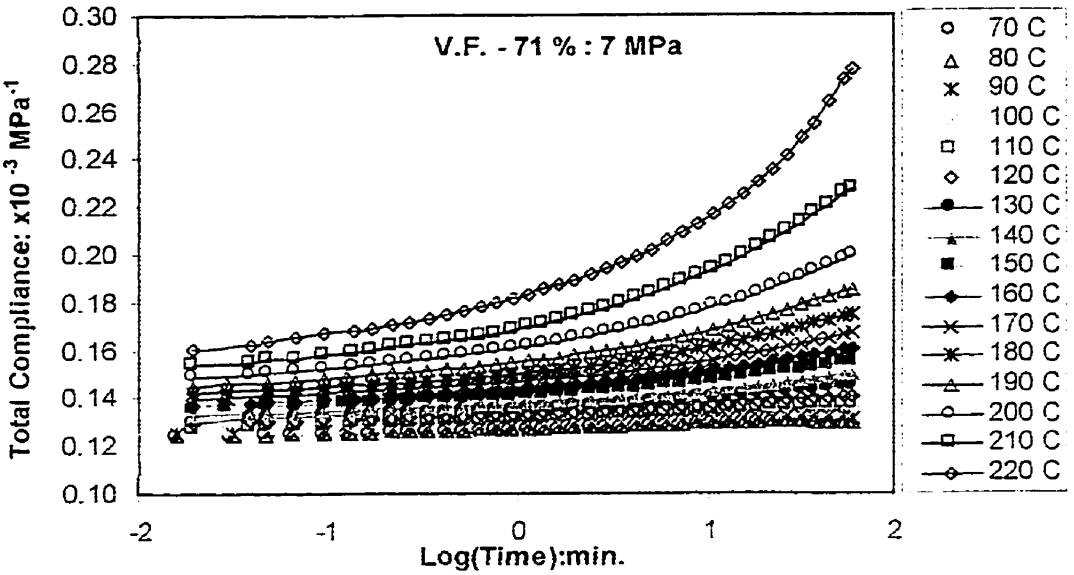

Figure B17: Compliance data at 7 MPa for $[90]_8$ composite (V_f : 71%)

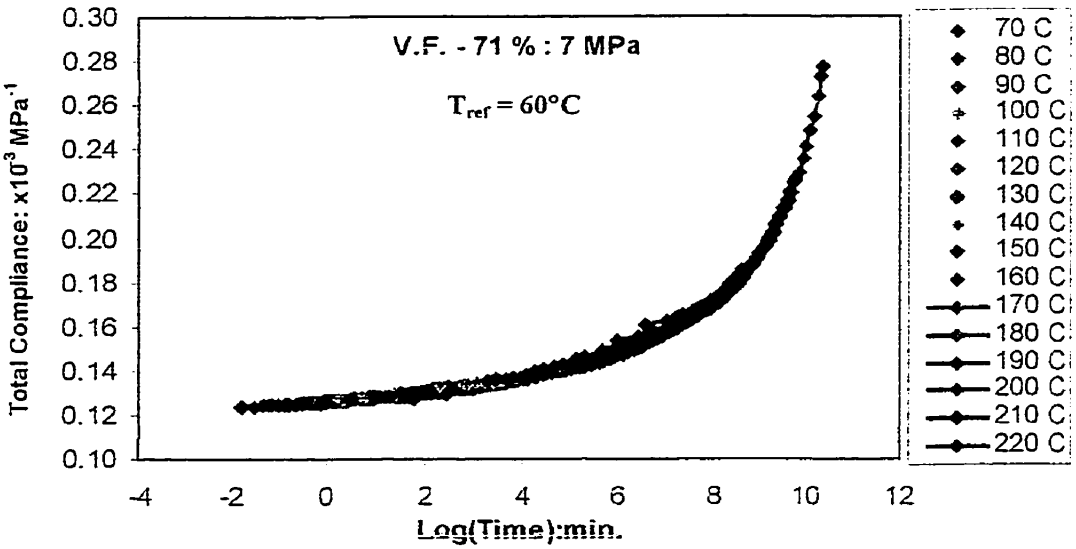

Figure B18: Master creep curve at 7 MPa for $[90]_8$ composite (V_f : 71%)

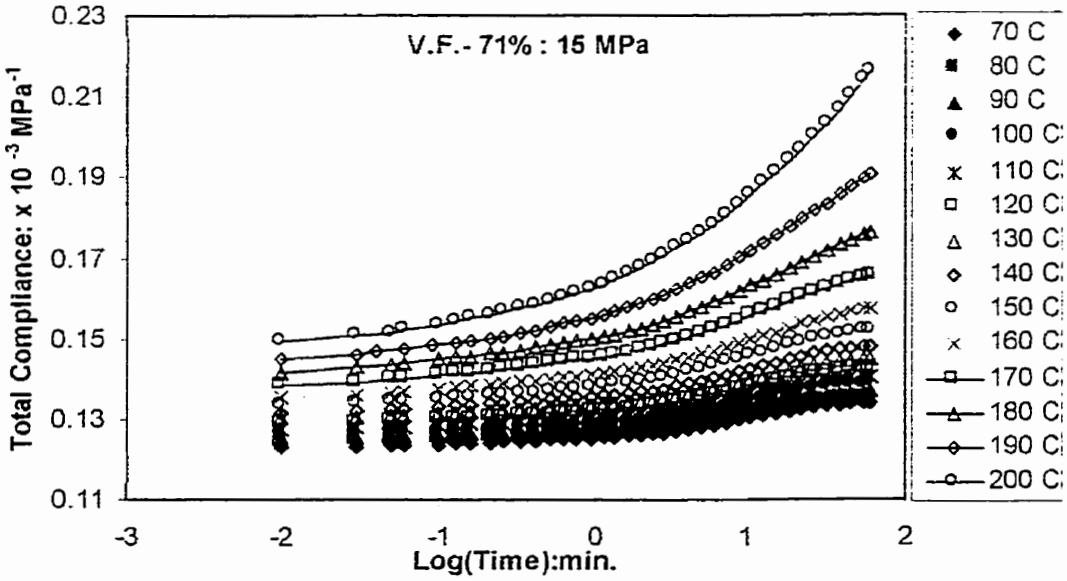

Figure B19: Compliance data at 15 MPa for $[90]_8$ composite (V_f : 71%) at various temperatures

APPENDIX - C

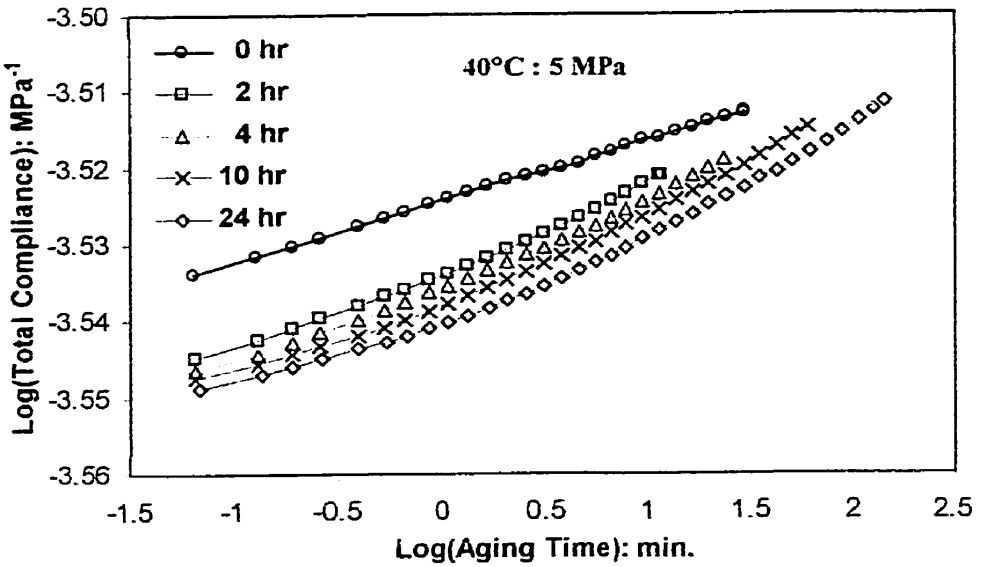

Figure C1: Compliance data at 5 MPa for resin at 40°C at various physical aging times

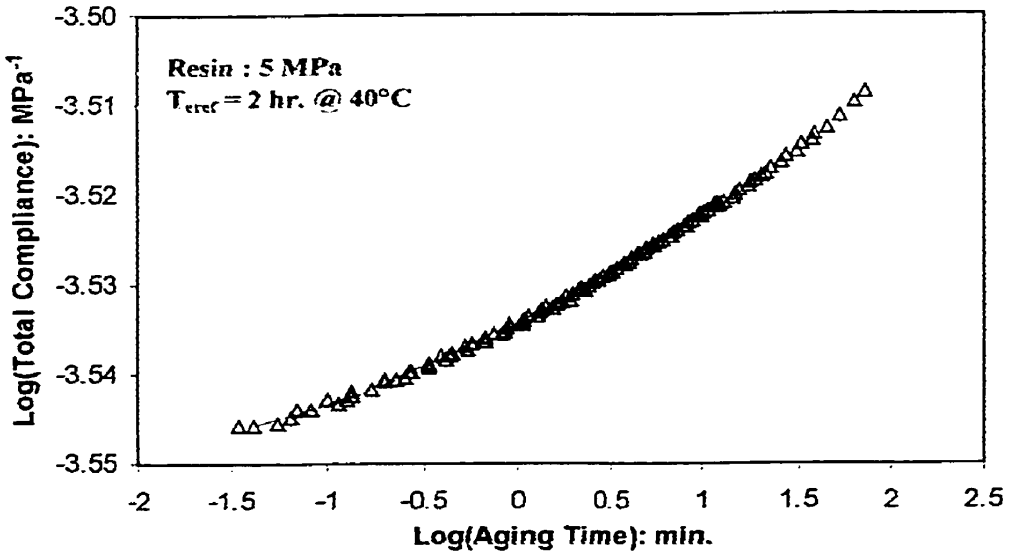

Figure C2: Momentary master curve at 5MPa for resin at 40°C

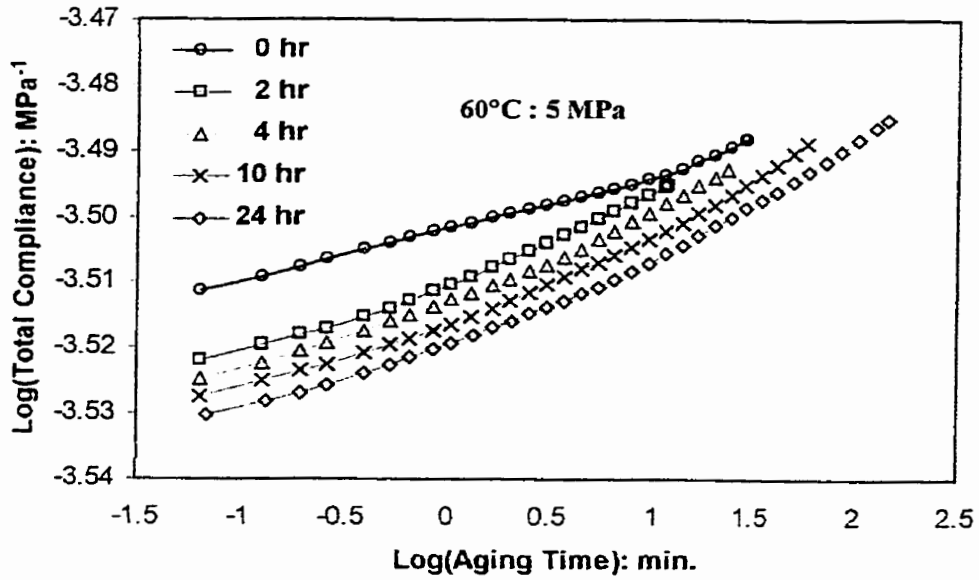

Figure C3: Compliance data at 5 MPa for resin at 60°C at various physical aging times

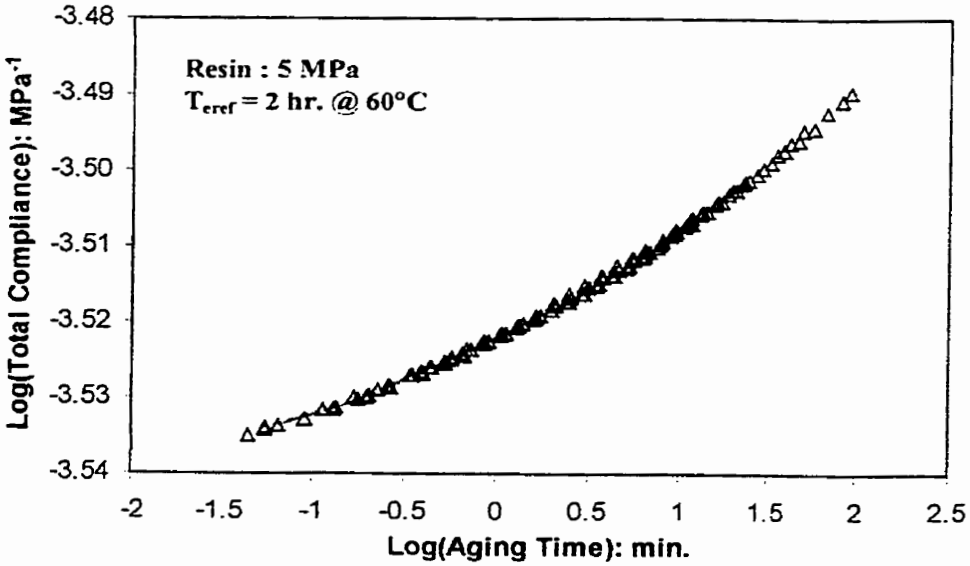

Figure C4: Momentary master curve at 5 MPa for resin at 60°C

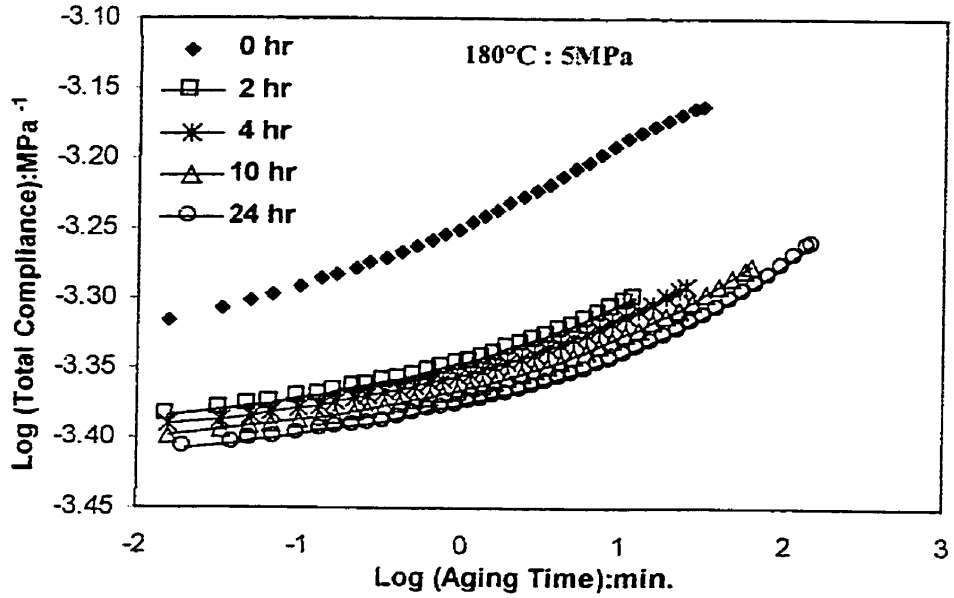

Figure C5: Compliance data at 5 MPa for resin at 180°C at various physical aging times

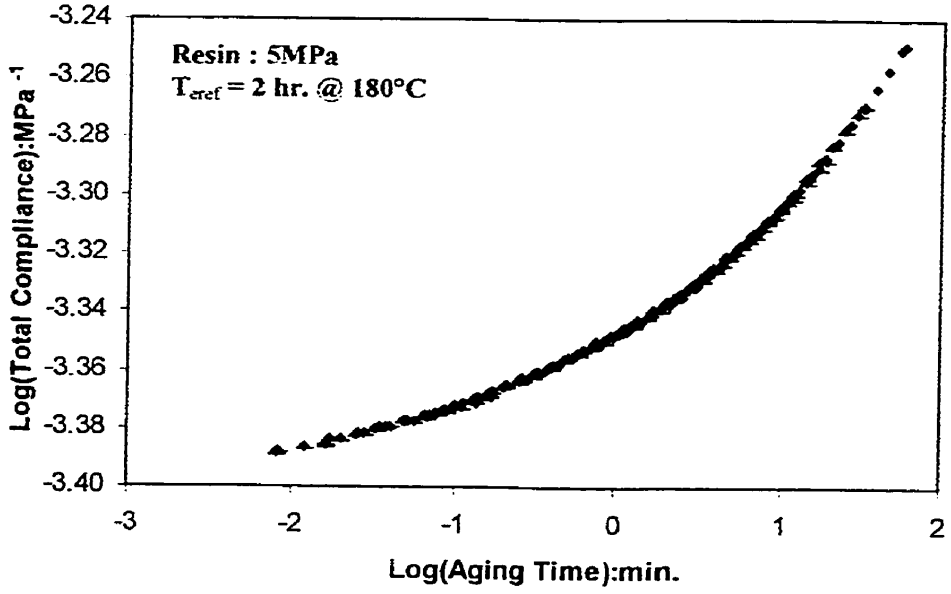

Figure C6: Momentary master curve at 5 MPa for resin at 180°C

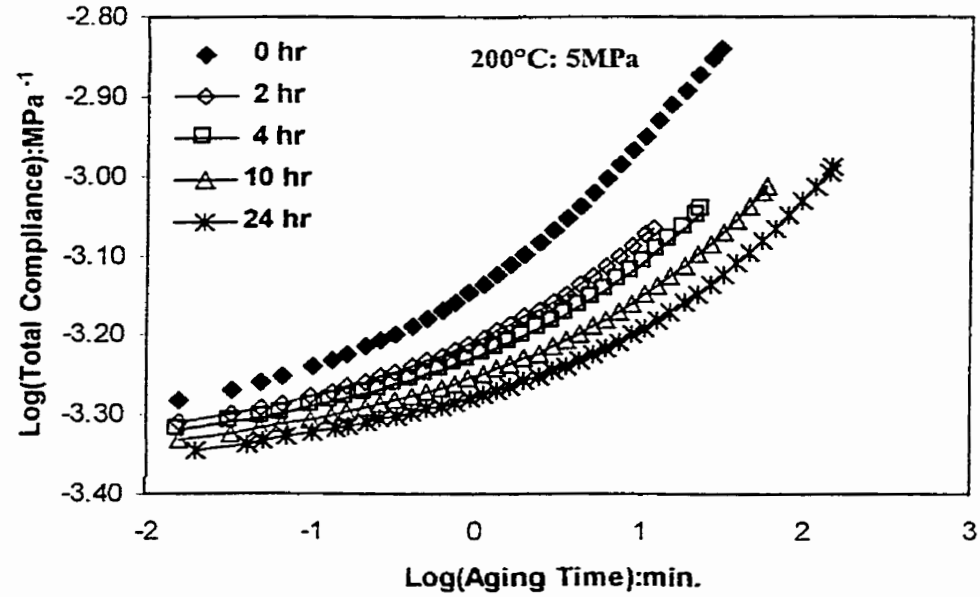

Figure C7: Compliance data at 5 MPa for resin at 200°C at various physical aging times

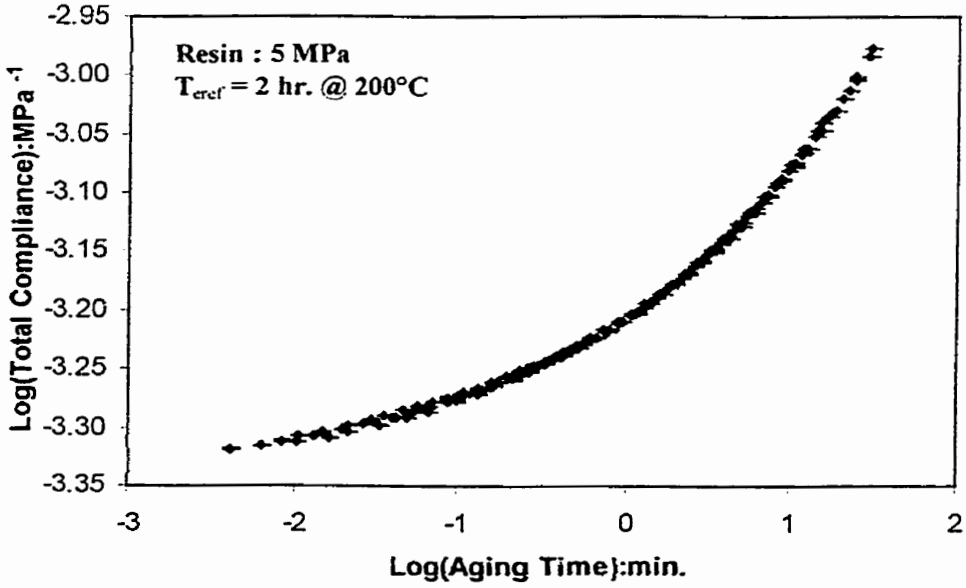

Figure C8: Momentary master curve at 5MPa for resin at 200°C

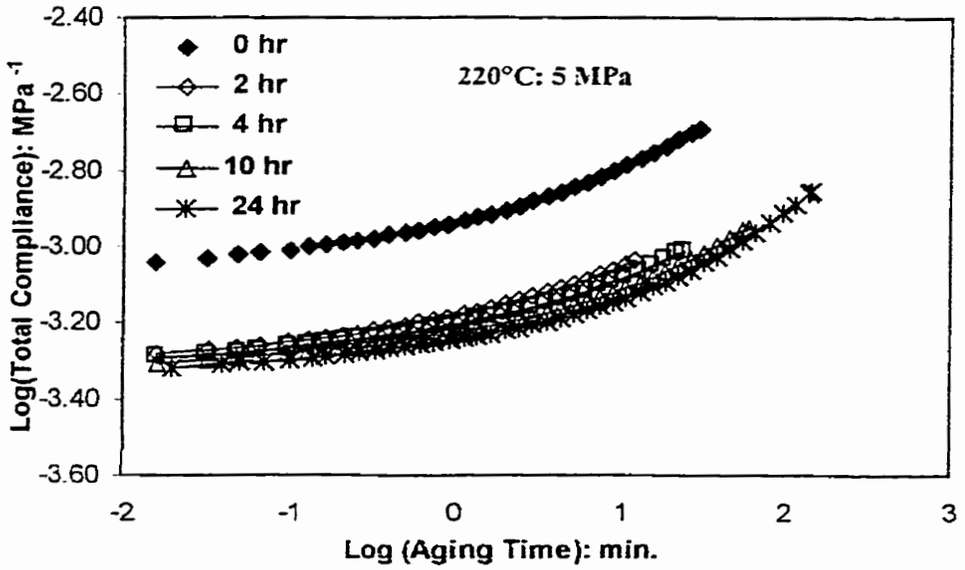

Figure C9: Compliance data at 5 MPa for resin at 220°C at various physical aging times

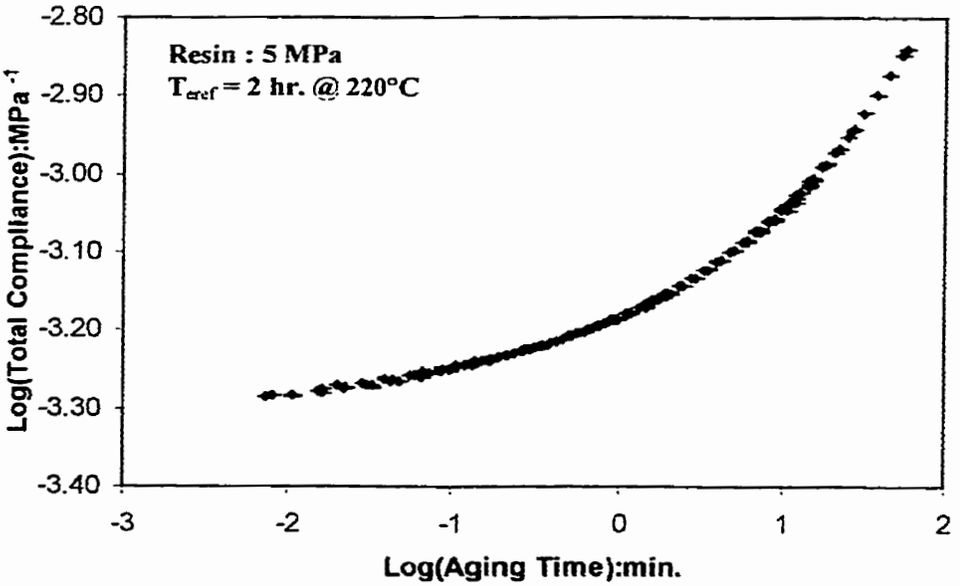

Figure C10: Momentary master curve at 5 MPa for resin at 220°C

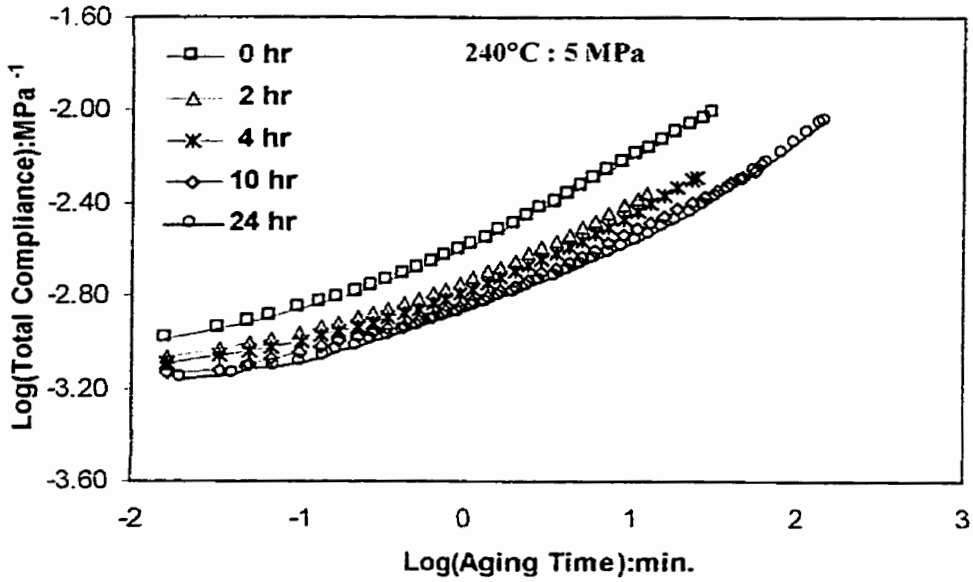

Figure C11: Compliance data at 5 MPa for resin at 240°C at various physical aging times

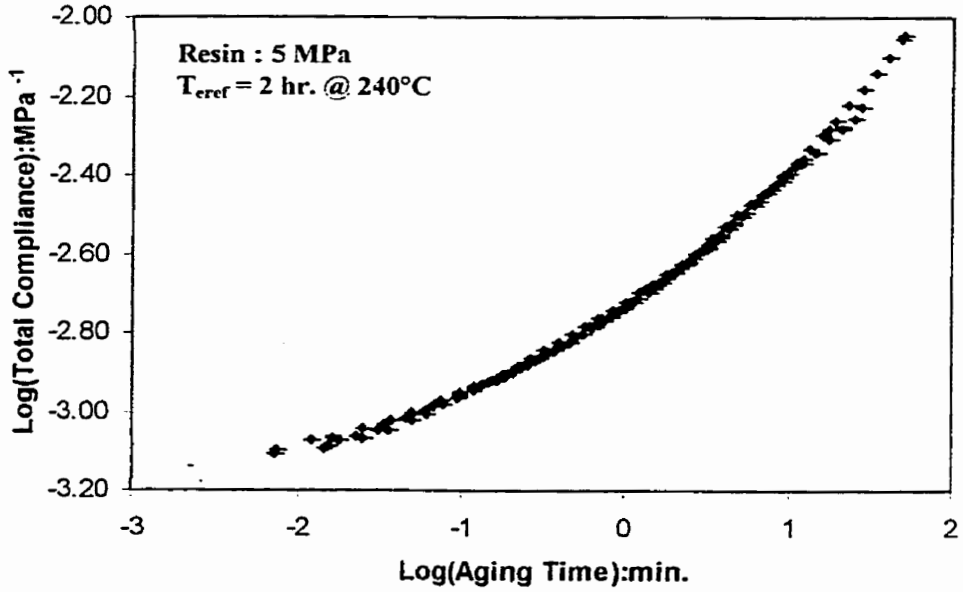

Figure C12: Momentary master curve at 5MPa for resin at 240°C

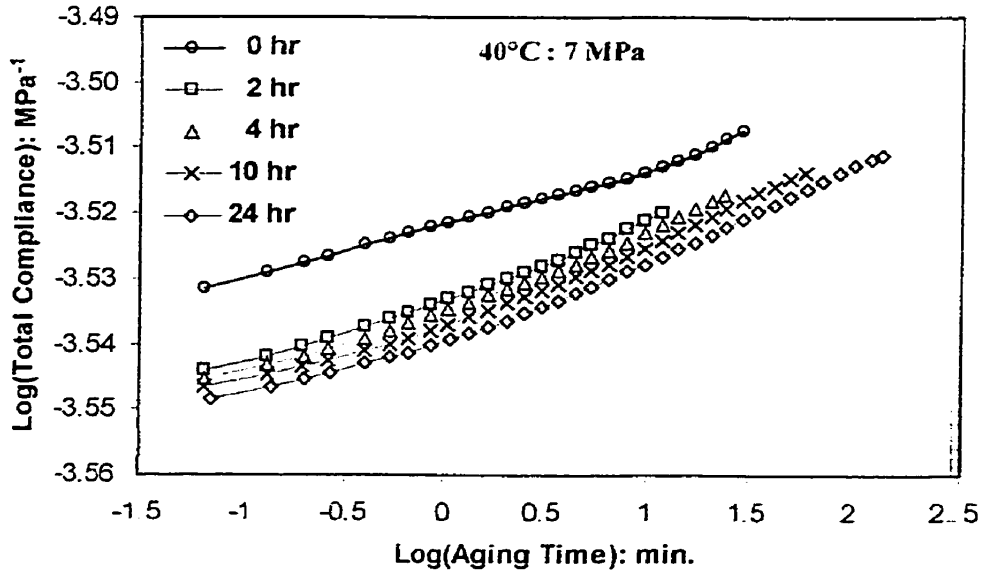

Figure C13: Compliance data at 7 MPa for resin at 40°C at various physical aging times

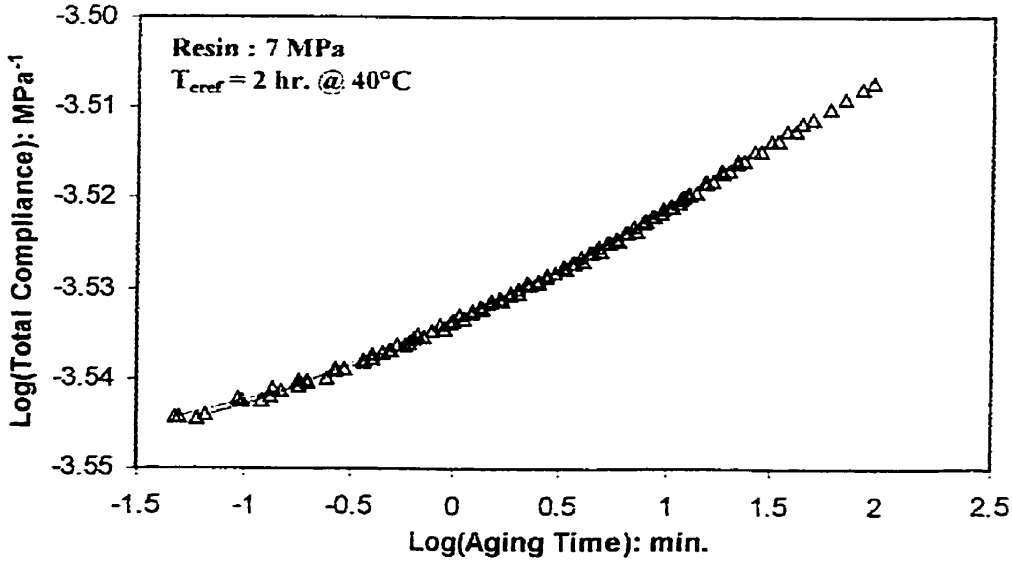

Figure C14: Momentary master curve at 7 MPa for resin at 40°C

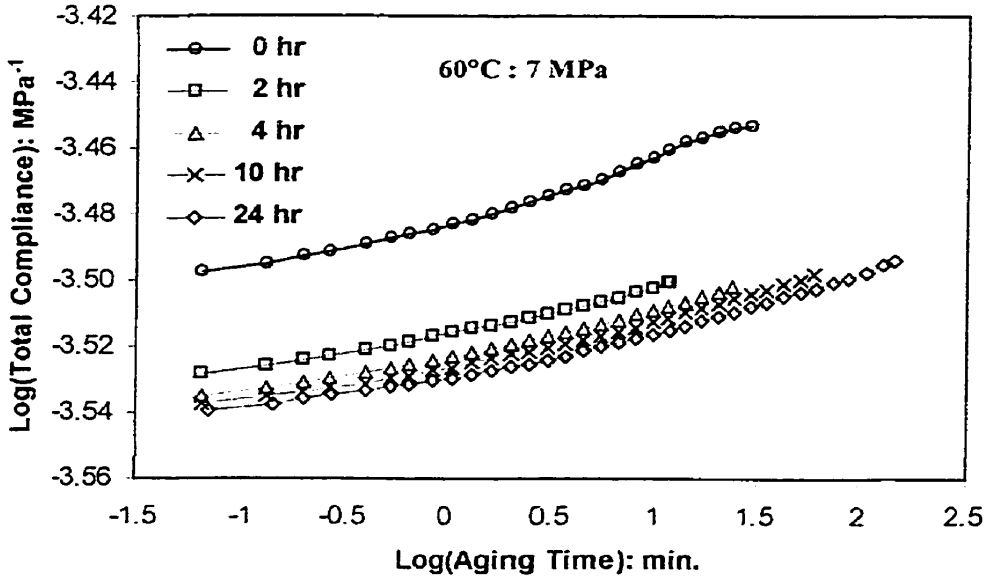

Figure C15: Compliance data at 7 MPa for resin at 60°C at various physical aging times

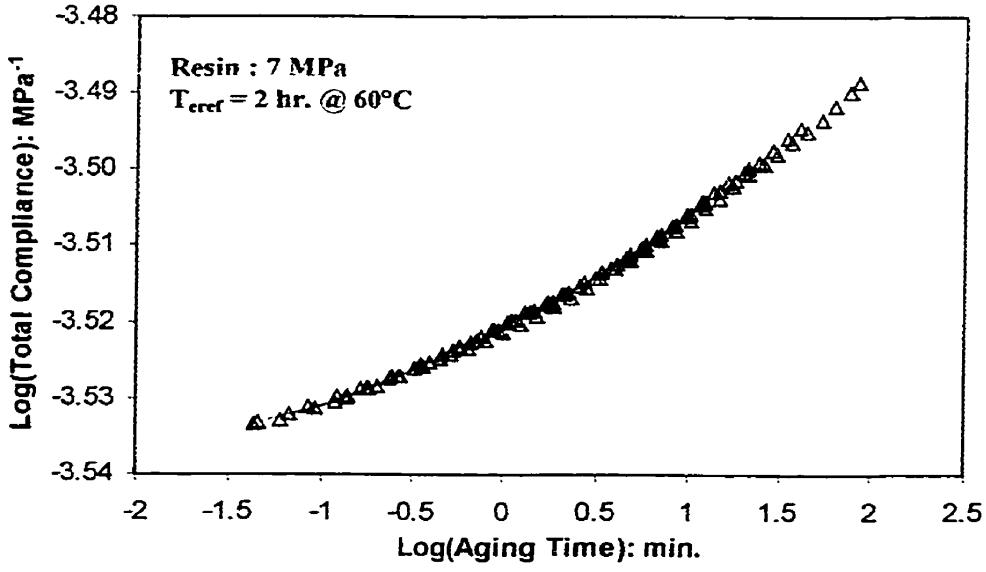

Figure C16: Momentary master curve at 7 MPa for resin at 60°C

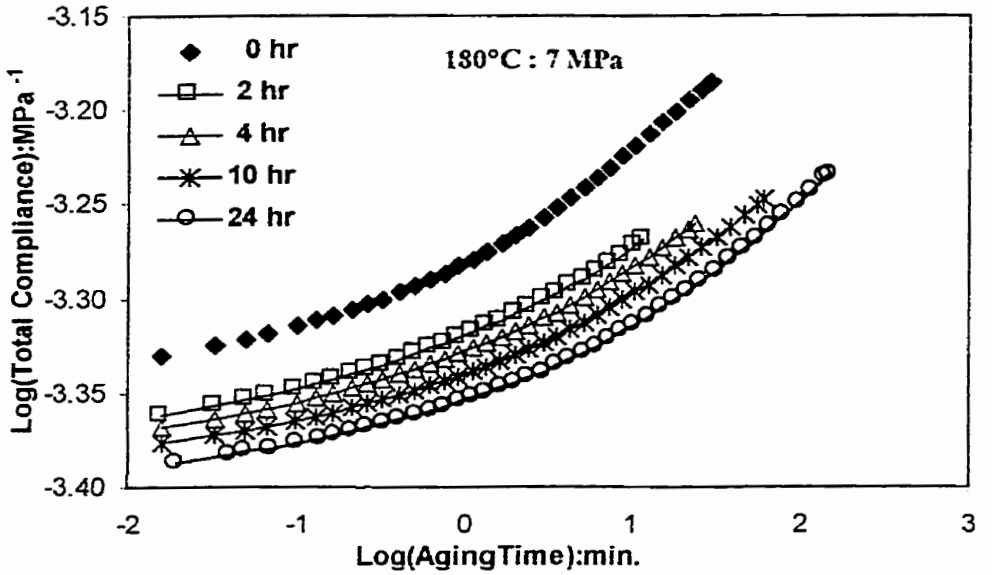

Figure C17: Compliance data at 7 MPa for resin at 180°C at various physical aging times

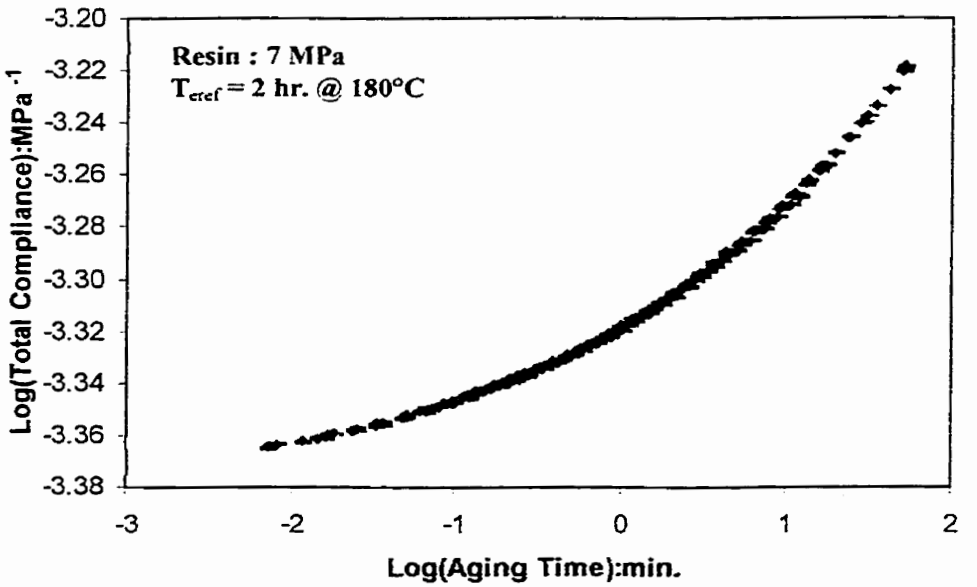

Figure C18: Momentary master curve at 7 MPa for resin at 180°C

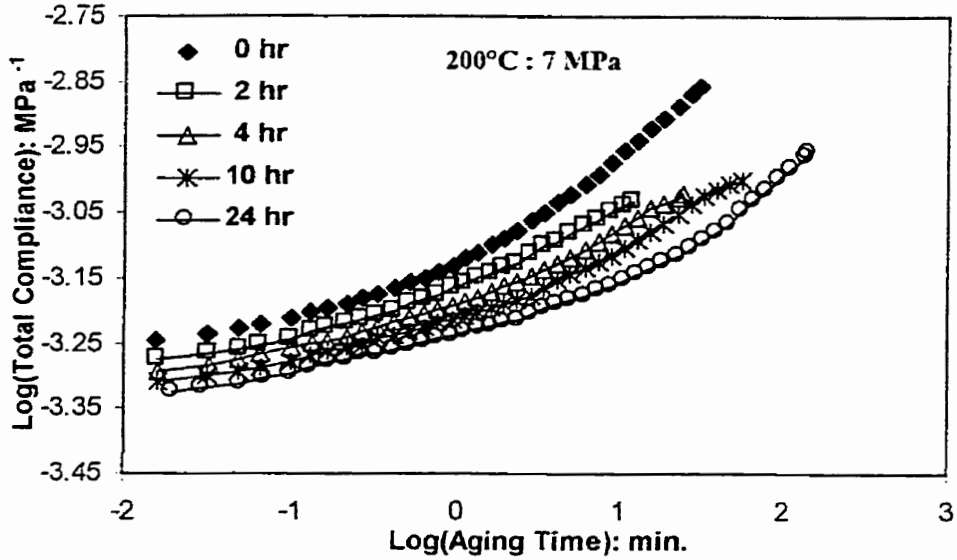

Figure C19: Compliance data at 7 MPa for resin at 200°C at various physical aging times

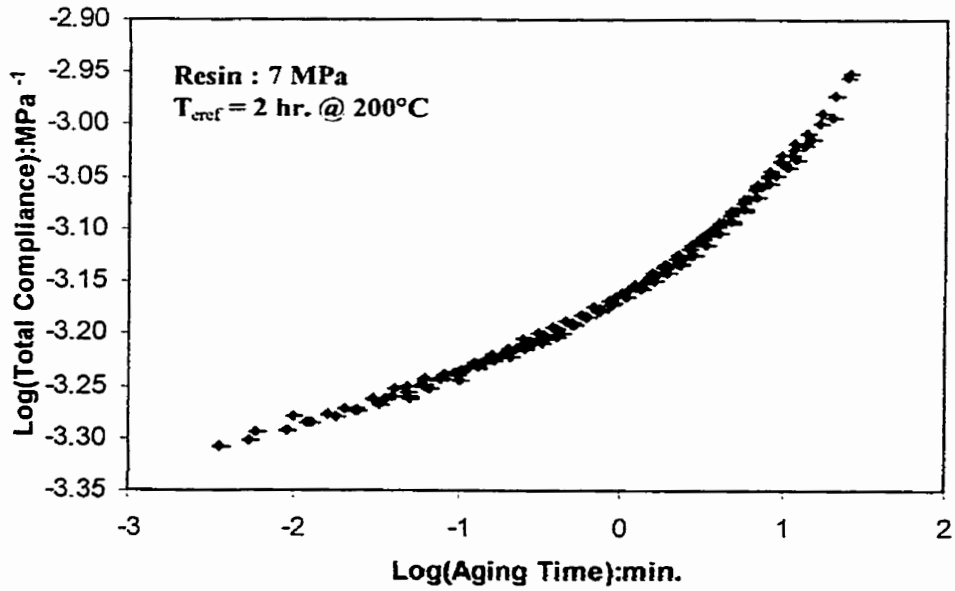

Figure C20: Momentary master curve at 7 MPa for resin at 200°C

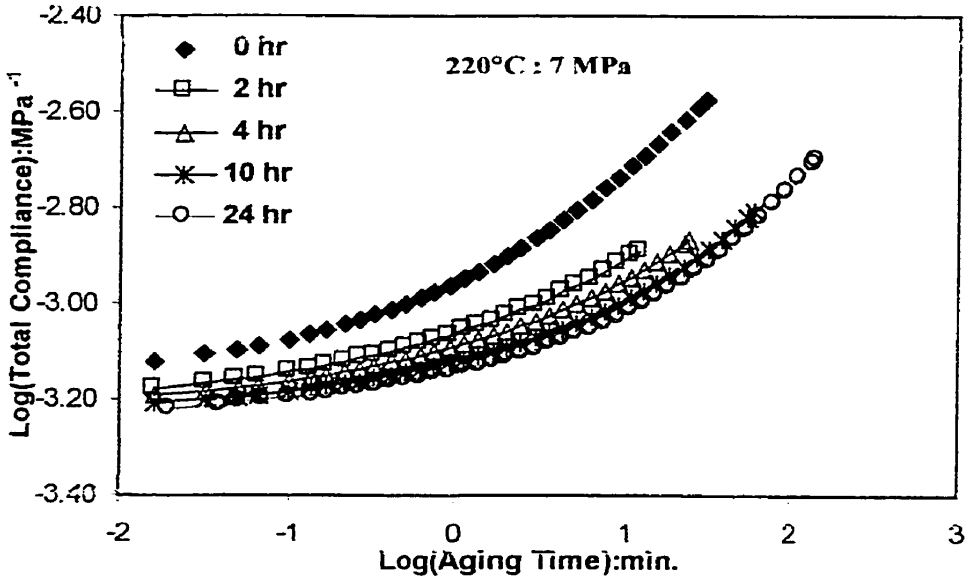

Figure C21: Compliance data at 7 MPa for resin at 220°C at various physical aging times

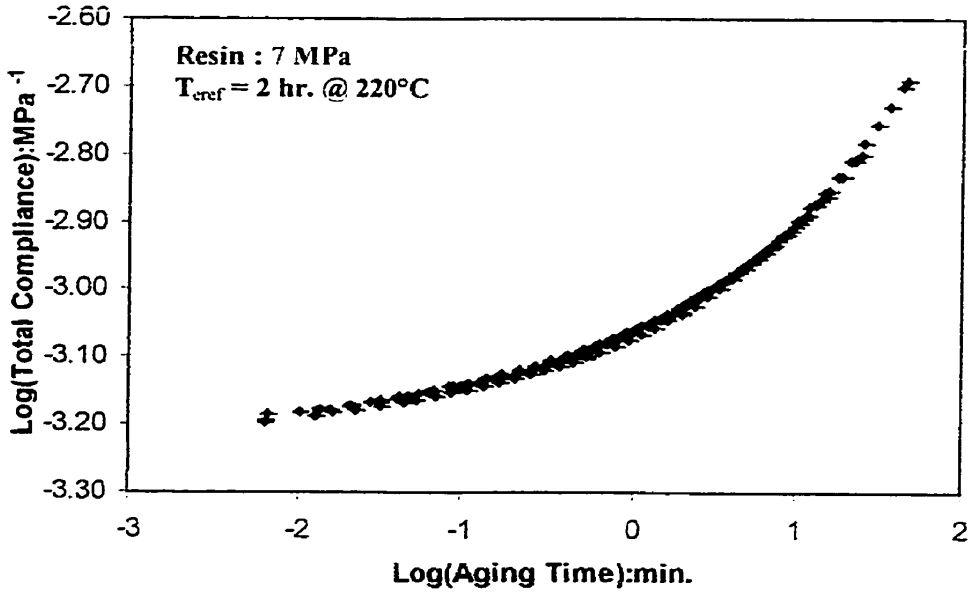

Figure C22: Momentary master curve at 7 MPa for resin at 220°C

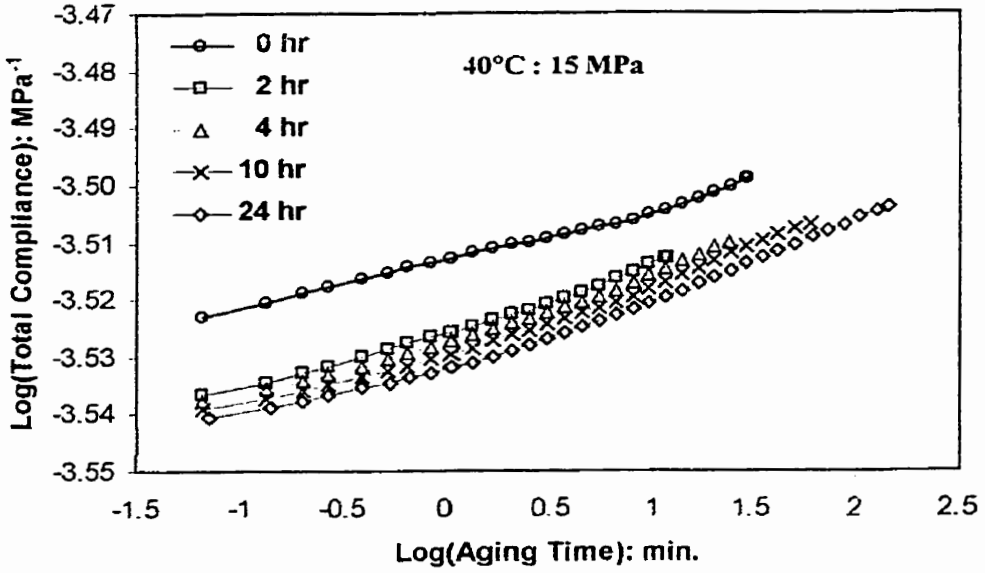

Figure C23: Compliance data at 15 MPa for resin at 40°C at various physical aging times

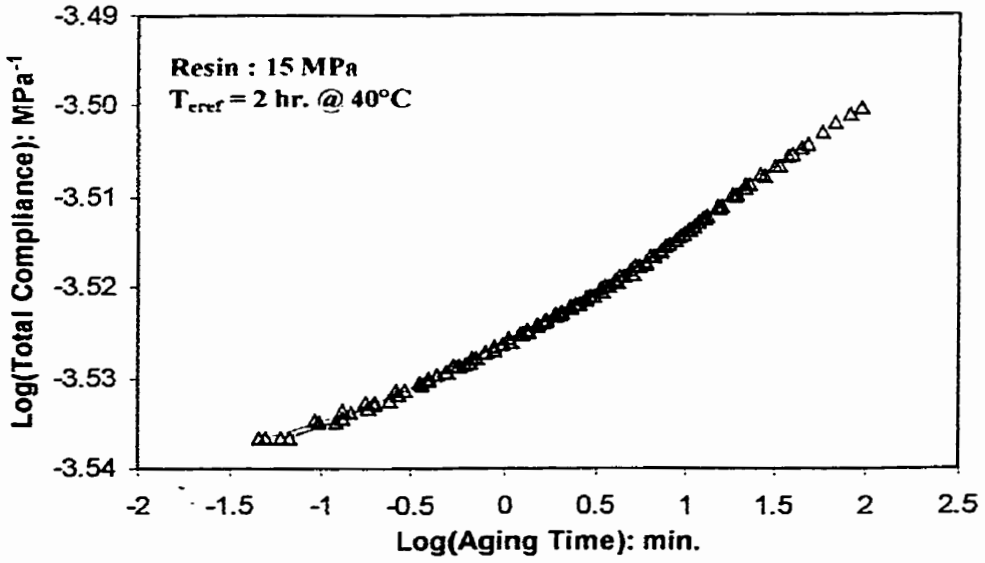

Figure C24: Momentary master curve at 15 MPa for resin at 40°C

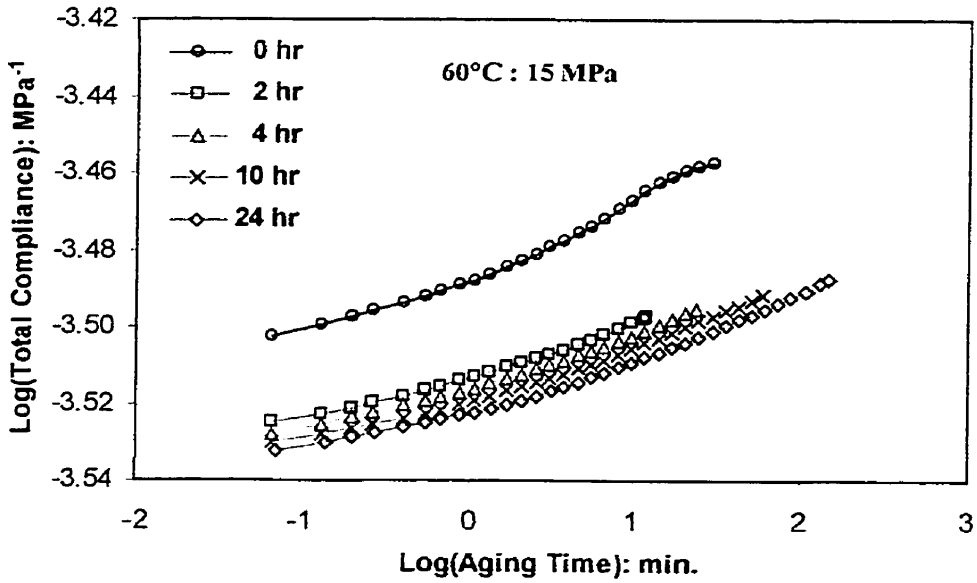

Figure C25: Compliance data at 15 MPa for resin at 60°C at various physical aging times

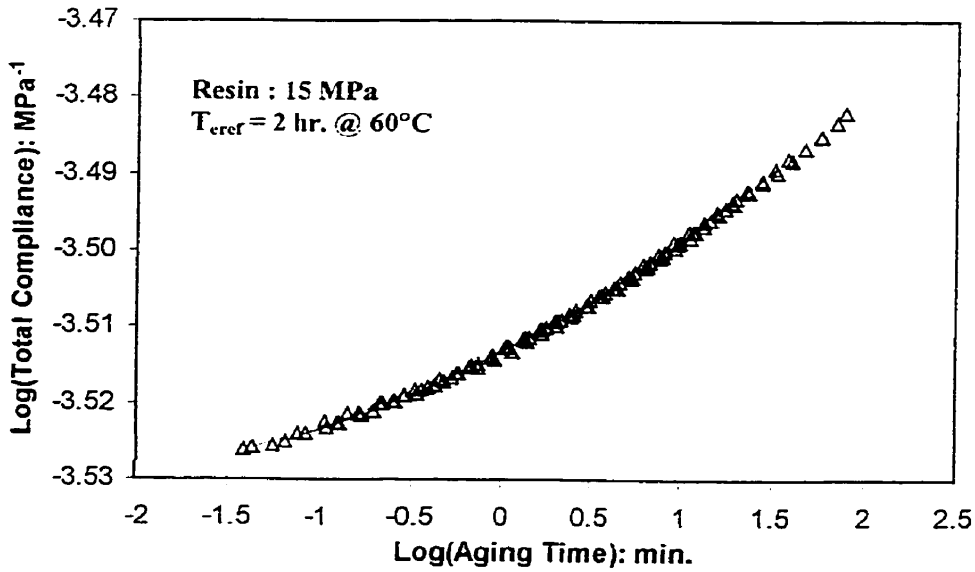

Figure C26: Momentary master curve at 15 MPa for resin at 60°C

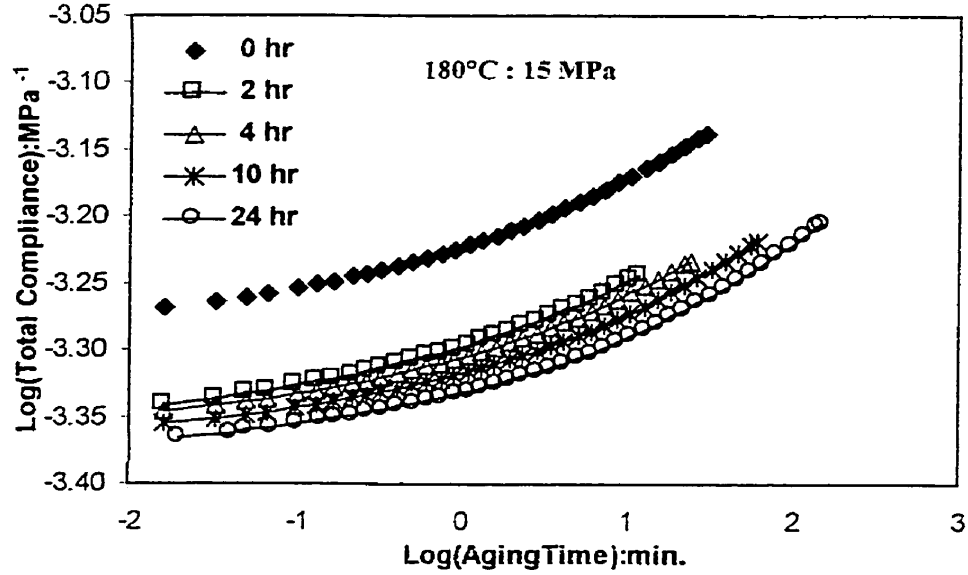

Figure C27: Compliance data at 15 MPa for resin at 180°C at various physical aging times

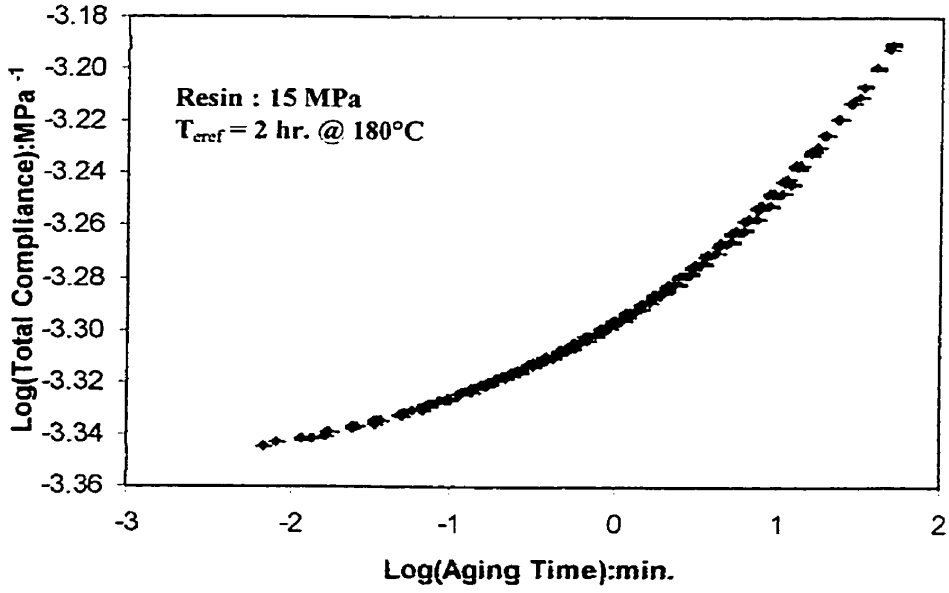

Figure C28: Momentary master curve at 15 MPa for resin at 180°C

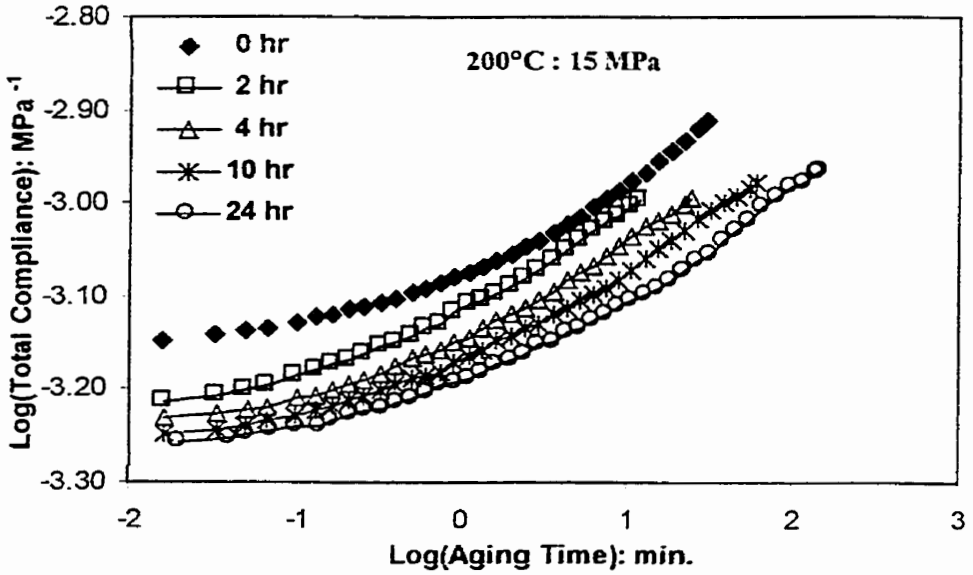

Figure C29: Compliance data at 15 MPa for resin at 200°C at various physical aging times

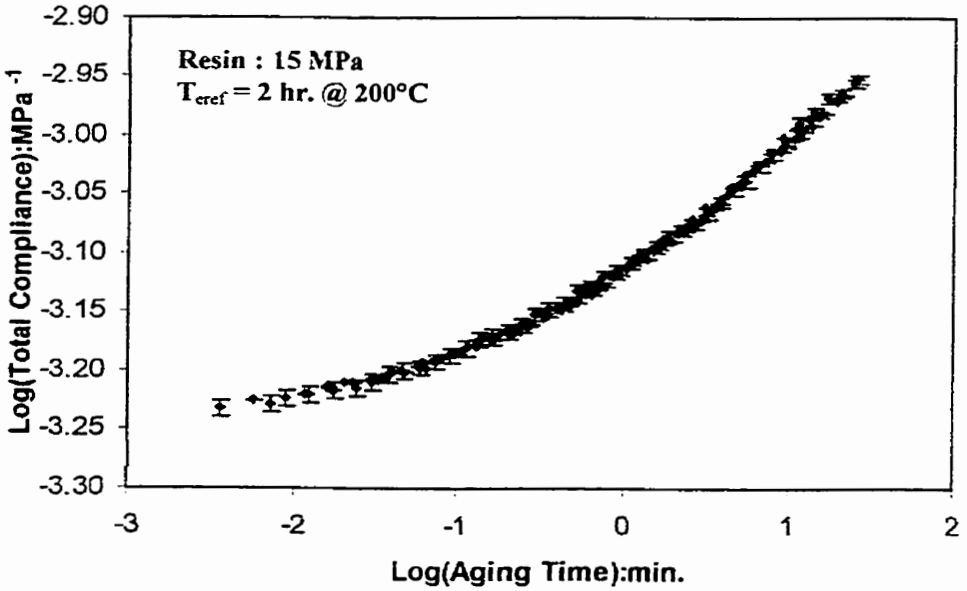

Figure C30: Momentary master curve at 15 MPa for resin at 200°C

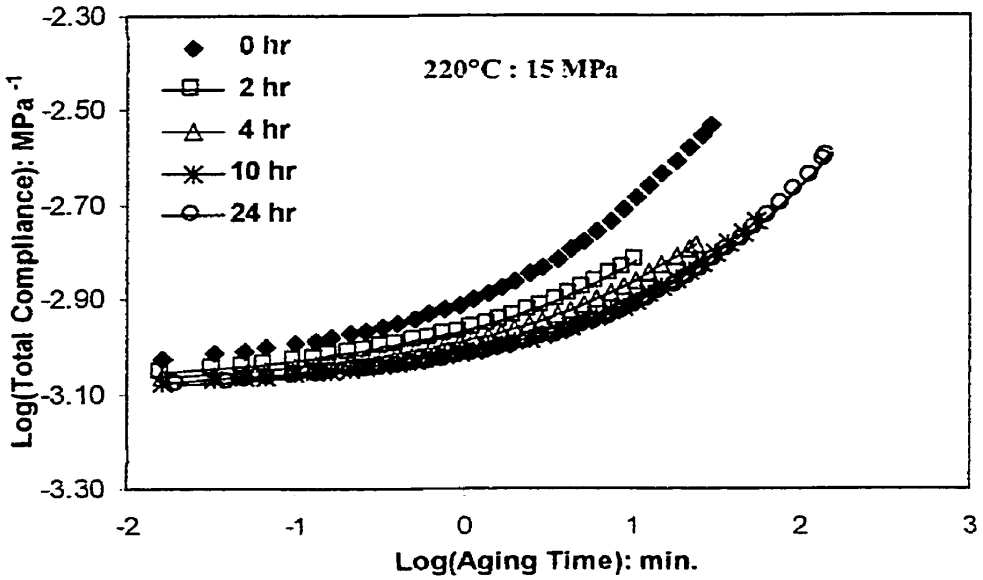

Figure C31: Compliance data at 15 MPa for resin at 220°C at various physical aging times

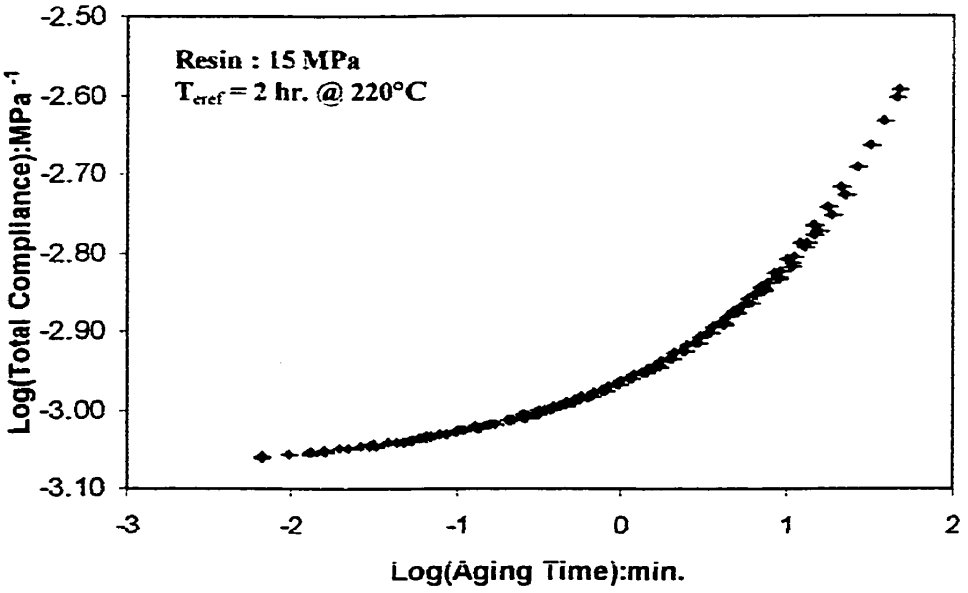

Figure C32: Momentary master curve at 15 MPa for resin at 220°C

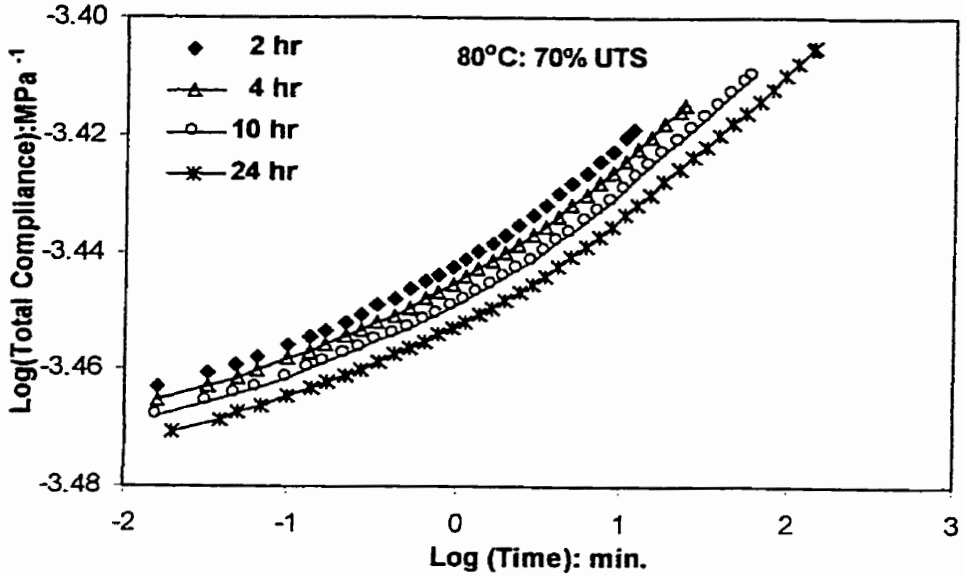

Figure C33: Compliance data at 70% of UTS for resin at 80°C at various physical aging time

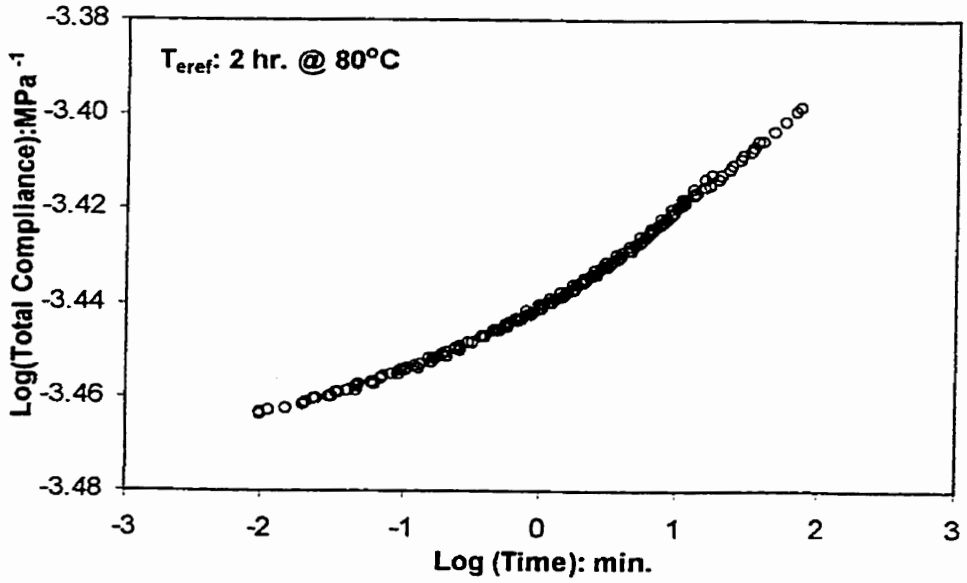

Figure C34: Momentary master curve at 70% of UTS for resin at 80°C

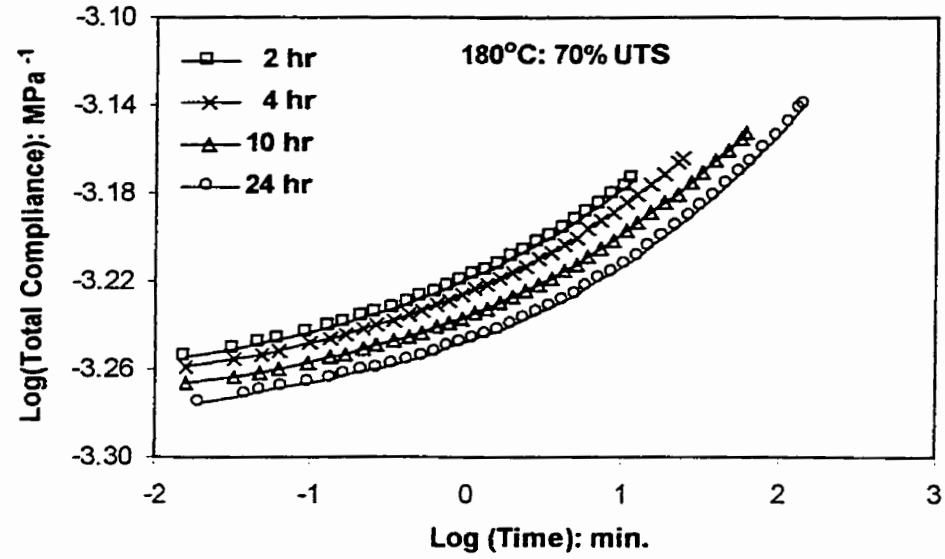

Figure C35: Compliance data at 70% of UTS for resin at 180°C at various physical aging times

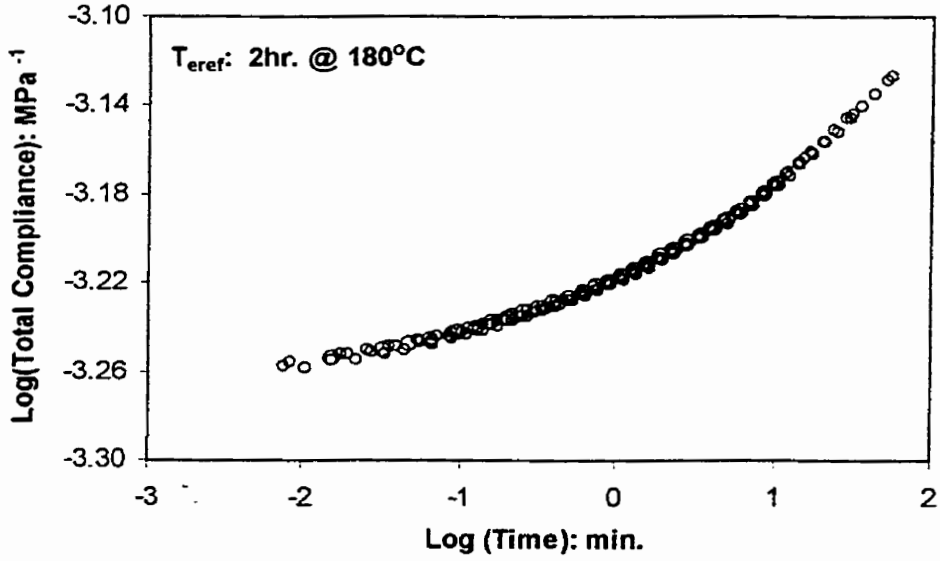

Figure C36: Momentary master curve at 70% of UTS for resin at 180°C

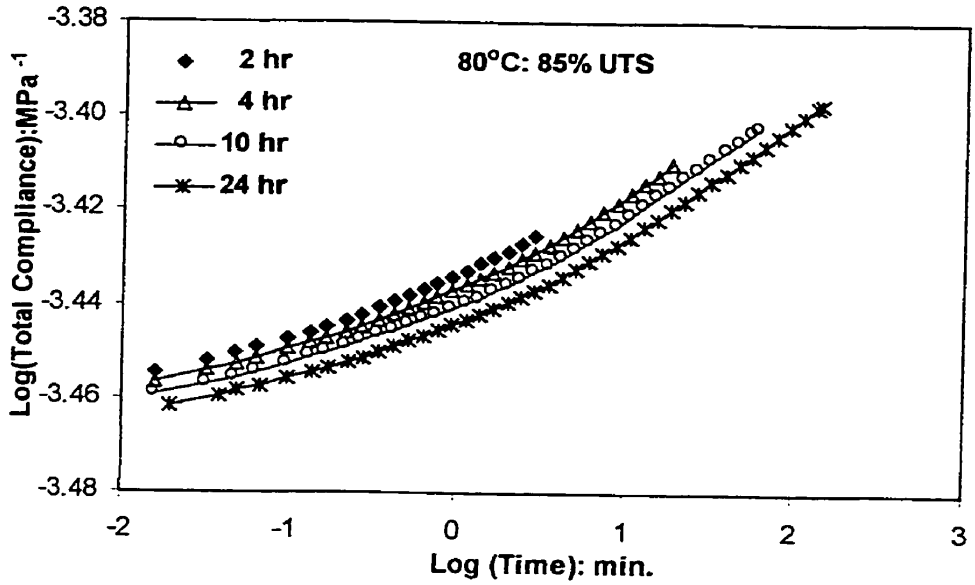

Figure C37: Compliance data at 85% of UTS for resin at 80°C at various physical aging times

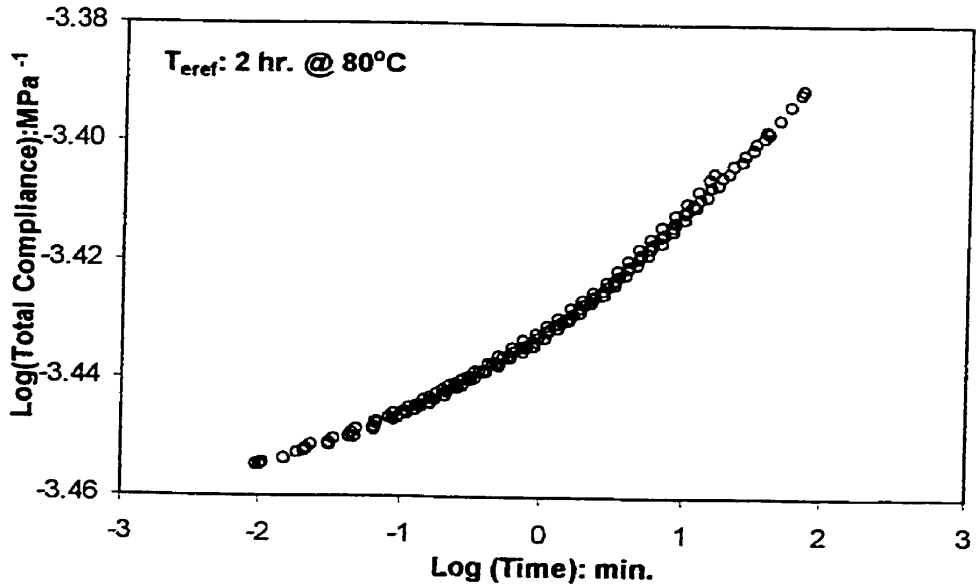

Figure C38: Momentary master curve at 85% of UTS for resin at 80°C

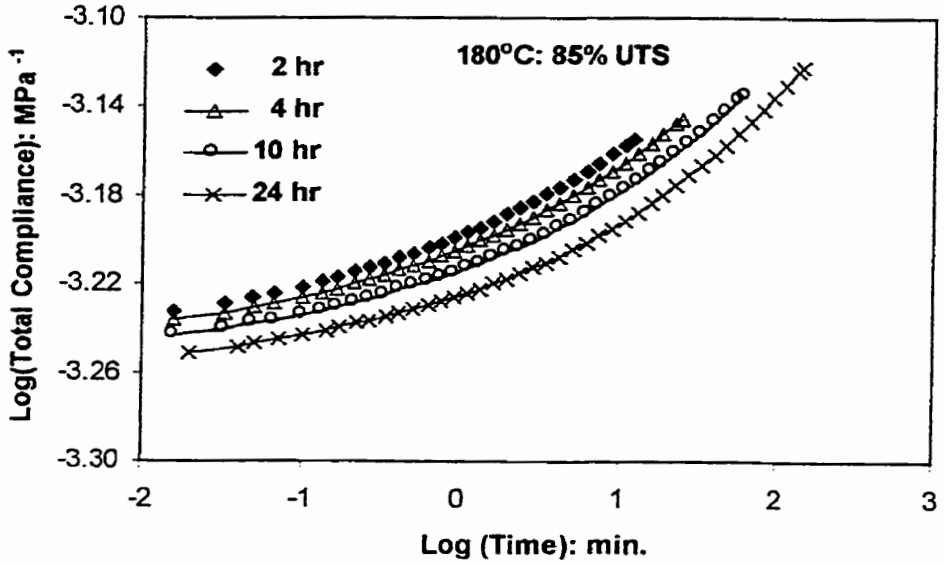

Figure C39: Compliance data at 85% of UTS for resin at 180°C at various physical aging times

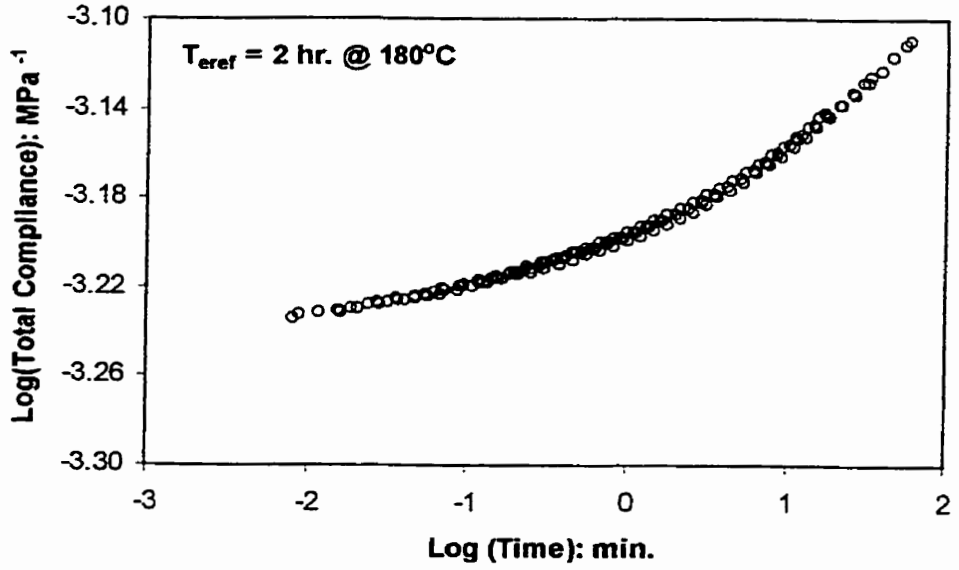

Figure C40: Momentary master curve at 85% of UTS for resin at 180°C

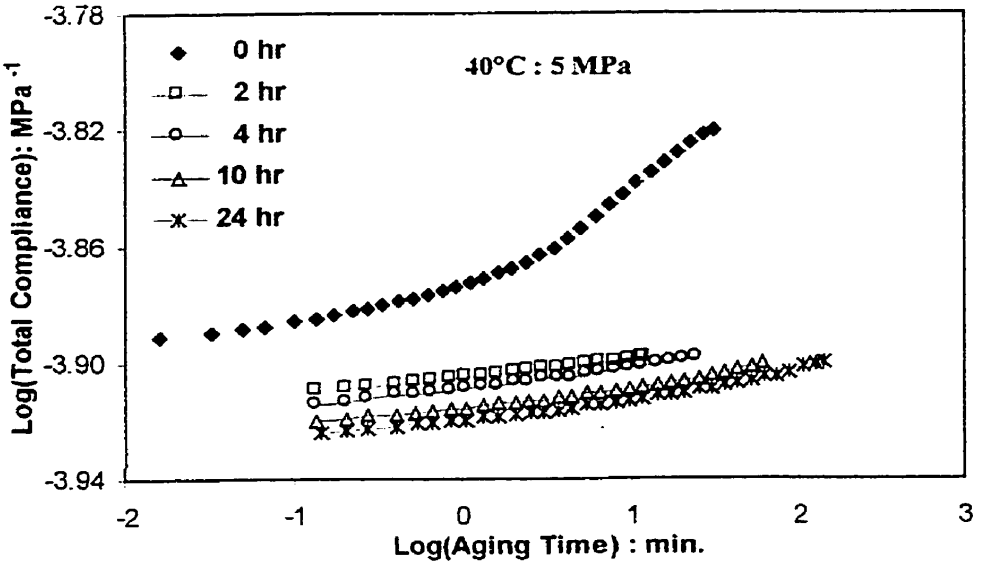

Figure C41: Compliance data at 5 MPa for $[90]_8$ composite (V_f:54%) at various physical aging times at 40°C

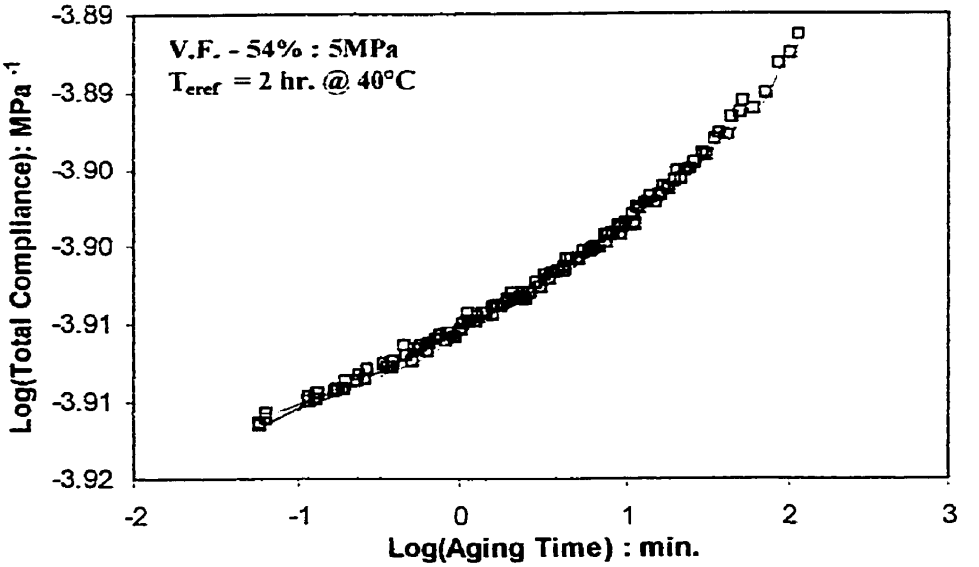

Figure C42: Momentary master curve at 5 MPa for $[90]_8$ composite (V_f:54%) at 40°C

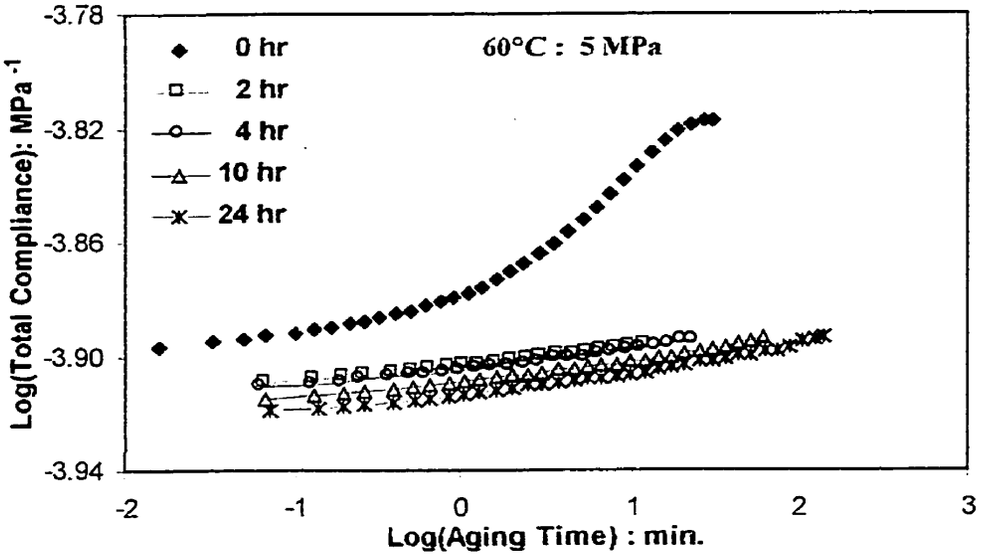

Figure C43: Compliance data at 5 MPa for $[90]_8$ composite (V_f:54%) at various physical aging times at 60°C

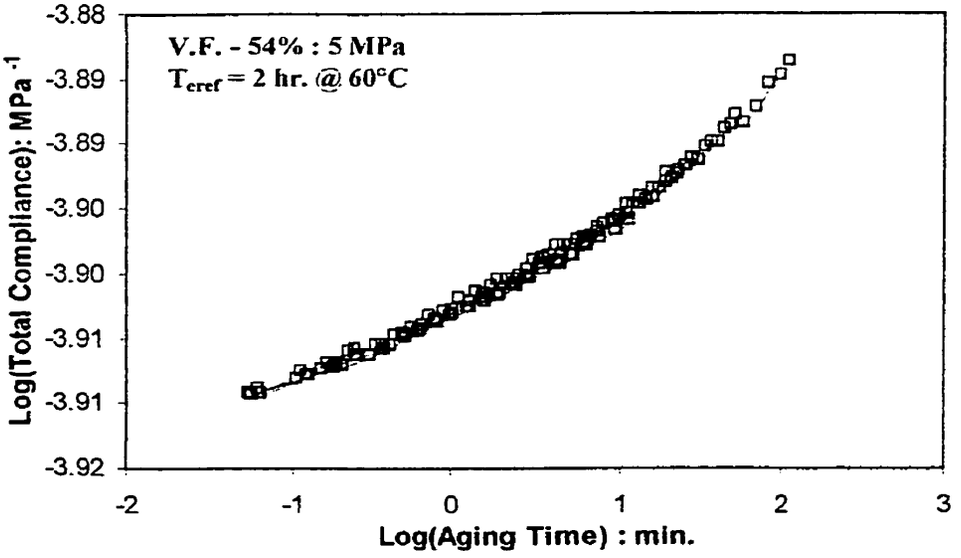

Figure C44: Momentary master curve at 5 MPa for $[90]_8$ composite (V_f:54%) at 60°C

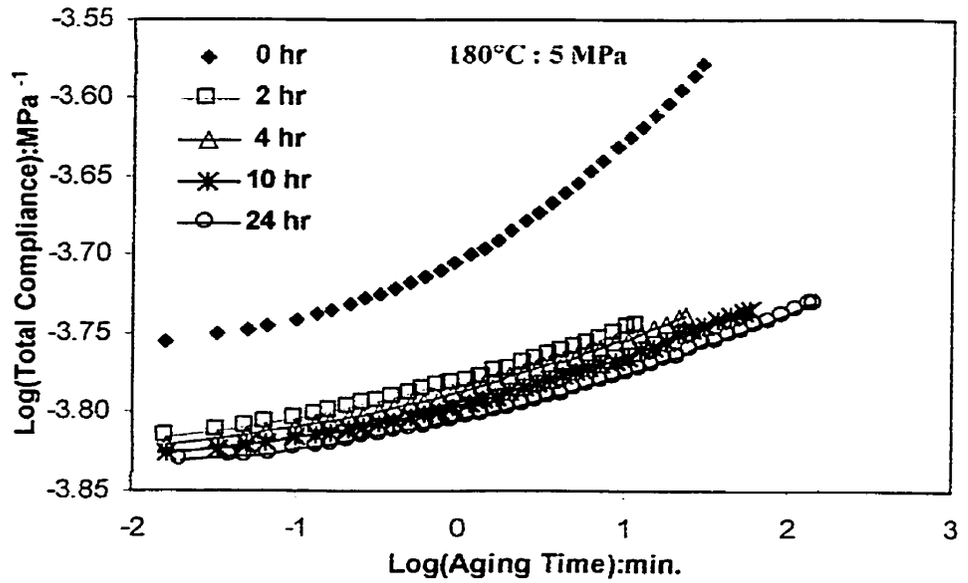

Figure C45: Compliance data at 5 MPa for $[90]_8$ composite (V_f:54%) at 180°C at various physical aging times

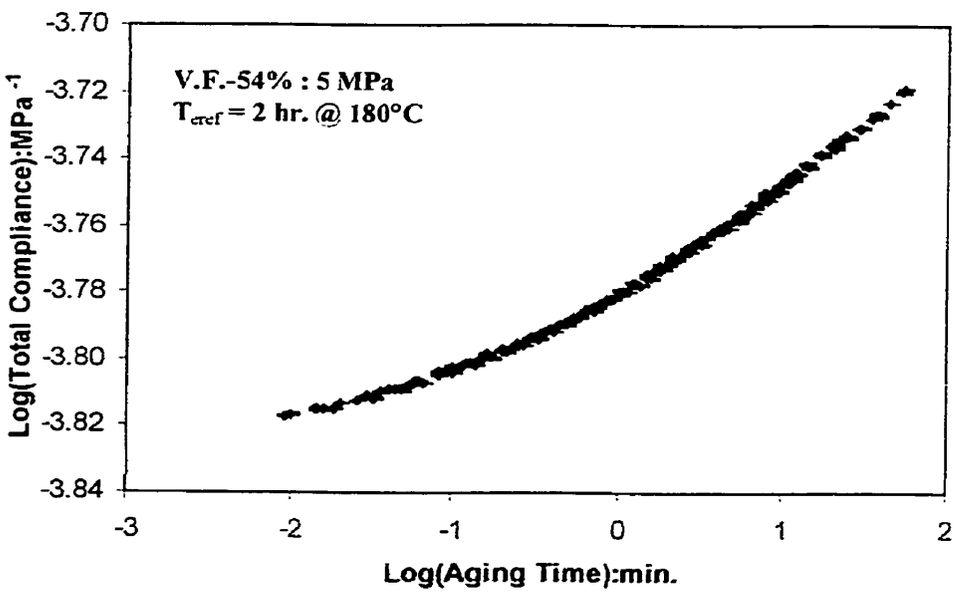

Figure C46: Momentary master curve at 5 MPa for $[90]_8$ composite (V_f:54%) at 180°C

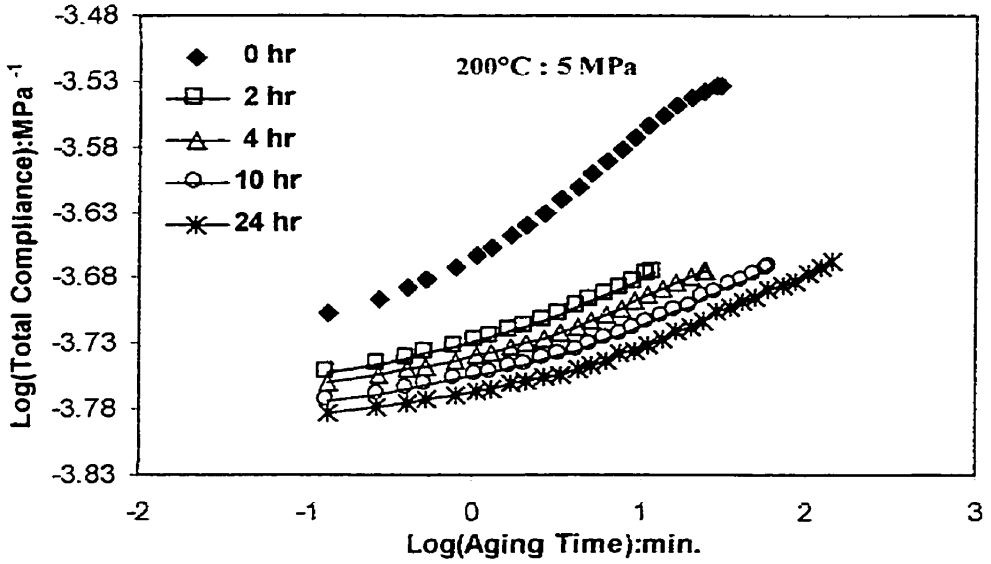

Figure C47: Compliance data at 5 MPa for $[90]_8$ composite (V_f:54%) at 200°C at different physical aging times

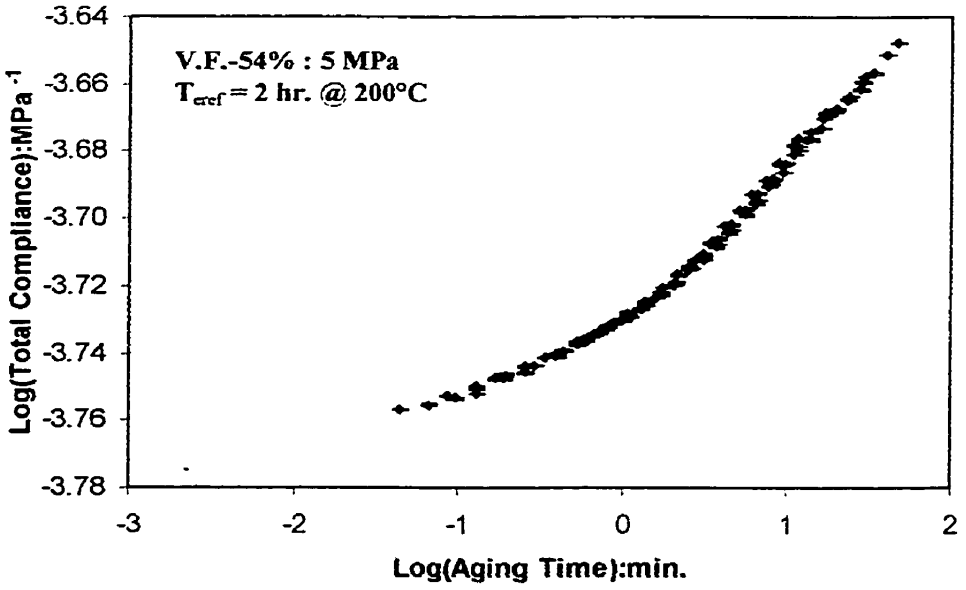

Figure C48: Momentary master curve at 5 MPa for $[90]_8$ composite (V_f:54%) at 200°C

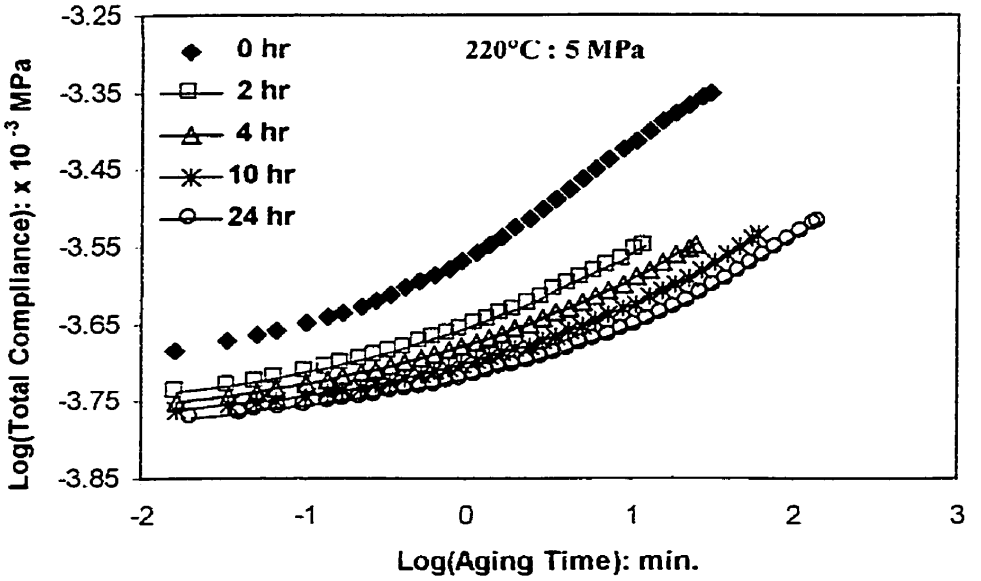

Figure C49: Compliance data at 5 MPa for $[90]_8$ composite (V_f:54%) at 220°C at various physical aging times

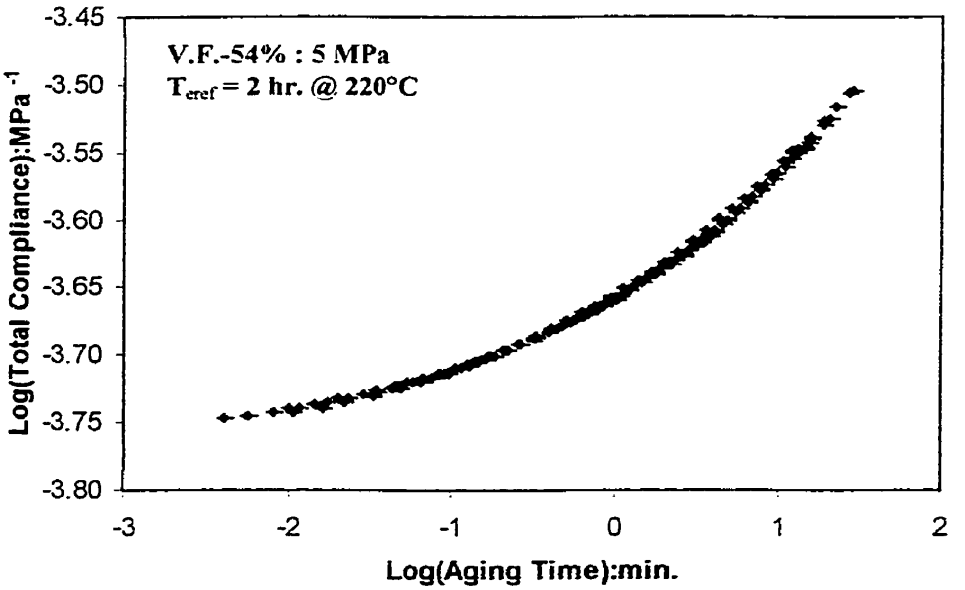

Figure C50: Momentary master curve at 5 MPa for $[90]_8$ composite (V_f:54%) at 220°C

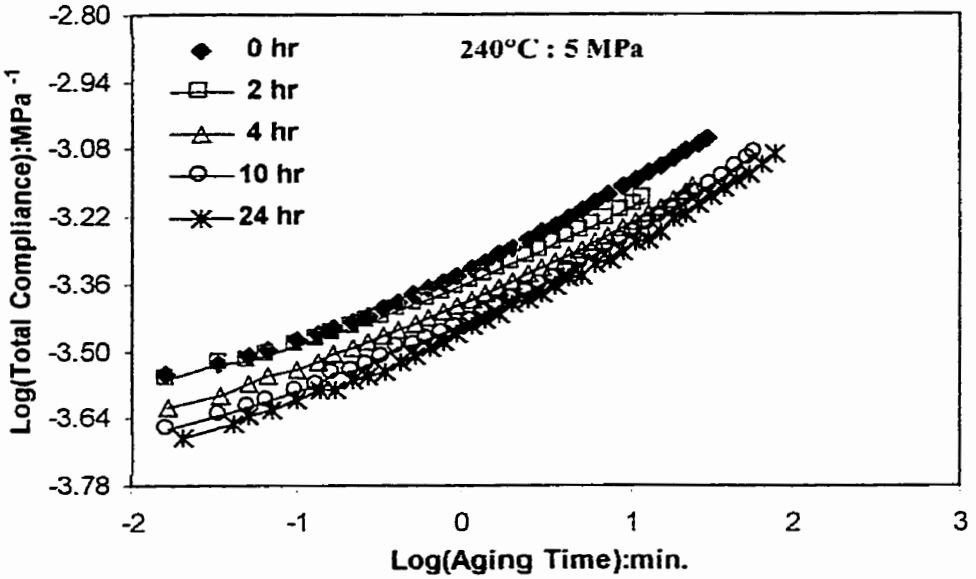

Figure C51: Compliance data at 5 MPa for $[90]_8$ composite (V_f:54%) at 240°C at various physical aging times

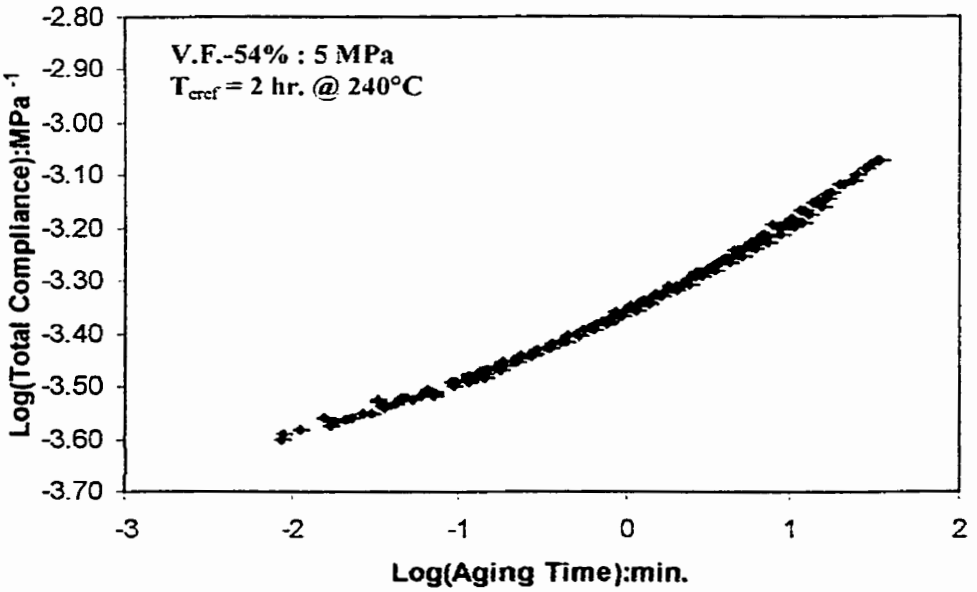

Figure C52: Momentary master curve at 5 MPa for $[90]_8$ composite (V_f:54%) at 240°C

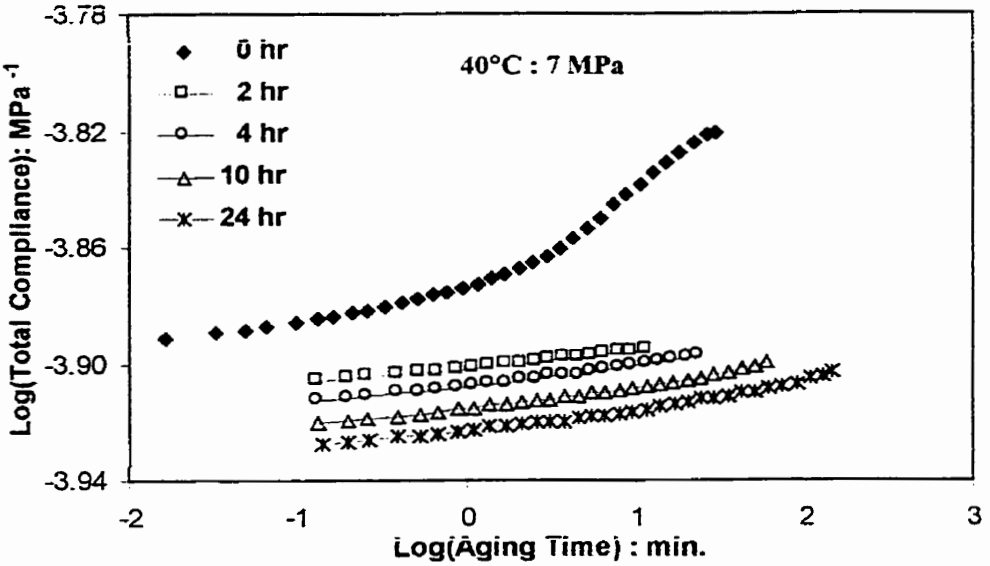

Figure C53: Compliance data at 7 MPa $[90]_8$ composite (V_f :54%) 40°C at various physical aging times

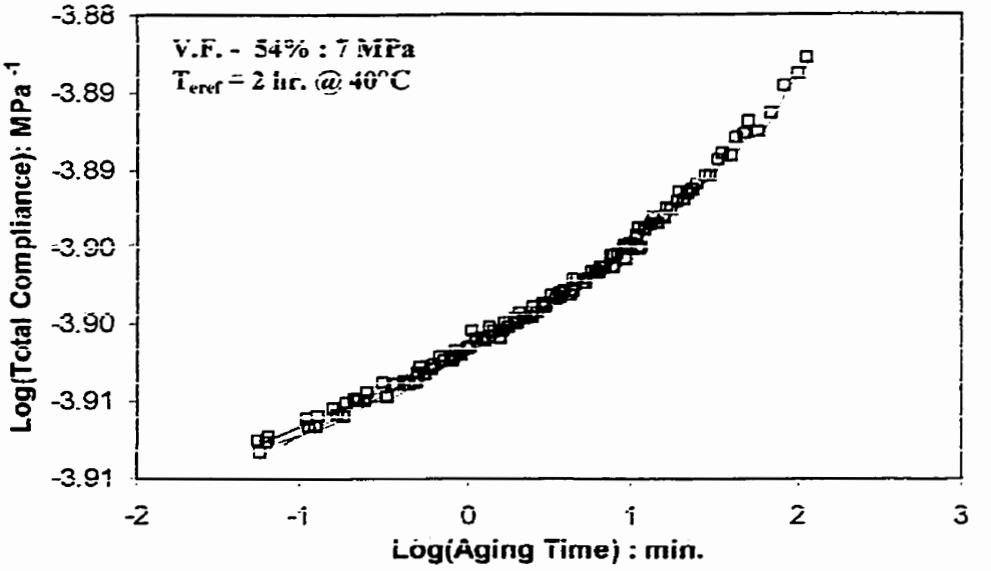

Figure C54: Momentary master at 7 MPa curve for $[90]_8$ composite (V_f :54%) at 40°C

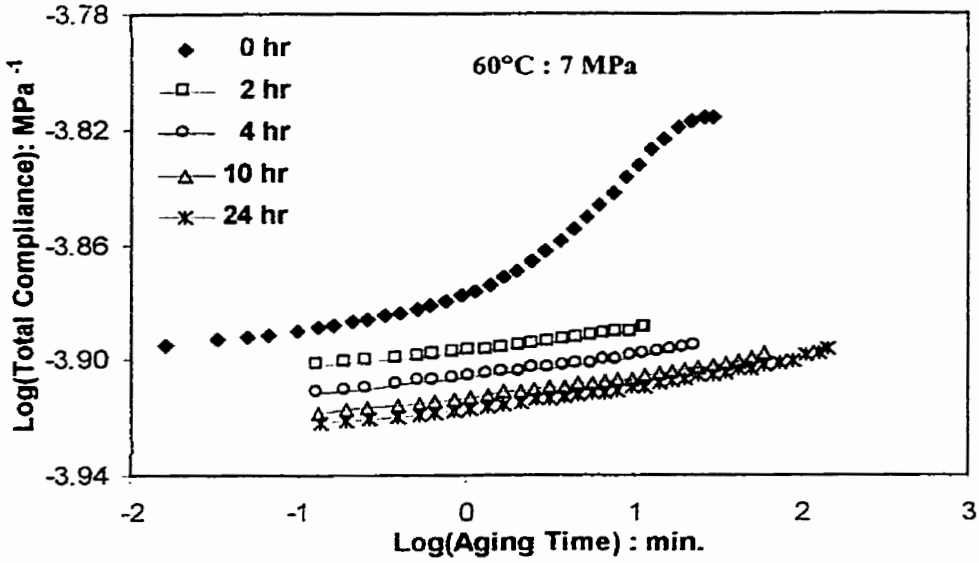

Figure C55: Compliance data at 7 MPa $[90]_8$ composite (V_f :54%) 60°C at various physical aging times

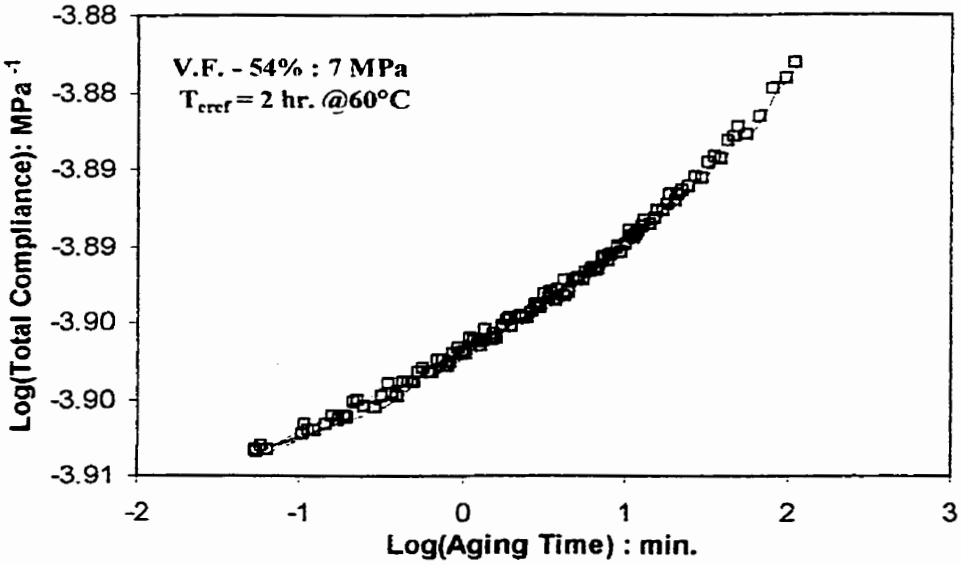

Figure C56: Momentary master at 7 MPa curve for $[90]_8$ composite (V_f :54%) at 60°C

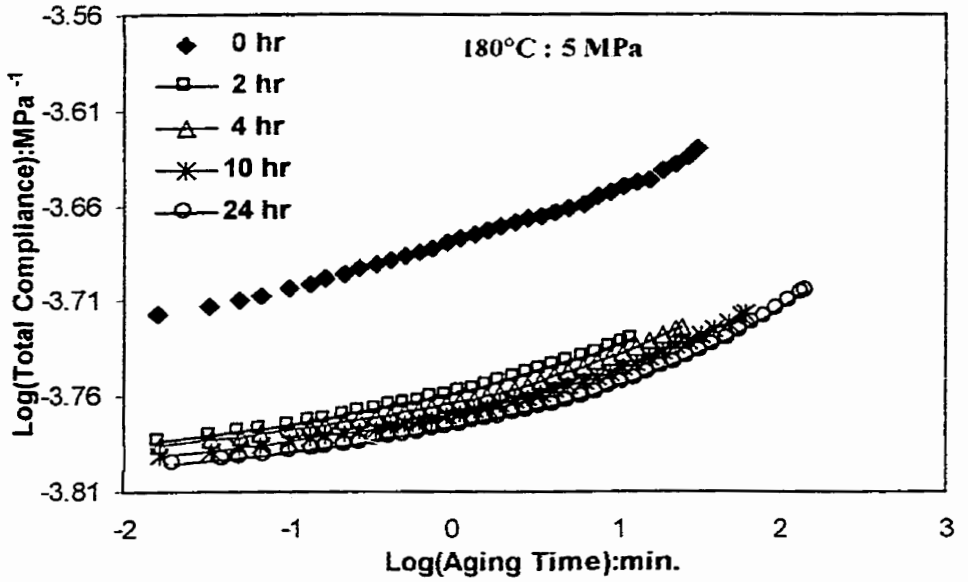

Figure C57: Compliance data at 7 MPa $[90]_8$ composite (V_f :54%) at 180°C at various physical aging times

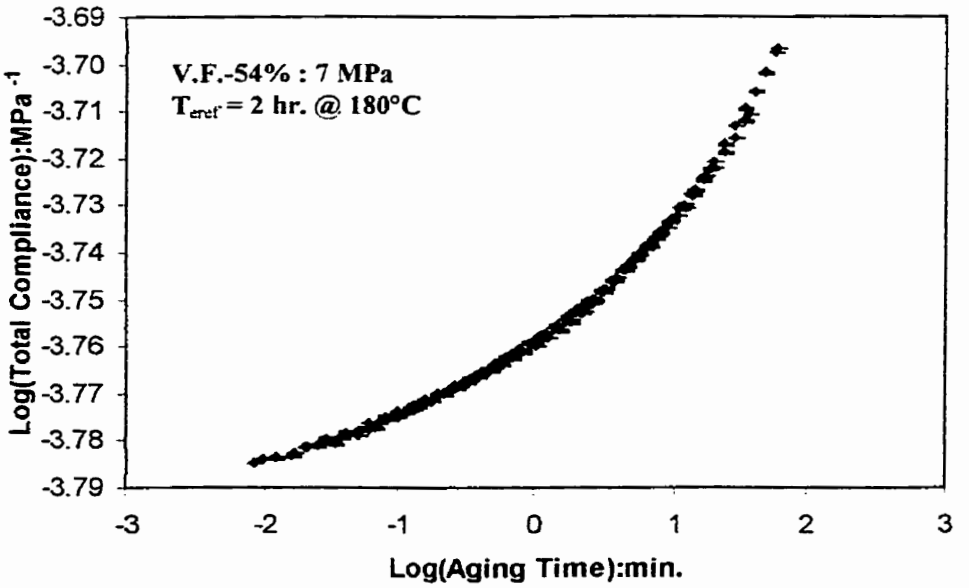

Figure C58: Momentary master at 7 MPa curve for $[90]_8$ composite (V_f :54%) at 180°C

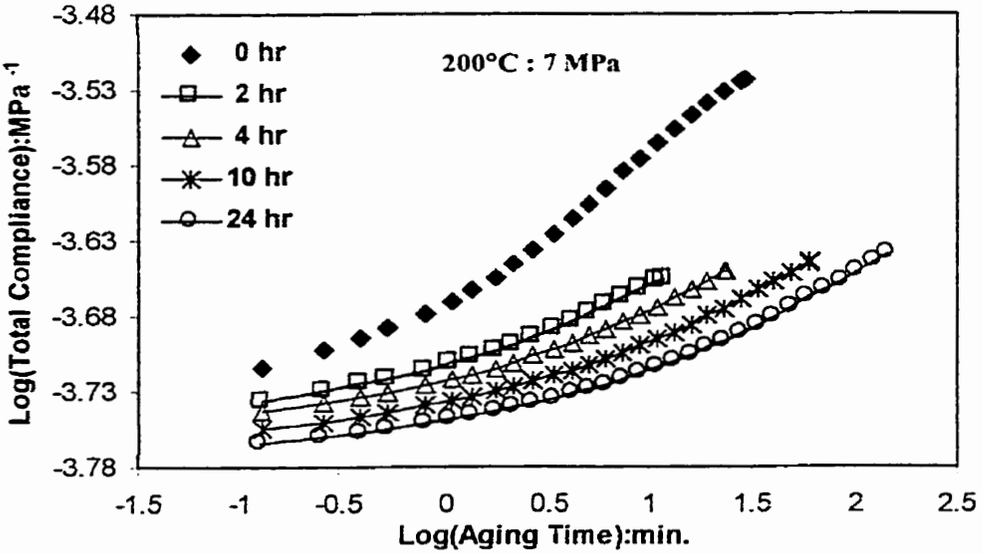

Figure C59: Compliance data at 7 MPa $[90]_8$ composite (V_f :54%) at 200°C at various physical aging times

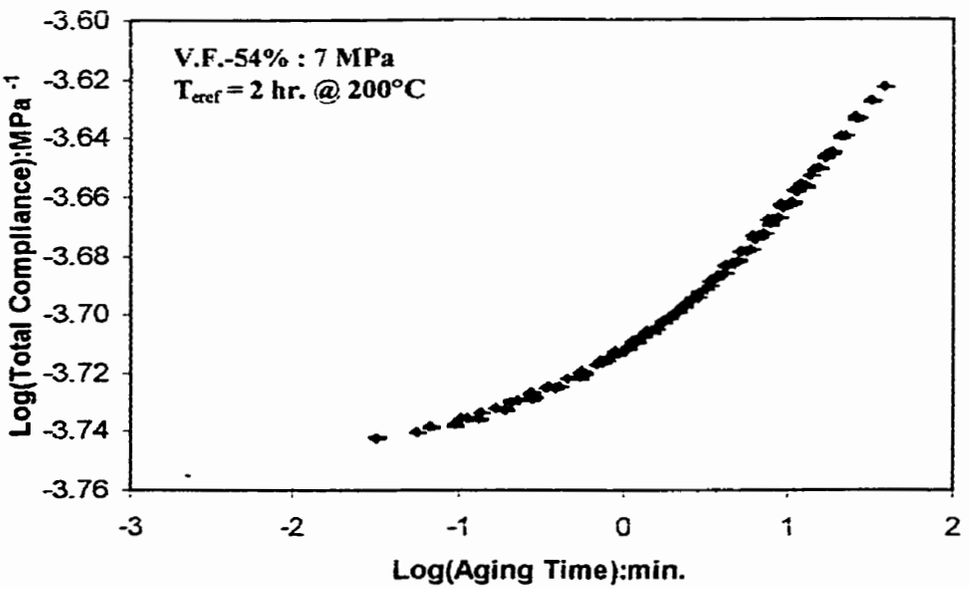

Figure C60: Momentary master at 7 MPa curve for $[90]_8$ composite (V_f :54%) at 200°C

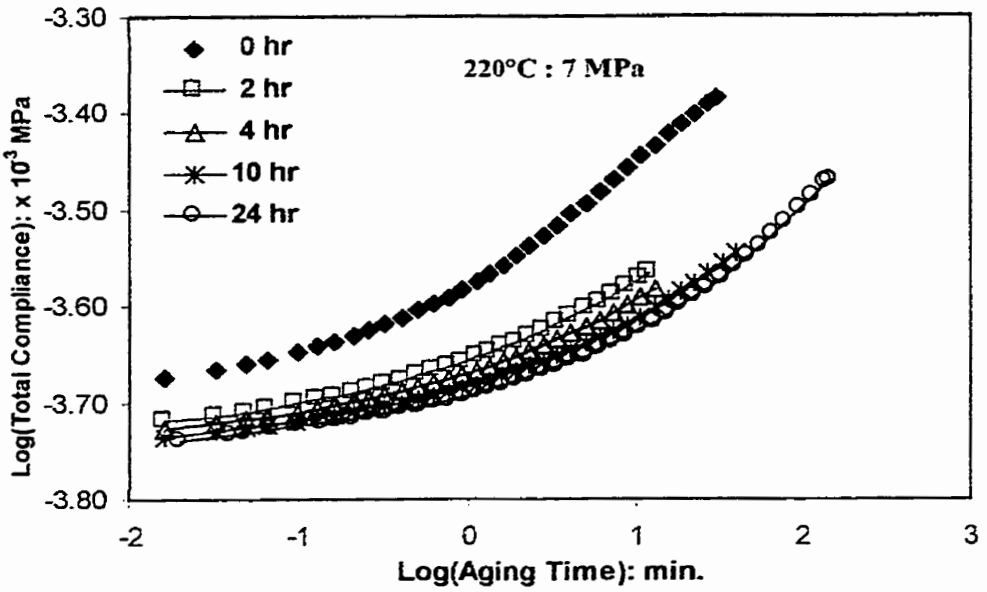

Figure C61: Compliance data at 7 MPa $[90]_8$ composite (V_f:54%) at 220°C at various physical aging times

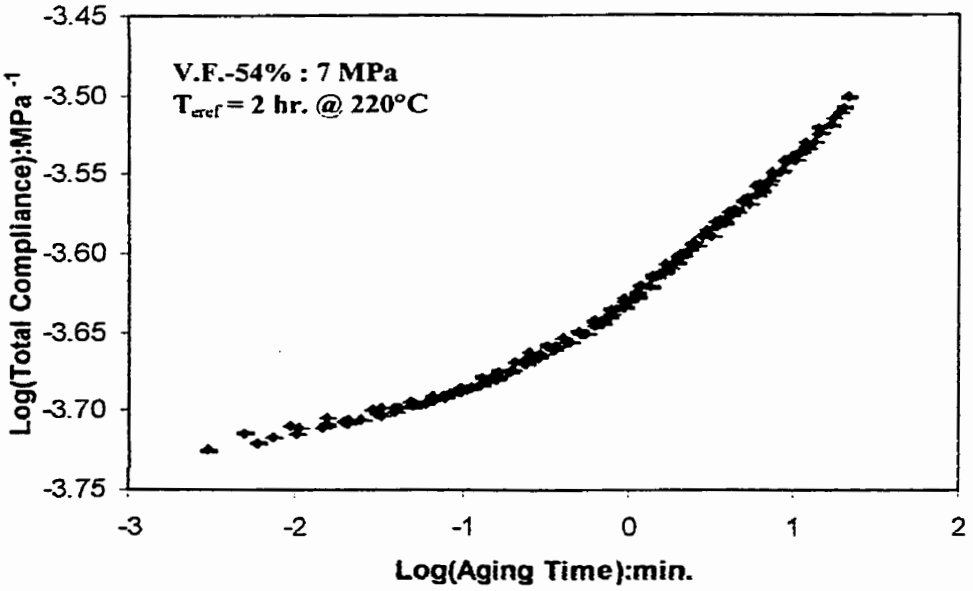

Figure C62: Momentary master at 7 MPa curve for $[90]_8$ composite (V_f:54%) at 220°C

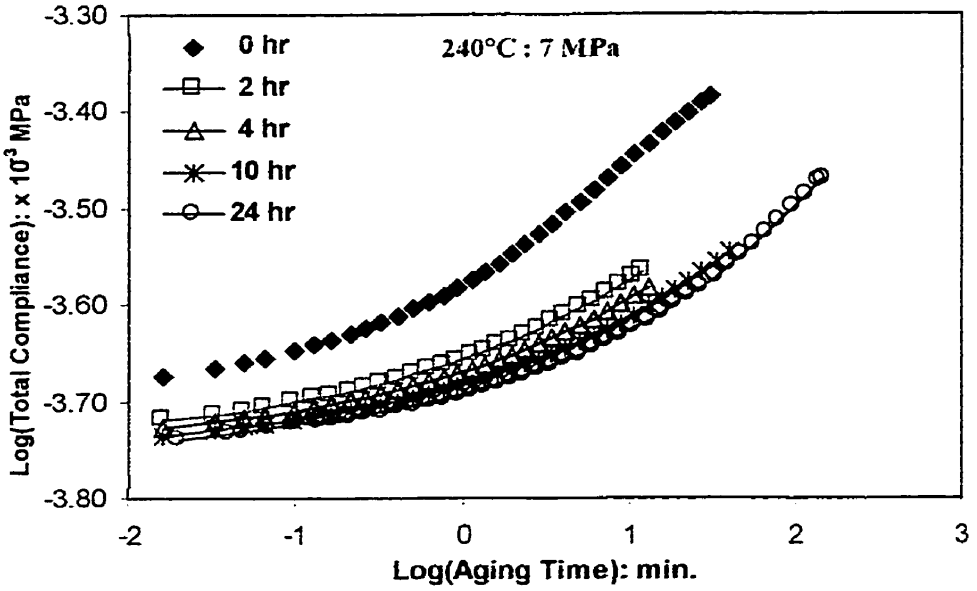

Figure C63: Compliance data at 7 MPa $[90]_8$ composite (V_f :54%) at 240°C at various physical aging times

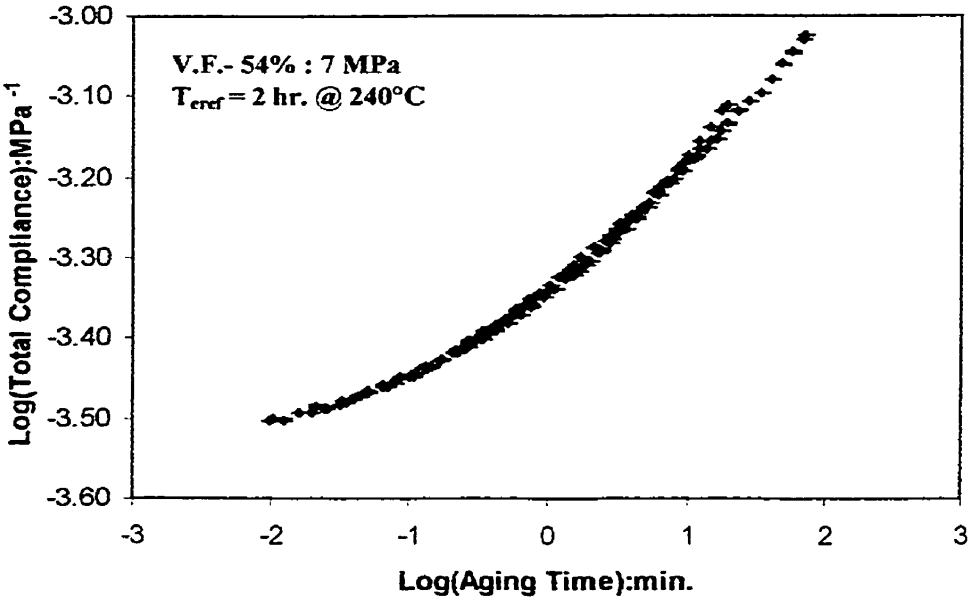

Figure C64: Momentary master at 7 MPa curve for $[90]_8$ composite (V_f :54%) at 240°C

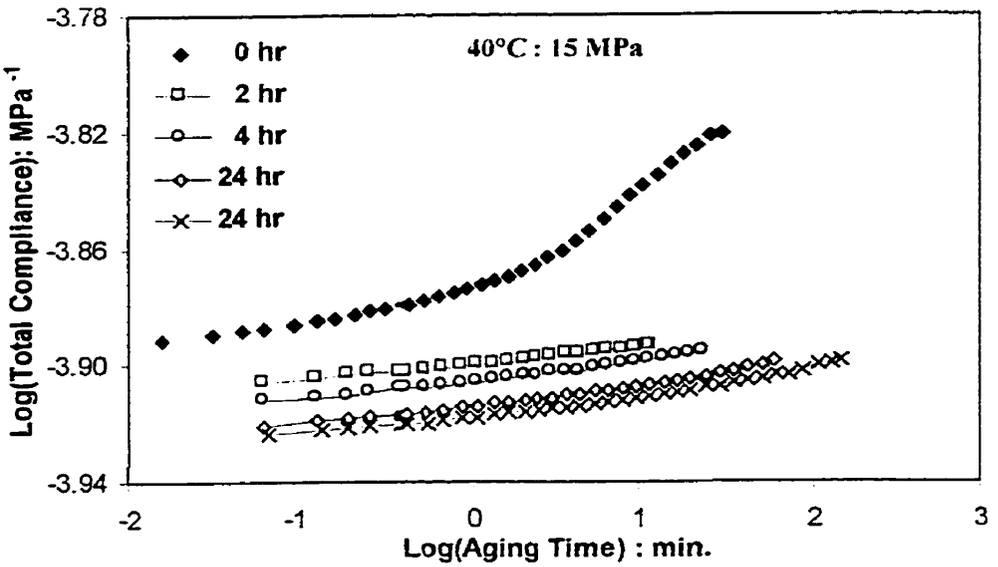

Figure C65: Compliance data at 15 MPa for $[90]_8$ composite (V_f:54%) at 40°C at various physical aging times

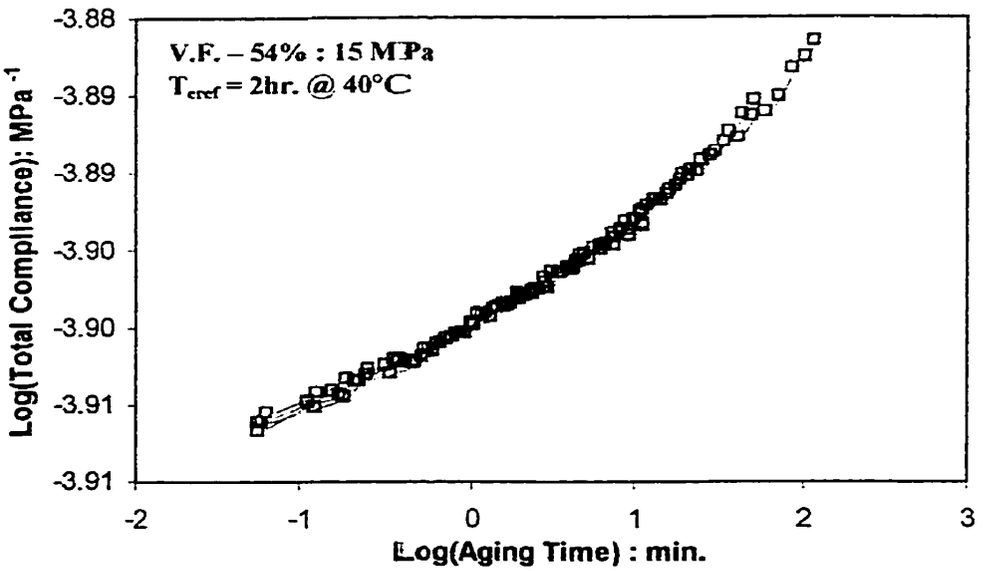

Figure C66: Momentary master curve at 15 MPa for $[90]_8$ composite (V_f:54%) at 40°C

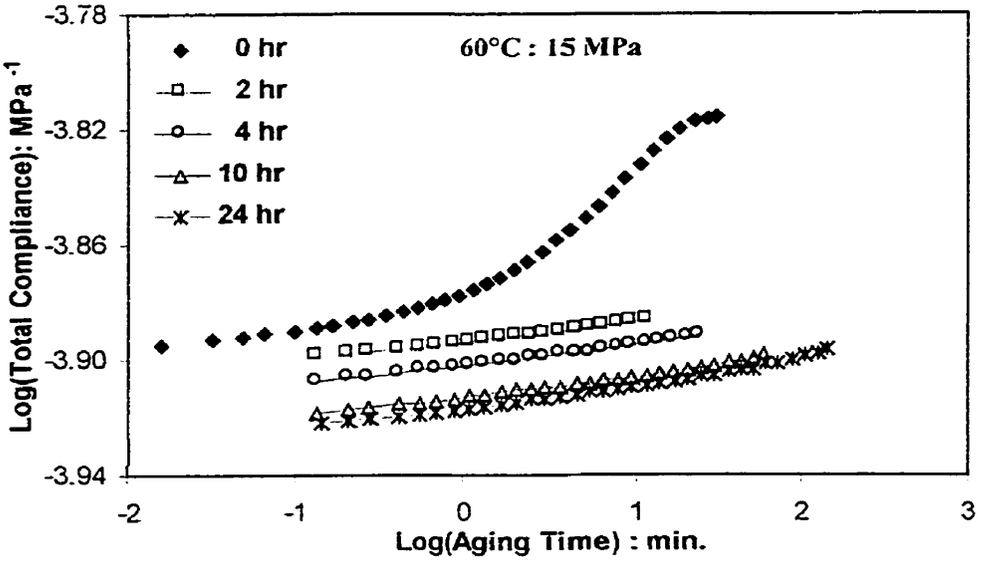

Figure C67: Compliance data at 15 MPa for $[90]_8$ composite (V_f:54%) at 60°C at various physical aging times

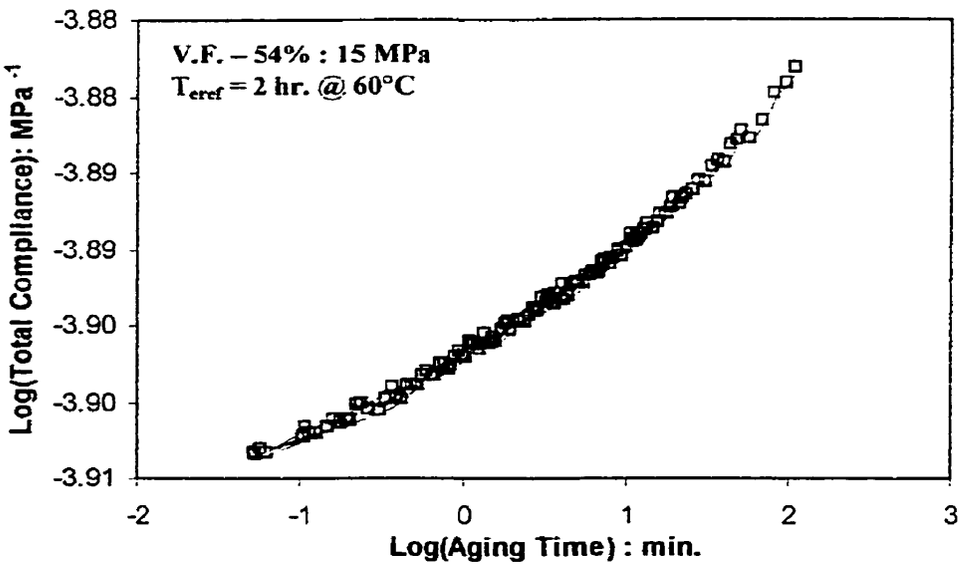

Figure C68: Momentary master curve at 15 MPa for $[90]_8$ composite (V_f:54%) at 60°C

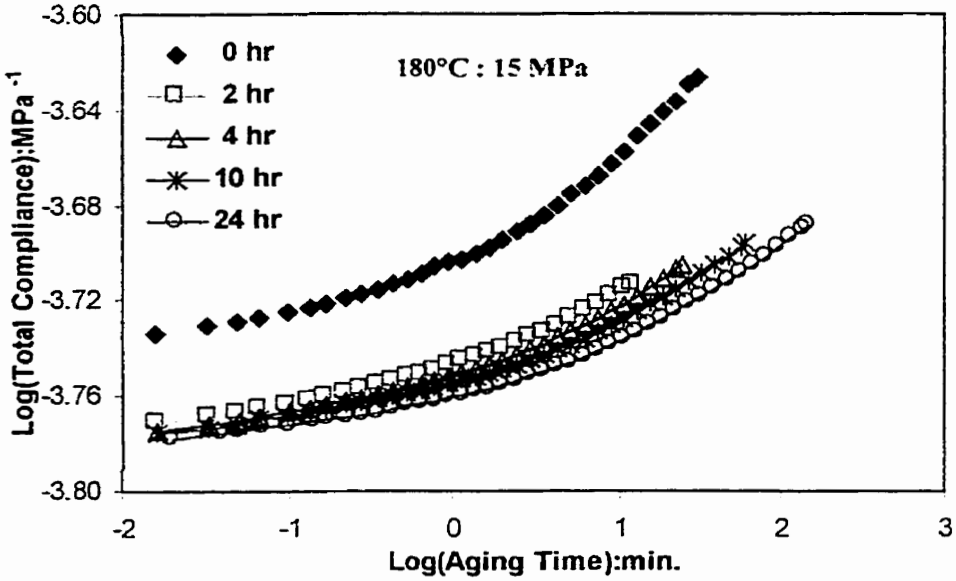

Figure C69: Compliance data at 15 MPa for $[90]_8$ composite (V_f:54%) at 180°C at various physical aging times

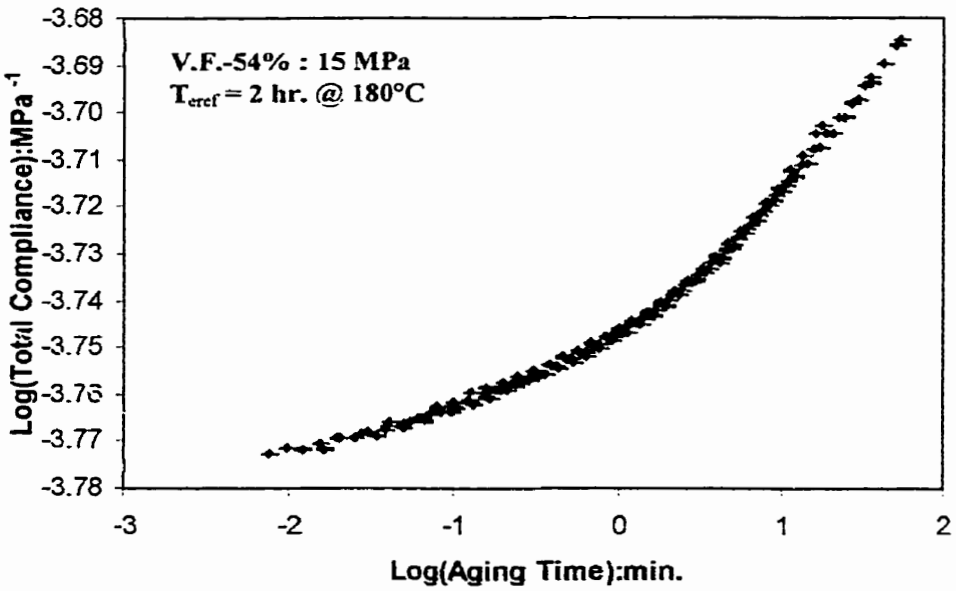

Figure C70: Momentary master curve at 15 MPa for $[90]_8$ composite (V_f:54%) at 180°C

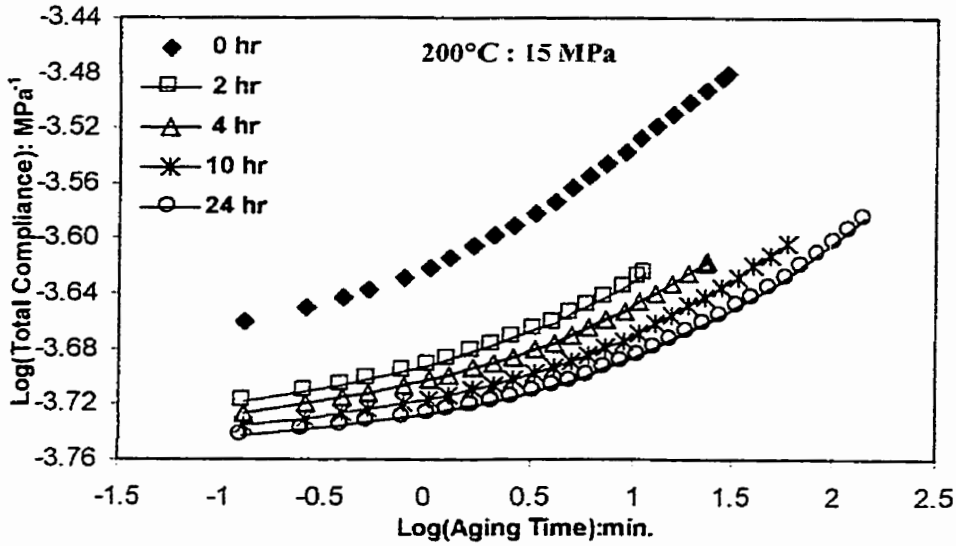

Figure C71: Compliance data at 15 MPa for $[90]_8$ composite (V_f:54%) at 200°C at various physical aging times

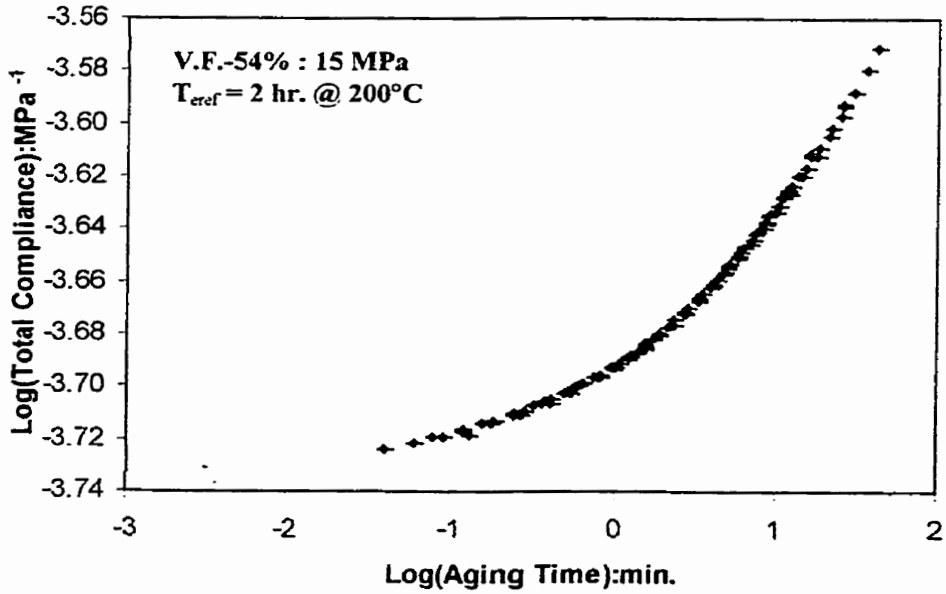

Figure C72: Momentary master curve at 15 MPa for $[90]_8$ composite (V_f:54%) at 200°C

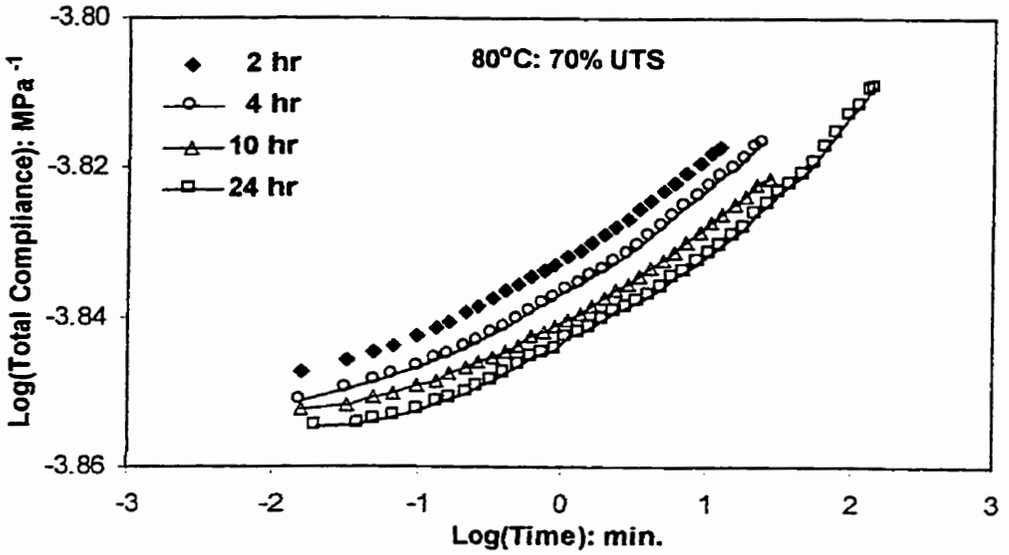

Figure C73: Compliance data at 70% of UTS for $[90]_8$ composite (V_f:54%) at 80°C at various physical aging times

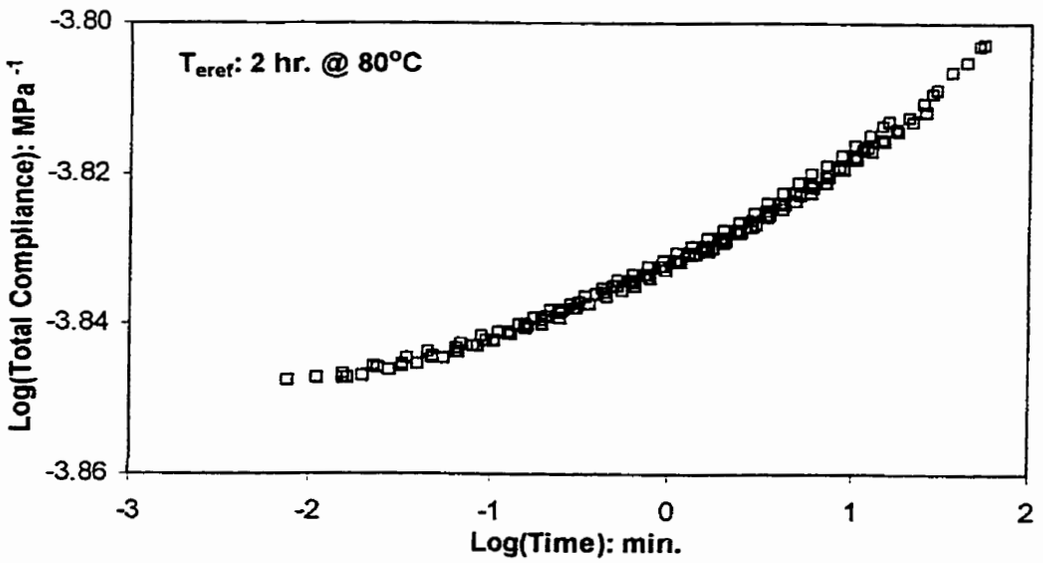

Figure C74: Momentary master curve at 70% of UTS for $[90]_8$ composite (V_f:54%) at 80°C

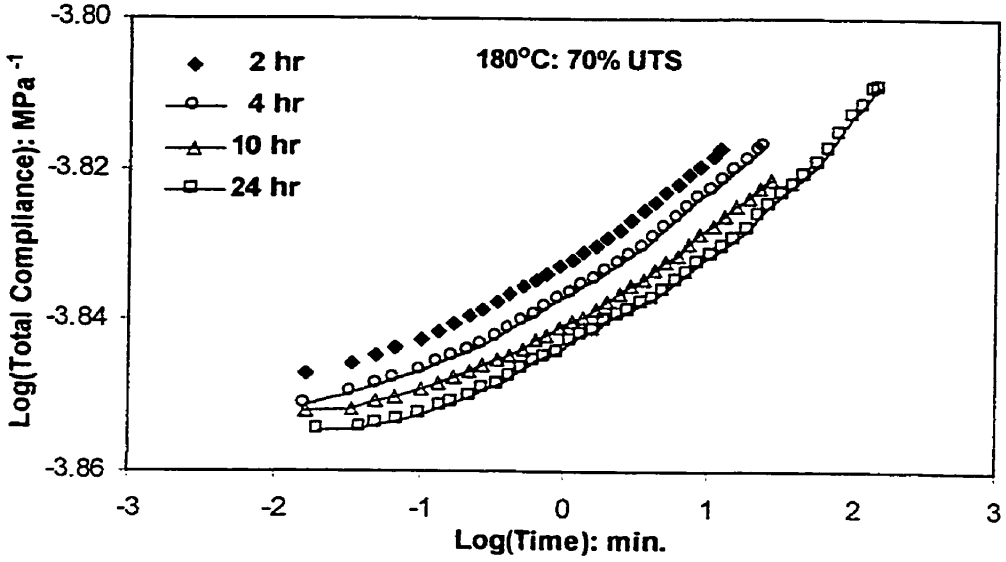

Figure C75: Compliance data at 70% of UTS for $[90]_8$ composite (V_f:54%) at 180°C at various physical aging times

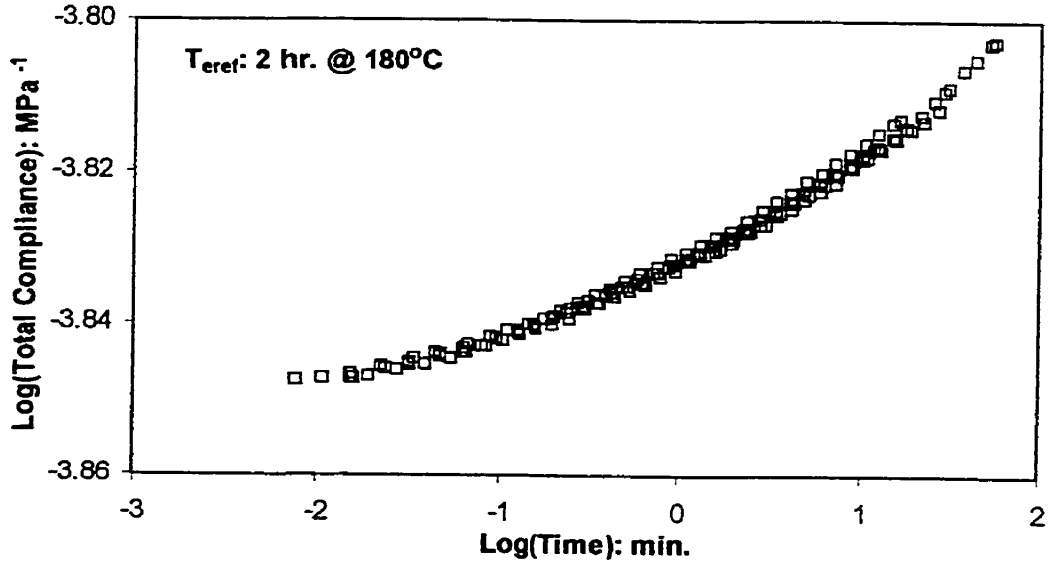

Figure C76: Momentary master curve at 70% of UTS for $[90]_8$ composite (V_f:54%) at 180°C

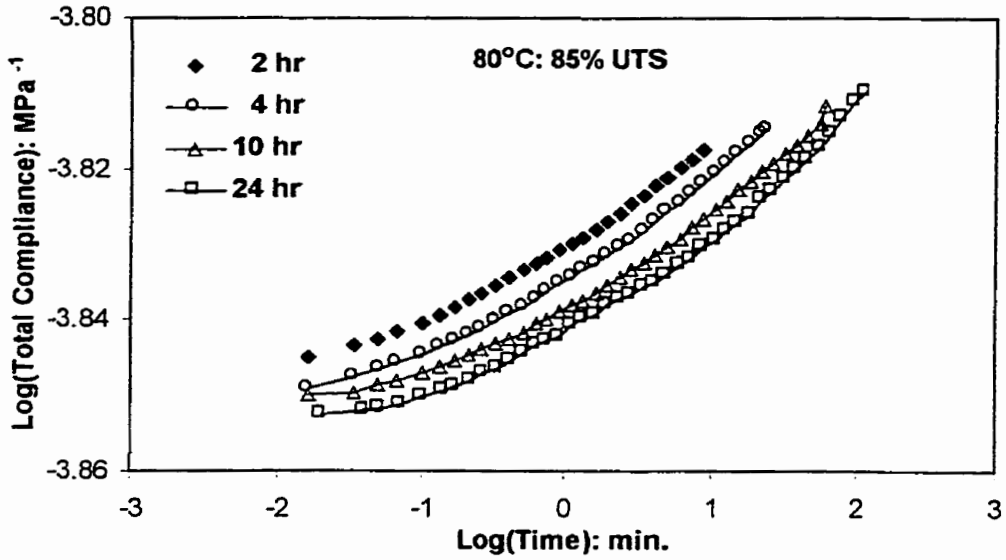

Figure C77: Compliance data at 85% of UTS for $[90]_8$ composite (V_f:54%) at 80°C at various physical aging times

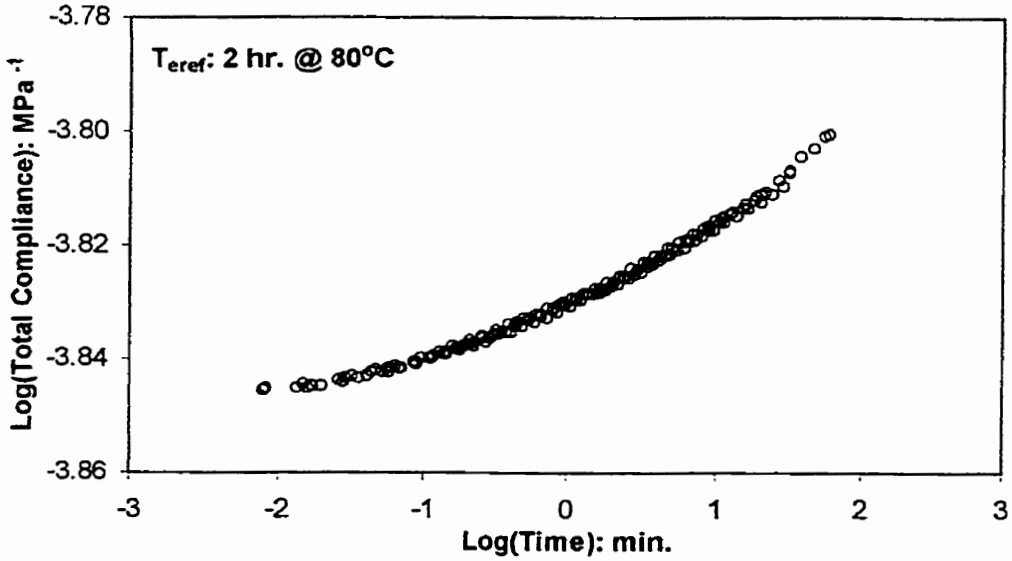

Figure C78: Momentary master curve at 85% of UTS for $[90]_8$ composite (V_f:54%) at 80°C

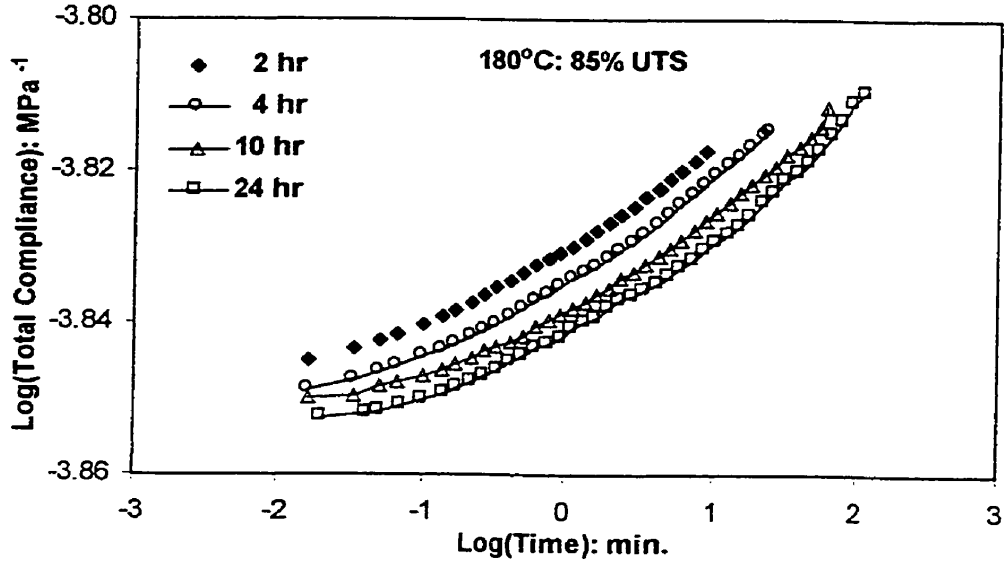

Figure C79: Compliance data at 85% of UTS for $[90]_8$ composite (V_f:54%) at 180°C at various physical aging times

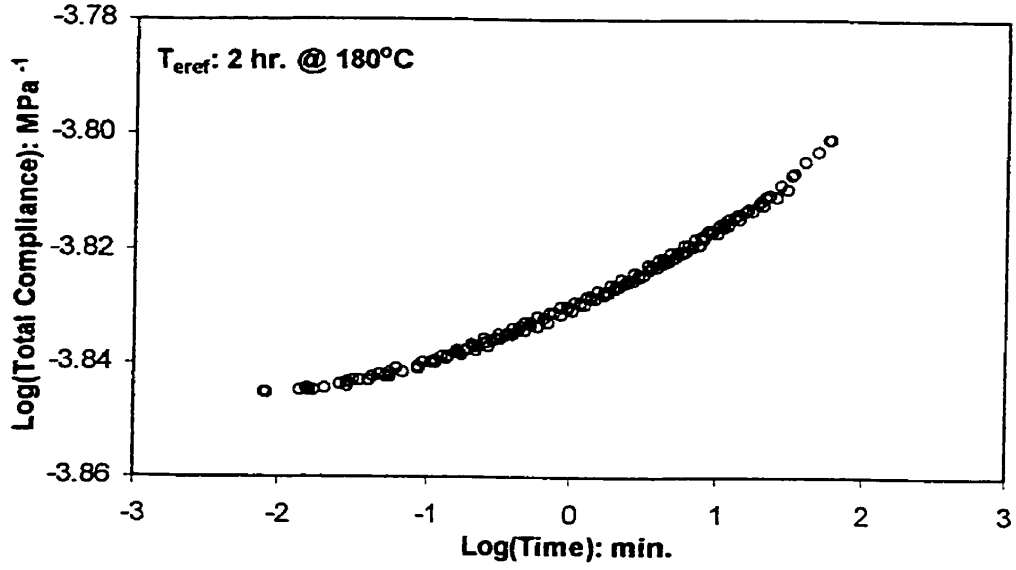

Figure C80: Momentary master curve at 85% of UTS for $[90]_8$ composite (V_f:54%) at 180°C

APPENDIX - D

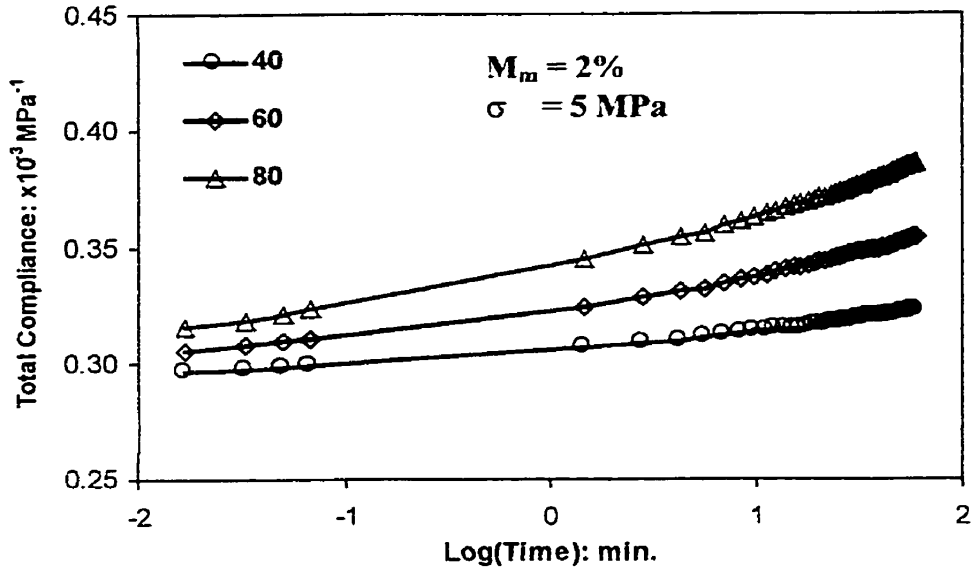

Figure D1: Compliance data at 5 MPa for 2 % moisture conditioned resin at various temperatures

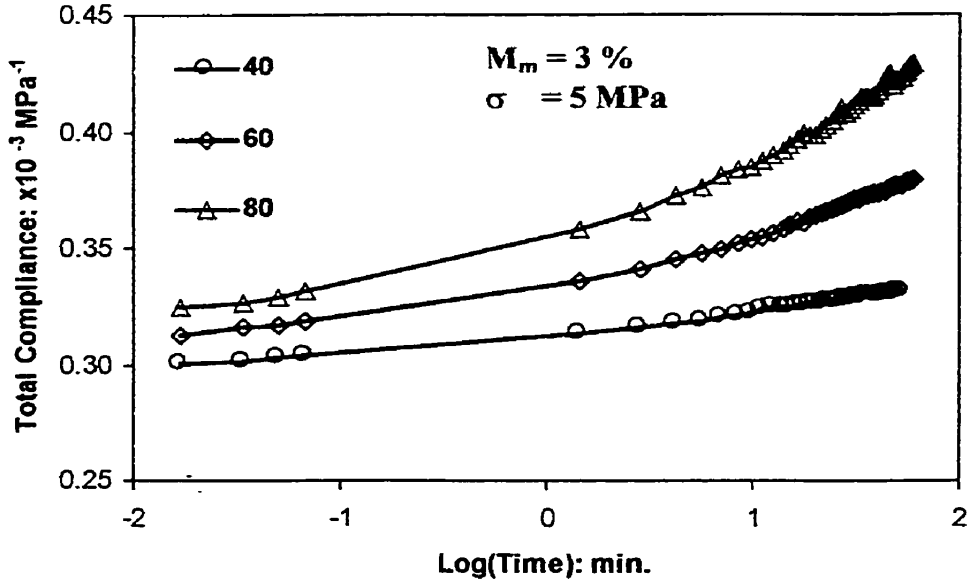

Figure D2: Compliance data at 5 MPa for 3 % moisture conditioned resin at various temperatures

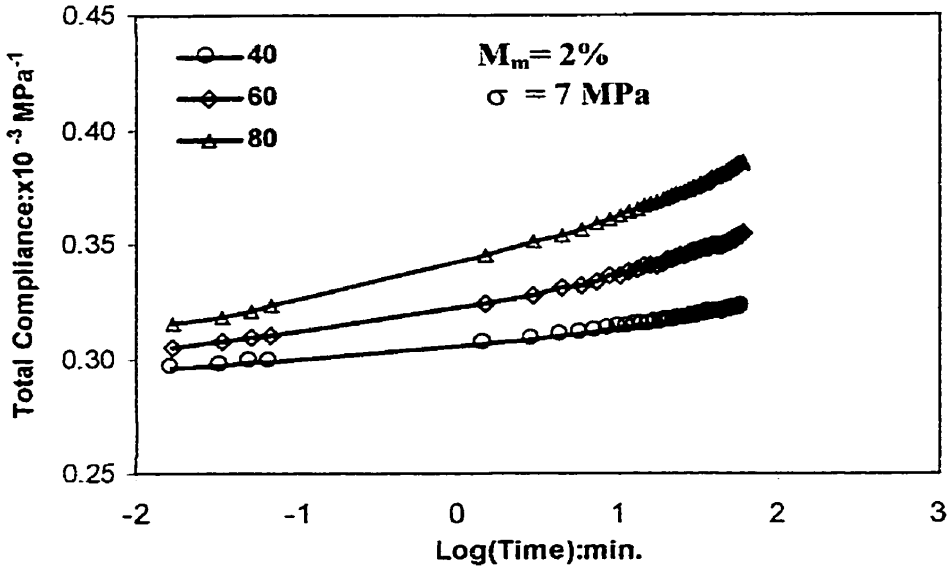

Figure D3: Compliance data at 7MPa for 2 % moisture conditioned resin at various temperatures

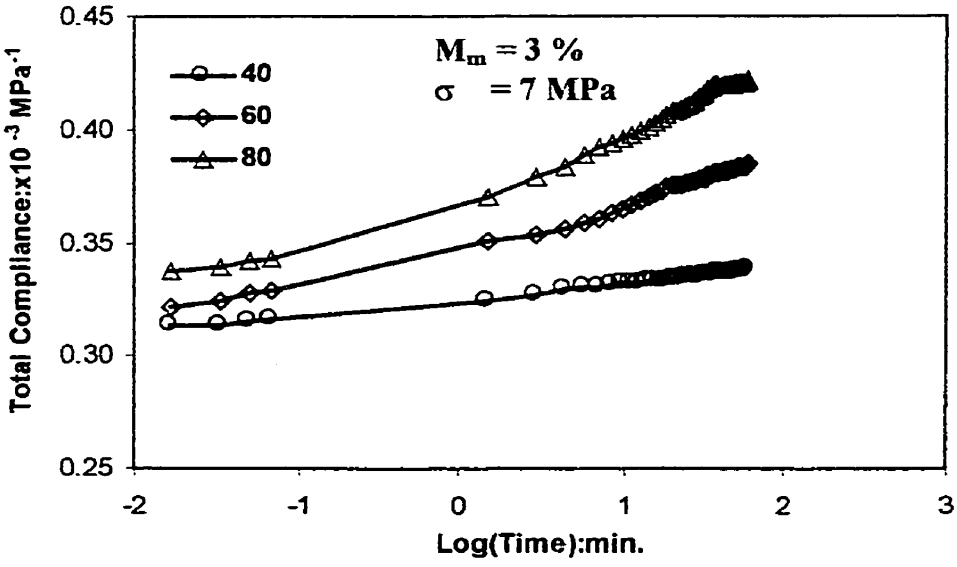

Figure D4: Compliance data at 7MPa for 3 % moisture conditioned resin at various temperatures

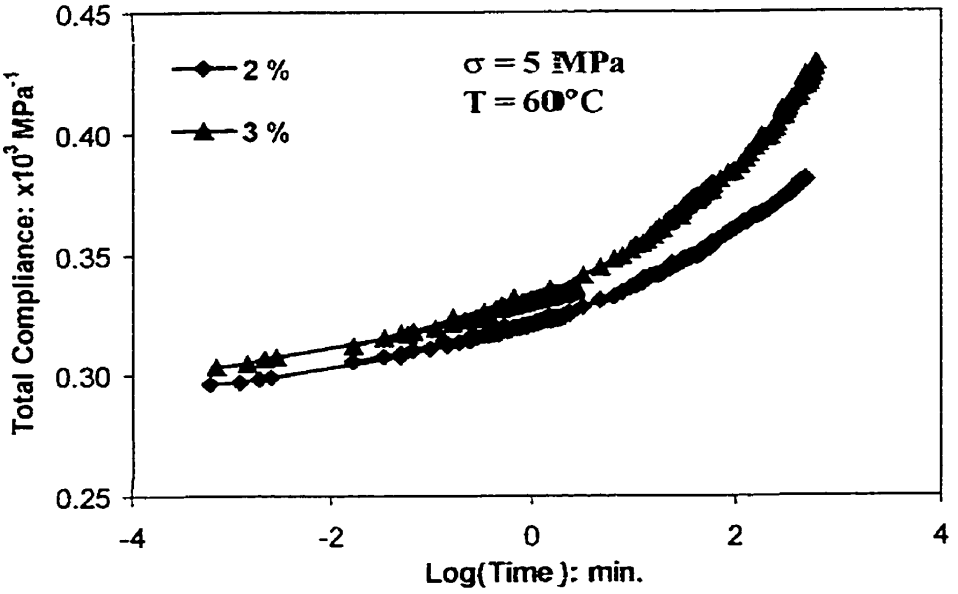

Figure D5: Master creep curve at 5 MPa for moisture conditioned resin

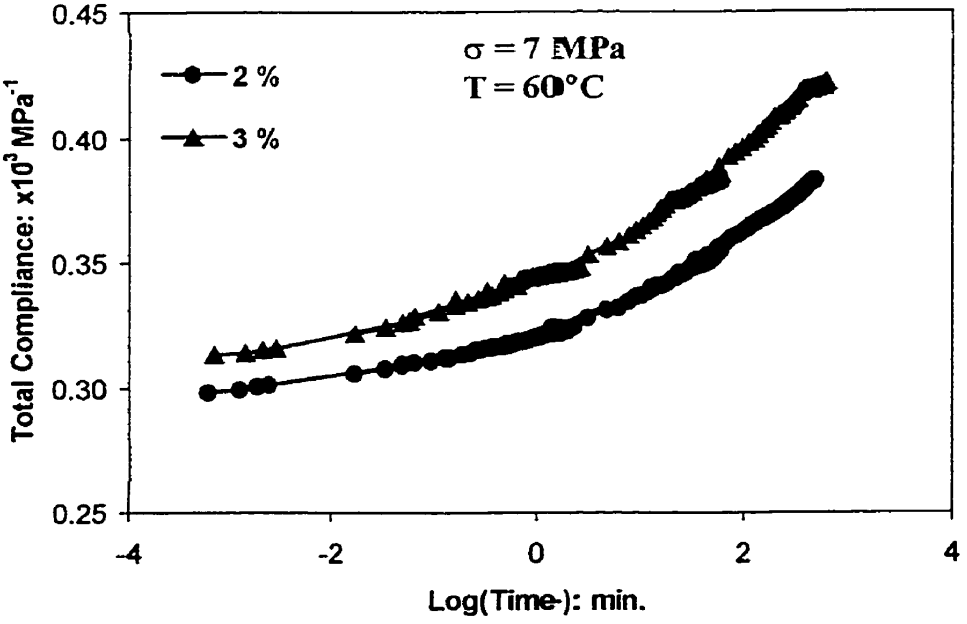

Figure D6: Master creep curve at 7 MPa for moisture conditioned resin

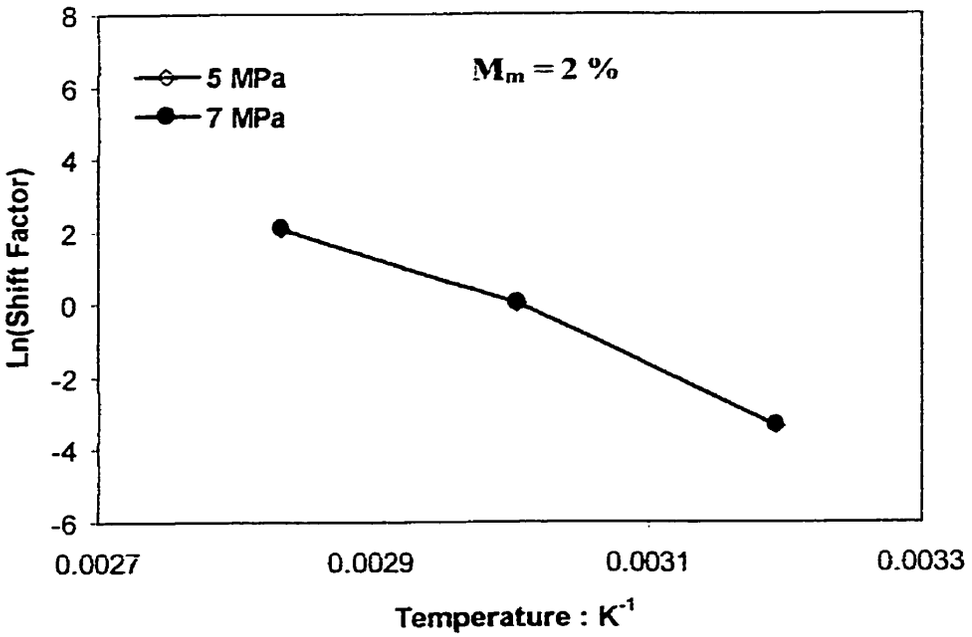

Figure D7: Shift factor as a function of temperature for 2 % moisture conditioned resin at 5 and 7 MPa

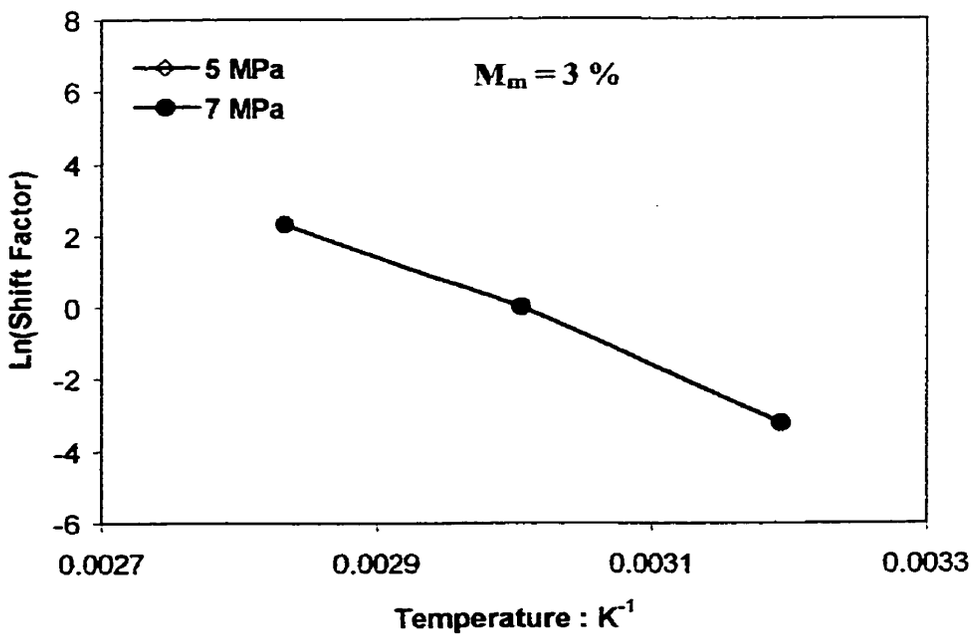

Figure D8: Shift factor as a function of temperature for 3 % moisture conditioned resin at 5 and 7 MPa

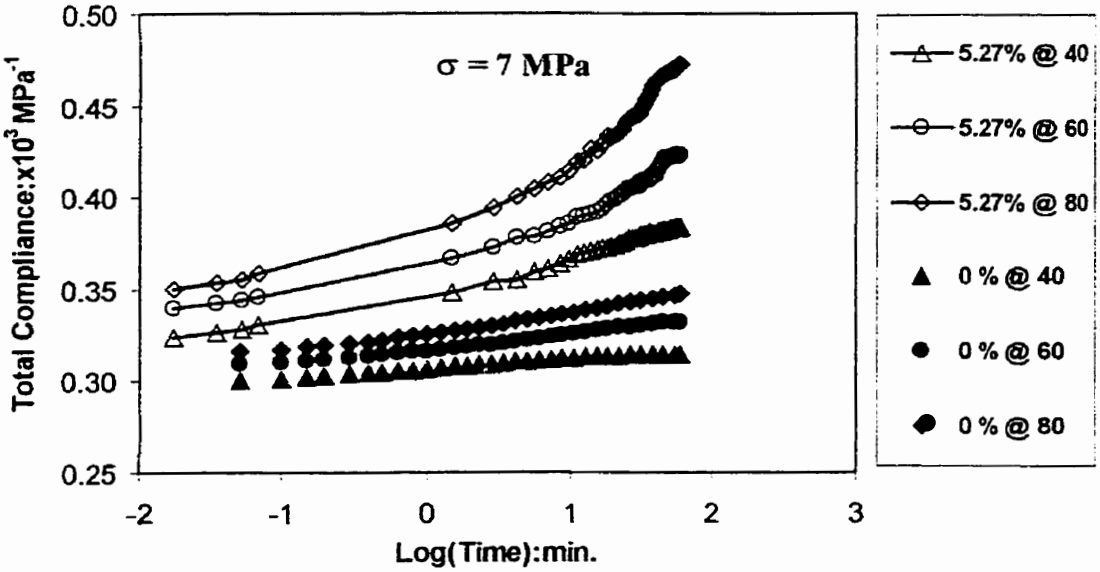

Figure D9: Compliance data at 7 MPa for dry and moisture conditioned resin at various temperatures

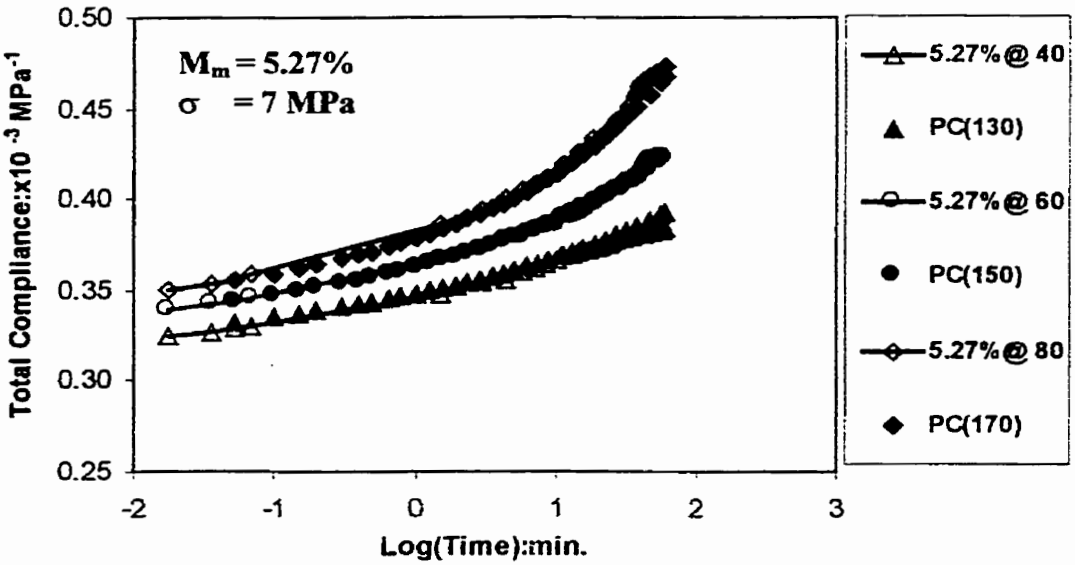

Figure D10: Validation of mechanism of creep acceleration by moisture for resin at 7 MPa

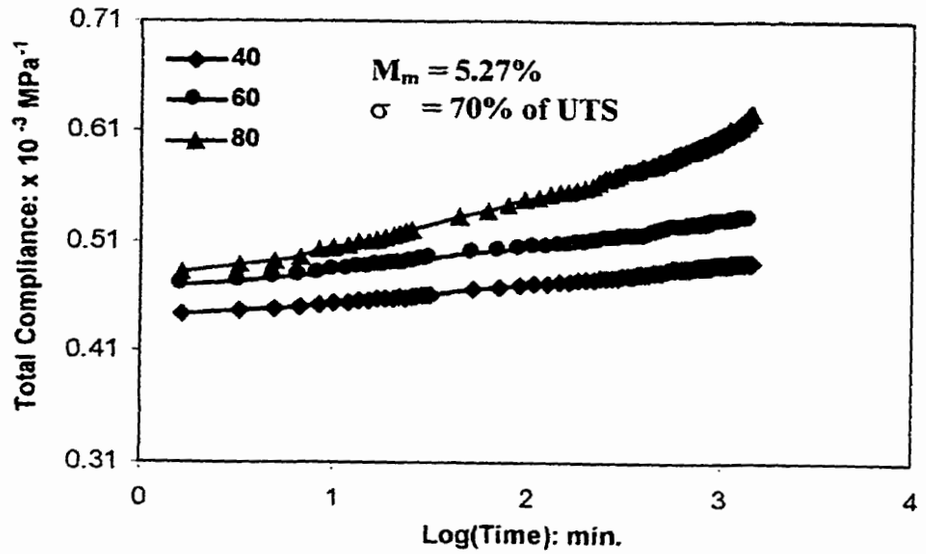

Figure D11: Compliance data at 70% UTS for 5.27 % moisture resin conditioned at various temperatures

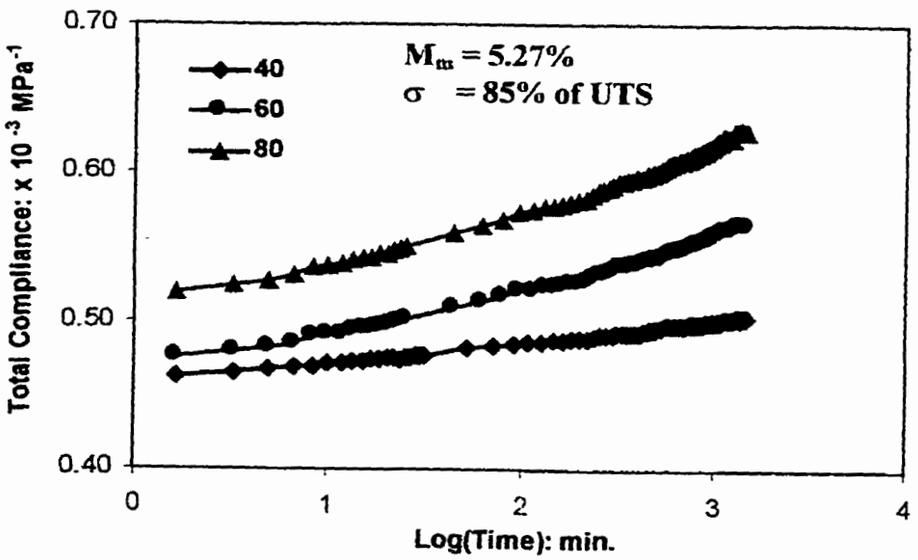

Figure D12: Compliance data at 85% UTS for 5.27 % moisture resin conditioned at various temperature

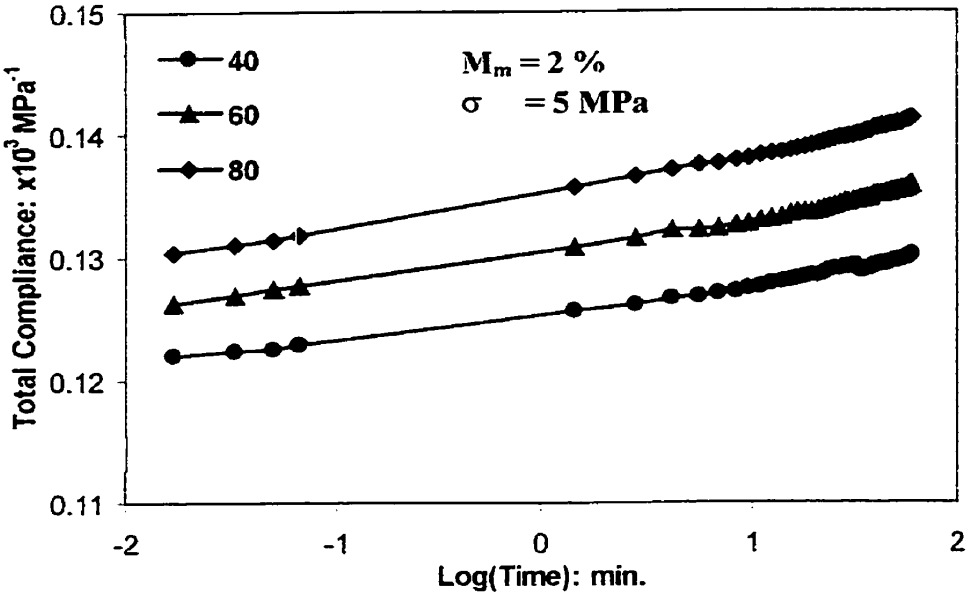

Figure D13: Compliance data of 2 % moisture conditioned composite with 54% V_f at 5 MPa at different temperatures

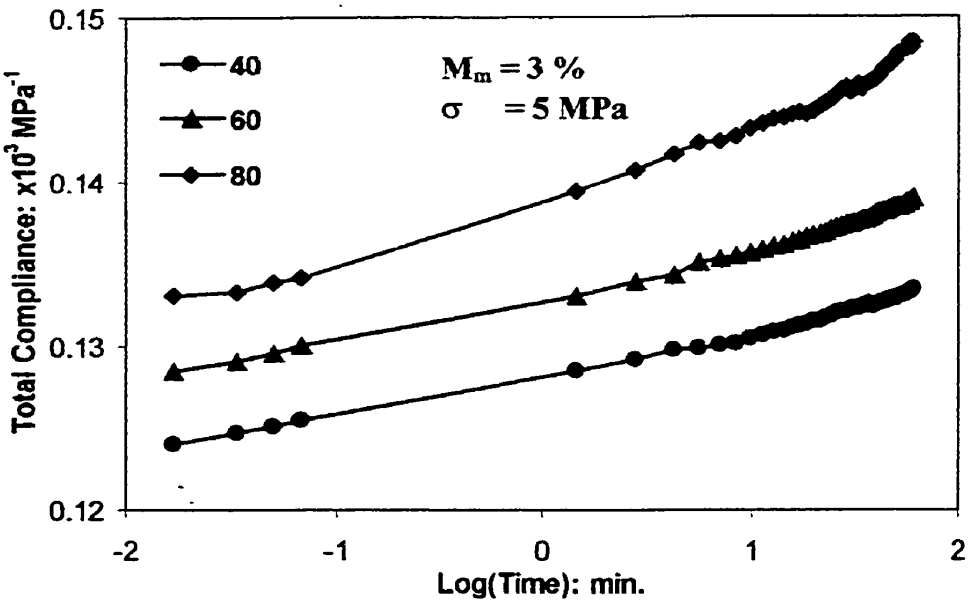

Figure D14: Compliance data of 3 % moisture conditioned composite with 54% V_f at 5 MPa at different temperatures

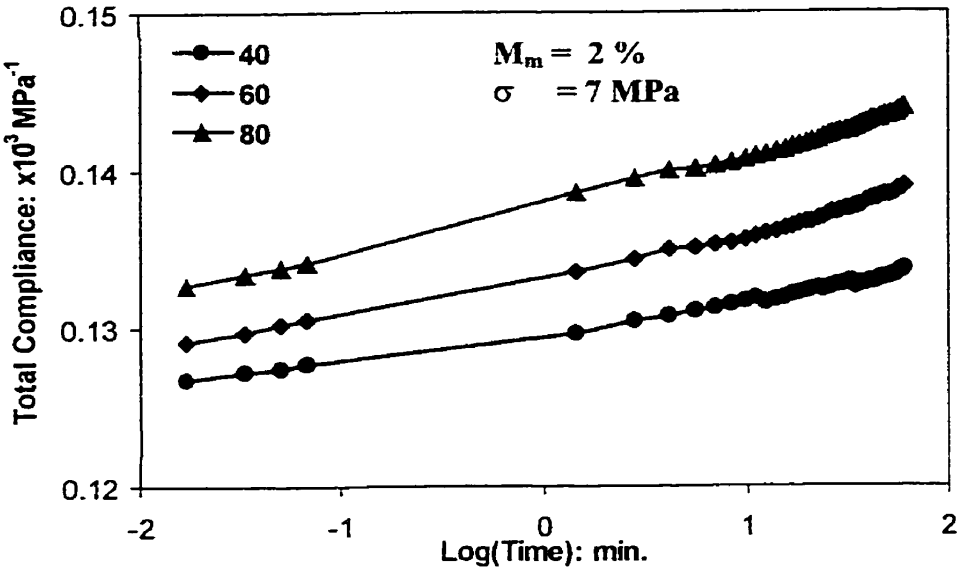

Figure D15: Compliance data of 2 % moisture conditioned composite with 54% V_f at 7 MPa at different temperatures

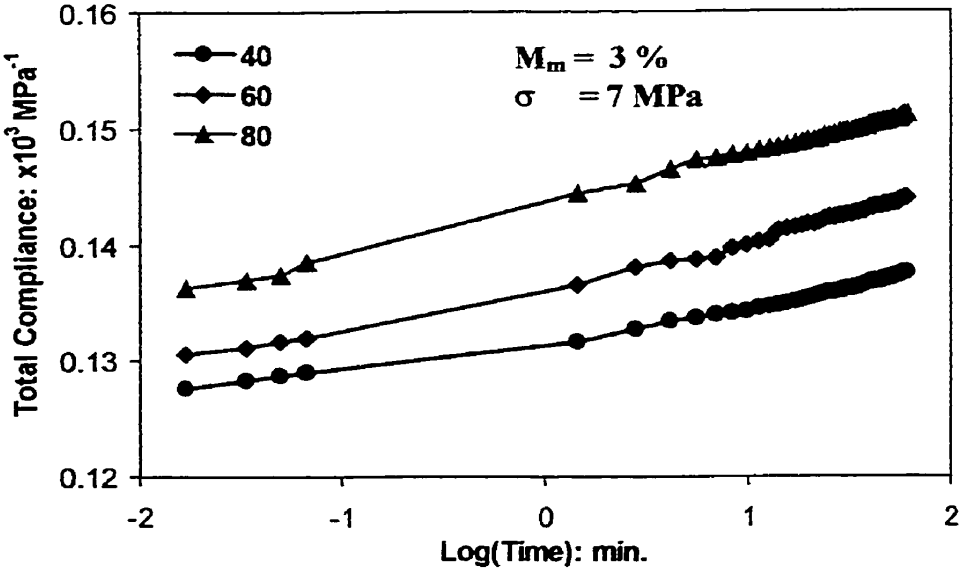

Figure D16: Compliance data of 3 % moisture conditioned composite With 54% V_f at 7 MPa at different temperatures

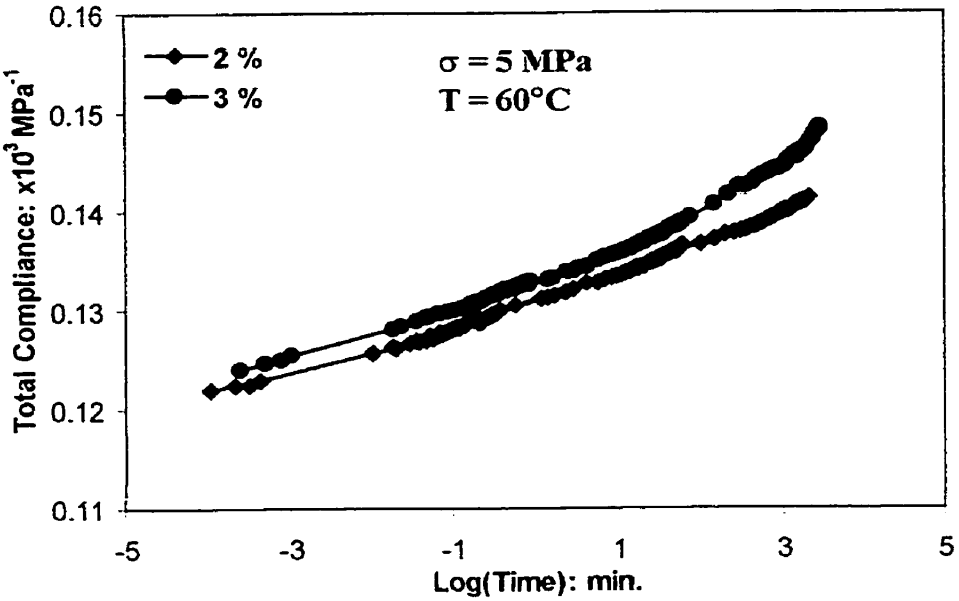

Figure D17: Master creep curve of moisture conditioned composite with 54% V_f at 5 MPa at 60°C

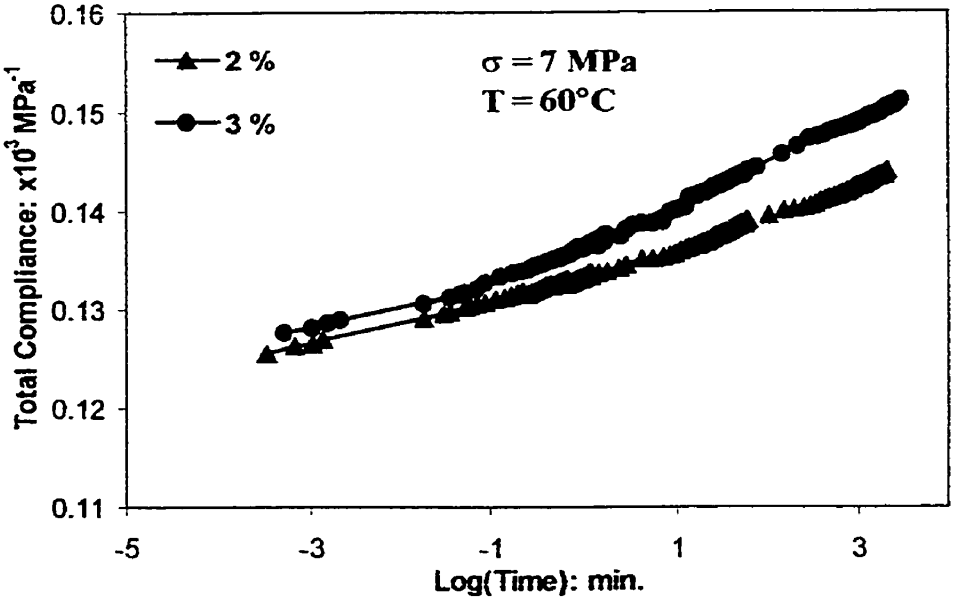

Figure D18: Master creep curve of moisture conditioned composite with 54% V_f at 7 MPa at 60°C

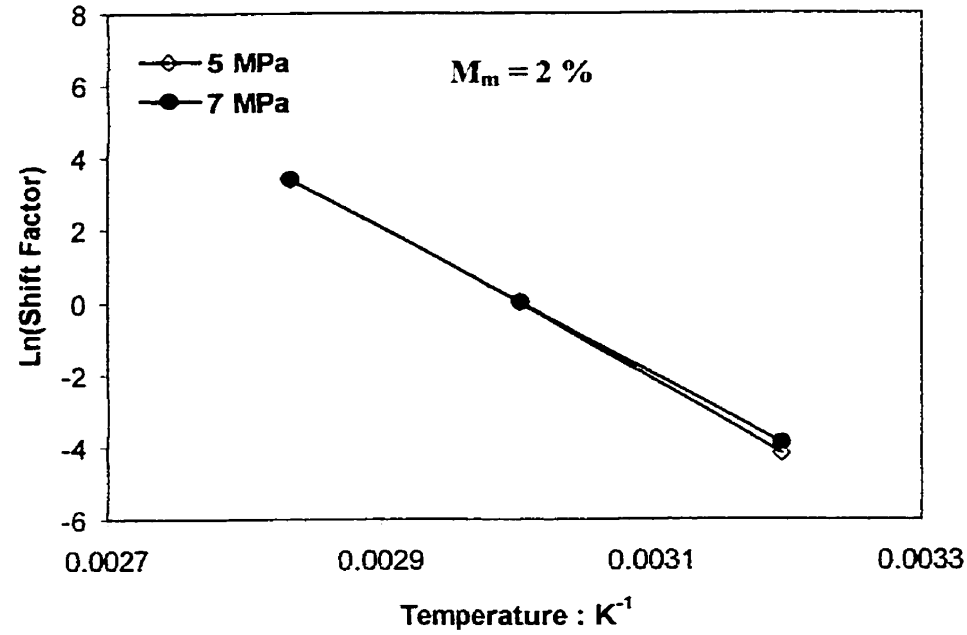

Figure D19: Shift factor as a function of temperature for 2% moisutre conditioned composite with 54% V_f at 5 and 7 MPa

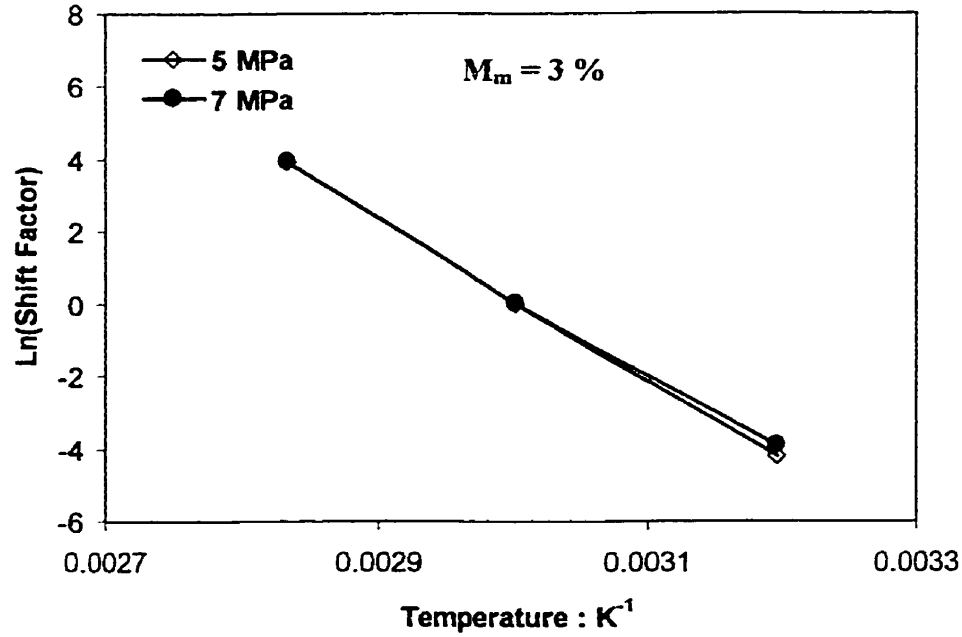

Figure D20: Shift factor as a function of temperature for 3% moisutre conditioned composite with 54% V_f at 5 and 7 MPa

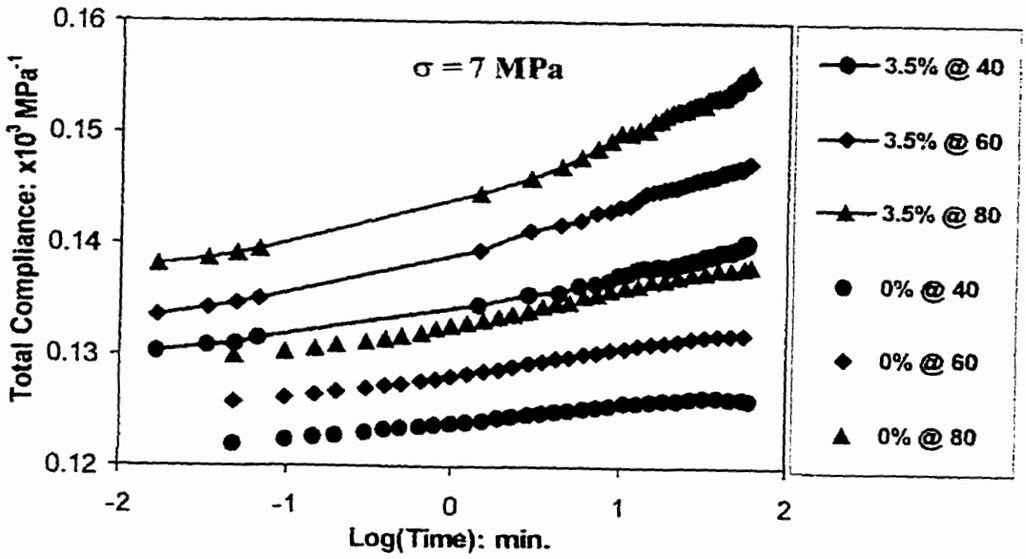

Figure D21: Compliance data of dry and moisture conditioned composite with 54% V_f at 7 MPa at different temperatures

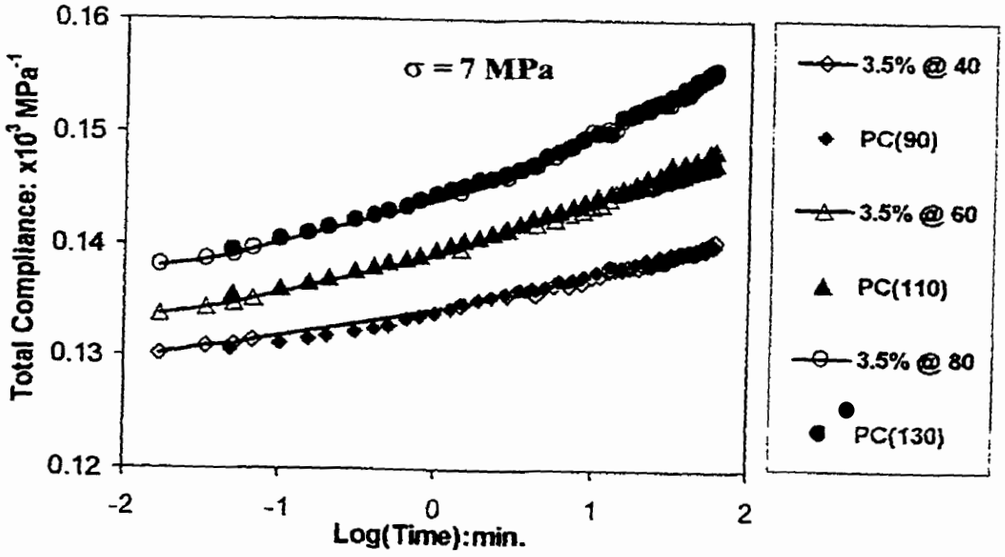

Figure D22: Validation of creep mechanism by moisture for composite (V_f :54%) at 7 MPa

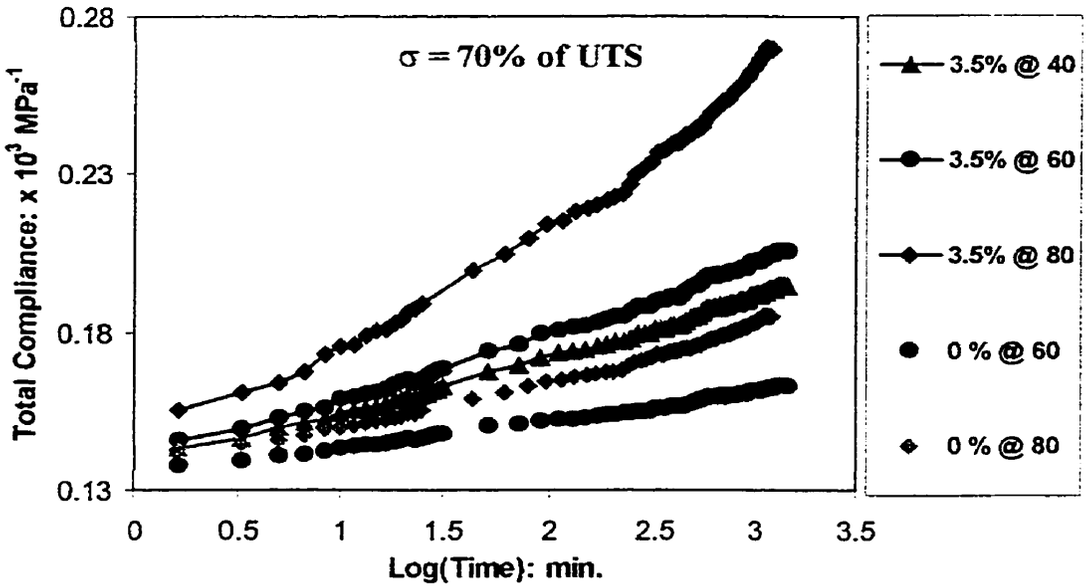

Figure D23: Compliance data of dry and moisture conditioned composite with 54% V_f at 70% of UTS at different temperatures

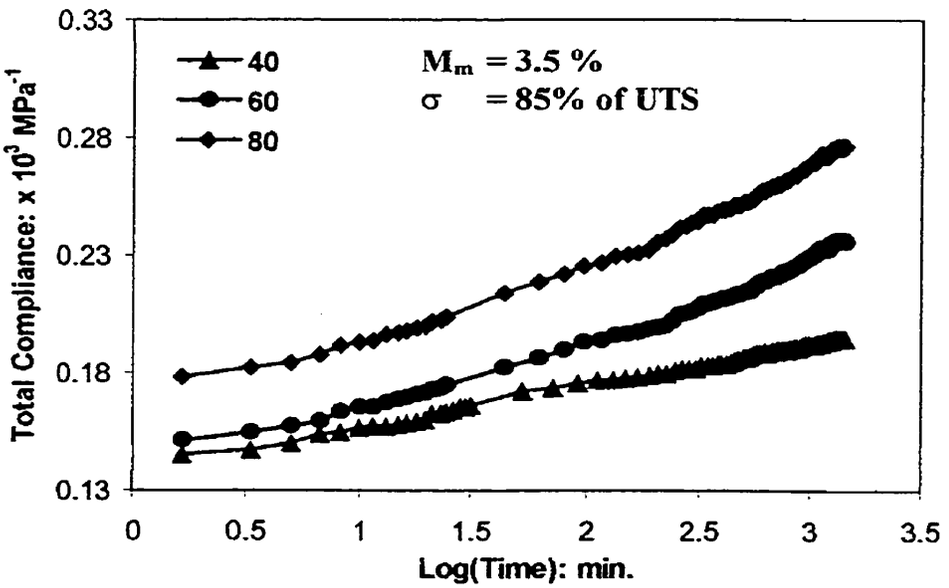

Figure D24: Compliance data of 3.5% moisture conditioned composite with 54% V_f at 85% of UTS at different temperatures

APPENDIX - E

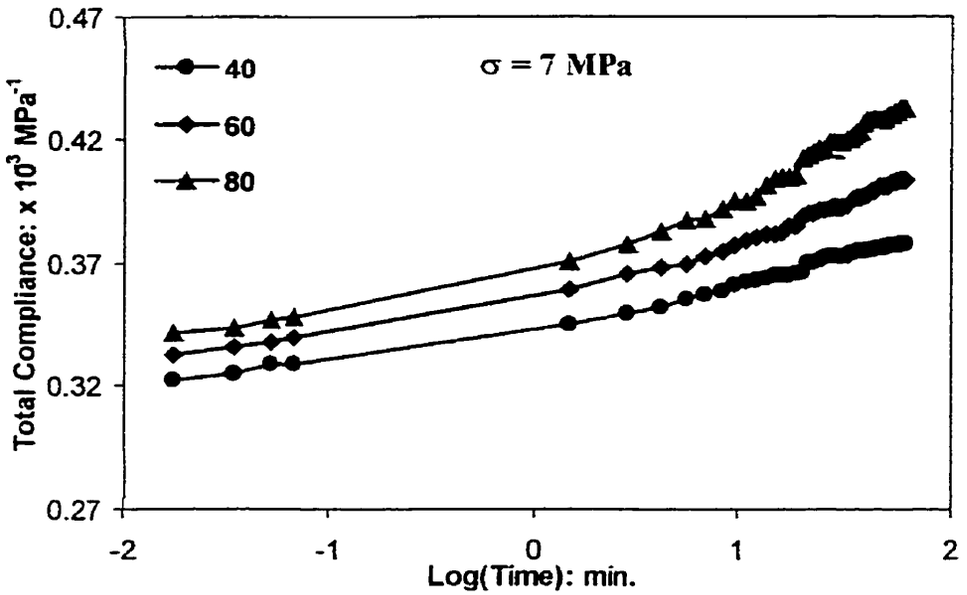

Figure E1: Compliance data at 7 MPa for aged-moisture conditioned resin at various temperatures

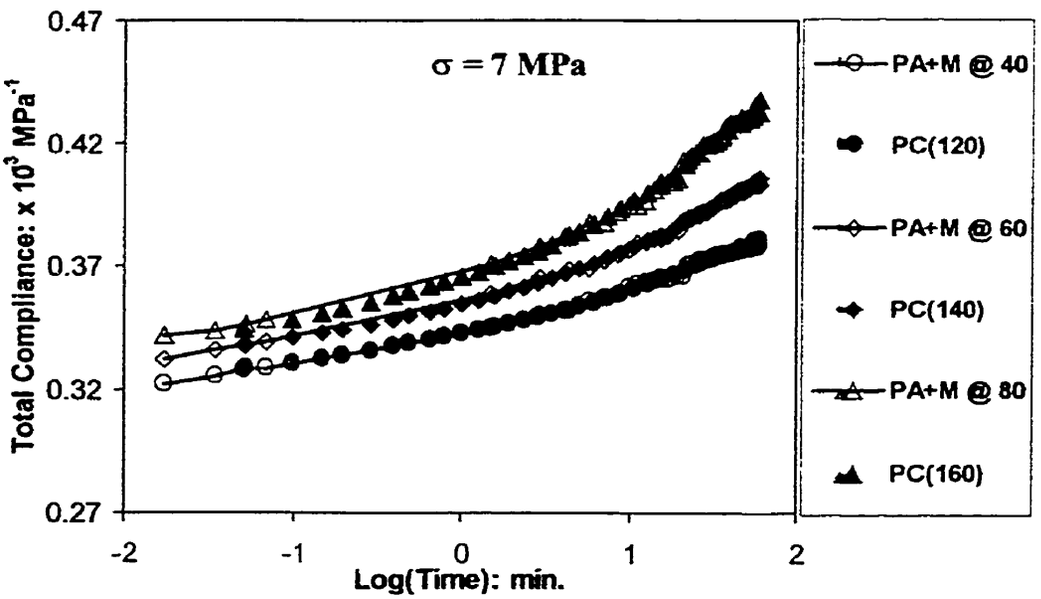

Figure E2: Validation of mechanism for interactive influence of aging and moisture for resin at 7 MPa

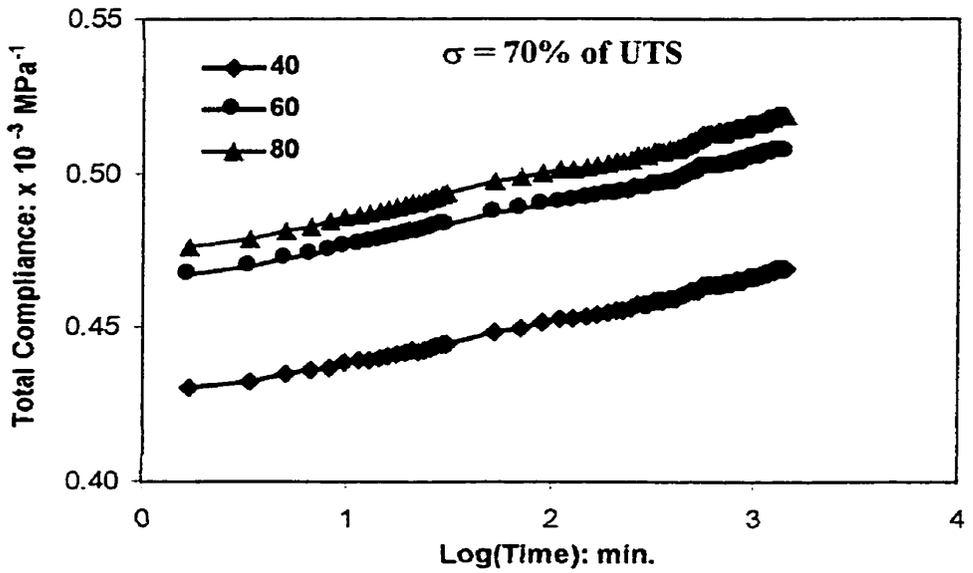

Figure E3: Compliance data at 70% UTS for aged-moisture conditioned resin at various temperatures

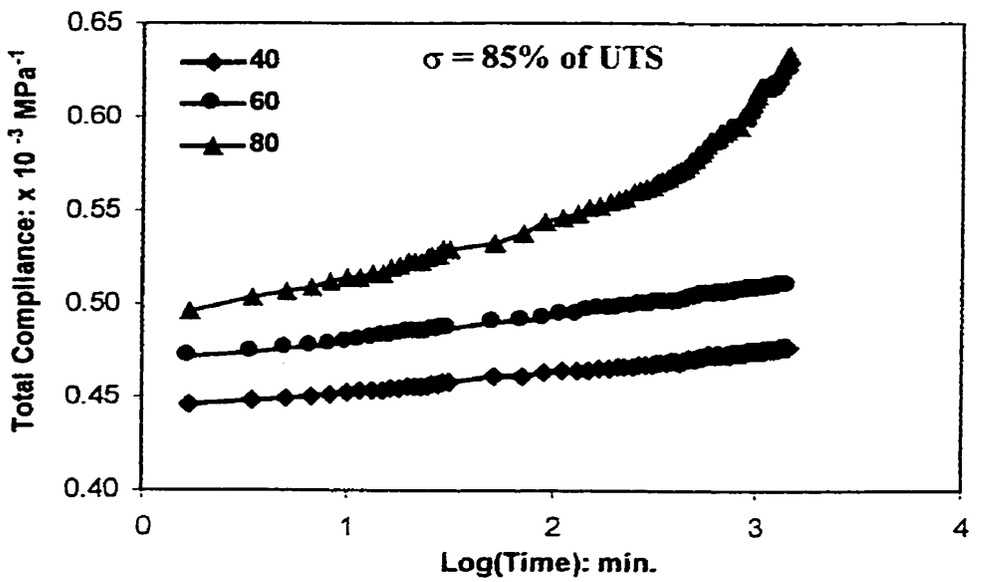

Figure E4: Compliance data at 85% UTS for aged-moisture conditioned resin at various temperatures

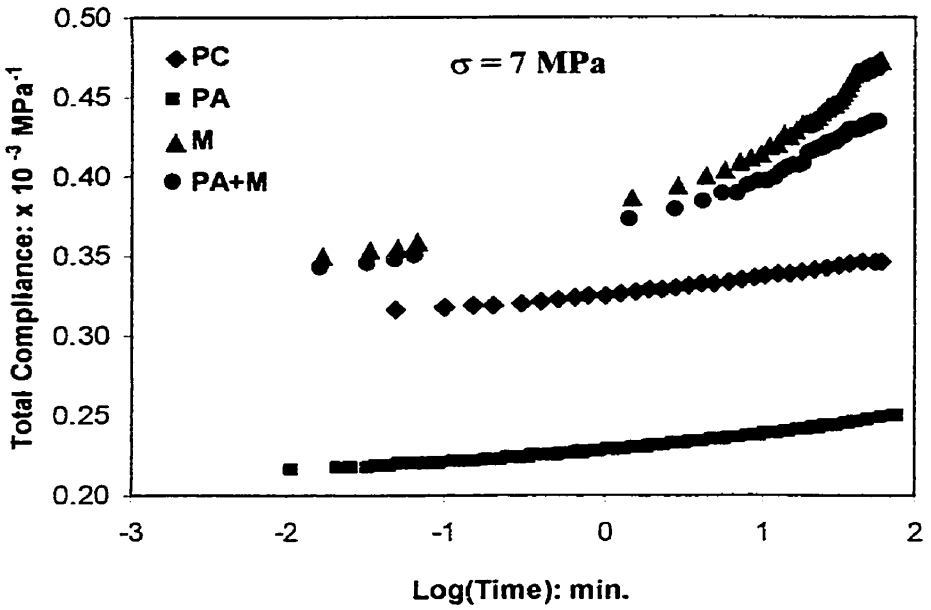

Figure E5: Compliance data at 7 MPa for postcured, physically aged, moisture-conditioned and aged-moisture conditioned resin at 80°C

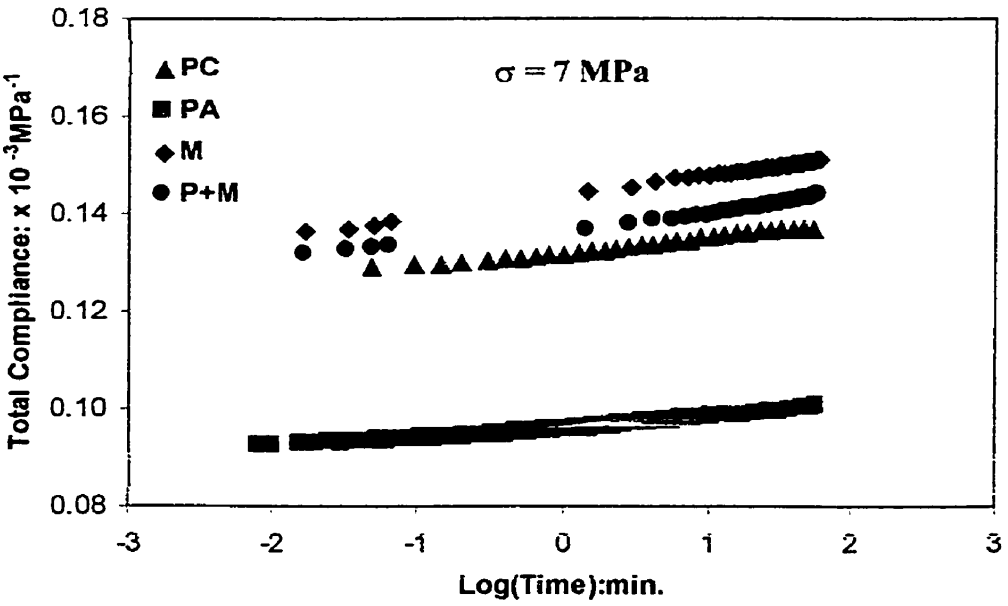

Figure E6: Compliance data at 7 MPa for postcured, physically aged, moisture-conditioned and aged-moisture conditioned composite (V_f:54%) at 80°C

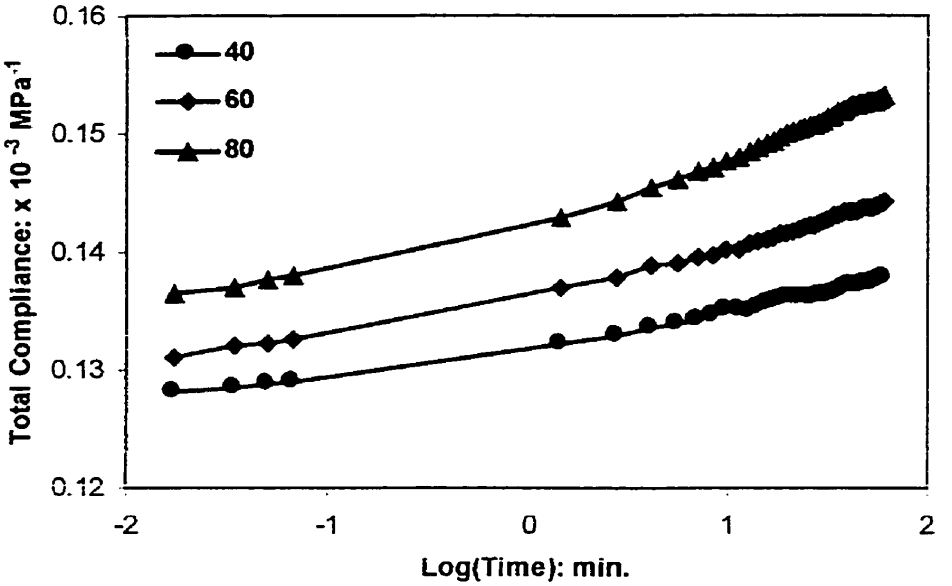

Figure E7: Compliance data at 7 MPa for aged-moisture conditioned composite (V_f:54%) at various temperatures

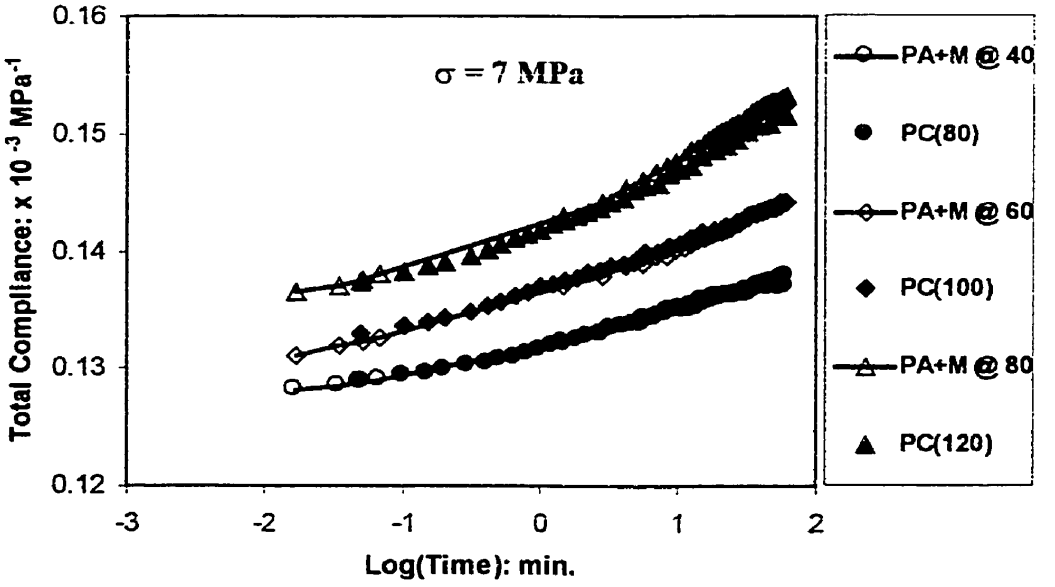

Figure E8: Validation of mechanism for interactive influence of aging and moisture for composite (V_f:54%) at 7 MPa

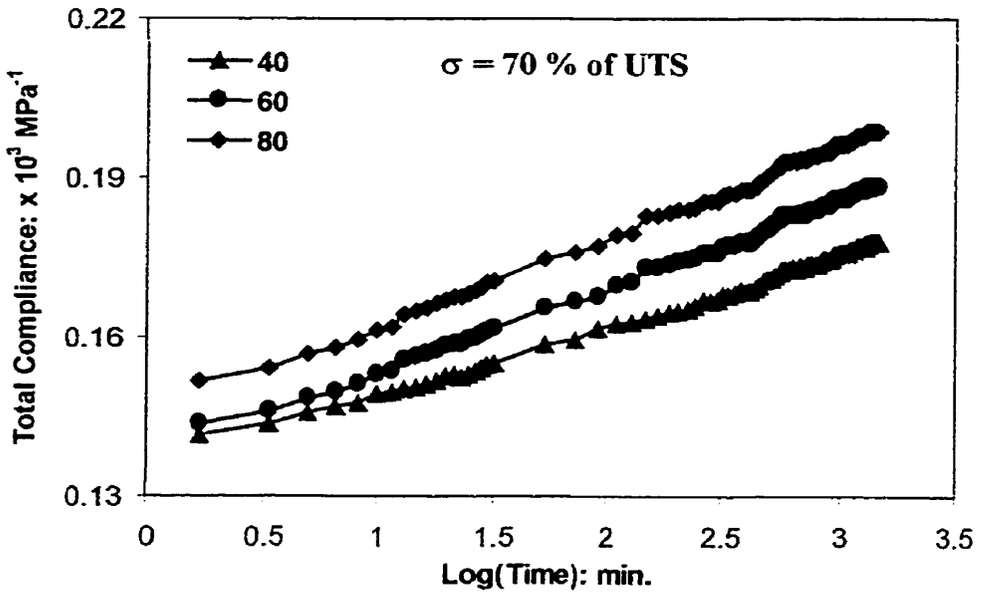

Figure E9: Compliance data at 70% of UTS for aged-moisture conditioned composite (V_f:54%) at various temperatures

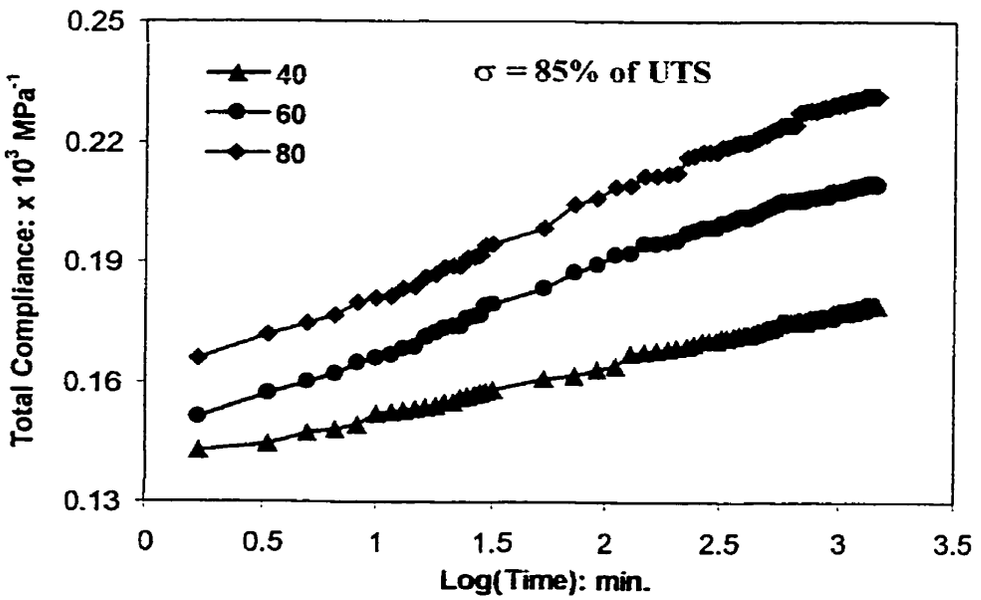

Figure E10: Compliance data at 85% of UTS for aged-moisture conditioned composite (V_f:54%) at various temperatures

APPENDIX - F

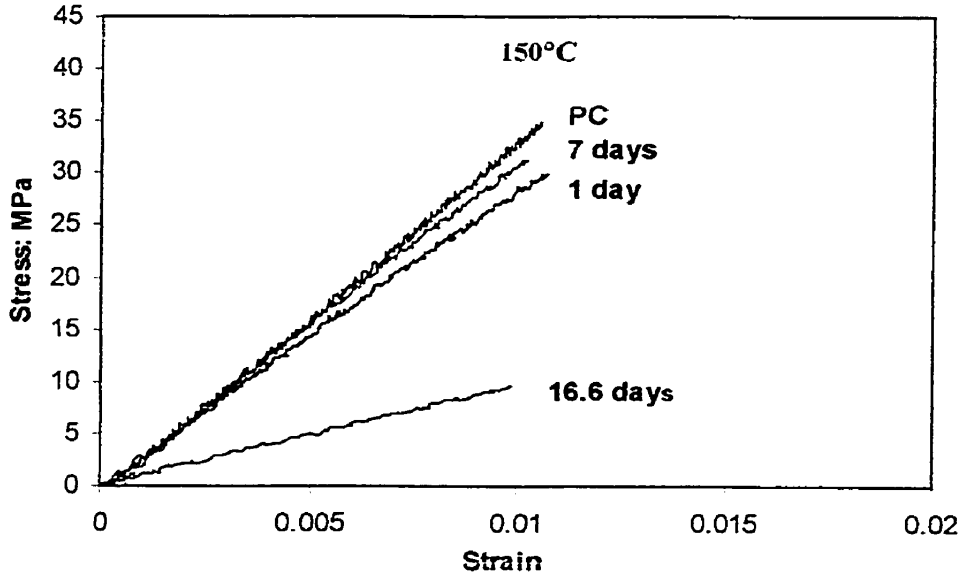

Figure F1: Stress-Strain plot of resin at different various aging times at 150°C

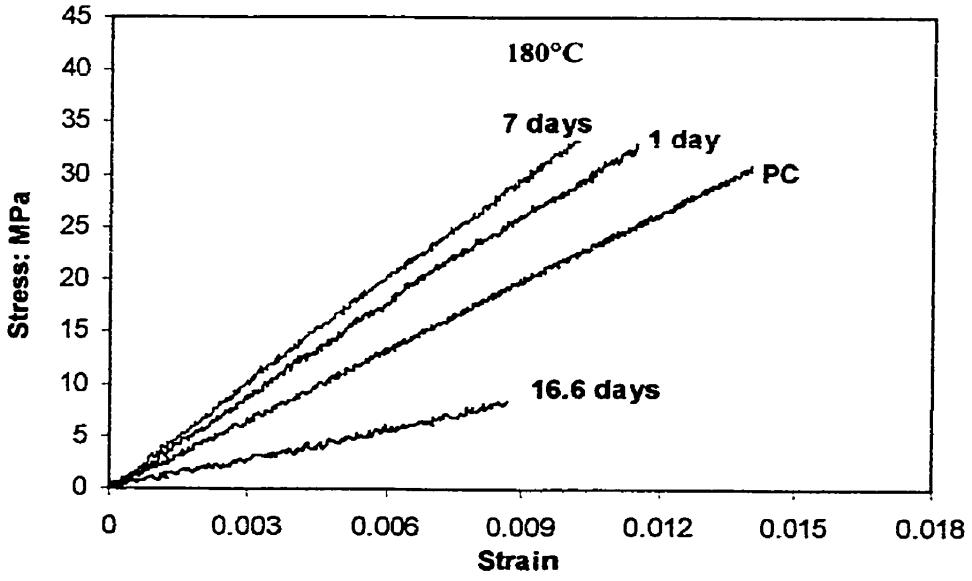

Figure F2: Stress-Strain plot of resin at various physical aging times at 180°C

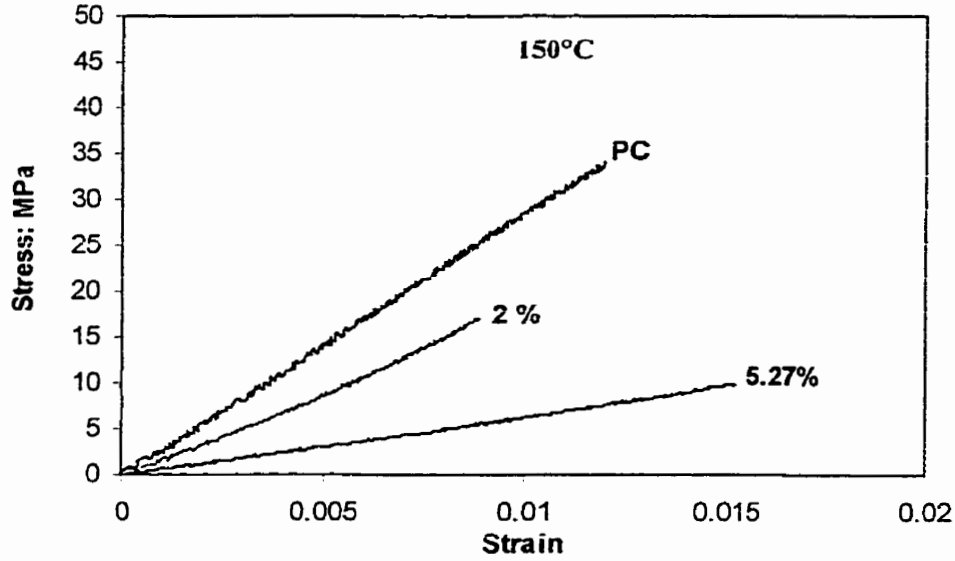

Figure F3: Stress-Strain plot of resin at 150°C at various moisture contents

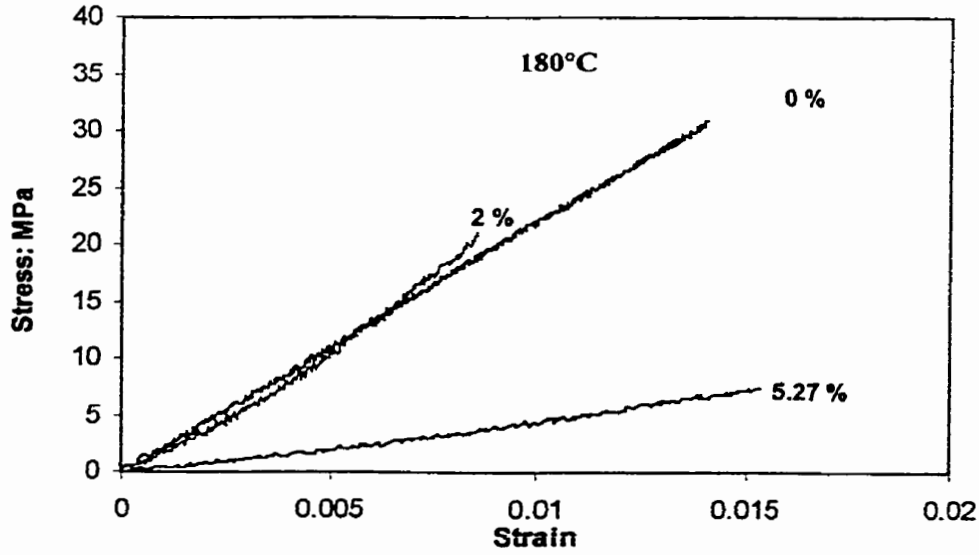

Figure F4: Stress-Strain plot of resin at 180°C at various moisture contents

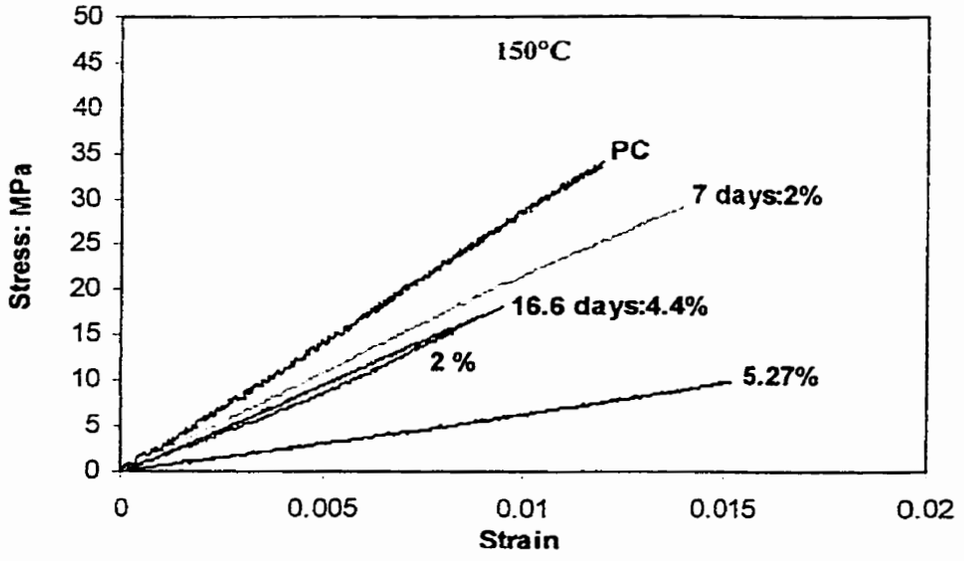

Figure F5: Stress-Strain plot of resin at 150°C at various physical aging times and moisture contents

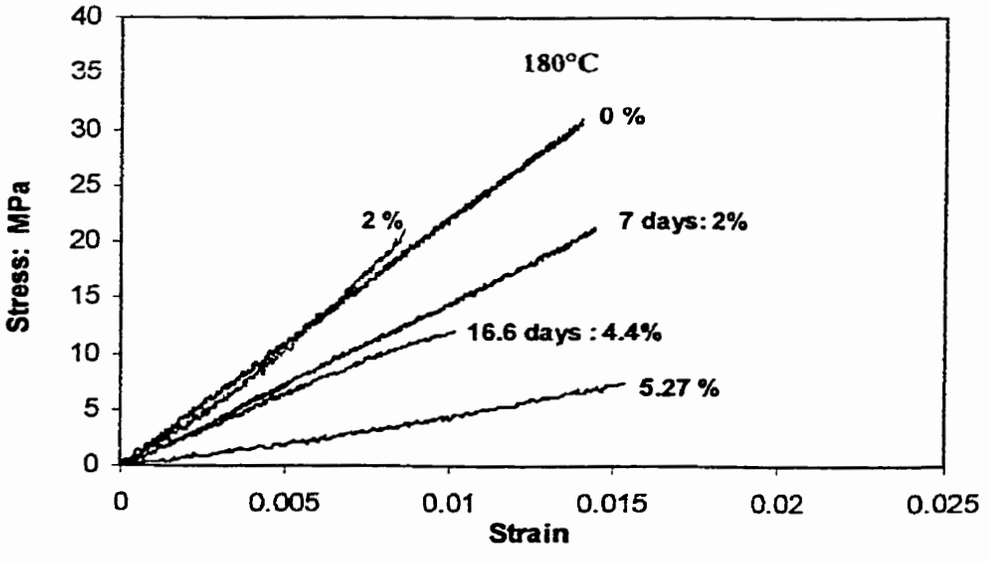

Figure F6: Stress-Strain plot of resin at 180°C at various physical aging times and moisture contents

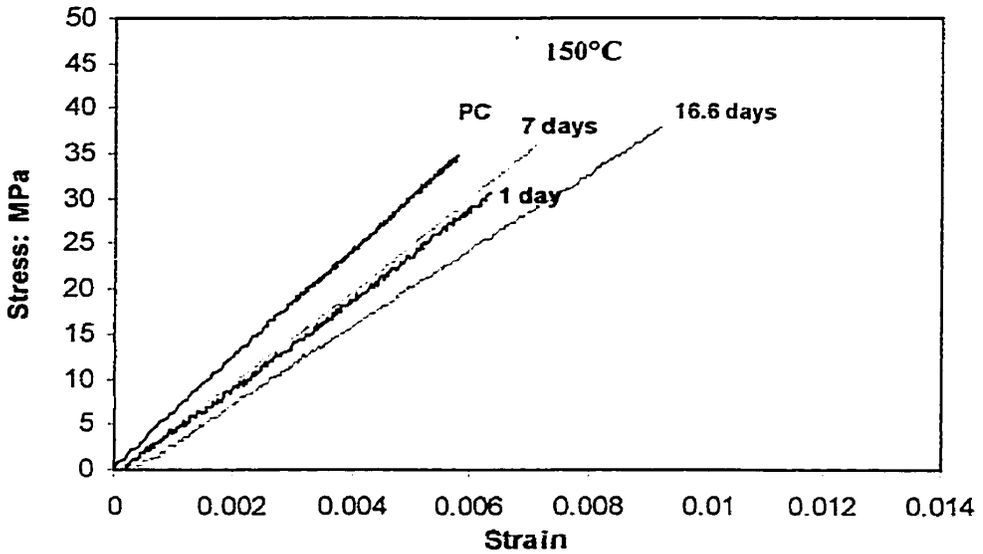

Figure F7: Stress-Strain plot of $[90]_{12}$ composite (V_f:54%) at various physical aging times at 150°C

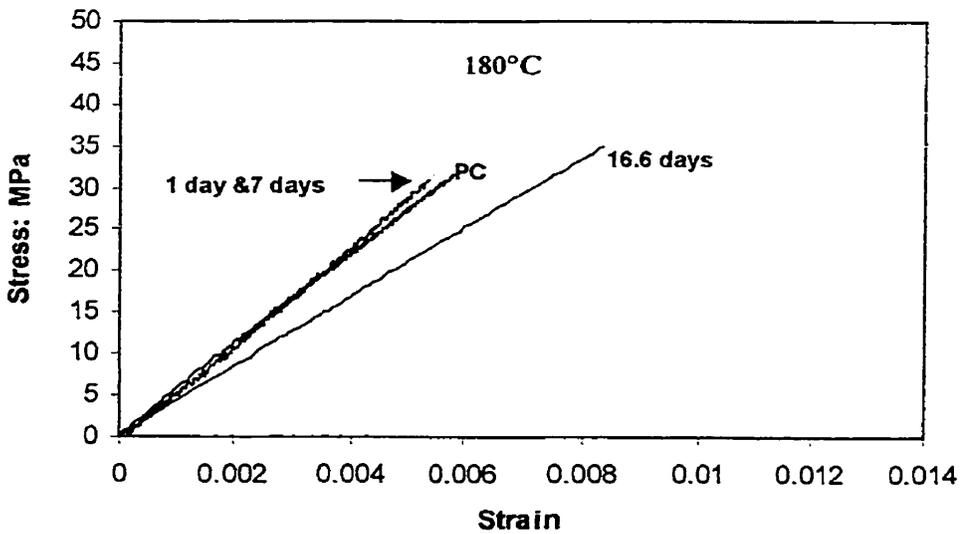

Figure F8: Stress-Strain plot of $[90]_{12}$ composite (V_f:54%) at various physical aging times at 180°C

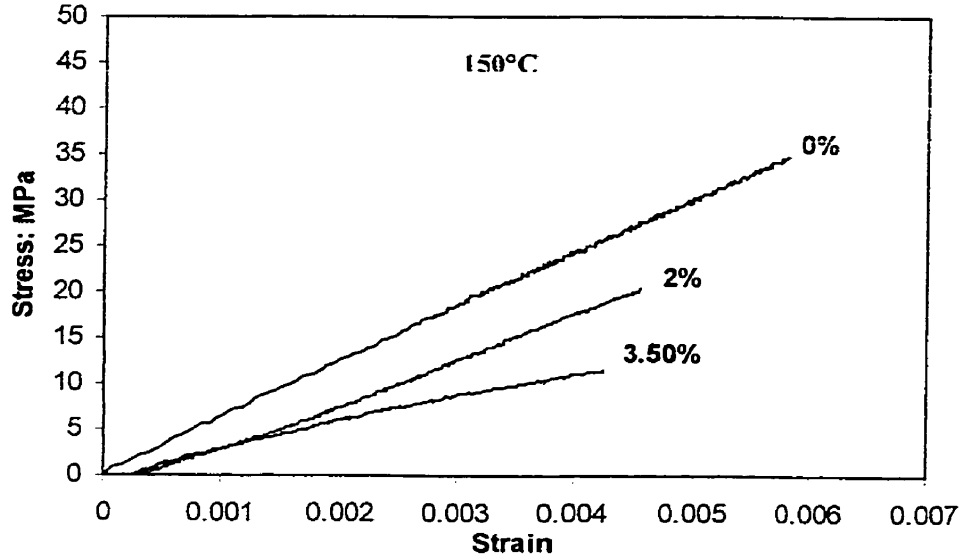

Figure F9: Stress-Strain plot of $[90]_{12}$ composite (V_f :54%) at various moisture contents at 150°C

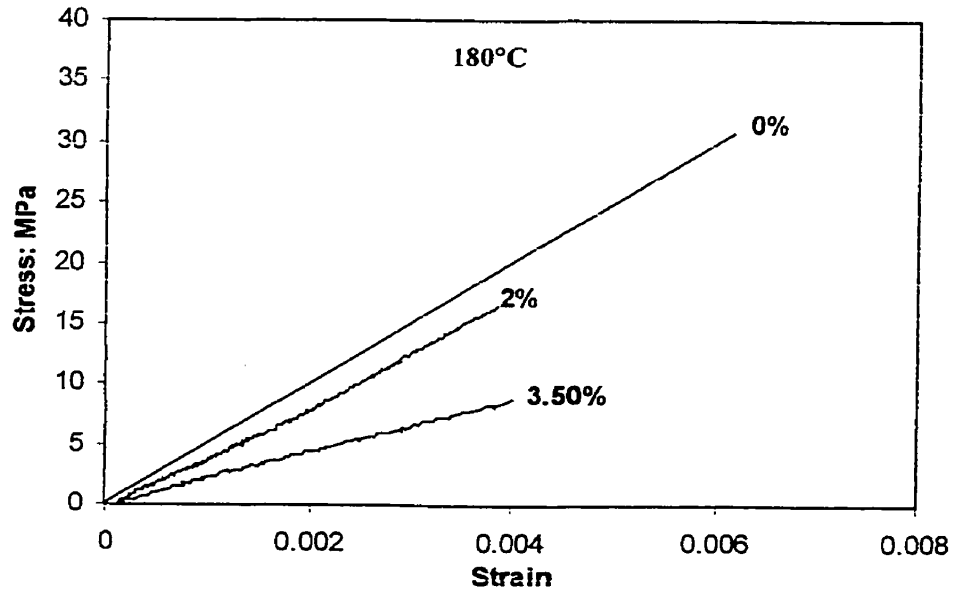

Figure F10: Stress-Strain plot of $[90]_{12}$ composite (V_f :54%) at various moisture contents at 180°C

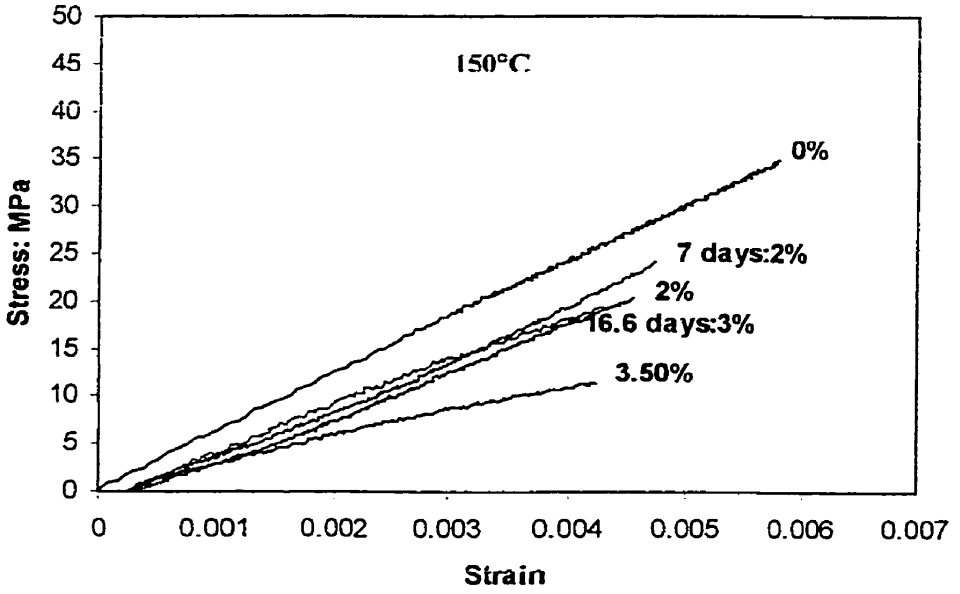

FigureF11: Stress-Strain plot of $[90]_{12}$ composite (V_f:54%) at 150°C at various moisture contents and physical aging times

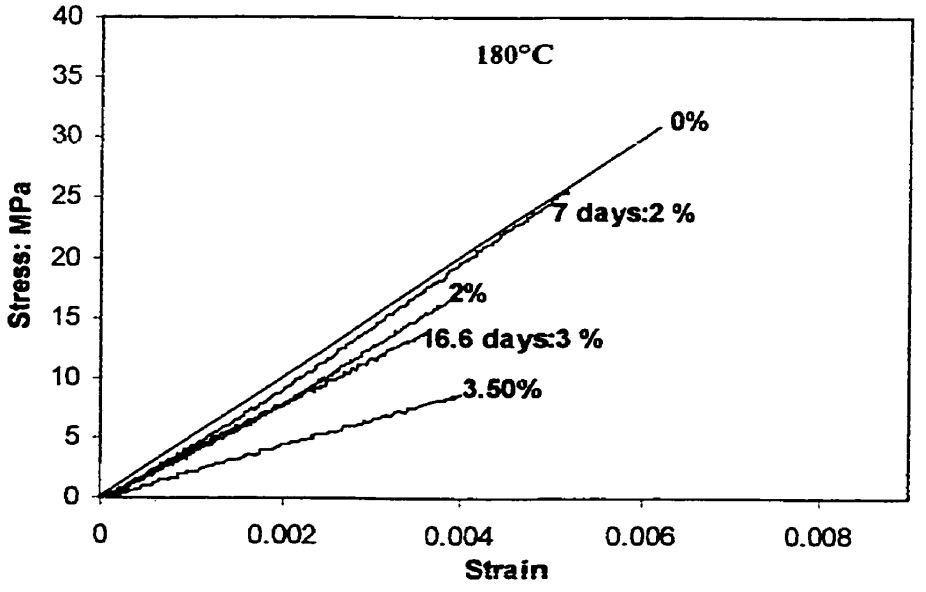

Figure F12: Stress-Strain plot of $[90]_{12}$ composite (V_f:54%) at 180°C at various moisture contents and physical aging times